1-1-2012

# Synthesis Of Molecular Probes For Cystic Fibrosis Research

Bashar Alkhouri
*Ryerson University*

# SYNTHESIS OF MOLECULAR PROBES FOR CYSTIC FIBROSIS RESEARCH

by:

**Bashar Alkhouri**

**B.Sc, Ryerson University, 2010**

A thesis presented to Ryerson University

in partial fulfillment of the requirements for the degree of

Master of Science in the program of

Molecular Science

Toronto, Ontario, Canada, 2012

## Author's Declaration

I hereby declare that I am the sole author of this thesis. This is a true copy of the thesis, including any required final revisions, as accepted by my examiners.

I authorize Ryerson University to lend this thesis to other institutions or individuals for the purpose of scholarly research.

I further authorize Ryerson University to reproduce this thesis by photocopying or by other means, in total or in part, at the request of other institutions or individuals for the purpose of scholarly research. I understand that my thesis may be made electronically available to the public.

**SYNTHESIS OF MOLECULAR PROBES AND MEDICINAL COMPOUNDS OF INTEREST IN CYSTIC FIBROSIS RESEARCH**

**Bashar Alkhouri**

**Master of Science, Molecular Science, Ryerson University, 2012**

## Abstract

Cystic fibrosis (CF) is caused by mutations in the gene coding for the cystic fibrosis transmembrane conductance regulator (CFTR) protein. In healthy individuals, CFTR acts as a phosphorylation and nucleotide regulated channel which mediates the flux of chloride ions across the membrane of epithelial cells. The most common genetic lesion is deletion of phenylalanine residue 508 (F508del-CFTR). The mutation leads primarily to misfolding of the protein, resulting in degradation of most of the protein before it reaches the cell membrane. Also, any F508del-CFTR in the membrane exhibits reduced ion channel activity. The drug-like small molecule VRT-532 has been shown to improve both the trafficking of F508del-CFTR to the cell membrane, as well as its channel function. The exact nature of the interaction of VRT-532 with mutant CFTR is not fully understood. The goal of this research is to help reveal the nature of interaction between VRT-532 and mutant CFTR protein by synthesizing derivatives useful in biochemical studies. Understanding the molecular basis for this interaction will provide us with a template for the development of therapeutically efficacious compounds.

## Acknowledgements

First and foremost I would like to express my sincere gratitude to Dr. Russell D. Viirre, Associate Professor in the Department of Chemistry and Biology, Ryerson University. I want to thank him for this research opportunity and his guidance along the way. His energy, enthusiasm, dedication and passion towards organic synthetic chemistry has undoubtedly motivated and inspired me. He has instilled all the necessary training, and expertise required to continue my journey as a chemist and for that I am most grateful.

I would also like to thank my fellow lab mates Augusto Matarazzo, Salma Elmallah, Rob Denning, and Vassilios Kanellis, and Salman Ansari, I want to thank them for their support, insight and always filling the lab with positive energy making it such an energetic atmosphere to be a part of, and for all the moral support along the way. I would also like to thank my committee members, Dr. D. Foucher, Dr. S. Wylie, and Dr. B. Koivisto for their insight and input on my project. I would also like to thank, Mahroo Taghvaee, Jesse Quinn, and Amanda Mocella and everyone in the Foucher, Gossage, McWilliams, Koivisto laboratory for simply being amazing individuals, I could not have asked for a better group of people to be surrounded by. Finally I would like to thank my parents Evleen, and Waheeb Alkhouri for all their love, support, and patience. Also, my three older brothers Justin, Waseem, and Louie and my cousin Haytham for being so down to earth and helpful in every step of my life. I would also like to thank, Rabei Uweis, Kevin Wahba, Nabil Dib, Rafik Zemo and Paul Wnuk, and Nader Lawen for being amazing individuals and for their endless support along the way. I would also like to thank the Dr. Christine Bear research group at the Hospital for Sick Children this project would not have been a success without their dedication, hard work and support.

**Table of Contents**

## List of Figures

## List of Schemes

List of Abbreviations

| | |
|---|---|
| 3-HA | 3-Hemagglutinin |
| ΔF508 | Deletion of a phenylalanine in position 508 |
| ABC | ATP binding cassette |
| ATP | Adenosine triphosphate |
| BHK | Baby hamster kidney |
| cAMP | Cyclic adenosine monophosphate |
| CF | Cystic Fibrosis |
| CFTR | Cystic fibrosis transmembrane conductance regulator |
| $Cl^-$ | Chloride ions |
| COPII | Coat Protein Complex II |
| COSY | Correlation Spectroscopy |
| DCC | *N,N'*-dicyclohexylcarbodiimide |
| DCM | Dichloromethane |
| DIPEA | Diisopropylethylamine (Hünigs base) |
| DMF | Dimethylformamide |
| DMSO | Dimethylsulfoxide |

| | |
|---|---|
| dppb | 1,4-bis(diphenylphosphino)butane |
| ELISA | Enzyme-Linked Immunosorbent Assay |
| ENaC | Epithelial Sodium Channel |
| $Et_3N$ | Triethylamine |
| $Et_2O$ | Diethyl ether |
| EtOAC | Ethyl acetate |
| ER | Endoplasmic reticulum |
| ESI-TOF MS | Electropray ionization-time of flight-mass spectroscopy |
| HMBC | Heteronuclear Multiple Bond Correlation |
| HMDS | 1,1,1,3,3,3-hexamethyldisilazane |
| HOBt | *N*-hydroxybenzotriazole |
| HPLC | High Pressure (Performance) liquid chromatography |
| Hr | Hour(s) |
| Hsc | Heat Shock Cognate |
| Hsp | Heat Shock Protein |
| HSQC | Heteronuclear Single Quantum Coherence |
| HTS | High-throughput screening |

| | |
|---|---|
| kDa | Kilodalton |
| LC/MS | Liquid chromatography–mass spectrometry |
| MeCN | Acetonitrile |
| Min | Minutes |
| Mp | Melting point |
| mRNA | Messenger ribonucleic acid |
| MSD | Membrane spanning domains |
| NBD | Nucleotide Binding Domain |
| NIH/3T3 | Mouse embryonic fibroblast 3-day transfer, inoculum 3 x $10^5$ cells |
| NMR | Nuclear magnetic resonance |
| $P_o$ | Open probability |
| PAL | Photoaffinity labels |
| $PdCl_2$dppf | Dichloro-1,1'-bis(diphenylphosphino)ferrocene-palladium (II) |
| PG | Photoreactive group |
| $pK_a$ | Acid dissociation constant |
| PMB | *p*-methoxybenzyl |
| PTC | Premature termination codons |

| | |
|---|---|
| R | Regulatory domain |
| $R_f$ | Retention factor |
| rt | Retention time |
| Sec | Seconds |
| *t*-BuOK | Potassium tert-butoxide |
| TEG | Tetraethylene glycol |
| TFE | 2,2,2-trifluoroethanol |
| TLC | Thin Layer Chromatography |
| THF | Tetrahydrofuran |
| TM | Transmembrane segments |
| TMS | Trimethylsilyl |
| UV | Ultraviolet |
| VRT-532 | 4-methyl-2-(5-phenyl-1H-pyrazol-3-yl)phenol |
| Wt | Wild type |

# 1. INTRODUCTION

## 1.1. Cystic Fibrosis

Cystic Fibrosis (CF) is one of the most common genetic diseases among the Caucasian population. Approximately one in every 3,600 children born in Canada has cystic fibrosis, and 60% of CF cases are diagnosed in the first year of life and 90% by the age of 10.[1] CF is an inherited autosomal recessive genetic disease of impaired epithelial transmembrane ion transport which is caused by mutations in the cystic fibrosis transmembrane conductance regulator (CFTR) gene.[2] The disease was first described by Anderson in 1938 as cystic fibrosis of the pancreas to point out the destruction of the pancreatic exocrine function.[3] In 1953 Di Sant' Agnese demonstrated that excessive salt loss occurs in the sweat of CF patients.[4] This finding led to the use of sweat electrolyte measurements as a diagnostic tool. CF is best known for affecting the respiratory system, and the major clinical characteristics of CF are pancreatic insufficiency and lung disease, caused by thick sticky and dehydrated mucus frequently infected by *Pseudomonus* and *Staphylococcus* bacteria, leading to respiratory failure and CF mortality.[5] In addition, most males are infertile, due to hereditary bilateral absence of the vas deferens. Other CF characteristics include bile duct obstruction, reduced fertility in females, high sweat chloride levels, intestinal obstruction, liver disease and diabetes.

### 1.1.2. Cause of Cystic Fibrosis

Cystic fibrosis is caused by mutations in the gene for the cystic fibrosis transmembrane conductance regulator (CFTR). The CFTR gene comprises 27 coding exons, which

spans over 250 kb on chromosome 7q31.2 and transcript 6.5 kb.[5] The major mutation found in CFTR results in the deletion of phenylalanine residue at position 508 of the amino acid sequence. This mutation leads to a serious folding defect, causing ΔF508-CFTR to be retained in the endoplasmic reticulum and prematurely degraded. Most chromosomes carrying the ΔF508 mutation share the same haplotype which is rare in the normal population, indicating that the ΔF508 mutation occurs only once.[5] There are over 1600 different CFTR mutations that have been described, however many are rare and the functional consequence of these rare occurrences are poorly understood. [6]

The protein encoded by the CFTR gene is a chloride ($Cl^-$) channel in the apical membrane of exocrine epithelial cells. Normally CFTR acts as a phosphorylation and a nucleotide regulated channel [7] which mediates the flux of chloride ions across the apical membrane of epithelial cells. In CF patients the mutated CFTR fails to mediate chloride flux from the inside to the outside of the apical membrane, which results in impaired transepithelial chloride, salt and water transport. This transport defect leads to dehydration of the airway surface fluid which in turn leads to mucus accumulation.[7] CF patients lack an effective mechanism to remove the thick sticky mucus layer which results in repeated cycles of inflammation and bacterial infection, eventually causing respiratory failure and ultimately death. The first clues to the structural basis for the trafficking defect came from protease susceptibility studies,[8] in which full-length ΔF508-CFTR proteins exhibited an enhanced susceptibility to digestion by lower concentrations of trypsin relative to wild-type CFTR protein. This supports the idea that mutant protein's conformation is altered and tryptic digestion sites are exposed.[9] Structural studies of protein fragments corresponding to Nucleotide Binding Domain 1(NBD1) and

molecular models of the full length CFTR protein suggest that Phe508 residue at the interface between NBD1 and NBD 2 and the deletion of this reside may disturb native intramolecular interactions.[9] Chemical cross-linking studies were performed using wild-type and ΔF508-CFTR proteins lacking endogenous cysteine residue, and possessing non-native cysteine pairs inserted into different domains.[9] The results of chemical cross-linking studies in the modified wild-type CFTR supported the molecular models for CFTR based on the crystal structure of the prokaryotic ABC protein Sav1866.[9] Sav1866 exhibits a cross-over pattern of domain-domain interactions where the NBD in half of the molecule interacts with the membrane spanning domain of the other half. It was shown that deletion of Phe508 impairs the chemical cross-linking that normally occurs between a non-native cysteine residue incorporated into NBD1, and a non-native cysteine introduced into the fourth intracellular loop.

### 1.2. The CFTR Gene Structure

Cystic fibrosis transmembrane conductance regulator (CFTR) is a cAMP-regulated chloride channel located in the apical membrane of epithelial cells **(Figure 1)**. CFTR is a member of the ATP binding cassette (ABC) superfamily of membrane proteins.[11] The CFTR protein is a 1480 amino acid complex with a molecular weight of approximately 170 kDa. The protein is comprised of five domains: two membrane spanning domains (MSD1 and MSD2), each comprised of six transmembrane segments (TM1 to TM12) that form the ion channel. Also, two nucleotide binding domains (NBD1 and NBD2) that mediate ATP binding and ATP hydrolysis which is necessary for channel opening.[5] Lastly, a regulatory domain (R) which contains numerous sites for phosphorylation,

which allow for domain-domain interactions within the CFTR that results in channel activity. The exact mechanism of R-domain regulation is not completely understood, there are data to support models in which phosphorylated R domain has an inhibitory action,[5] as well as data to support a model in which R domain phosphorylation regulates domain-domain interactions within the CFTR molecule which then results in channel activation.

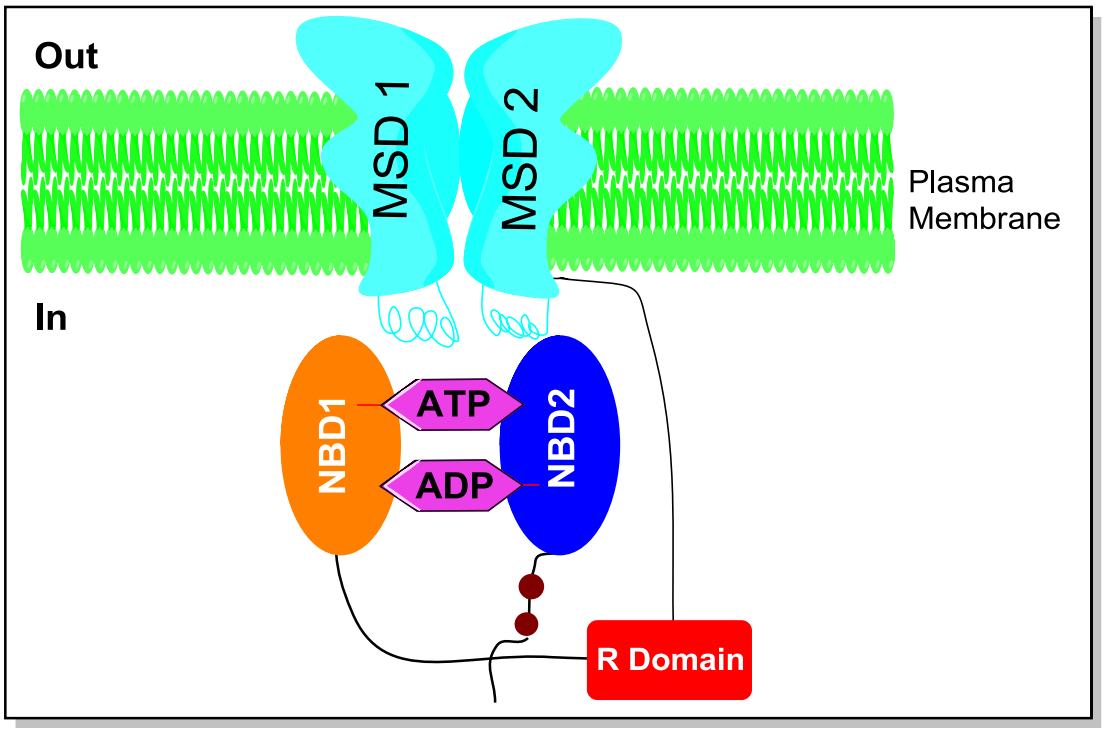


**Figure 1:** Domain structure of CFTR.

In addition to its role as an anion channel, CFTR has been shown to interact with other intracellular proteins. For instance, CFTR regulated the activity of other membrane channels including the epithelial sodium channel (ENaC) and the outward rectifying chloride channel.[12] This is important for the development of new drug therapies that will only improve epithelial chloride transport, but not other aspects of CFTR function. The

CFTR modifies the function and properties of other ion transporters including chloride, sodium, and potassium channels and the $Cl^-$/ $HCO_3^-$ exchanger, which in turn has an effect on water permeability, ATP transport, and mucus secretion.[12]

### 1.2.1. CFTR Folding and Misfolding

The folding of CFTR is thought to occur both co- and post-translation, and involves the formation of multiple intradomain contacts.[13] Structural studies have revealed a complicated folding pathway in which the MSDs of CFTR likely interact with one another to form a 2-winged pore where each wing contains helices from both MSDs.[13] Also, there is communication between the cytosolic nucleotide binding domains with both membrane spanning domains, therefore co- and post-translational folding and assembly of these domains is essential for both the trafficking and function of the CFTR protein. The folding and processing of CFTR is a complex process, to begin the nascent polypeptide is folded and inserted into the ER lipid bilayer, where both cytoplasmic and ER luminal chaperones assist in the folding process.[13] Studies have identified core chaperones Hsp40/70, Hsp 90 and calnexin that play a major role in this process, also the Hsp40, Hdj-2, and Hsc70 chaperones have been shown to play a role in the early steps of the folding pathway.[14] Despite the assistance of the chaperones approximately 55-80% of newly synthesized wild-type CFTR protein are improperly folded, which gets recognized by the ER quality control system (ER QC) and targeted to the cytoplasmic proteasomes for degradation. The properly folded CFTR leaves the ER via the coat protein complex II (COPII) coated vesicles; the CFTR then enters the golgi apparatus

thereby creating a mature CFTR protein.[14] The mature CFTR protein is then delivered to the plasma membrane where it functions as a chloride ion channel.

Mutations in the CFTR that affect the folding process can be very lethal. The ΔF508 mutation causes misfolding and the CFTR protein is retained in the ER, causing approximately 99% of this protein are prematurely degraded.[15] The F508 residue is localized on the NBD1 domain, and interestingly the ΔF508-CFTR is temperature sensitive, and can be corrected by the addition of chemical chaperones or by treatment at low temperature in cultured cells.[15] Therefore understanding the misfolding events which occur with the mutation could aid in the development of therapeutics for CF

### 1.3. Classification of CFTR Mutations

The different CFTR mutations can be divided into five major classes according to the functional effects the mutation has on CFTR production and (or) function. The five classes of CF related mutation have different ways of impairing a cell's membrane's $Cl^-$ conductance.[5] Normally, cystic fibrosis transmembrane conductance regulator (CFTR) is transcribed into mRNA, which in turn is translated into protein in the endoplasmic reticulum. But, prior to being stationed in the cell membrane the protein undergoes posttranslational modification via glycosylation in the Golgi apparatus this process is summarized in **Figure 2**.

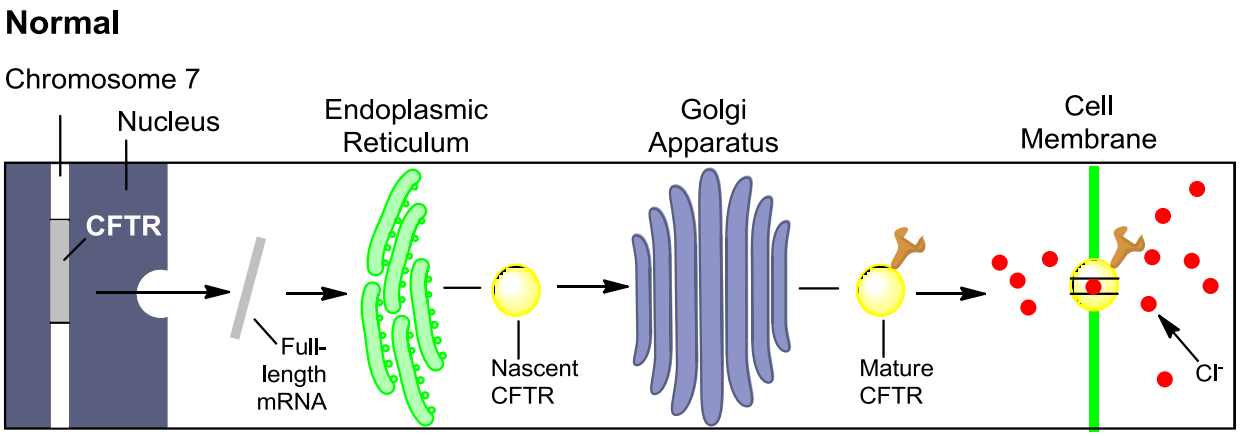


**Figure 2**: A normal Cystic Fibrosis Transmembrane conductance Regulator (CFTR).

### 1.3.1. Class I: Defective Protein Synthesis

Class I are null mutations that result in no CFTR production. This class contains CFTR mutations that leads to nonsense and frameshift, which leads to premature termination codons (PTC). This class is exemplified by the mutation G542X in which a premature termination codon creates truncated protein.[5] Therefore, such mutations decrease the life span of mutant mRNA which results in little or no protein production.

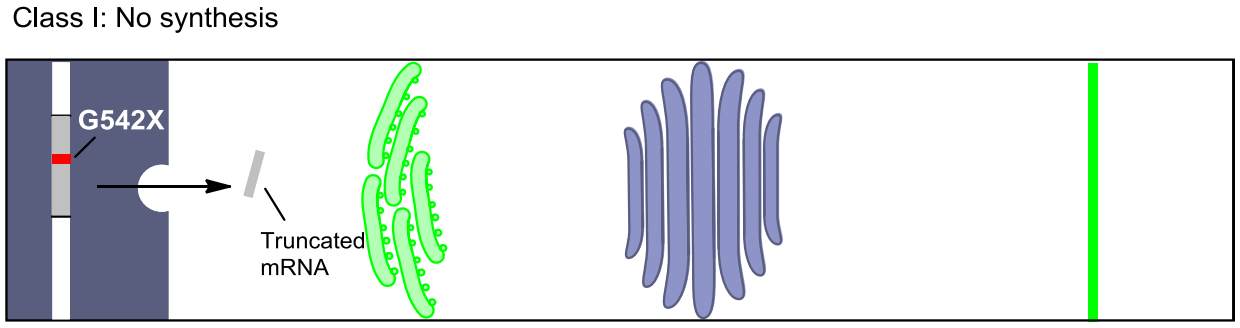


**Figure 3**: Class I mutation which result in no protein synthesis.

The premature termination codons result in truncated proteins that dramatically decrease the half-lives of mutant mRNAs by the nonsense-mediated mRNA decay pathway, as well as alter the pattern of pre-mRNA splicing.[16] Thus these mutations produce little to no protein. The truncated proteins are usually unstable, and are recognized by chaperone proteins in the ER and are rapidly degraded

### 1.3.2. Class II: Defective Protein Processing

Class II mutations are usually associated with defective protein processing. Upon completion of translation a normal CFTR protein undergoes a series of processes which include glycosylation and folding which enable the protein trafficking to the apical cell membrane.[5] This class of mutation causes this process to be impaired, and eventually leads to degradation of the mis-folded protein. ΔF508 is the major mutation which results in the synthesis of a CFTR protein that is unable to correctly fold into its appropriate configuration. This improper configuration results in the protein being retained in the endoplasmic reticulum (ER) and eventually degraded (approximately >99%).

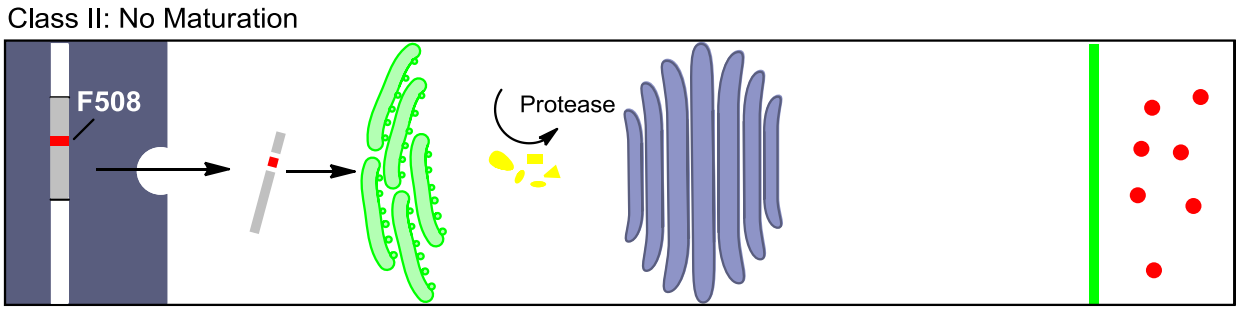


**Figure 4:** Class II mutation results in defective processing of the transcribed CFTR protein.

When the ΔF508 CFTR proteins reach the plasma membrane they undergo abnormal exocytosis and recycling into the membrane. However, most of the exocyted ΔF508 proteins will be marked for degradation and will not be recycled into the plasma membrane.[5] This process reduces the level of defective protein in the membrane.

### 1.3.3. Class III: Mutations Affecting $Cl^-$ Channel Regulation/Gating

Mutations of the CFTR gene in class III result in limited CFTR expression on the cell epithelial membrane but with defective regulation of the $Cl^-$ channel. [5] All mutations attributed to this disease are located within the nucleotide binding folds which affect the binding of ATP or the coupling of ATP binding to activation of channels. Class III mutations; lead to the production of proteins with mutations such as G551D, which alter the normal gating cycle of the CFTR. These alterations cause defects in the chlorine channel regulation and gating and cannot be activated by ATP or cAMP.

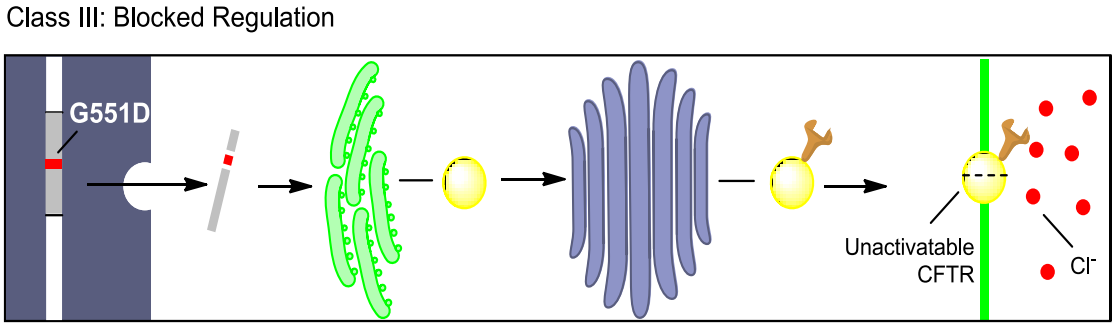


**Figure 5:** Class III mutation results in some CFTR expression but with defective regulation of the CFTR $Cl^-$ channel.

Class III mutations lead to the production of proteins which reach the plasma membrane, however their regulation is defective and thus cannot be activated by ATP

of cAMP.[16] All mutations attributed to this class are located within the nucleotide binding folds, and are likely to affect the binding of ATP or the coupling of ATP binding to activation of the channel, such as by preventing transmission of a conformational change.

### 1.3.4. Class IV: Mutations Affecting $Cl^-$ Channel Conductance

Class IV mutations are associated with cases in which the CFTR gene encodes a protein that is trafficked to the cell membrane and responds to a stimulus but generates a reduced $Cl^-$ current. This class is exemplified by the mutation R347P which affect a transmembrane segment causing decreased $Cl^-$ conductance.[5] The ion channel has the ability to open but the ion throughput is low. Most of the mutations associated with class IV mutations are located on the membrane spanning domains.

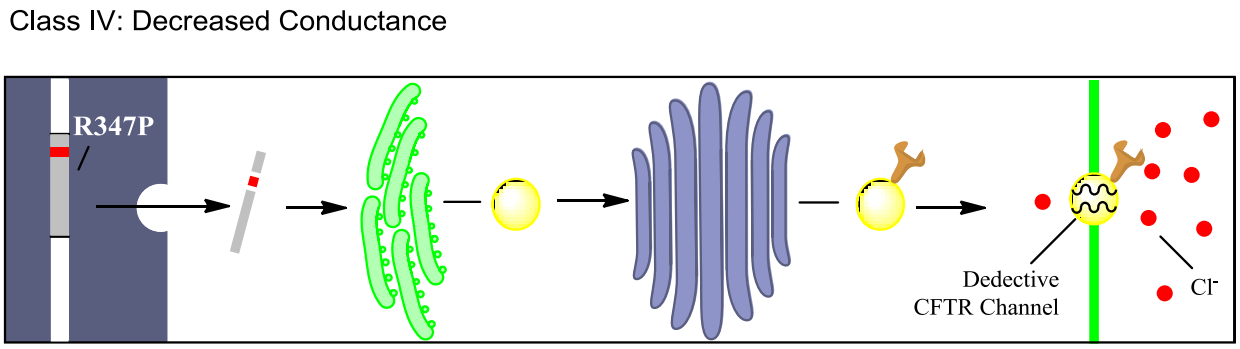


**Figure 6**: Class IV result in CFTR expression on the epithelial cell surface, but have altered conduction of $Cl^-$.

Class IV mutations include cases where the CFTR gene encodes a protein that is correctly trafficked to the cell membrane and responds to stimuli but generates a reduced $Cl^-$ current (for example R117H).[16] Regulation by ATP appears to be normal;

however, the current was much reduced due to a decrease in amplitude of a single channel current and also a lower open state probability.

### 1.3.5. Class V: Reduced CFTR Levels

Class V mutations lead to the production of normal proteins but at a reduced level. This class includes promoter mutations that reduce transcription and amino acid substitution that cause inefficient protein maturation.[16] Most of these mutations are splicing mutations which affect the normal splicing of the pre-mRNA which in turn reduce the level of correctly spliced mRNA. The class is illustrated by a nucleotide substitution that apparently leads to a mixture of mRNAs, some of them correctly spliced.[14]

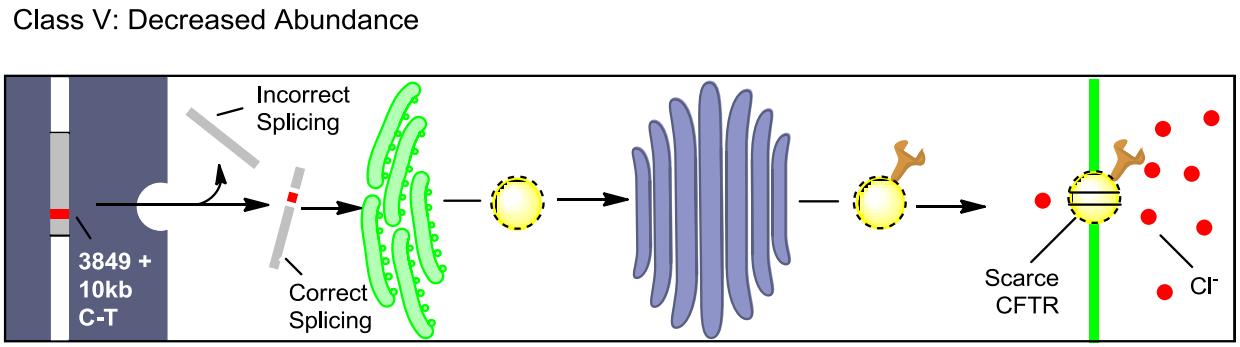


**Figure 7**: Class V result in some CFTR expression on the epithelial surface, but in reduced amounts compared to wild type.

## 1.4. Discovery of small molecules for CF treatment

CF treatment options are mainly focused to help control the disease as opposed to curing it. Existing treatment strategies for cystic fibrosis are primarily symptomatic and do not address the underlying defects caused by this disease. Mainly, CF is monitored

addressing areas such as nutrition, physiotherapy, and maintaining an active lifestyle.[18] Acceptable treatment include antibiotics which are used to treat mild lung infections. Inhaled antibiotics are often used to prevent or control infections caused by the bacteria strain *Pseudomonas aeruginosa.* Anti-inflammatory medicines such as Pulmozymecan[18] help reduce swelling in the airways of the lungs caused by mucus that clogs the airways, which improves lung function and helps prevent respiratory infection. Current drug discovery are focused primarily on two classes of small molecules which may prove to be useful in the pharmacological treatment of CF.[18] The first class is referred to as “Correctors”; these are molecules which through either direct interactions with mutant CFTR or perhaps any various chaperone proteins, recuse the cell’s ability to correctly traffic the protein to the cell membrane. The second class of small molecules is referred to as “Potentiators” which restore the normal channel activity in the mutant protein once it appears in the cell membrane.

### 1.4.1. Small Molecule Therapeutics for Cystic Fibrosis

The first generation of chemical chaperones that were identified to assist in ΔF508 folding and trafficking were nonspecific osmolytes, such as glycerols **(I, Figure 8)**, and trimethylamine N-oxide (TMAO) **(II)**.[18] These chemicals protect proteins against both thermal and chemical denaturants and stabilize the native conformation of proteins. Myoinositol **(III),** and 4-phenylbutyrate **(IV)** were shown to promote ΔF508 folding, however high doses of the chemical are needed to obtain correction, which limits the efficacy of these compounds.[18] There was a great deal of excitement over the initial discovery that the SERCA pump inhibitors curcumin **(V)**, and thapsigargin **(VI)** which

had potentiator capabilities, however; the effect of these targets were variable amongst cell types and mouse strains.[19]

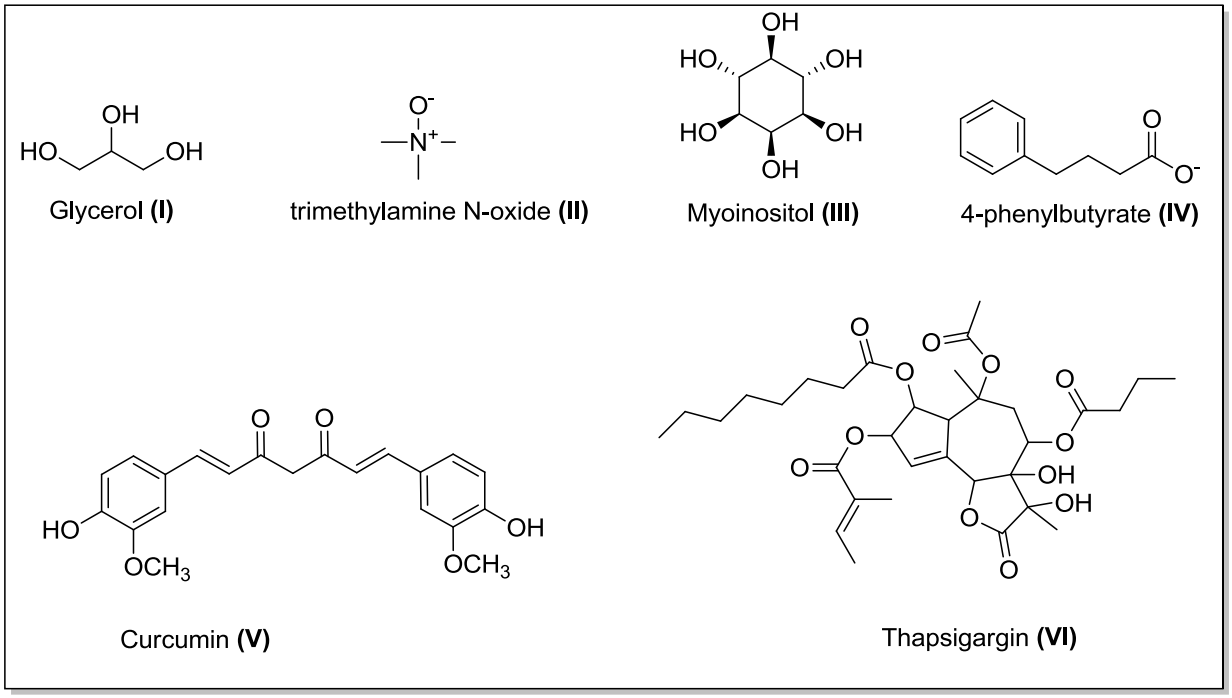


**Figure 8:** First generation of chemical chaperones that were identified to assist in ΔF508 folding and trafficking.

Research towards identifying novel target compounds for CF treatment has been geared towards the use of high throughput screening (HTS). In 2005, the Verkman group[20], screened over 150,000 diverse small molecules and were analyzed for their ability to correct ΔF508 trafficking. This screen identified 4 classes of corrector molecules which were grouped based on chemical structure **(Figure 9)**. Class 1 molecules were, 2-aminobenothiazoles, class 2 were 2-amino-4-arylthiazoles, class 3 were 2-quinazolinyl-4-aminopyrimidinones, and class 4 include bisaminomethylbithiazoles. All members of these classes were identified to be corrector molecules that increase the abundance of ΔF508 CFTR at the plasma membrane, also

an increase in the forksolin-genistein stimulated apical membrane chloride current was observed. [20]

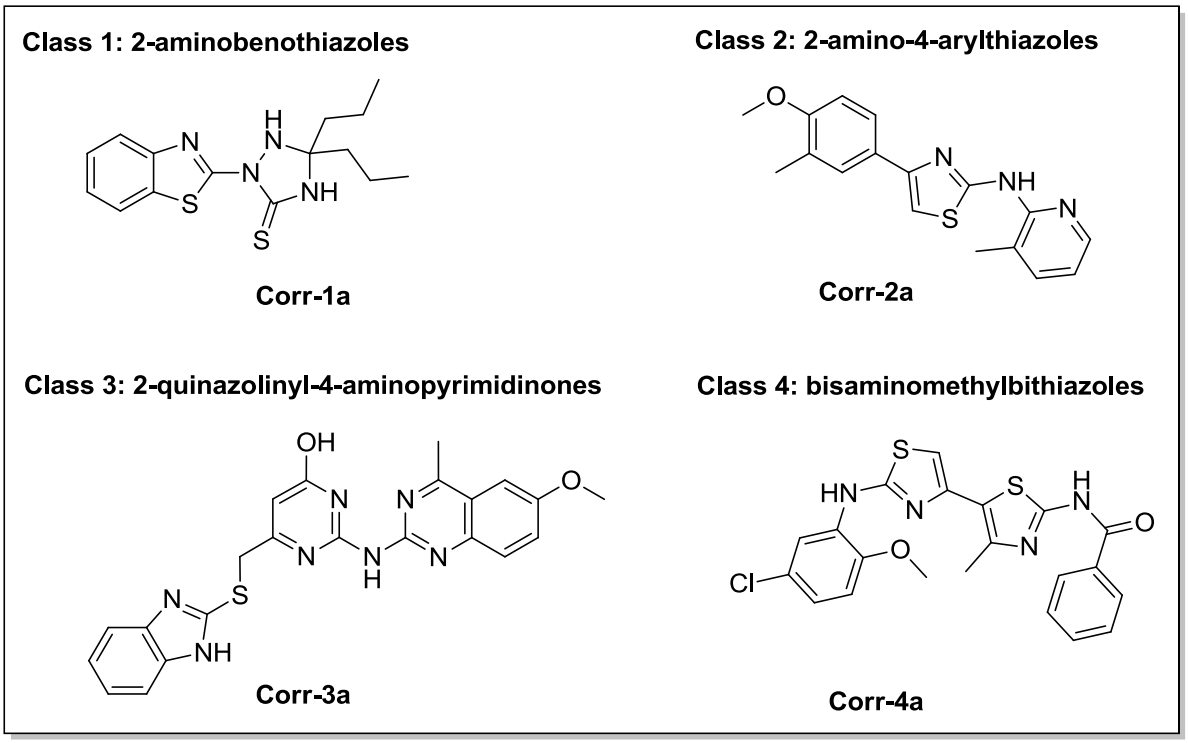


**Figure 9:** Four classes of corrector molecules that were identified via HTS.

Upon further analysis, the class 4 bisaminomethylbithiazoles showed the highest functional correction of the mutant ΔF508 CFTR upon measurements using an iodide efflux essay, which measures iodide release using an iodide sensitive probe.[21] When these classes of molecules were tested for their effects on human bronchial epithelial cells isolated from patients homozygous for ΔF508 mutation, only class 4 molecules resulted in a significant increase in the CFTR dependent $Cl^-$ secretion. Corr-4a has been studied and suggests that Corr-4a may exert an effect on ΔF508 CFTR folding by binding to the transmembrane region of the protein, but the direct binding site on the

CFTR is unclear.[21] Overall Corr-4a not only improves trafficking of ΔF508 CFTR to the plasma membrane, but it was also found to enhance the cell surface stability of the rescue mutant protein. Corr-4a interacts in such a way that allows mutant CFTR protein to bypass multiple quality control checkpoints.

A recent study described a screening assay for CF correctors which focused on identifying molecules based on their ability to promote delivery of 3-hemagglutinin (3-HA) tagged ΔF508 CFTR to the plasma membrane of baby hamster kidney (BHK) cells.[21] This screen measured the transport of ΔF508 CFTR to the cell surface as opposed to screening molecules based on halide conductance. Upon screening of 2000 compounds there were several classes of trafficking correctors identified, some of which were previously identified to play a role in CFTR trafficking. Two hits which Robert *et al*. chose for further investigation were sildenafil and carboplatin.[21]

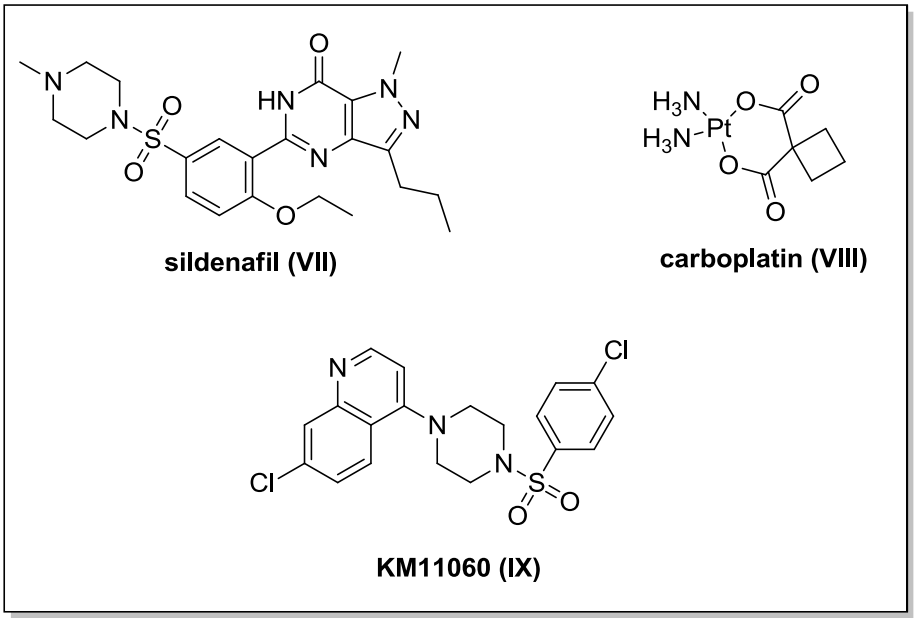


**Figure 10**: CFTR correctors that were identified by a three stage ELISA assay.

Sildenafil more commonly known as Viagra was previously identified to correct CFTR trafficking when applied in high molecular doses.[22] Analysis showed that low doses of sildenafil was sufficient to promote trafficking but did not result in the accumulation of functional channels at the plasma membrane. Upon increased dosage, sildenafil did result in a strong increase in iodide efflux responses. Further screening of sildenafil derivatives identified a molecule named KM11060, which was more potent in its ability to increase both the amount of mature ΔF508 C band as well as the function of ΔF508-CFTR in iodide efflux assays. Carboplatin was a novel hit which was able to increase maturation of ΔF508 CFTR, but only caused a slight increase in iodide efflux regardless of dosage.[23]

### 1.4.2. Identification of novel ΔF508-CFTR potentiators

In the search for small molecule modulators for ΔF508-CFTR, a research group from Vertex pharmaceuticals[24] developed cell-based assays of membrane potential for either potentiators or correctors using NIH/3T3 mouse fibroblast cells expressing ΔF508-CFTR. In order to identify novel ΔF508-CFTR potentiators, high-throughput screening (HTS) of over 122,000 synthetic compounds from a library database was undertaken. Of the 122,000 compounds from the database, only 278 of those compounds were selected for further testing based on activity. Of these, 145 compounds were removed because of impurities (<85% purity by LC/MS) along with poor chemical attractiveness. The remaining 133 compounds were selected for dose-response analysis using HTS assay and were counterscreened in NIH/3T3 cells that did no express ΔF508-CFTR. Based on those results, 53 compounds containing 10 structurally distinct scaffolds were selected for further studies. Amongst the compounds tested, 4-methyl-2-(5-phenyl-1H-

pyrazol-3-y)phenol (VRT-532 **1**, **Figure 11**), was the most potent and efficacious potentiators identified in the HTS using ΔF508-CFTR-NIH/3T3 cells. [24]

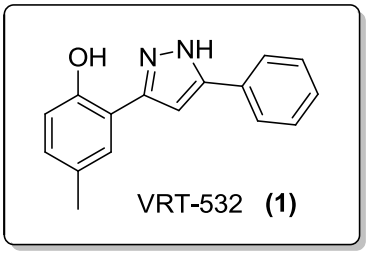


**Figure 11:** Structure of VRT-532 [4-methyl-2-(5-phenyl-1H-pyrazol-3-yl)phenol].

Potentiator activity was confirmed by inside-out patch clamp recording in ΔF508-CFTR-NIH/3T3 cells. Patch clamping is used to measure ion currents across biological membranes which allows the study of single or multiple ion channels in cells. In a concentration of 20μM VRT-532 in the presence of ATP and $pK_a$ increased the open probability ($P_o$) approximately 4 fold. The $P_o$ of ΔF508-CFTR in the presence of VRT-532 was similar to that of wild type-CFTR (wt-CFTR) under identical conditions.[24] The CFTR potentiator VRT-532 has the ability to potentiate the gating not only with wt-CFTR and ΔF508-CFTR but also G551D-CFTR which is a rare mutation found in ~5% of CF patients.

### 1.4.3. The use of VRT-532 as a corrector molecule for protein trafficking

Since VRT-532 was identified as a ΔF508-CFTR channel potentiator, Wang et al. tested whether it could enhance channel activity of ΔF508-CFTR.[25] In doing so, baby hamster kidney cells (BHK-cells) were used that express ΔF508-CFTR and channel activity was monitored using iodide efflux assays. It was observed that upon addition of forskolin

with VRT-532 the iodide efflux drastically increased, but in the absence of forskolin VRT-532 did not increase channel activity suggesting that it acts as a potentiator. Therefore the ability to enhance channel activity indicates direct binding to the CFTR protein.

Van Goor *et al*., suggested that the potentiating effects of VRT-532 is likely mediated by inhibition of the intrinsic ATPase activity of the mutant protein, an activity associated with channel closure.[24] The effect of VRT-532 on the ATPase activity of partially purified ΔF508-CFTR provides the most compelling evidence for direct binding to the protein and elucidates the mechanism underlying its potentiating effect on channel activity. Bear *et al*., showed ATPase studies suggesting binding probably does not occur at the nucleotide binding site formed from the NBD1-NBD2 heterodimer because little change in the apparent ATP affinity was observed.[26] Further findings suggest that direct binding of VRT-532 induces and/or stabilizes a structure that promotes the channels open state which closely resembles that of a wild-type CFTR and that this interaction is sufficient to partially rescue both protein biogenesis and channel activity. The site at which VRT-532 binds to ΔF508-CFTR still remains unidentified, and the determination of this specific interaction can lead to a breakthrough in drug development and treatment for cystic fibrosis. [26]

### 1.5. Research objectives

VRT-532, identified by Vertex pharmaceuticals by HTS has the ability to act as a potentiator and a corrector molecule. Based on limited proteolysis studies, this molecule may modify the conformation of ΔF508-CFTR such that it more closely

resembles a wild-type protein. Understanding the molecular basis for this interaction will provide insight into the mechanism of action of VRT-532 and the mutated CFTR protein. An understanding of the interaction between the two can provide a template for the development of therapeutically efficacious compounds. To help reveal the nature of interaction between VRT-532 and the ΔF508-CFTR proteins derivatives modified with functional groups useful in biochemical studies will be synthesized. These derivatives include a photoaffinity label that contains a recognition element for specific interaction with a site on a target protein. Photoaffinity labels also include a photoactivatible functional group that reacts to form a covalent bond to the protein upon photoirradiation. Another aspect this work will entail the synthesis of a fluorescent probe, which can be a useful probe for the binding interaction between VRT-532 and CFTR. Furthermore, developing a working protocol for hydrogen isotope exchange to be used as a radiolabeled version of the parent compound is another aspect of this research. A radiolabeled version of VRT-532 would be extremely useful for quantitative studies of its binding properties to CFTR. Finally the synthesis of a stationary phase to be used for affinity chromatography is of great interest. In doing so, the stationary phase with comprise a tether compound coupled to the parent compound and attached to a solid support resin (agarose beads).

## 2. RESULTS AND DISCUSSION

### 2.1. Synthesis of VRT-532 and its derivatives

To elucidate the nature of interaction between the parent compound **1** and mutant CFTR, VRT-532 must be prepared along with useful molecular probes based on the structure of **1** to be used for biochemical studies. Starting with 2′-hydroxy-5′-methylacetophenone **2** which was added to an ice cooled suspension of 4-iodobenzoyl chloride **3** in pyridine acting as the base and the solvent to eventually afford the expected ester **4** in 86% yield **(scheme 1)**.

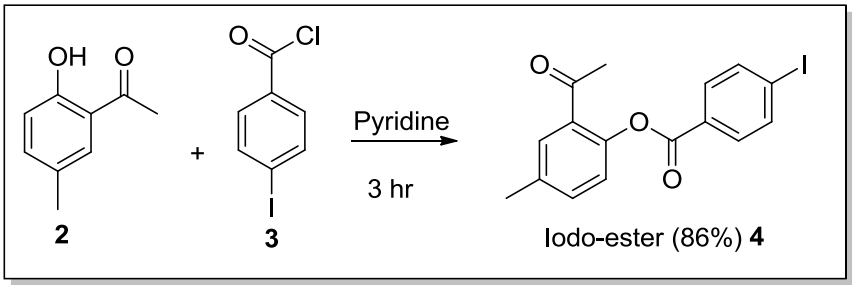


**Scheme 1:** Synthesis of 2-acetyl-4-methylphenyl 4-iodobenzoate.

The ester **4** is then subjected to a Baker-Venkataraman rearrangement[35] using potassium tert-butoxide (*t*-BuOK) in hopes to isolate the diketone **(Scheme 2)**. This rearrangement reaction involves the base-induced transfer of the ester acyl group in an *o*-acylated phenol ester, leading to a 1,3-diketone, which proceeds through the formation of an enolate, followed by intramolecular acyl transfer.

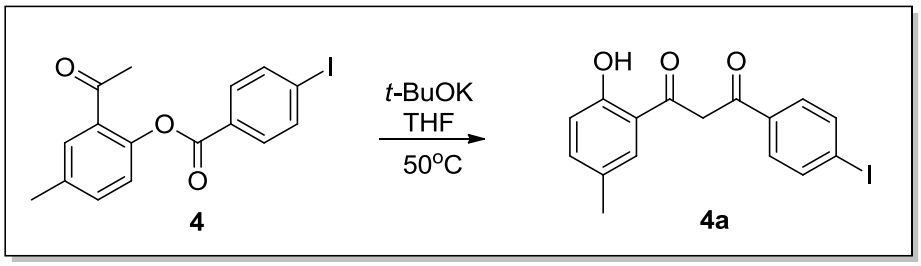


**Scheme 2**: The Baker-Venkataraman rearrangement of ester 4a.

The crude $^{1}$H-NMR ($CDCl_3$) spectroscopy of **4a** revealed the presence of numerous species and repeated attempts at purification via recrystallization failed to materialize a product with improved purity. The additional signals were reasoned to be attributed to a mixture of keto-enol tautomers, which should to be compatible in the subsequent pyrazole formation; therefore it was decided to carry the crude solid material onto the next step. The crude material was then exposed to a Paal-Knorr pyrazole synthesis[36], with the treatment of hydrazine in acetic acid to afford the desired pyrazole (i-VRT, **5**) in a 68% yield.

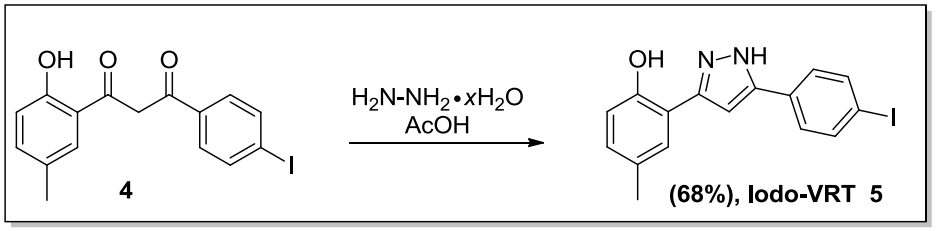


**Scheme 3:** Paal-Knorr pyrazole synthesis involving the crude diketone **4**.

Following the same sequence of reactions as described above the nitro derivative **9** was synthesized in a 67% yield. Starting with 2′-hydroxy-5′-methylacetophenone and using 4-nitrobenzoyl chloride **6** the desired ester was achieved in a 98% yield. Ester **7** was subjected to a Baker-Venkataraman rearrangement with the intention of not isolating the

di-ketone intermediate but rather taking the crude reaction mixture and subsequently performing a Paal-Knorr pyrazole synthesis. The crude material was treated with hydrazine and acetic acid in order to achieve the desired **9 (scheme 4)**.

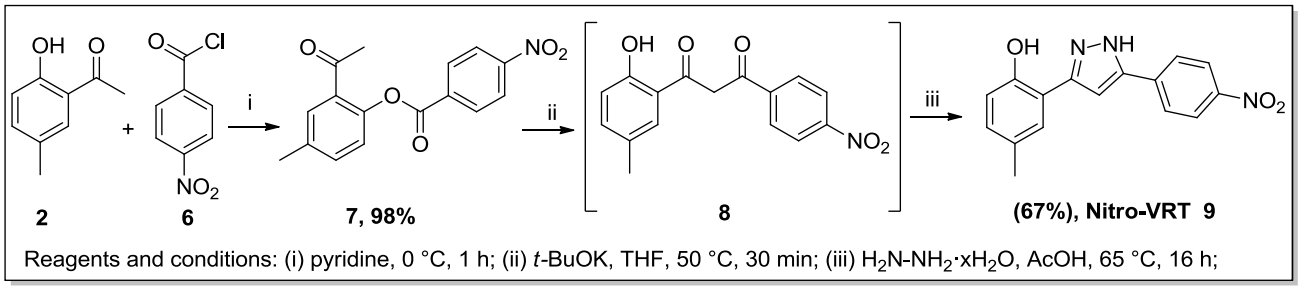


**Scheme 4**: Synthetic route towards the synthesis of nitro derivative of **1.**

Subsequent to these experiments, it was discovered that the entire synthesis of the pyrazole core starting from 2′-hydroxy-5′-methylacetophenone and varying the benzoyl chlorides could be achieved in a one-pot synthesis. The reaction between the acetophenone and the benzoyl chloride was heated to 50°C using pyridine as the solvent and monitoring by TLC for complete conversion of the 2′-hydroxy-5′-methylacetophenone. At this point, *t*-BuOK was added, and again gauging the complete consumption of the ester intermediate by TLC. Finally, aqueous hydrazine was added followed by acetic acid **(scheme 5)**. With one final extraction followed by purification via column chromatography the desired compound can be obtained, all in less than one day of reaction time and in one pot. Iodo-VRT (**5**, 41%), Nitro-VRT (**9**, 24%), and VRT-532 (**1**, 65%) were all synthesized by the one-pot method in moderate yields. This synthetic route is a quick and effective method towards the synthesis of VRT-532 derivatives. Simply by changing the benzoyl chloride we can create a variety

of useful derivatives with varying substituents at the 4-position of the parents compound's phenyl ring.

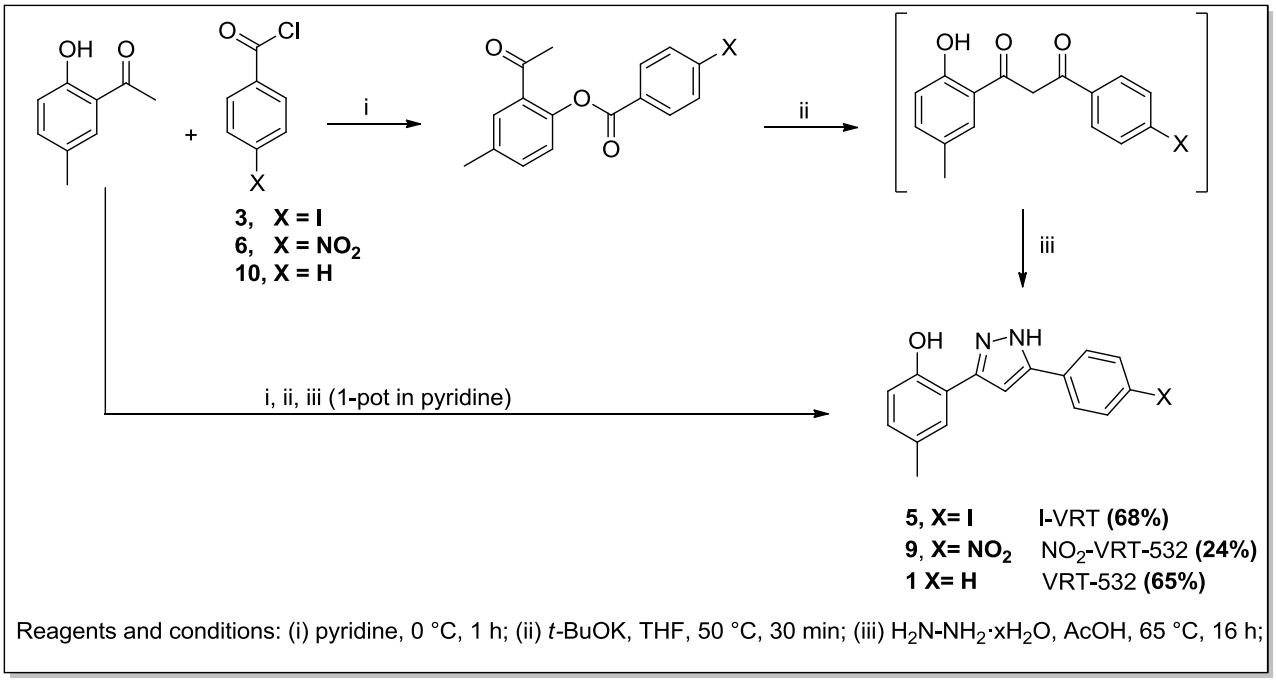


**Scheme 5:** One pot-synthesis towards VRT-532 and its derivatives.

## 2.2. Synthesis of a photoaffinity label

One way to help elucidate the nature of interaction between VRT-532 and mutant CFTR is to prepare derivatives with functional groups that are useful in biochemical studies. Derivatives such as photoaffinity labels (PAL) are an ideal tool for this purpose. In the process of photoaffinity labeling a compound of interest is covalently modified with a photoreactive group (PG). A photoaffinity label is a molecule that contains a recognition element for specific interactions with a site on a target protein, as well as a PG that reacts to form a covalent bond to the protein upon photoirradiation. After covalent

modification the new labeled site can then be identified using any number of biochemical techniques, for instance limited proteolysis followed by gel electrophoresis and/or mass spectrometry to suggest the location of the binding site for the unlabeled ligand. Three major types of PGs are commonly used in PAL: benzophenones **(X)**, aryl azides **(XI)** and diazirines **(XII) (Figure 12).**

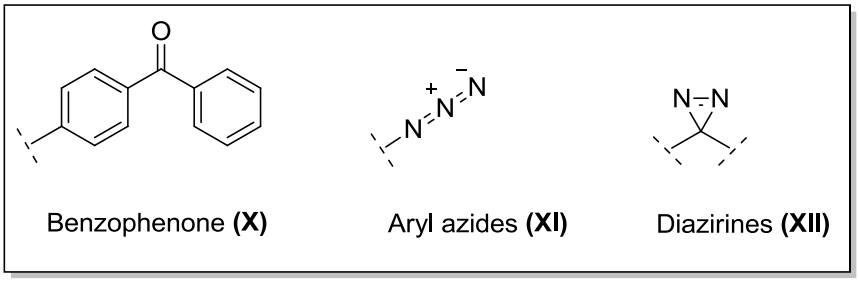


**Figure 12**: Common photoreactive groups used in photoaffinity labeling.

For our synthetic efforts in preparing a photoaffinity label, aryl azide was chosen because of the relative ease in preparing such a derivative. Starting with the nitro-VRT **9** a stannous chloride reduction was performed in ethanol which provided the amine derivative **11** in a 71% yield **(Scheme 6)**.

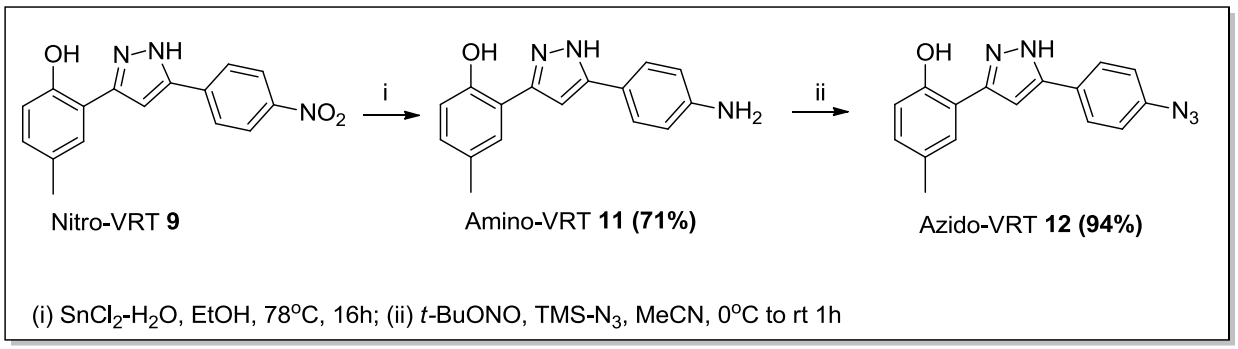


**Scheme 6**: Synthesis of aryl azide to be used as a photoaffinity label.

Having amine **11** at our disposal allows for a diazotization reaction[37] with the treatment of *t*-butyl nitrite in acetonitrile, followed by the addition of azidotrimethylsilane at 0°C. Upon completion of the reaction, the acetonitrile was evaporated and the crude material was purified via column chromatography to afford the aryl azide derivative **12** as a yellow solid in a 94% yield.

Upon photoexcitation under UV irradiation, aryl azides extrude a molecule of $N_2$; thereby forming a highly reaction and short lived intermediate known as a nitrene. The nitrene readily rearranges to form an electrophilic cyclic ketenimine.[38] In photoaffinity labeling experiments, this occurs within a protein binding site, and the ketenimine is quenched by a nucleophilic functional group from the protein, thus forming a covalent linkage between the label and the protein **(Figure 13)**.

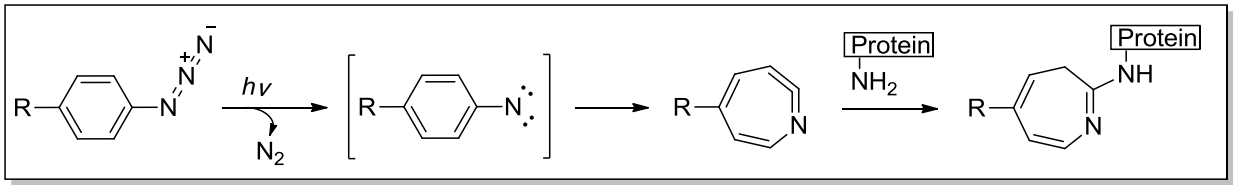


**Figure 13**: Typical photoreaction of aryl azide photoaffinity labels.

Following a literature procedure by Sydnes *et. al*. we set out to demonstrate that this type of chemistry could apply to our azide compound **12.** They had shown previously that 2,2,2-trifluoroethanol (TFE) is an efficient solvent for trapping[39] intermediates derived from photochemical reactions, possibly as a result of the unique physical properties of TFE, therefore the use of this solvent was pursued. Azido-VRT **12** (20 mg, 0.069 mmol) was dissolved in 30 mL of 2,2,2-trifluoroethanol (TFE) in a glass dish and was irradiated using a hand held UV lamp. The excess use of TFE was due in part to

solubility issues. Working with such low concentrations issues of detection were apparent by TLC.

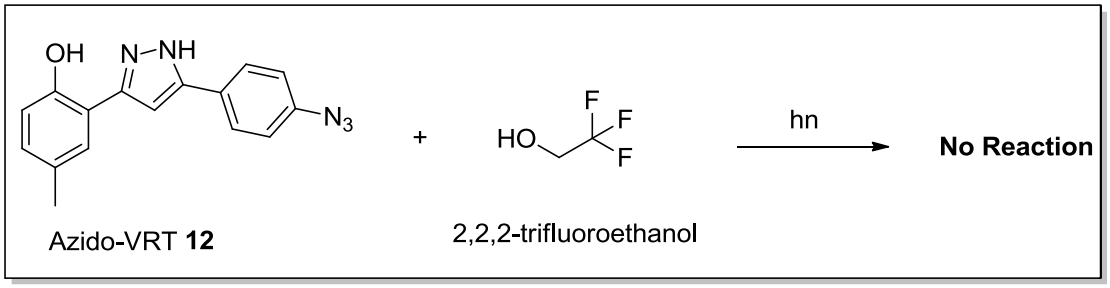


**Scheme 7:** UV irradiation of Azido-VRT using TFE.

After 10 min of constant exposure, a colour change was observed with the solution changing from a yellow to a dark orange colour. The solution was exposed for another 60 min with no additional colour change. The TFE was evaporated off and a crude $^{1}$H-NMR ($CDCl_3$) spectrum indicated no major reaction had occurred to the original azide-VRT compound.

Continuing with this methodology, we decide to use UV-Vis spectroscopy in order to track any changes that occur once the solution is exposed to UV. Azido-VRT **12** (1 mg) was dissolved in 1 mL of TFE and series dilutions were performed until a final concentration 0.01 $\mu$g/mL was achieved. The solution was placed in a quartz cuvette and placed 15 cm away from the UV light source, and exposed in 15 sec increments and changes measured using a Perkin Elmer UV/Vis Spectrometer Lambda 40 instrument. **Figure 14** shows the degradation product for azide **12** over time. The graph shows an absorption maximum (λmax) at 275 nm, in addition to an isosbestic point at 314 nm. The isosbestic point on a graph refers to a specific wavelength at which two chemical species have the same molar absorptivity (ε). This result indicated

that there is a chemical change occurring, and it is improbable if there were more than two products present in the mixture.

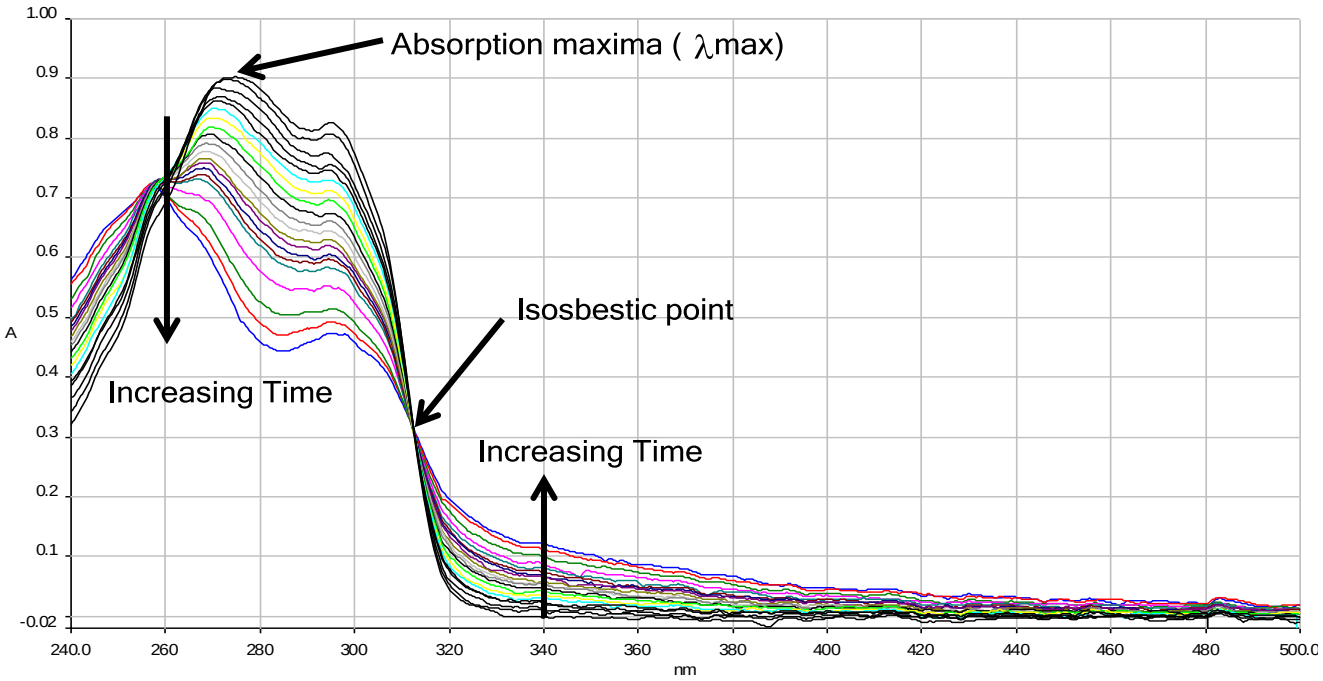


**Figure 14:** UV/Vis spectra for the photoirradiation of azide **12** in TFE.

The UV/VIS results showed great promise, but repeated trials using $^{1}$H-NMR ($CDCl_3$) to track changes in the photoreaction that were expected to occur were inconclusive. This methodology was abandoned, and instead of using TFE, diethylamine was used along with heptane as a solvent. In a 25 mL volumetric flask, containing a concentration of 0.2 mg/mL of azide **12** in heptane, the sample was placed 15 cm away from the light source for 15 second increments and placed for UV/VIS analysis. The result was almost identical to the previous trial with TFE.

In an additional attempt to trace the photoreaction that occurs once aryl azides are exposed to UV light, another $^{1}$H-NMR experiment was performed. Taking 40 mg of

azide-VRT **12**, along with 0.4 mL of diethylamine in 2 mL of deuterated benzene ($C_6D_6$) placed in a quartz NMR tube and irradiated using a 140 W Hanovia Utility ultraviolet quartz lamp. The experiment was performed in a closed vessel to avoid exposure to the harmful radiation. Prolonged exposure from the light source eventually caused the contents within the NMR tube to heat up and boil off. This experiment was then repeated with a stream of air blowing over the vessel to avoid overheating of the sample. The sample was observed at t=0 min prior to exposure to confirm the azide-VRT **12** and diethylamine functionalities. After 30 min of exposure, analysis of the proton spectrum indicated evidence that a change has occurred. Observing the region from 7.7 ppm to 6.6 ppm the most profound changes were the appearance of three new resonance peaks, three doublets at 7.44 ppm, 7.22 ppm, and 6.74 ppm. Also, the doublet at 7.09 ppm, the doublet of triplets at 6.82 ppm, and the singlet at 6.78 ppm of **12** were diminished to about ~65% of their original intensities. The clear doublet of doublets at 6.94 ppm which was observed prior to UV exposure has now become a multiplet. It is apparent that modifications have occurred to the original azido-VRT compound.

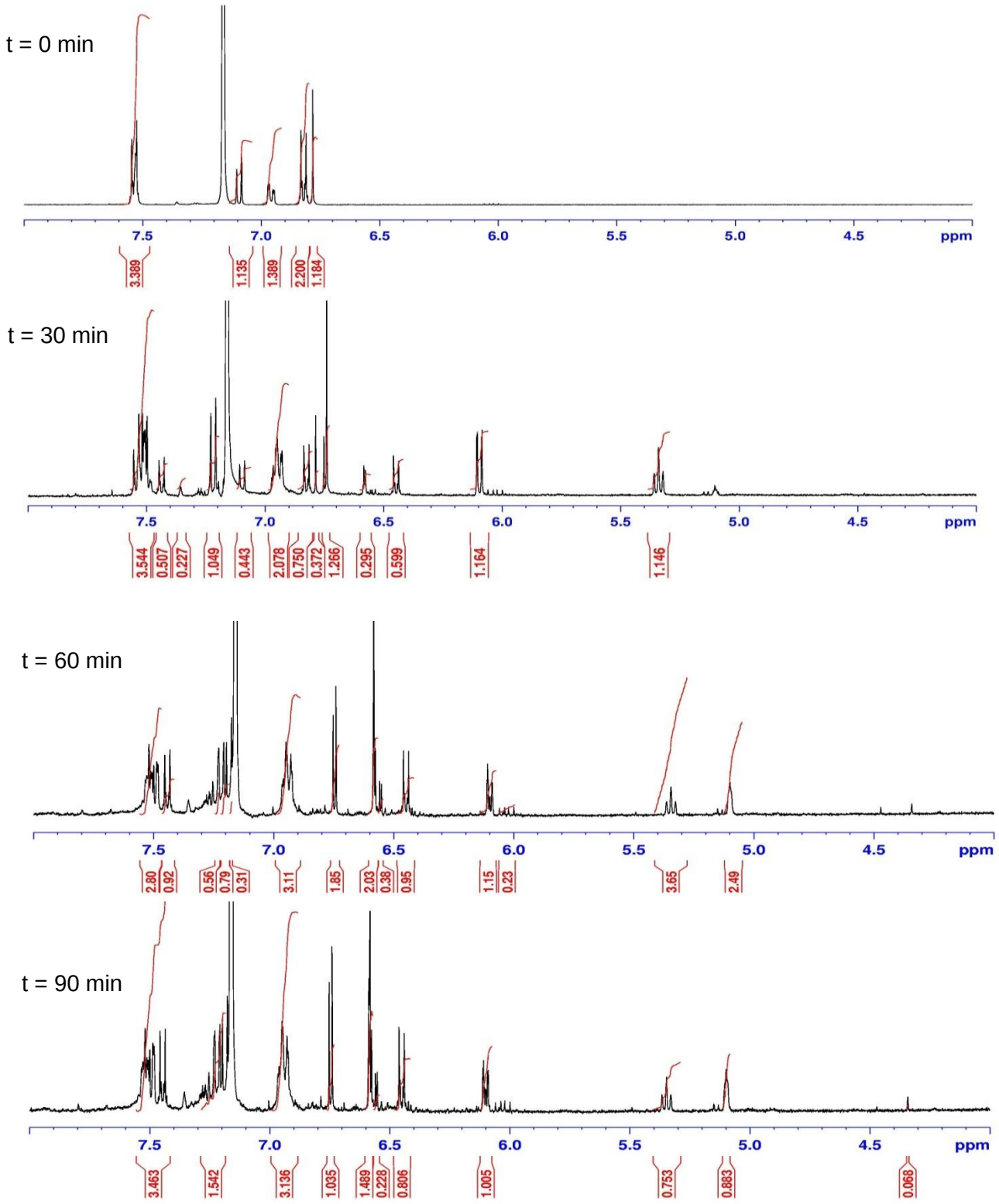


**Figure 15:** A) $^{1}$H-NMR spectra of Azido-VRT with no exposure to UV light. B) 30 min. C) 60 min exposure. D) 90 min of exposure from the region 8.0-4.0 ppm.

The region from 6.5-4.0 ppm in the original sample at t = 0 min displays a flat baseline indicating that **12** has no proton resonances in this range **(Figure 15 A)**. After 30 min of exposure the formation of a new species is observed with 3 new resonances including; a doublet at 6.45 ppm, a doublet of doublets at 6.10 ppm, and a clear triplet at 5.34 ppm **(Figure 15 B)**. After 60 min of exposure noticeable changes were occurring. The aromatic resonance of **12** at 7.06 ppm, 6.82 ppm and 6.78 ppm have completely disappeared, indicating the complete consumption of azide-VRT **12 (Figure 15 C)**. The sample was exposed for an additional 30 min, and not much change was observed at all from the previous trail **(Figure 15 D)**. By observing the region from 6.5-4.0 ppm we notice a new peak develop 5.10 ppm, and at t = 60 min. No change in spectrum was observed when the sample was irradiated for an additional 30 min. The disappearance and appearance of signals is consistent with the formation of **13**. Since no further change was observed, the reaction was deemed complete. The reaction mixture was evaporated to a solid brown product and purified by column chromatography. Thorough NMR spectroscopy analysis 1-D and 2-D (shown below) was performed on the purified product to determine the exact structure of the material isolated and it was deemed that the diethylamine adduct **13** was attained in a 40% yield.

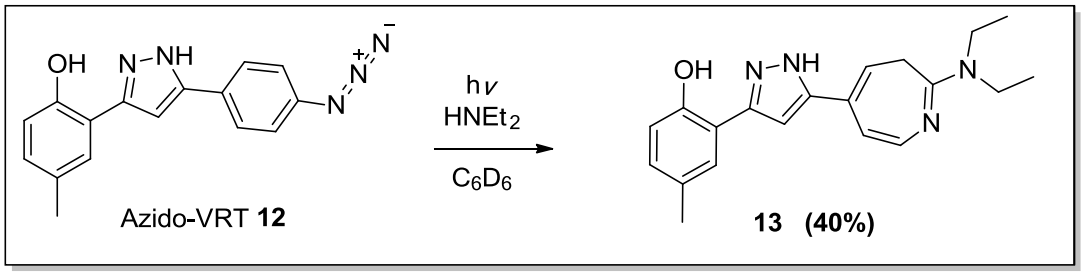


**Scheme 8**: Photoreaction of **12**, towards the formation of diethylamine adduct **13.**

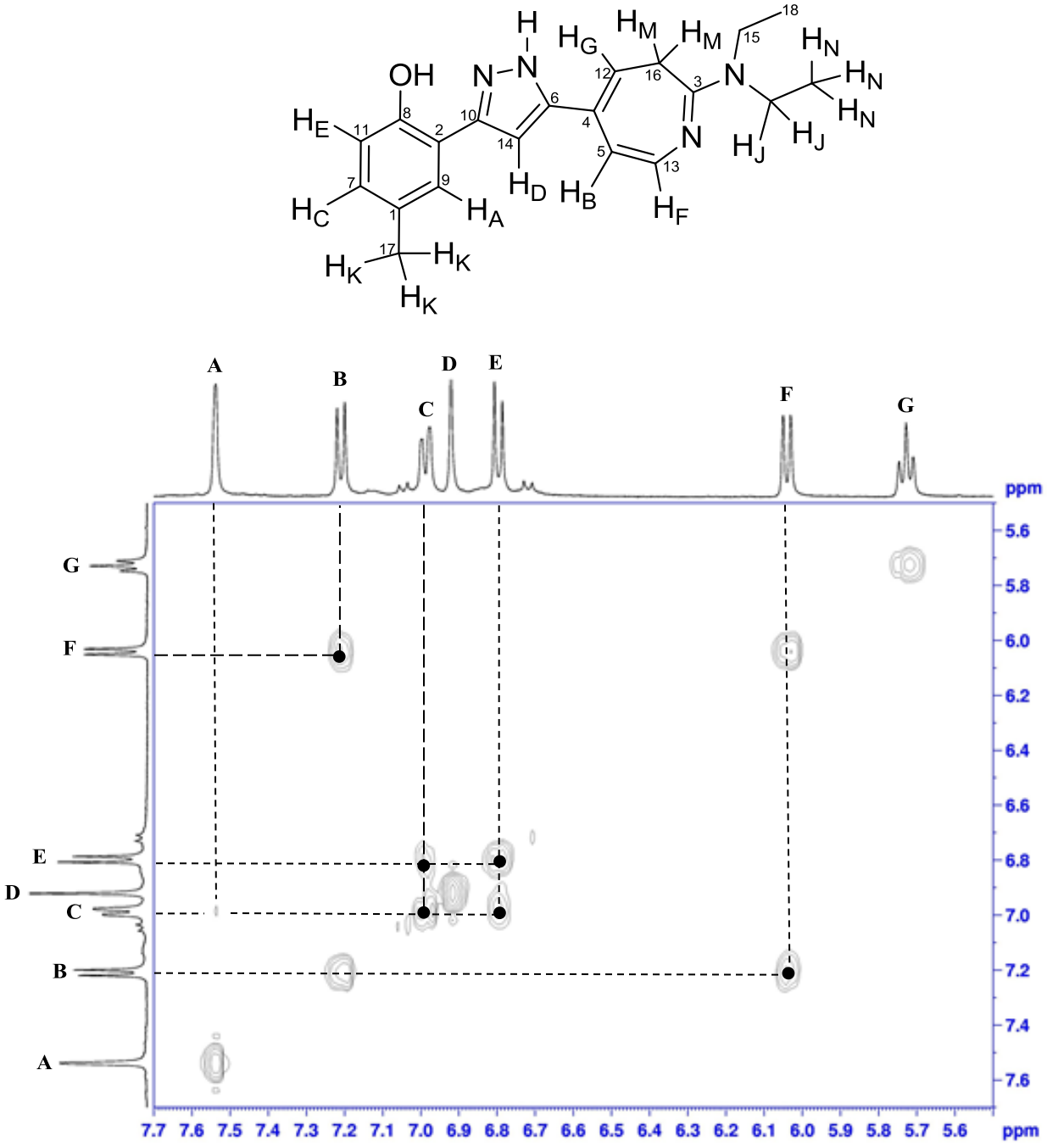


**Figure 16:** $^{1}$H,$^{1}$H-COSY-spectrum of photolysis product **13.**

By observing the 2-D COSY spectrum which displays protons coupled to one another, coupling were observed between the arbitrary labeled proton B-F, E-C,

a faint interaction between A-C and J-N, but missing interactions between G-M.

Another 2-D process that will help in the determination of the structure of the photolysis product would be the use of HSQC, which determines the correlation between $^{13}C$ atoms and directly attached protons.

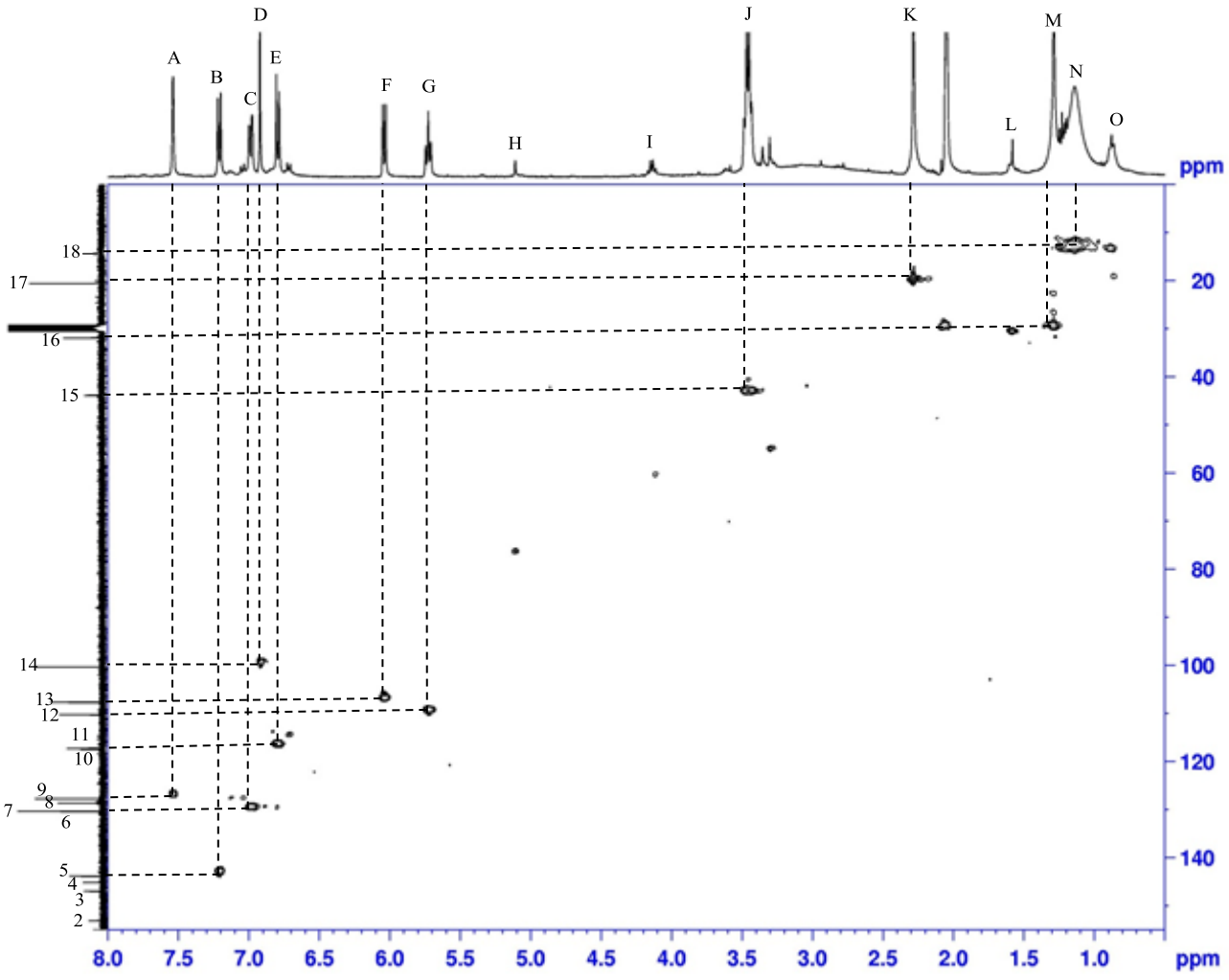


**Figure 17**: $^{1}H,^{13}C$-HSQC spectrum of the photolysis product **13.**

By observing the HSQC spectrum we notice interactions between; A-9, B-5, C-7, D-14, E-11, F-13, G-12, J-15, K-17, M-16, and N-18. Based on the results from COSY and

HSQC conclusions can be reached about certain classifications of protons and carbon atoms on the target compound **13**. The singlet proton K which integrates for 3H is a clear indication of a methyl peak, which is in association with carbon 17. The quartet resonance signal at 3.46 ppm J which integrates for 4 protons results from the two -$CH_2$ on the diethylamine adduct, therefore carbon 15 reflects this moiety. Proton N which is attributed to the two–$CH_3$ protons on the diethylamine adduct correlates to carbon 18.

The singlet at 6.92 ppm D which correlates to carbon 14 must be attributed to pyrazole proton, due to the fact that it is the only aromatic proton that can give rise to a singlet on the proposed structure.

HMBC was used to help decipher the remaining correlations between the proton and carbon signals which is useful for determining heteronuclear correlations over 2 or 3 bonds away. Carbon 1: has correlation to four protons; A, C, E, K, but no correlation on HSQC indicating that C-1 is a quaternary carbon. Protons K, which resonates from the methyl substituent C-1 must be located in the position para to the phenolic substituent. Carbon 2: shows correlation with protons; A, D, but no correlation is observed via HSQC indicating a quaternary carbon. Since proton D is attributed to the pyrazole proton C-2 must be the carbon ortho to the phenol. Carbon 7: has correlation with protons A, B, E, K, and direct interaction with proton C via HSQC, therefore the position indicated on the photolysis product is considered to be an accurate depiction. Carbon 9: has correlation with protons C, E, and K and HSQC reveals direct interaction with A, therefore the location of this carbon atom must be meta to the phenolic moeity. Carbon 8: has correlation with C, and E, and no direction interaction via HSQC indicating a quaternary carbon and the position indicated on the photolysis product is an accurate

representation. Carbon 4: has correlations with D, F, and G yet no HSQC correlation indicating a quaternary carbon. Carbon 12: shows interaction with proton F and M, and is directly bond to proton G (via HSQC).

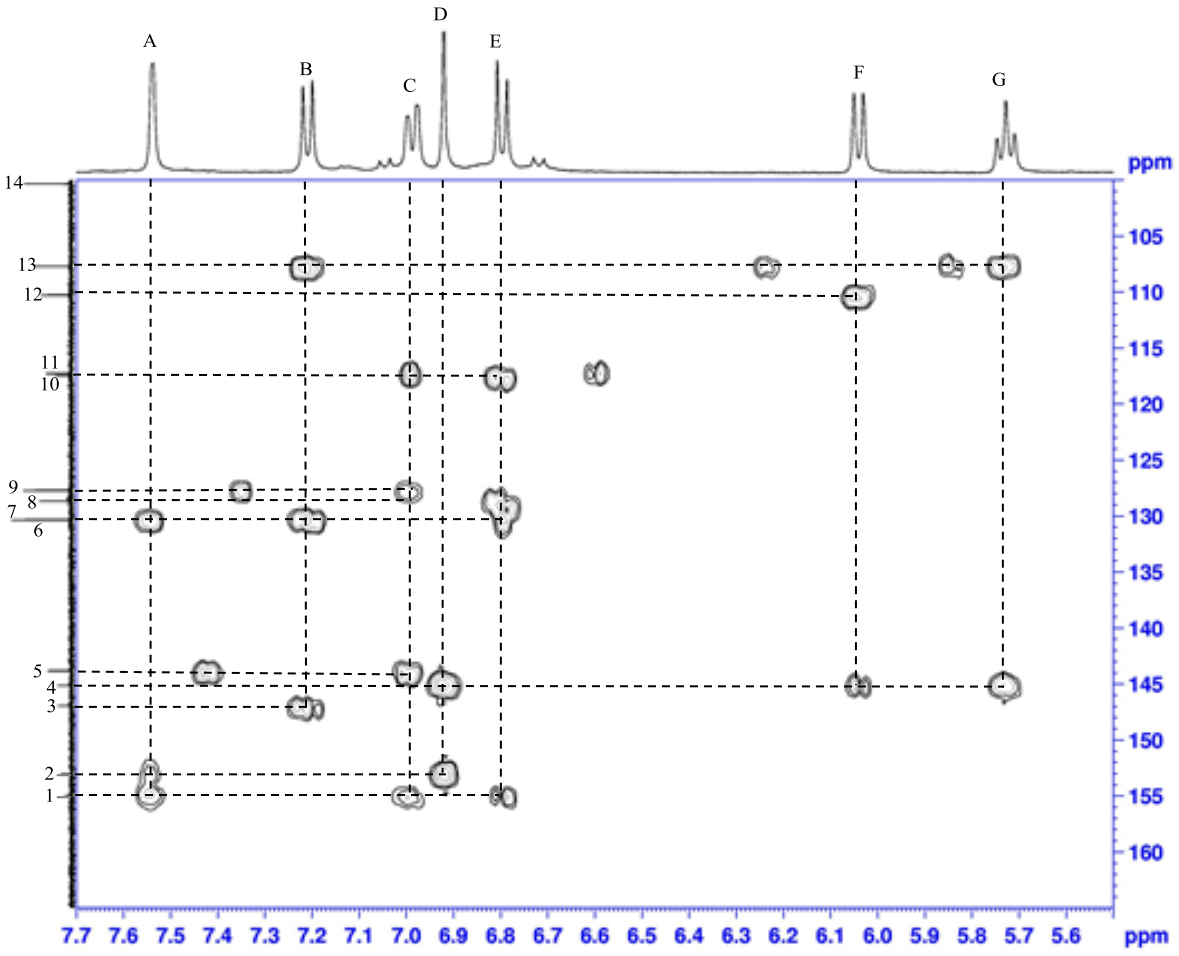


**Figure 18:** $^{1}H,^{13}C$-HMBC spectrum of the photolysis product **13.**

Therefore the position indicated in the photolysis product is an accurate indication of its true position. Carbon 16: shows direct interaction with proton M and correlation with G, therefore it must be adjacent to carbon 12, and the position in the photolysis product appears to be an accurate depiction of its position. The 2-D spectra(COSY, NMBC,

HSQC) analyzed helped in the determination of the exact configuration of the photolysis product of azide **12**.

### 2.3. Synthesis of a Fluorescent Conjugate

A fluorescent conjugate of VRT-532 would be a useful probe for biochemical experiments with CFTR. The amino group on compound **11** was envisioned to be a suitable nucleophile for reactions with fluorescent electrophiles like; 4-chloro-7-nitrobenzofurazan (NBD chloride)[40] and 5-(dimethylamino)naphthalene-1-sulfonyl chloride (dansyl chloride).[41] Unfortunately, no reaction was observed when **11** was exposed to these reagents **(Scheme 9)**.

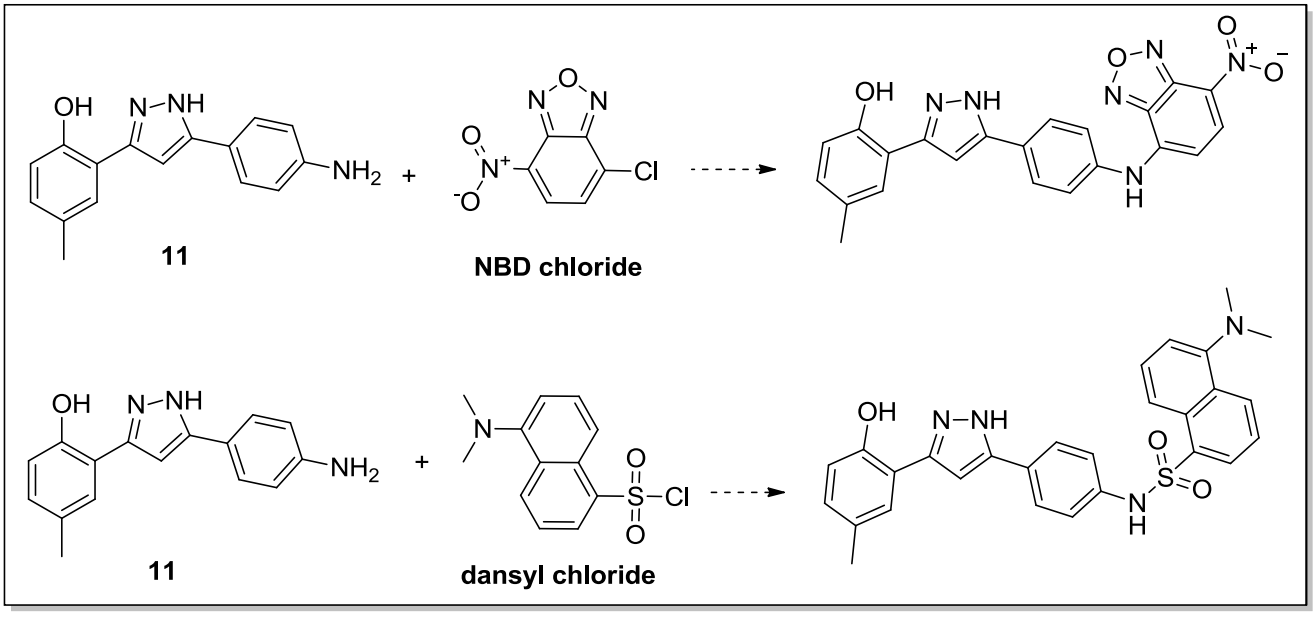


**Scheme 9:** Functionalization of amino-VRT in order to synthesize a fluorescent conjugate

Ultimately this methodology was abandoned and an approach focusing on palladium-catalyzed cross-coupling chemistry to install a fluorophore was pursued. Following a procedure by Zaccheroni *et al*., dansyl chloride **14** was reacted with propargyl amine[42] under basic condition to afford the *N*-propargyl dansyl amide **15** in a 70 % yield**.**

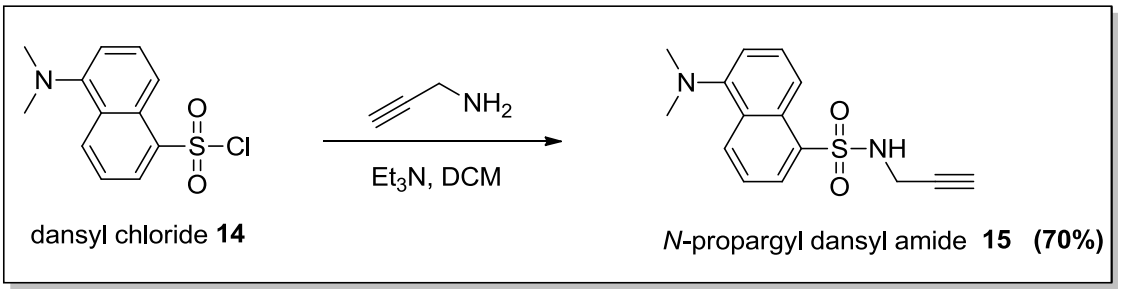


**Scheme 10:** The synthesis of *N*-propargyl amide **14**, using dansyl chloride.

Having the terminal alkyne in place from the dansyl amide, it was reacted with I-VRT under Sonogashira conditions[43] using a palladium and a copper source under inert atmosphere to produce the cross coupled fluorescent probe **16,** in a 47% yield.

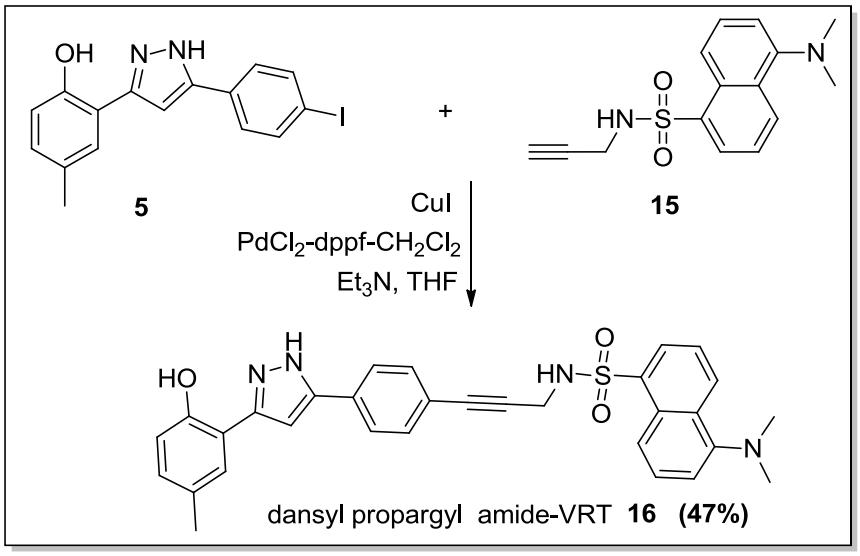


**Scheme 11:** Sonogashira cross coupling between I-VRT and dansyl amide **15.**

The fluorescent probe **16,** which contains a recognition element of **1**, is expected to be a useful probe for the binding interaction between VRT-532 and CFTR. The direct binding of the probe to CFTR and/or conformational change which mediate protein folding and function can be detected by anisotropy measurements. **Figure 19** displays the fluorescence emission spectra of **16** in various solvents. Our collaborators (Dr. Christine Bear's research group in the Programme in Molecular Structure and Function in the Research Institute at the Hospital for Sick Children) performed this experiment to show how the dansyl derivative **16** behaves in various conditions.[31]

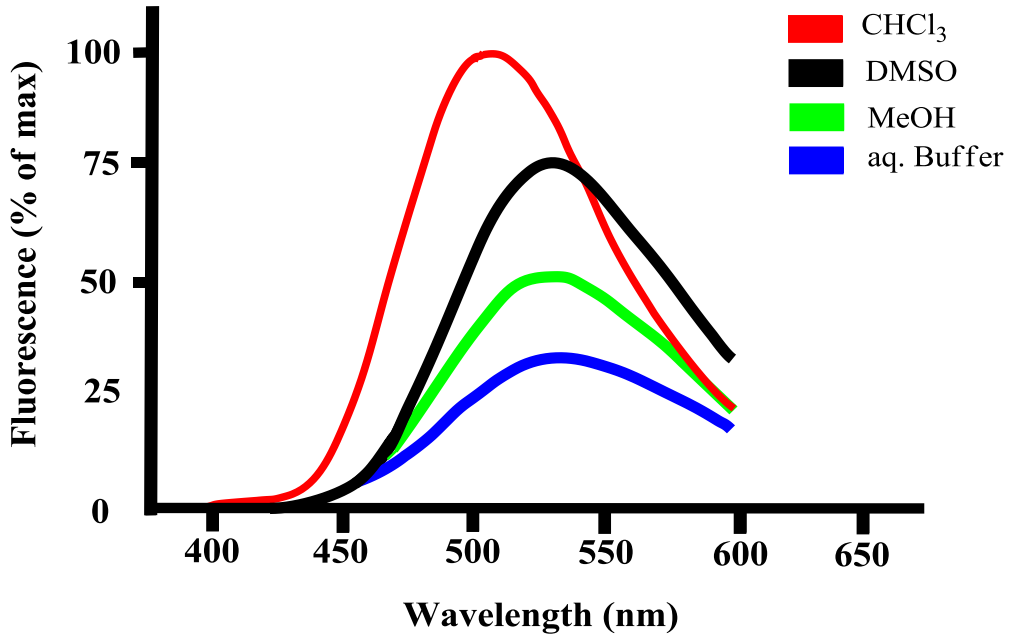


**Figure 19:** Fluorescence emission spectra of **16** in various solvents.

A stock solution of **16** (5 mM DMSO) was diluted to 20 $\mu$M in 100% chloroform, 100% methanol, 100% DMSO, or aqueous buffer solution and the emission spectra were obtained using a Quantmaster QM/80 steady state spectrofluorimeter. When dissolved in chloroform, the fluorescence emission is maximal and centered at 504 nm (red). In

the aqueous buffer solution, the most polar of the media tested, the emission maximum is red shifted by 37 nm to 541 nm with a 68% decrease in intensity relative to the emission in $CHCl_3$. By increasing the polarity of the solvent relative to that of $CHCl_3$, MeOH and DMSO showed emission maxima (529 nm for both) that were intermediate between aq. buffer and $CHCl_3$ with the intensity decreasing for increasing polarity. The experiment shows that the fluorescent probe **16** displays fluorescence specific to its environment. Therefore the fluorescence intensity or emission maxima may change upon binding to a hydrophobic pocket of CFTR, which can be monitored by fluorescence experiments. Alternatively, as the emission for the tryptophan residues in CFTR overlaps with the excitation of this dansyl derivative, there may be measurable resonance energy transfer upon binding to the protein. Lastly, it is anticipate that competition experiments with unlabeled drugs will identify other small molecules that bind directly to CFTR and permit quantification of their relative binding constants.[31]

## 2.4. Synthesis of Peptide coupling derivatives

Given the success of the Sonogashira cross-coupling reaction, another derivative was pursued. The primary amine on propargylamine was protected[44] using di-*tert*-butyl dicarbonate, to afford Boc-propargylamine **17**, in a 66% yield **(Scheme 12)**.

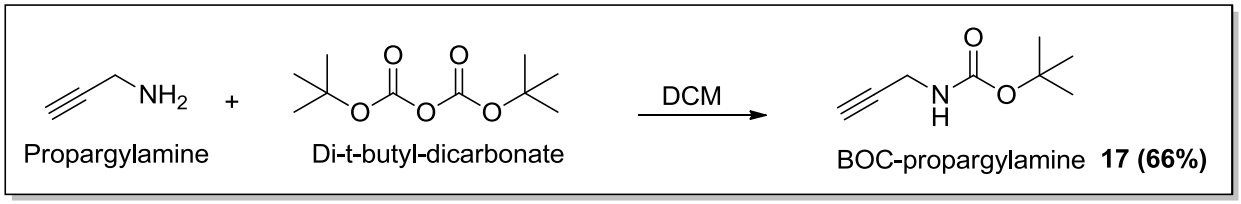


**Scheme 12:** Boc protection of propargylamine, using Di-*t*-butyl dicarbonate.

Having the terminal alkyne in place on the Boc-propargylamine allows for coupling to occur with the Iodo-VRT.[43] The cross coupled product Boc-propargylamine-VRT **18** was achieved in a 69% yield **(Scheme 13**).

Upon Boc-deprotection, compound **18** will afford a nucleophilic primary aliphatic amine, which can be readily derivatized with electrophiles.

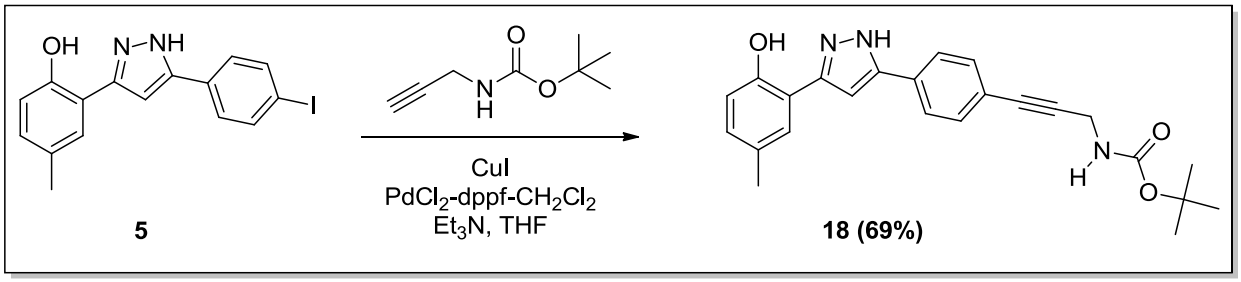


**Scheme 13:** Sonogashira cross-coupling between iodo-VRT and Boc-propargylamine.

Taking advantage of the strong nucleophilic nature of the deprotected product of **18**, derivatives involving biotin were pursued. Biotin is used in many biochemical experiments to study various processes which include; protein localization, protein interactions, DNA transcription and replication.[45] Biotin is known to form one of the strongest known protein-ligand interaction to a tetrameric protein known as avidin with a dissociation constant ($K_d$) of about $10^{-15}$ M. With avidin having such a strong affinity for biotin, this makes it useful for a wide range of biochemical assays, which include western blot, enzyme-linked immunosorbent assay (ELISA), enzyme-linked immunosorbent spot (ELISPOT), and pull-down assays or immunoprecipitation (IP).[45]

The first step towards the synthesis of a biotin derivative involves the deprotection of Boc-propargylamine-VRT **18,** using trifluoroacetic acid. The deprotection affords a

nucleophilic primary aliphatic amine which attacks the carbonyl ester attached to the succinimide moiety on biotinamidohexanoic acid 3-sulfo-*N*-hydroxysuccinimide ester sodium salt.[46] This displaces the 3-sulfo-*N*-hydroxysuccinimide and forms the new covalent bond, in hopes to form target compound **19**.

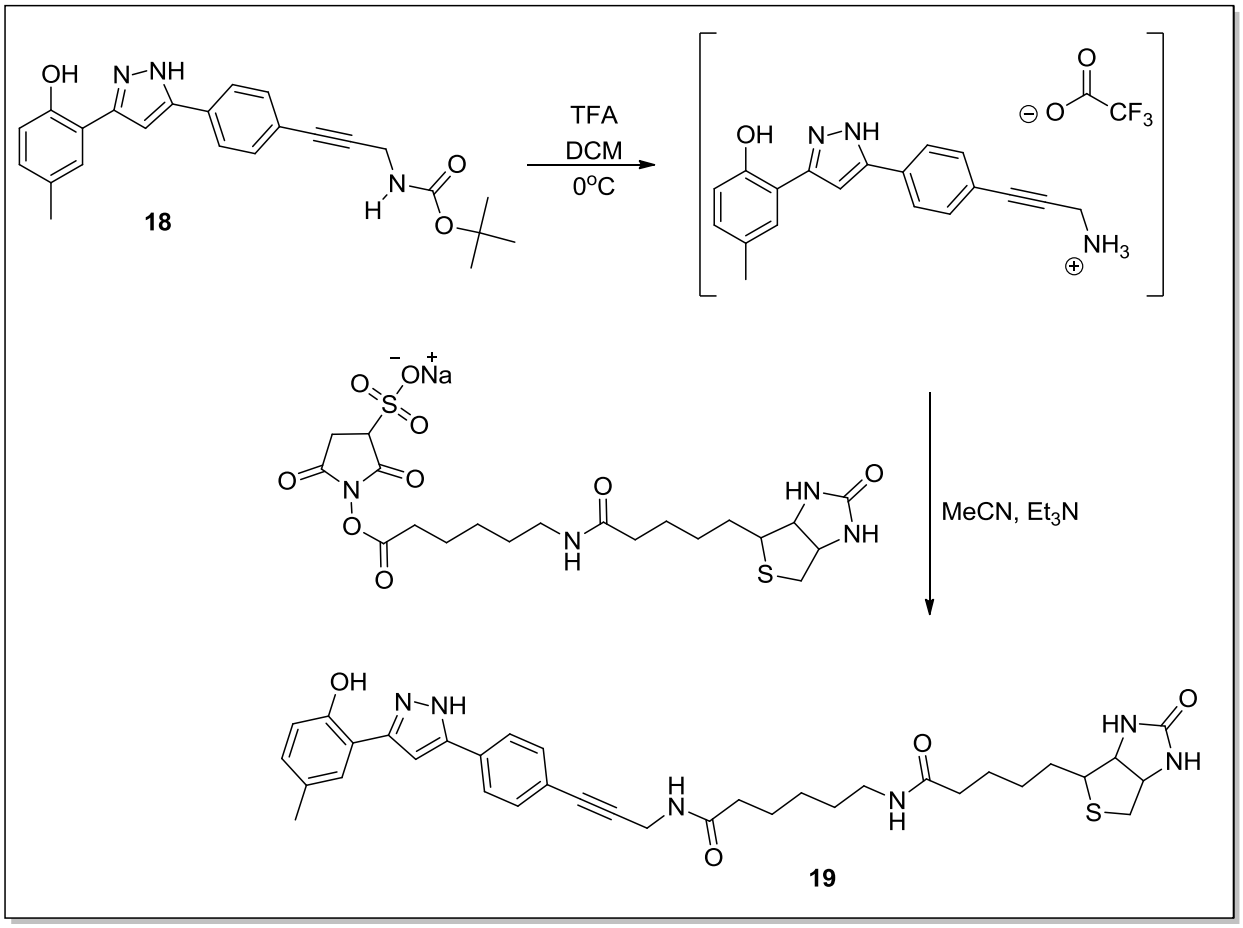


**Scheme 14:** Synthesis of a Biotin-Hex-Gly-NH- VRT-532 **19.**

Due to the limited quantity of the biotin analog this reaction was attempted on a relatively small scale using MeCN as the solvent and triethylamine as the base. Purification became problematic, and the column fractions containing product were inconclusive via $^{1}$H-NMR analysis and the product of interest was not obtained. An

alternative method or a scale up of reagents must be gauged in order to make such a derivative in an effective manner.

In an attempt to synthesize a biotin analog of VRT-532, another methodology was evaluated. Again beginning with Boc-propargylamine-VRT **18** as the starting material, the Boc functionality was deprotected using trifluoroacetic acid which generates the nucleophilic primary aliphatic amine **(Scheme 15)**.

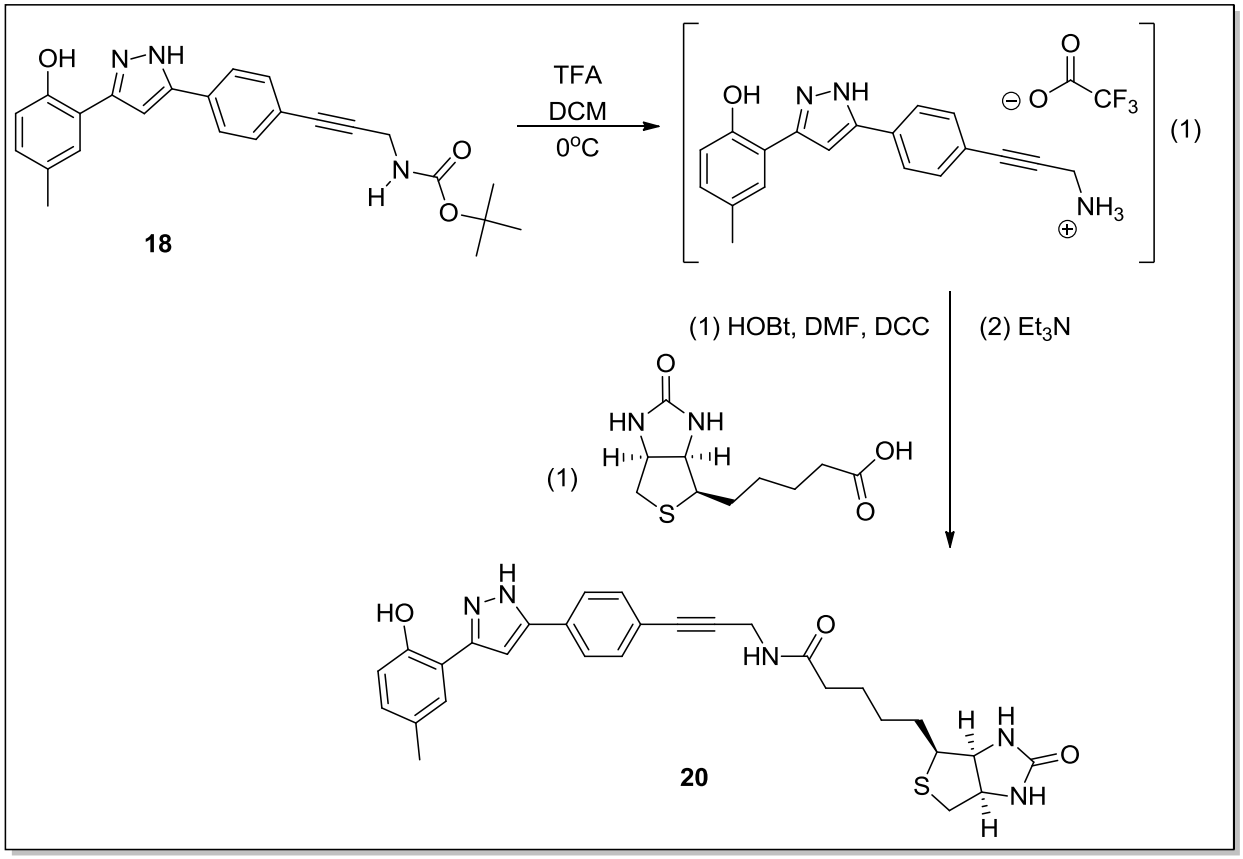


**Scheme 15:** Synthesis of a Biotin derivative of VRT **20**, using the deprotected version of **18.**

In a separate flask containing D-biotin in DCM, *N*-hydroxybenzotriazole (HOBt), and *N,N'*-dicyclohexylcarbodiimide (DCC) were also added.[47] The solution containing the

deprotected propargylamine-VRT is combined with the activated biotin solution along with triethylamine and the reaction was allowed to proceed. HOBt and DCC are two reagents commonly used in peptide synthesis which are required to form the activated ester of D-biotin. The activated ester will react with the primary amine on the deprotected version of **18** to form a new amide bond

After a work up procedure followed by column chromatography analysis of the product via $^{1}$H-NMR spectroscopy indicated the desired coupled product was not obtained. Having limited material of both the biotin reagent and the Boc-propargylamine-VRT compound this reaction was not revisited in order to obtain the desired product **20.**

### 2.5. Synthesis of a radiolabeled derivative

Another useful tool for studying the interaction between VRT-532 **1** and mutant CFTR would be the use of radiolabeling. Binding of CFTR modulators have been detected using functional assays which give results based on the consequence of binding rather than the actual binding, thereby the use of a radiolabel derivative would be a beneficial biochemical tool for quantitative studies of binding properties. The radiolabeled derivative would provide insight into potential genotype-specific structural differences[48] in the binding site. The concept involves the use of a radioligand which is a radioisotope-labeled substance used in the quantitative measurement of an unlabelled substance by its binding reaction to a specific antibody or other receptor site.[48] Radioligands have shown to be an influential tool for understanding the mechanism of action of membrane proteins, receptors, transporters, and channels.[49]

For the development of a radiolabeled version of **1**, the ultimate goal would be to replace as many non-readily exchangeable hydrogen atoms in place for a radioactive isotope of hydrogen, tritium ($^3$H, or T). An ideal methodology would use readily available tritiated water as a $^3$H-source, and would be operationally simple with minimal purification, so that it can be carried out by biochemist collaborators who are qualified and equipped to handle radioisotopes, but with no training in synthetic organic chemistry. As a model for this study, the incorporation of a less expensive, more safely handled and nonradioactive deuterium ($^2$H, D) was used.

A small sample of VRT-532 (25 mg) was dissolved in 1 mL of 1M NaOH in $D_2O$ and heated to 90°C for a 48 hr period and the progress of the reaction was monitored by $^1$H-NMR **(Scheme 16)**.

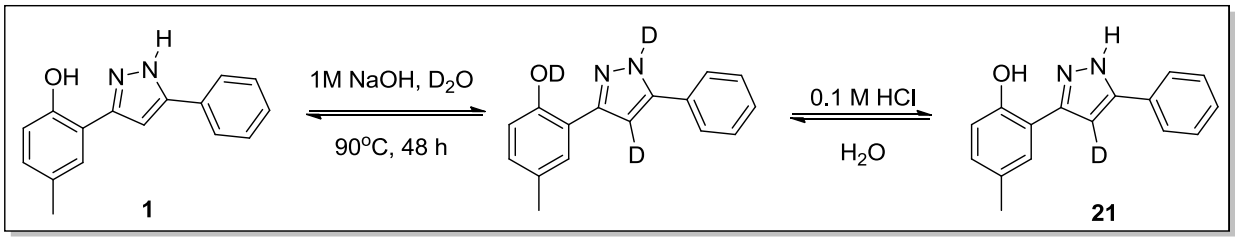


**Scheme 16:** Experimental conditions for hydrogen/deuterium exchange.

The $^1$H-NMR of VRT-532 was taken prior to, during and after the experiment for comparison purposes. As expected, the phenolic O-H, and the pyrazole N-H readily exchange in solution with deuterium. It was also observed that the proton on the C4 position on the pyrazole ring also underwent deuterium exchange **(Figure 19)**. The singlet at 6.7 ppm is attributed to the proton on the pyrazole C4-H **(Figure 19, A)** which integrates for a single proton. After 48 hr **(Figure 19, B)** the singlet at 6.7 ppm was

decreased to ~20% of its original integration. The reaction was then followed by an aqueous extraction involving 0.1 M HCl solution to re-exchange the phenolic O−H and the pyrazole N−H for protons. After TLC purification, **1** was re-isolated in an 88% yield and determined to have ~80% deuterium incorporation at the C4 position on the pyrazole.

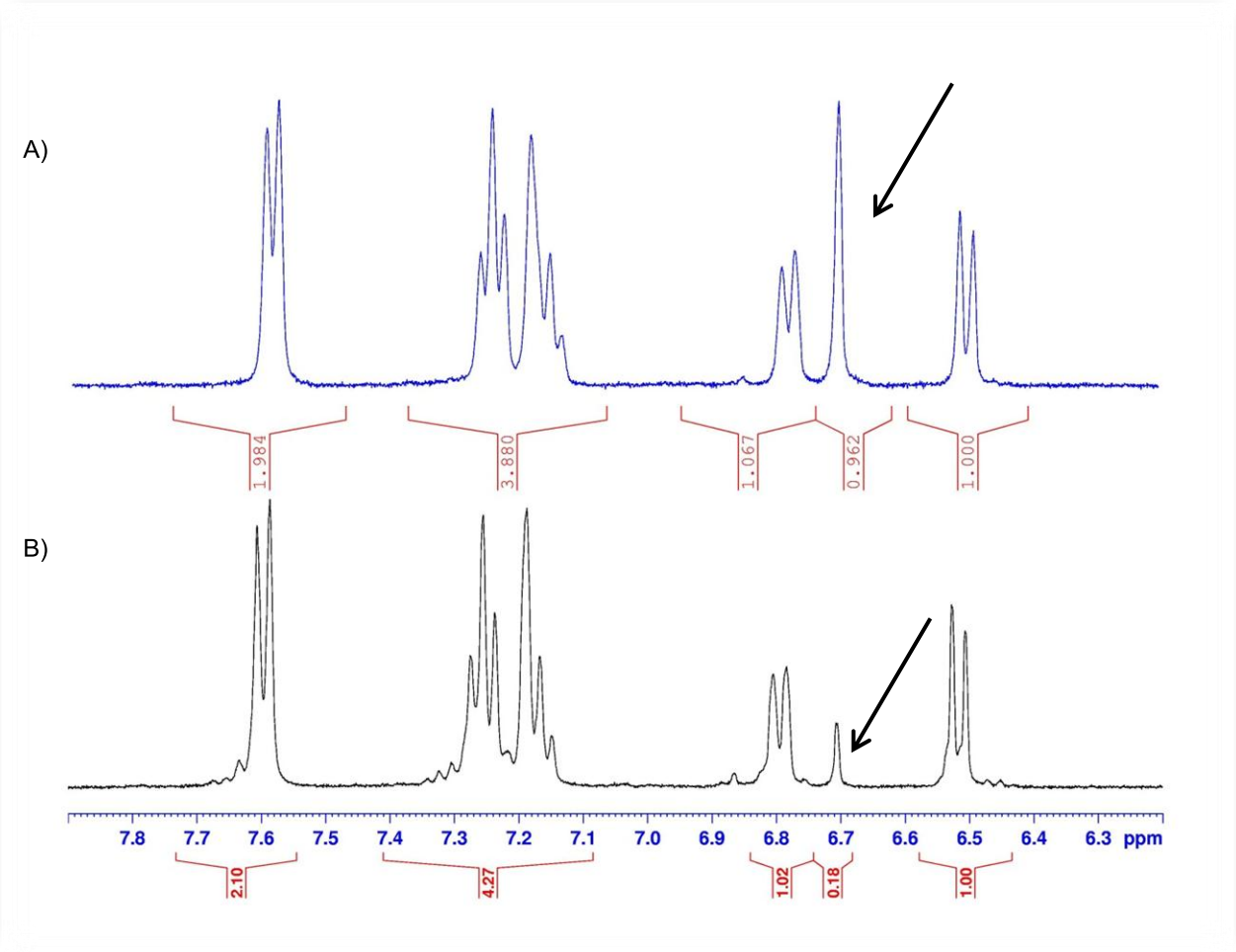


**Figure 20:** A) $^{1}$H-NMR spectra of VRT-532 at t=0 hrs. B) VRT-532 after 48 hrs of heating in 1 mL of 1 M NaOH in $D_2O$.

Given the fact that this methodology was only able to incorporate 80% deuterium inclusion into the parent compound with a high abundance of deuterium atoms in $D_2O$,

repeating this with lower abundance of tritium in tritiated water ($T_2O$) would not be effective. Along with the low inclusion of deuterium atoms, this methodology utilizes harsh conditions such as prolonged heat, long reaction times, acidic extractions and the need for purification therefore making this methodology unviable process for convenient incorporation of useful amounts of tritium

For the development of a radiolabeled derivative of VRT-532, the methodology must be an effective, which involves limited to no extractions or purification and must be a time effective process. Upon completion of a working model that can effectively incorporate a non-radiolabeled deuterium atom, we can share this methodology with our collaborators, to perform this experiment using radiolabeled tritium atoms in hopes for a radiolabeled version of **1**.

Towards the synthesis of a radiolabeled derivative of **1**, the concept of protodesilylation is an area that was pursued. The concept involves a substitution reaction between a silyl groups being replaced by a hydrogen atom. In an attempt to incorporate silyl groups onto the Iodo-VRT **5** a literature procedure by Fathabad *et. al* was followed in which iodo-VRT was dissolved in MeCN, followed by the addition of 1,1,1,3,3,3-hexamethyldisilazane (HMDS).[50] The reaction then proceeds by the addition of ammonium molybdate(VI) tetrahydrate acting as the catalyst. The mixture was stirred at room temperature and the progression of the reaction was monitored by TLC **(Scheme 17)**.

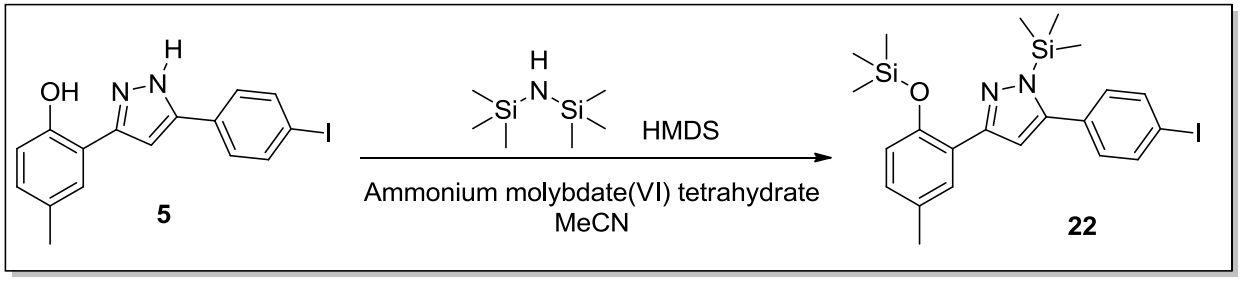


**Scheme 17**: Silylation of I-VRT using HMDS and ammonium molybdate(VI) tetrahydrate.

After 1 hr a new product was observed by TLC indicating the formation of a new species. To drive the reaction to completion, 0.4 mL of HMDS and 3 mg of the catalyst was added. Upon consumption of the starting material, the reaction was filtered to remove any insoluble catalyst, the remaining solution was evaporated and a crude NMR was taken. The characteristic singlets for the trimethylsilyl (TMS) groups were not observed, indicating no inclusion of TMS groups onto the iodo-VRT, therefore an unsuccessful reaction.

In another attempt at this type of reaction, iodo-VRT was dissolved in DCM along with HMDS and stirred at room temperature. This was followed by the addition of tetrabutylammonium tribromide **(Scheme 18)**[51] and continued to stir at room temperature.[52] The progress of the reaction was monitored by TLC for the appearance of a new species.

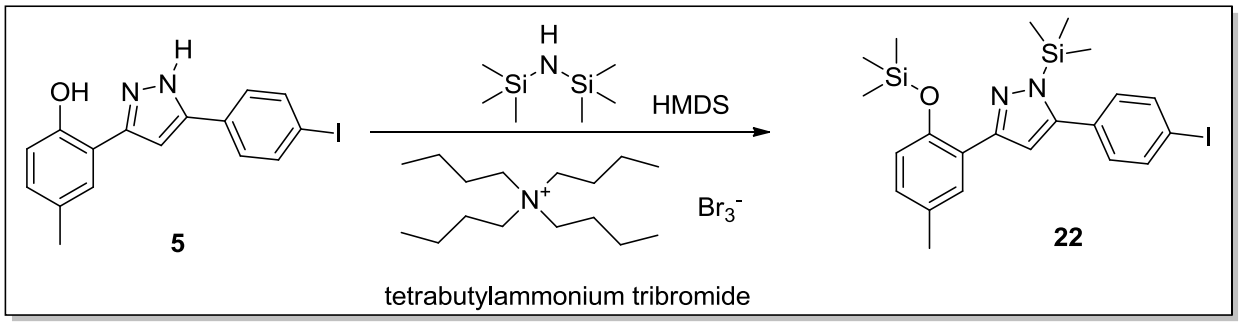


**Scheme 18**: Silylation of I-VRT using HMDS and tetrabutylammonium tribromide.

After a few hours, TLC indicated that no reaction had occurred, so the reaction vessel was heated overnight. After doing so the solution turned black but still no indication of a new species via TLC. There is the possibility of the expected product having the same retention factor, a problem that has plagued previous reactions. The solution was filtered and evaporated and crude $^{1}$H-NMR of the product was taken which indicated no appearance of the expected TMS peaks.

This synthetic process was abandoned and a new route was taken in order to synthesize a radiolabeled derivative. Sticking with the concept of protodesilylation, the intention was to synthesize a VRT analog with multiple carbon-silicon bonds present on the molecule. The more carbon-silicon bonds present only increases the probability of protodesilylation occurring with non-labeled deuterium atoms and eventually tritium atoms. The synthesis of such a “radiolabeled kit molecule” would entail synthesizing a VRT derivative with multiple halogens present to allow for silylation to occur.

Following a procedure that has been utilized in the synthesis of varying VRT derivatives, our sights were set on synthesizing a new derivative with multiple halogens present on

the parent compound. 3'-Bromo-2'-hydroxy-5'-methylphenylethanone **23**, which was previously synthesized in the Viirre research lab, was added to an ice cooled suspension of 4-iodobenzoyl chloride in pyridine and stirred for two hours. The resulting solution was quenched by pouring into an ice/HCl mixture and extracting with DCM, and the resulting organic phase was also extracted using aqueous 1 M HCl, $NaHCO_3$, and NaCl, followed by column chromatography in order to afford the iodo-bromo ester **24**.

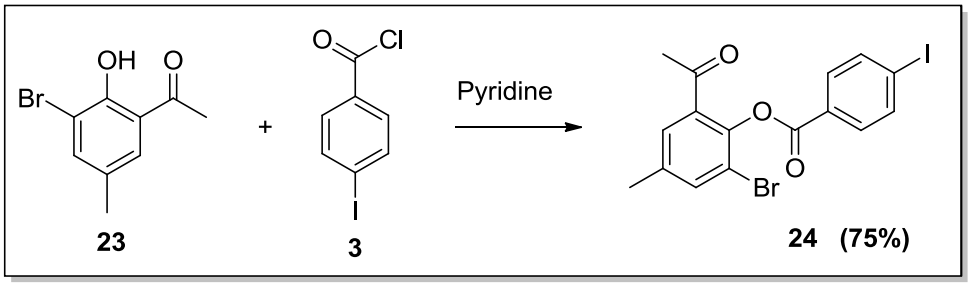


**Scheme 19:** The synthesis of I,Br-Ester.

The ester **24** is then subjected to a Baker-Venkataraman rearrangement using *t*-BuOK in THF and heating the solution to 50°C for 4 hr. Additional *t*-BuOK was required to ensure consumption of the starting material. The reaction mixture was cooled to 0°C to allow the addition of acetic acid (10% v/v) and extracted multiple times with DCM, dried and evaporated. The resulting solid material was taken up in glacial acetic acid and cooled in an ice bath, followed by the slow addition of hydrazine. The reaction mixture was heated to 65°C for 16 hrs and the expected product **25** with two halogens present was isolated in a 31% yield **(Scheme 20)**.

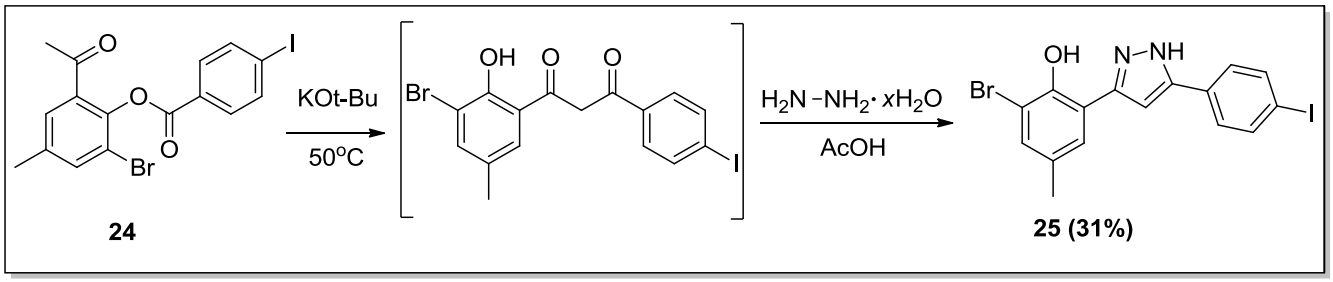


**Scheme 20**: Synthetic route towards the formation of I,Br-VRT.

Having the two halogens present on the VRT derivative allows for the eventual inclusion of TMS groups. The first step towards doing so is protecting the phenolic O-H and the N-H on the pyrazole ring, mainly because their acidities would be expected to interfere with the lithium-halogen exchange reaction. Once the O,N are protected, lithium halogen exchange can take place, followed by silylation to form the carbon-silicon bond. The next step encompasses the deprotection of O and N atoms without interfering with the C-Si bond, if successful in making target compound **26,** protodesilylation using fluoride and $D_2O$ can be done to form target compound **27** with deuterium atom taking place of the C-Si bond. Once the "Radiolabeled Kit Molecule" has been synthesized and the reaction for protodesilylation has been optimized, compound **26** can then be sent to our collaborators at the Hospital for Sick Children, along with a set of instructions for optimal protodesilylation. The radiolabeled derivative can be synthesized, which they carry out the reaction with tritiated water.

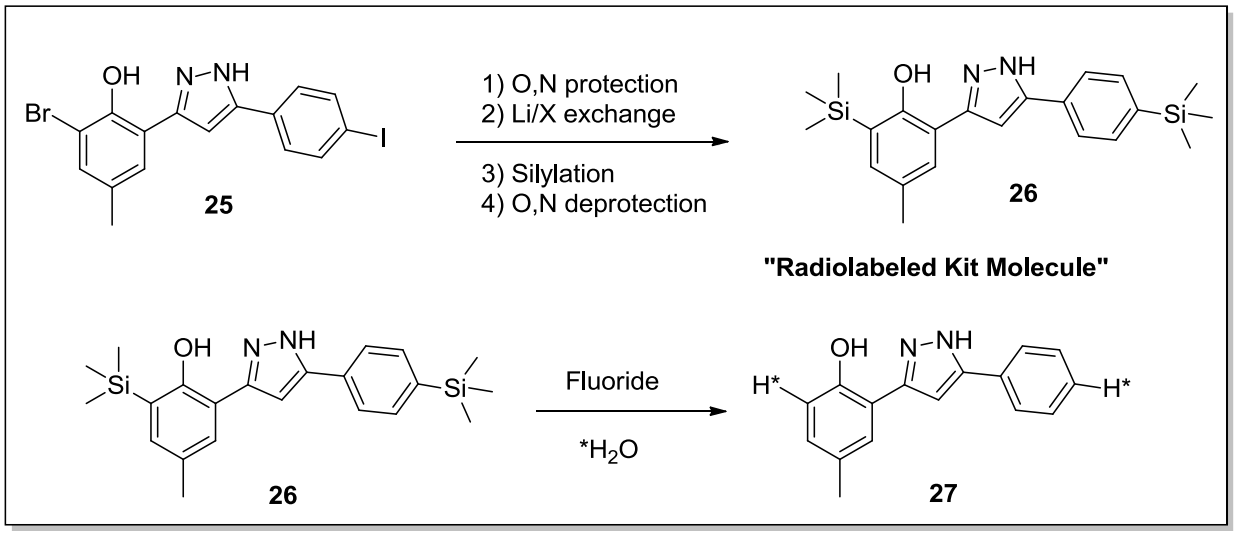


**Scheme 21**: Synthesis of the Radiolabeled Kit Molecule for protodesilylation.

To protect the functionalities of the O and N, the *p*-methoxybenzyl group was chosen as the protecting group. The protection reaction was first attempted on the iodo-VRT derivative owing to the limited availability of the I,Br-VRT analog **25**. Iodo-VRT **5**, was first dissolved in DMF at 0°C, followed by the addition of NaH to allow for deprotonation of the phenolic O-H and pyrazole N-H. A solution of 4-methoxybenzyl-chloride in DMF[53] was then added dropwise over a 30 min period. The reaction proceeded at room temperature for 16 hrs **(Scheme 21)**.

The reaction mixture was extracted followed by column chromatography to afford the bis-PMB protected iodo-VRT **29** in a 33% yield. Since the amount of PMB protected iodo-VRT derivative was limited it was decided to implement a test model system in order to optimize the conditions of lithium-halogen exchange, silylation and eventually protodesilylation prior to working on VRT derivatives.

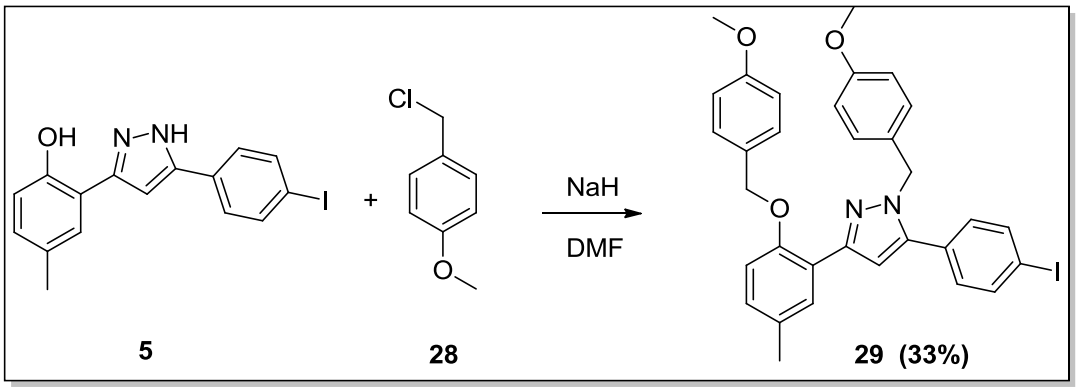


**Scheme 22:** Synthesis of PMB protected Iodo-VRT.

The test model; 1-bromo-2-naphthol **30** was chosen mainly because of the aryl halide present along with the phenolic alcohol; these are both functional groups present on the VRT analog therefore this appears to be a suitable system. The first reaction involves the protection of the alcohol functionality, where 1-bromo-2-napthol **30** was dissolved in DMF at 0°C, followed by the slow addition of NaH. PMB-Cl in DMF was added dropwise over a 30 min period at 0°C and stirred for 16 hrs at room temperature.[53] The PMB protected bromo-naphthalene **31** was obtained in a 75% yield as a white crystalline solid **(Scheme 23)**.

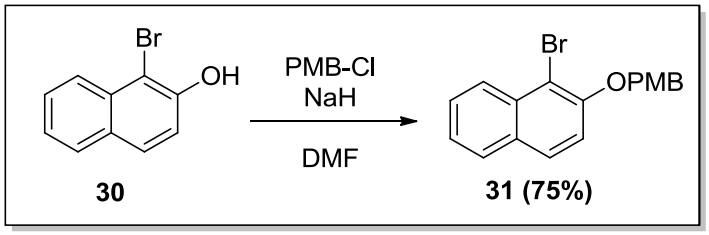


**Scheme 23:** PMB protection of 1-bromo-2-napthol.

Having the PMB protected bromo-naphthalene in place the next step involves the lithium-halogen exchange and silylation of the compound. A literature procedure by Katz *et. al.* which entailed dissolving PMB-naphthalene in THF, followed by the addition of trimethylsilyl chloride at -78°C. This was followed by the slow addition of *n*-BuLi over a 30 min period **(Scheme 24)**. The reaction mixture was warmed to room temperature for and hr, taken up in hexanes and extracted with saturated sodium bicarbonate and the solvent was evaporated.[54] Crude $^{1}$H-NMR ($CDCl_3$) revealed the desired singlet integrating for 9 protons which corresponds to the TMS protons.

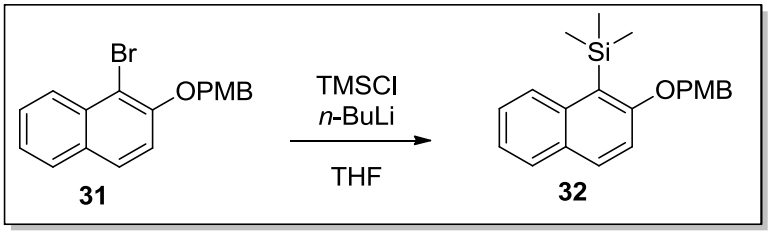


**Scheme 24:** Silylation of PMB protected bromo-naphthalene using TMS-Cl.

The crude material was then purified via column chromatography, and the resulting fractions indicated by $^{1}$H-NMR the disappearance of the TMS peaks. This suggests that the reaction was either decomposing or simply not reacting according to plan. The same reaction was repeated on a larger scale, and the same result was achieved. Another route was followed in order to synthesize the silylated product **32**. Following a procedure of Wataru *et. al.*, the moisture and oxygen sensitive manipulation were performed in the glove-box, in which PMB-naphthalene **31** was mixed along with ethoxytrimethylsilane[55] and solid magnesium, anhydrous THF was added and the solution heated to reflux **(Scheme 25)**.

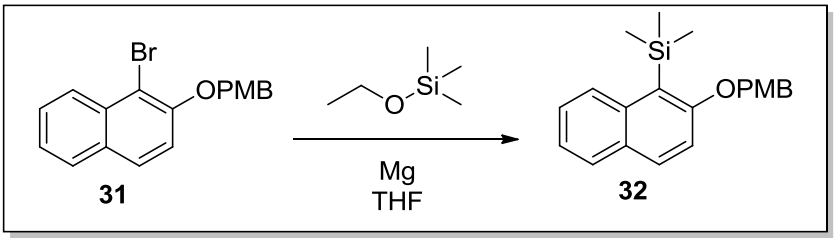


**Scheme 25:** Silylation of PMB protected bromo-naphthalene using ethoxytrimethylsilane.

After 16 hrs the TLC indicated no appearance of a new species, therefore heating was continued for an additional 16 hrs and no difference was observed by TLC. The crude $^{1}$H-NMR indicated only the presence of starting material and that no reaction had taken place. This reaction was attempted yet again, and the outcome remained the same. Work is currently needed to progress this methodology for incorporating a radiolabeled substituent into the VRT core, but due to time constraints along with the viability of the model system this area of research has been postponed.

## 2.6. Synthesis of a Stationary Phase for Affinity Chromatography

A useful tool to help reveal the nature of the interaction between the parent compound **1** and mutant CFTR would be a stationary phase to be used for affinity chromatography. The theory behind this process involves synthesizing a stationary phase comprised of three features; a solid support resin (agarose beads), iodo-VRT, and a linker or tether molecule which joins the resin and the VRT compound. Upon completion of the stationary phase our collaborators will perform affinity chromatography with fragments of mutated CFTR protein. The idea is to identify fragments of the protein that have a

strong affinity for the VRT core, in hopes to locate the specific binding of VRT to the mutated protein.

Tetraethylene glycol (TEG) was chosen as the linker between the resin and the VRT compound mainly because TEG has the alcohol functionality at either end which can be functionalized, also a long enough spacer between the two to deter any sort of interaction between the polymeric bead and the recognition element (VRT-532).

To begin, TEG **33** was dissolved in THF at 0°C followed by the addition of a slight excess of NaH to allow the deprotonation of a single terminal alcohol to take place. A solution of propargyl bromide[56] in THF was added dropwise over a 20 min period at 0°C. The reaction was run at room temperature for 16 hrs, after which the reaction mixture was filtered, evaporated and purified. After purification, the desired mono-alkyne **34**, is isolated in a 24% yield **(Scheme 26)**. The major product of this reaction is the di-alkyne species **35**, which was isolated in 53% yield. Both **34** and **35** are useful compounds. The reason for such a high yield for the di-alkyne as opposed to the mono results from the difficulty to control alkylation only at one end of the TEG.

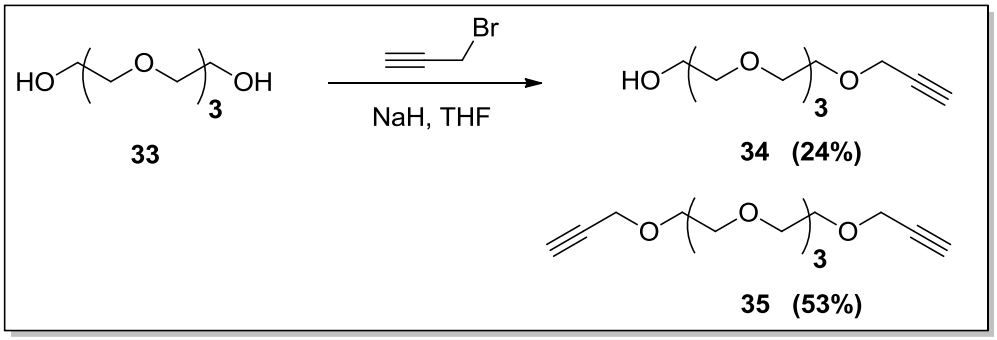


**Scheme 26:** Synthesis of mono-alkyne derivative of TEG.

This reaction was run multiple times with varying solvents and the yields ranged from 9-24% for the desired mono-alkyne product. This reaction resulted in poor yields along with problematic purification processes, but nonetheless enough material was generated to carry on to the next step. The reason behind introducing a terminal alkyne into the TEG moiety is to allow for the coupling between the linker compound and the iodo-VRT under Sonogashira conditions.

Having the mono-alkyne **34** in place allows for the addition of a desired ester at the terminal alcohol, which is required in order to attach the solid support resin to the linker molecule. TEG propargyl ether **34** was taken up in THF at 0°C and NaH was added. This was followed by the slow addition of ethyl bromoacetate[57] in THF for a 1hr period, the reaction vessel was then stirred at room temperature for overnight. The crude material was purified by column chromatography, and confirmation by $^{1}H$ and $^{13}C$-NMR revealed a high purity of ester derivative of the mono-alkyne **36**, which was isolated in a 30% yield **(Scheme 27)**.

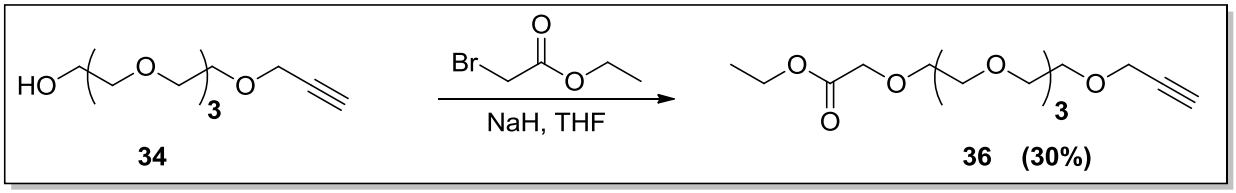


**Scheme 27:** Synthesis of ethylacetate ester of mono-alkyne **34.**

The reaction was also repeated using cesium carbonate as the base in acetonitrile; the yield achieved was consistent with the previous methodology (27%). For this reaction using various conditions the yield ranged from 5-30%.[57, 58, 59]

Having synthesized compound **36**, a coupling reaction with Iodo-VRT was attempted. Under inert atmosphere Iodo-VRT, TEG derivative **36**, along with catalysts; [1,1′-Bis(diphenylphosphino)ferrocene]dichloropalladium(II), complex with dichloromethane and CuI, were mixed under basic conditions and heated to 50°C under Sonogashira conditions **(Scheme 28)**. After 20 hrs of reaction time, TLC showed the appearance of new species. The reaction mixture was taken up in ethyl acetate and extracted with 0.1M HCl, the organic layer was then extracted with saturated NaCl, then dried over $Mg_2SO_4$.

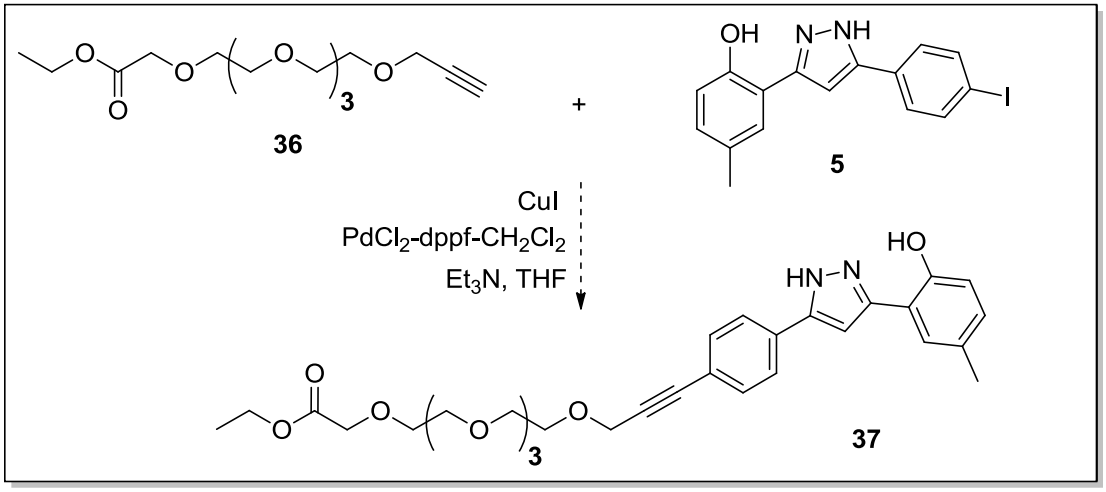


**Scheme 28**: Sonogashira coupling between Iodo-VRT and TEG derivative **36**.

After column chromatography, the fractions that were collected did not appear to have the desired compound present. Due to the water solubility of these TEG mioeties, it was hypothesized that the compound of interest was lost during extractions; therefore precautions must be taken in avoiding aqueous work up. Having the di-alkyne in place another route was taken in order to synthesize the linker moiety. Di-alkyne **35**, under basic conditions in acetonitrile was reacted with ethyl bromoacetate with the intention of

synthesizing **38 (Scheme 29)**. Many species were observed by TLC and purification became challenging. Multiple attempts at purification lead to constant co-elution of species, working on such a small scale further purification became non-viable; therefore this methodology was abandoned.

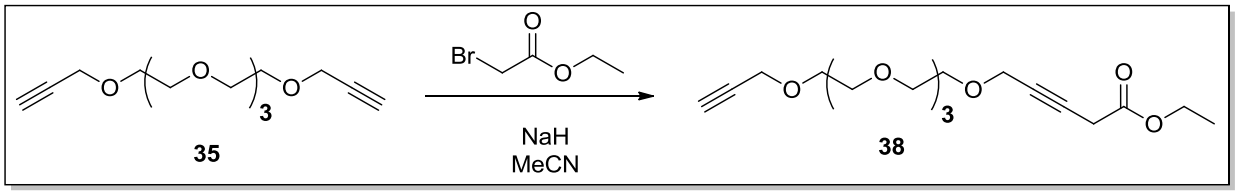


**Scheme 29**: Addition of ethyl bromoacetate to dI-propargyl-TEG.

Another route that was taken involved using the Sonogashira method which was been particularly success in previous occurrences. Potassium carbonate ($K_2CO_3$)[60] which is used to remove the acidic proton from *p*-iodobenzoic acid was used along with iodoethane which is an excellent substrate to promote the $S_N2$ substitution reaction for the ethylation process. The desired ester **40** was achieved in a 73% yield **(Scheme 30)**.

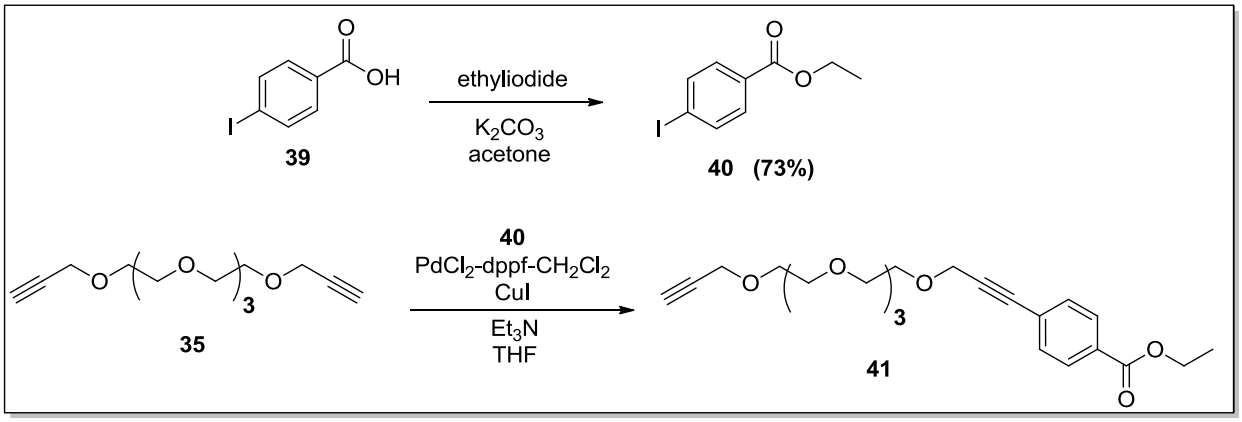


**Scheme 30**: Cross-coupling of ethyl 4-iodobenzoate with di-propargyl-TEG.

A coupling reaction was attempted using the di-alkyne **35,** along with ethyl 4-iodobenzoate **40** under Sonogashira conditions in hopes to isolate the coupled product **41 (Scheme 30).** The resulting reaction mixture was filtered through celite in order to remove any insoluble byproducts evaporated under reduced pressure and purified by column chromatography. The results obtained by $^{1}$H-NMR were inconclusive, further identification of the isolated materials was not pursued.

It was hypothesized that if the TEG moiety had enhanced leaving functional group functionality that the efficiency of these reactions would be greatly improved. Following a procedure by Bacaro *et. at*. TEG was dissolved in $CHCl_3$ and placed in a -20°C NaCl ice bath. Pyridine was then added followed by *p*-toluenesulfonyl chloride the reaction was stirred at -20°C for 5 hrs[61] **(Scheme 31)**. The $CHCl_3$ was then evaporated off and the reaction mixture placed in ice water and the aqueous phase was extracted three times with DCM. The organic phase was then extracted once each with; 1M HCl, sat. $NaHCO_3$ and finally water. After purification the mono-tosylated TEG was isolated in a 28% yield and the di-tosylated-TEG in 20% yield, the remaining product was unreacted starting material. Both the di-and mono-tosylated products **42** and **43** are useful target compounds.

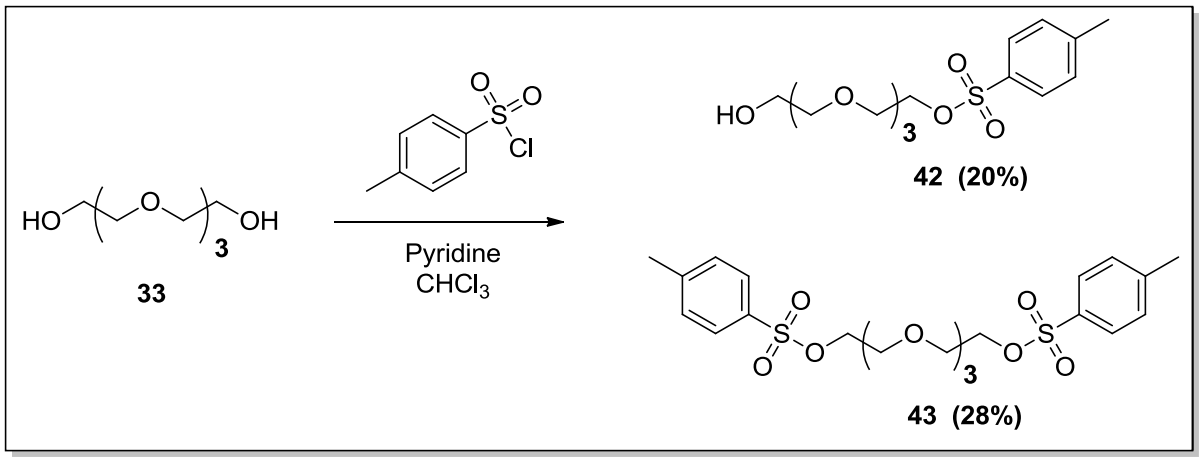


**Scheme 31:** Synthesis of tosylated TEG derivatives **42** and **43.**

Towards the synthesis of tosylated esters of TEG another methodology was attempted. TEG was taken up in THF, followed by the addition of aqueous NaOH at 0°C.[62] The desired mono-tosylated TEG derivative was isolated in a 60% yield, which proved to be a more effective process.

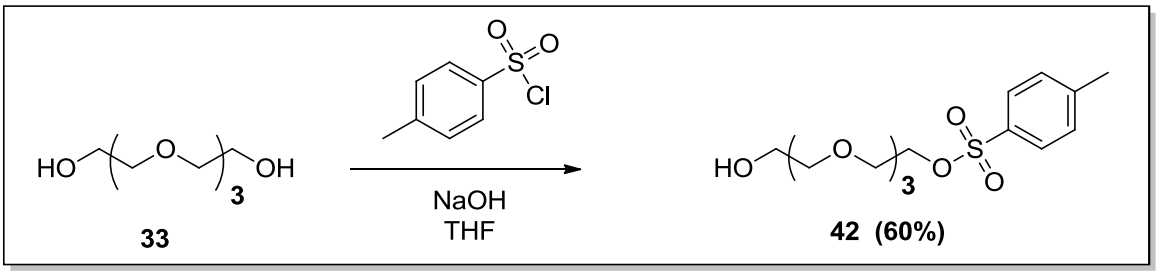


**Scheme 32:** Improved synthesis of tosylated TEG derivatives 42.

The mono-tosylated TEG derivative **42** was dissolved in acetonitrile; $K_2CO_3$ and ethyl-4-hydroxy benzoate were added and stirred at room temperature. A substitution reaction occurs to form the desired ether. After purification, ether **44** was formed in a 74% yield.

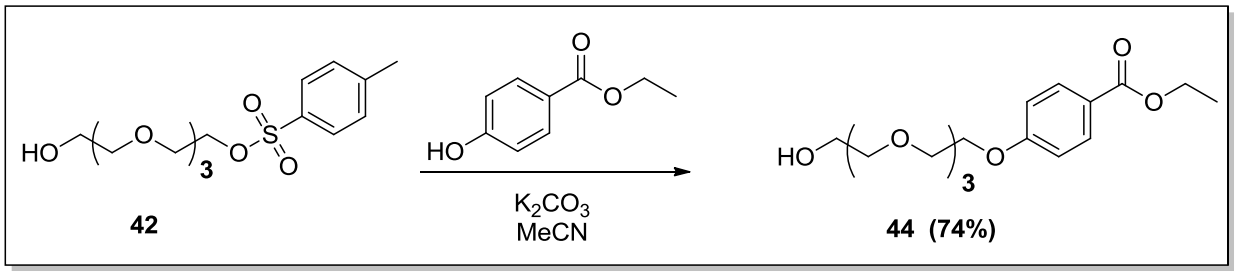


**Scheme 33**: Synthesis of the benzoate derivative of TEG **44**.

Making use of the di-tosylate **43**, under basic conditions propargyl alcohol was added in an equimolar ratio to **43**, with the intention of isolating a terminal alkyne at one end, and maintaining the tosylate functionality at the other **(Scheme 34)**. The intended product was isolated but in a 2% yield, the amount of material generated was not sufficient to proceed onward. The major product isolated was the di-alkyne **35**, in a 41% yield.

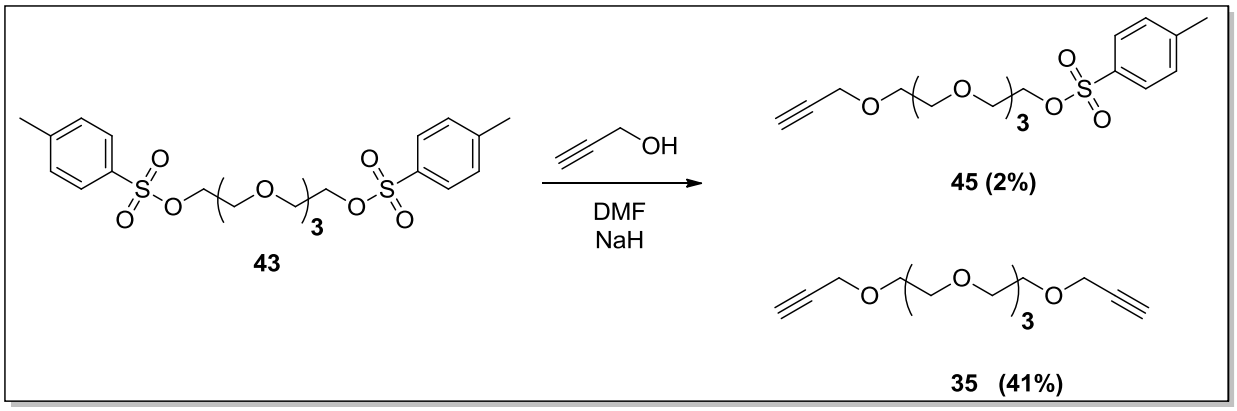


**Scheme 34**: Intended synthesis of propargyl- tosylated-TEG derivative **45.**

Since the previous methodology for incorporating a terminal alkyne was ineffective an alternate route was pursued. Utilizing the good leaving group ability of the tosylate esters, propargyl alcohol was reacted with *p*-toluenesulfonyl chloride, which generated the propargyl tosylate moiety **46**, in a 66% yield **(Scheme 35)**. With the benzoate ester

derivative of TEG **44** previously synthesized and having generated the tosylated propargyl the two were reacted under basic conditions **(Scheme 35)**[63] and the TEG derivative with a terminal alkyne and the benzoate ester at the other end was generated in a 63% yield.

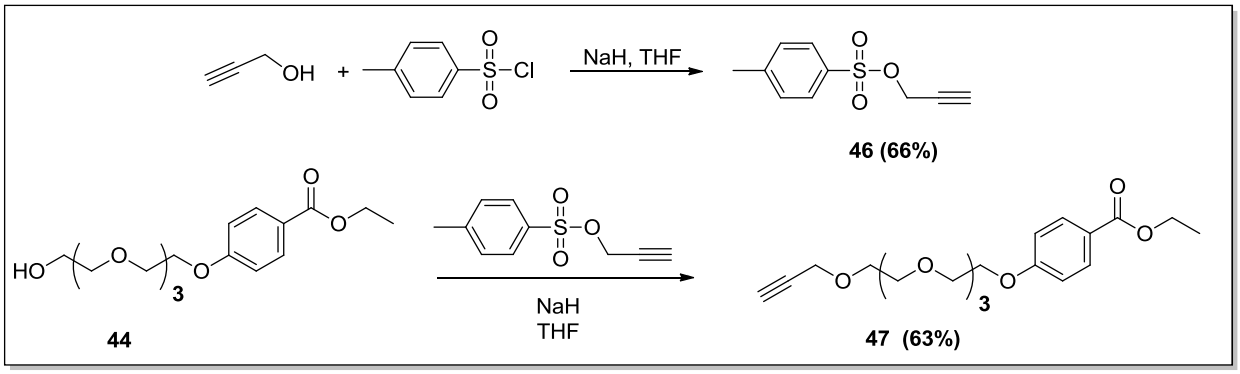


**Scheme 35**: Using the tosylate ester of propargyl alcohol TEG derivative **47** was synthesized.

The next step towards the synthesis of the stationary phase is the coupling between i-VRT **5** and linker **47**. Under inert atmosphere i-VRT along with $PdCl_2$-dppf-$CH_2Cl_2$ were added in the Schlenk flask followed by the addition of **47** in THF and $Et_3N$, followed by CuI. The reaction vessel was heated to 50°C for 16 hrs, which was then filtered through celite and evaporated to dryness, aqueous extractions was avoided to reduce loss of product based on the water solubility of these compounds. Purification via column chromatography followed by analysis of the species isolated by $^{1}H$ and $^{13}C$-NMR indicated the desired cross coupled product **48** was achieved in an 84% yield **(Scheme 36)**.

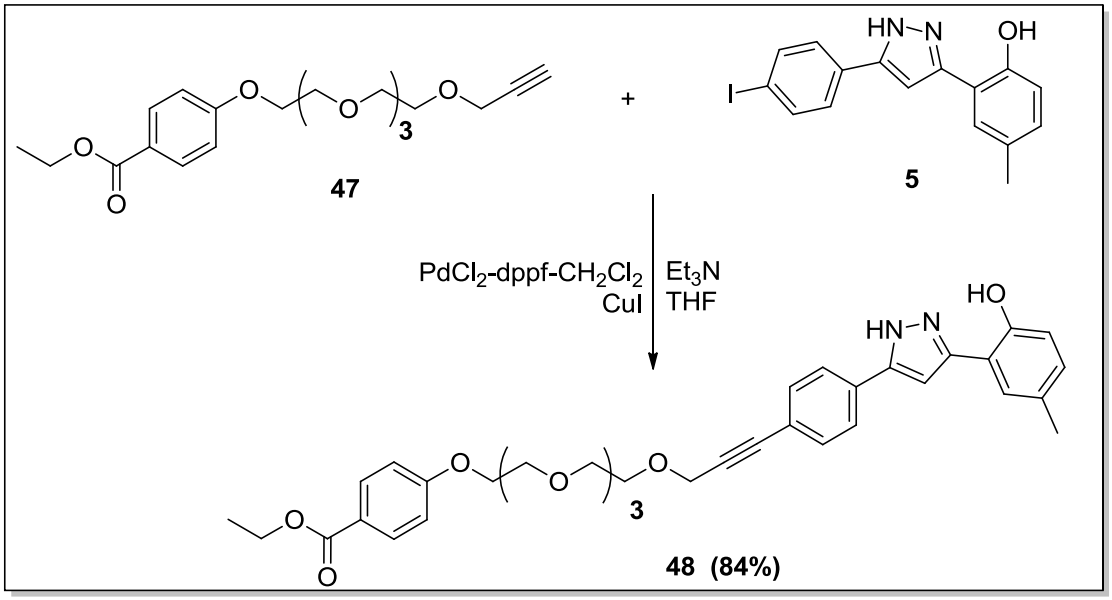


**Scheme 36:** Sonogashira cross-coupling reaction forming the desired linker **48.**

The final steps toward the synthesis of a stationary phase, involve ester hydrolysis of the linker **48**, followed by peptide coupling to a solid support resin. Compound **48** was first dissolved in MeCN followed by the addition of NaOH **(Scheme 37)**. The disappearance of the starting material was noticed by TLC, which was followed by the addition of TFA which generates the carboxylic acid moiety, purification and analysis is currently in progress. This allows for peptide coupling to proceed with the primary amine on the solid support resin. This product can now be utilized by our collaborators at the Hospital for Sick Children for affinity chromatography using fragmented mutant CFTR protein, to help elucidate the nature of interaction between VRT-532 and mutant CFTR.

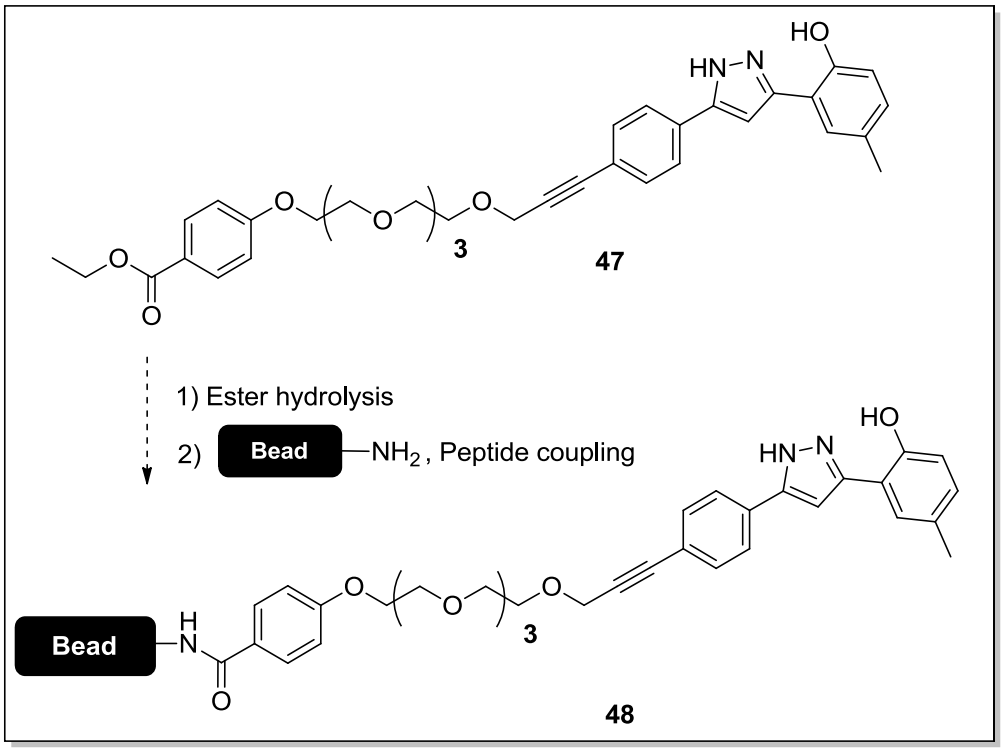


**Scheme 37:** Peptide coupling to generate the solid support attached to the tethering molecule.

## 2.7. Biological Activity for the Molecular Probes Synthesized

For all the molecular probes that have been synthesized it must be demonstrated that, substitutions at the 4'-positions of the phenyl ring of the parent compound **1** does not interfere with the compound's ability to interact with the protein in order to be useful for biochemical studies. All the biological testing and results have been obtained by our collaborators in the Dr. Christine Bear research group at the Hospital for Sick Children. To demonstrating the effect of compounds **5, 9, 11, 12** and **16** on CFTR channel function a patch clamp electrophysiology experiment was performed. In this experiment baby hamster kidney (BHK) cells that express ΔF508-CFTR are loaded with NaI and

stimulated using forksolin (10 $\mu$M) at the 120 s mark **(i, Figure 21)**. Then the cells are treated with the **12** at the 500 s mark **(ii, Figure 21)**. The potentiation of the channel function is observed as an increased rate of iodide efflux from the cells, the amount of iodide released is measured using an iodide sensitive electrode positioned in the cell bath. Finally the cells are lysed at the 800 s **(iii, Figure 21)** mark which releases the remaining iodide. This experiment was also repeated with compounds **5, 9, 11,** and **16.**

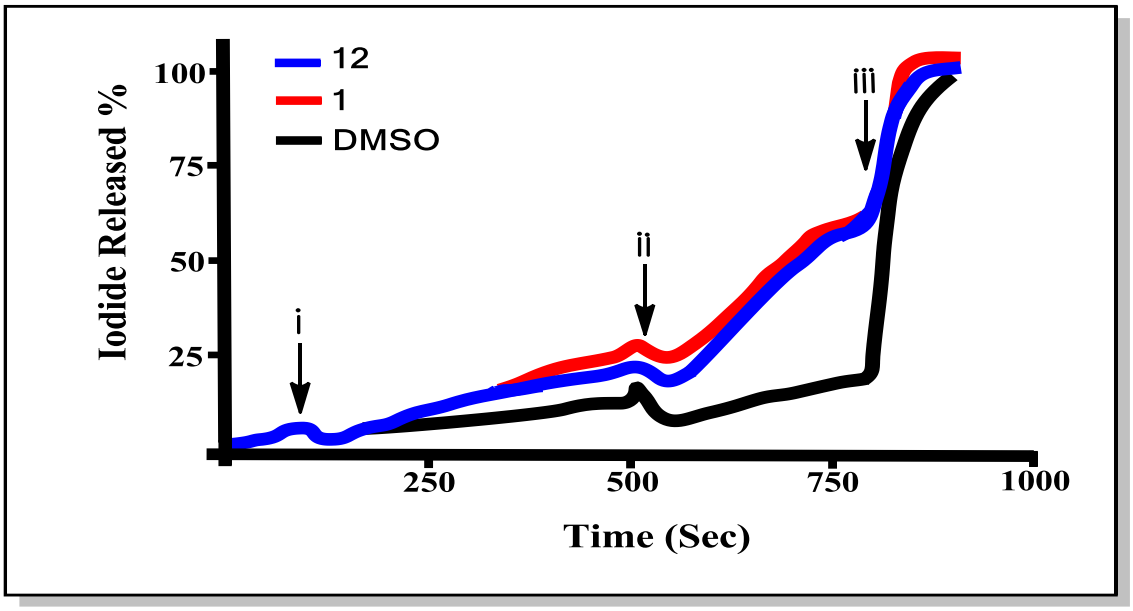


**Figure 21**: Depicting the iodide efflux of compound **12** in a cultured cell bath over time.

The channel potentiating effects of the compounds are measured as the maximum slope of the line prior to addition subtracting maximum slope after addition of the compound. The channel potentiating effects of all the compounds tested are depicted in **Figure 22**.

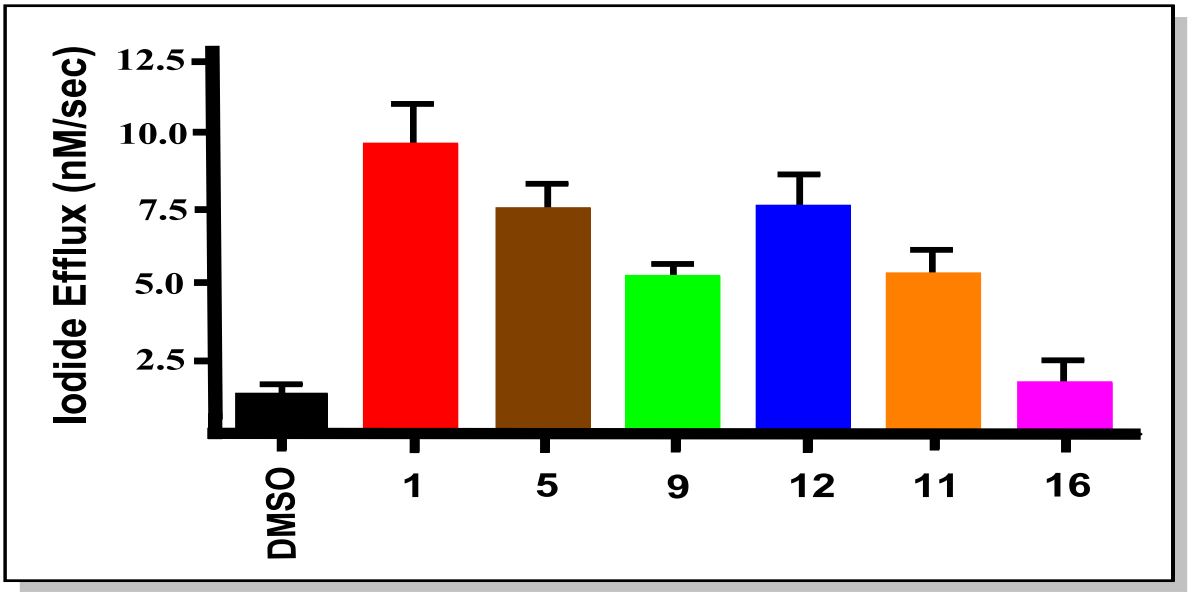


**Figure 22:** Channel potentiating effects of all the compounds tested.

DMSO was used as a control and showed negligible change in halide efflux (1.4 ± 0.4 nM/s) whereas the addition of **1** displayed a drastic increase in efflux post forskolin stimulation (9.9 ± 2.3 nM/s). All the other analogs with the exception of **16** were found to be biologically active, with efflux rates ranging from 5.1-7.5 nM/s. The rates observed for the derivatives were not significantly different than the rates observed for the parent compound **1**, thus suggesting that substitution at the 4'-position of the phenyl ring is not detrimental to the function of the molecule as a potentiator of CFTR channel function.

The inactivity of the dansyl conjugate **16**, in iodide efflux assay may be attributed to the compounds inability to permeate through the cell's membrane rather than some hindered interaction with the CFTR protein. To test this hypothesis, another experiment was utilized to test the effect of **16** on CFTR. A G551D CFTR mutation was reconstructed into liposomes of egg phosphatidylcholine. Typically in this reconstructed system, the protein molecules are oriented randomly within the liposomes (some

proteins molecules exposed the portion that would normally be intracellular toward the exterior of the liposomes); therefore the compound does not need to cross the membrane in order to interact with the protein. If **16** does retain the ability to interact with CFTR, it should potentiate channel activity. For this experiment the liposomes were loaded with KI and suspended in a 10 $\mu$M solution containing the dansyl-VRT **16** in buffer lacking iodide. The release of iodide outside the liposomes is continuously measured using an iodide sensitive probe. **Figure 23** shows the traces of iodide concentration vs time for the parent VRT (**1**), dansyl derivative (**16**), and DMSO (Black line) as a control. Around the 40 s mark the CFTR is activated using; protein kinase A and ATP. Valinomycin is also added to prevent charge build up across the membrane due to CFTR-mediated efflux.

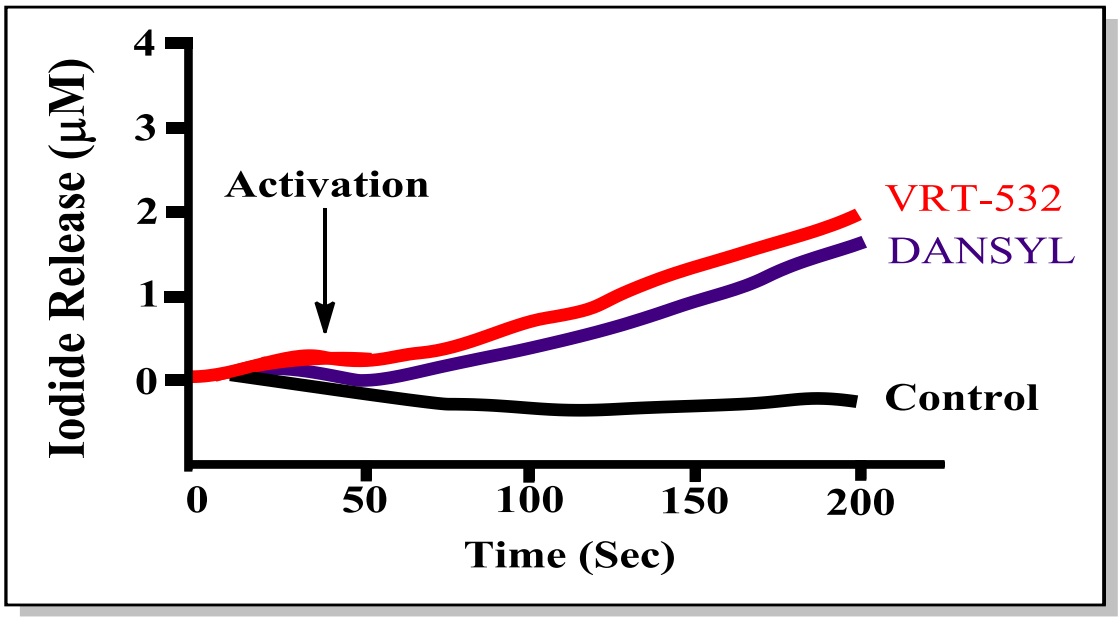


**Figure 23**: Iodide efflux assay on purified G551D-CFTR for compound **16**.

By observing **Figure 24** it is evident that the iodide release from the fluorescent derivative is similar to that of the VRT-532 **1**.

**Figure 24** shows the effect of each of these compounds measured as the maximum slope of iodide efflux followed by valinomycin activation. Under these conditions compound **16** proved to be an effective potentiator of channel activity with an iodide efflux rate of 11.18 ± 2.08 nM/s.

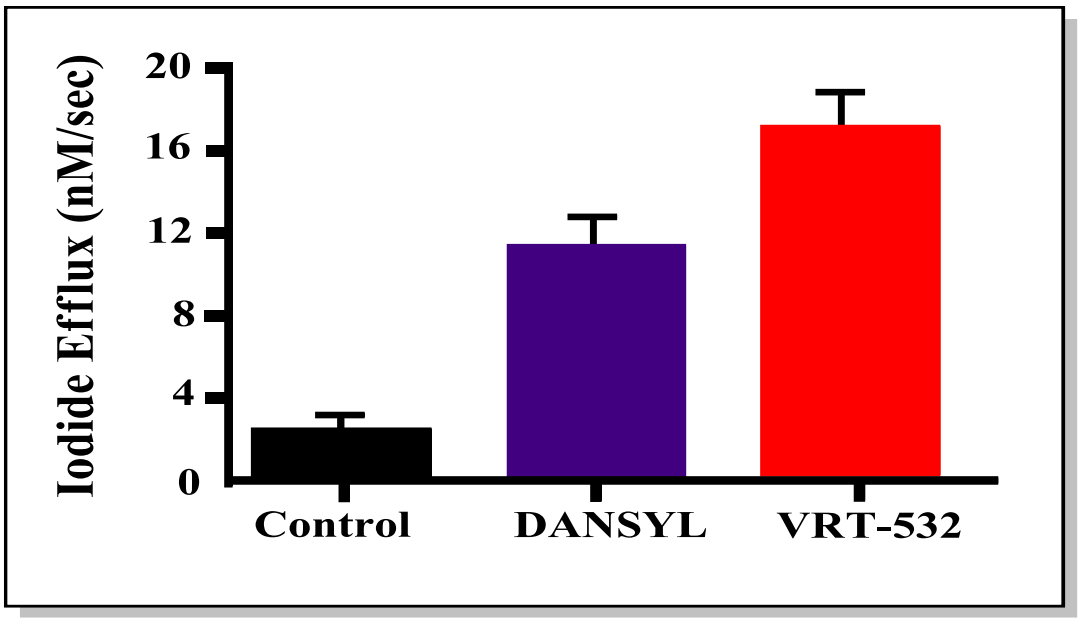


**Figure 24**: The effect of VRT-532 and Fluorescent probe 16, on iodide efflux in the system.

This suggests that compound **16** does maintain the ability of the parent compound to interact with CFTR and modulate its activity, but has a diminished ability to cross the cell membrane.

## 2.8: Future work and Considerations

With respect to synthesizing new VRT target compounds, the idea of synthesizing a biotin analog has great biochemical relevance and would be an extremely useful compound. Extensive research must be completed in order to synthesize a radiolabeled derivative of **1.** The idea of isotope labeling is an appealing feature which will help elucidate the nature of interaction between the recognition element of VRT-532 and mutant CFTR protein. With the fluorescent probe previously synthesized only useful for purified and reconstructed protein but not whole live cells, alternate probes must be analyzed. Some of the probes that should be investigated include compounds such as; Atto dyes and Alexa dyes which are a series of fluorescent labels which covers a spectral range from 390 nm in the UV up to 740 nm in the near infrared allowing excitation with most commonly used light source. This property makes the use of Atto and Alexa dyes useful for bio chemical studies.

# 3. EXPERIMENTAL

## 3.1. General Considerations

All reagents and solvents were used as received from commercial suppliers, except for tetrahydrofuran, which was dispensed under nitrogen from an Mbraun solvent purification system immediately prior to use as a reaction solvent. TLC was carried out on silica gel 60 F254 aluminum backed plates, supplied by EMD chemicals, eluting with the solvent system indicated, and visualizing with UV light. Column chromatography was carried out on Silicycle SiliaFlash P60, 40−63 μm silica gel, eluting with the solvent system indicated below for each compound. Nuclear magnetic resonance ($^{1}$H NMR, 400 MHz, and $^{13}$C NMR, 100 MHz) spectroscopy was carried out on a Bruker Avance 400 instrument in the deuterated solvents indicated below for each compound, and spectra were referenced to the solvent residual $^{1}$H and $^{13}$C peaks. High-resolution mass spectrometry was performed using ESI-TOF or DART-TOF as indicated. UV/Visible spectroscopy was performed using a Perkin-Elmer Lambda 20 instrument. Melting points were determined in open air and are uncorrected. The purity of all compounds subjected to biological assays was determined to be ≥95% by HPLC analysis, using an Agilent Zorbax Rx-C8 4.6 mm × 150 mm column, eluting at 0.6 mL/min with a binary gradient of 100% $H_2O$ to 100% MeCN over the course of 1 h, except for compound **16**, for which the gradient was 100% $H_2O$ to 50% MeCN over the course of 1 h.

**Method 3.2.1. Procedure for the esterification of 2′-(4-Iodobenzoyloxy)-5′-methylacetophenone**

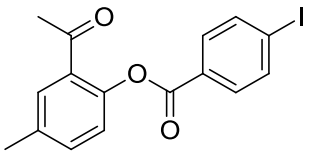


**2′-(4-Iodobenzoyloxy)-5′-methylacetophenone (4)** 2′-hydroxy-5′-methylacetophenone (3.95 g, 26.3 mmol) was added to an ice-bath cooled suspension of 4-iodobenzoyl chloride (7.01 g, 26.3 mmol) in pyridine (140 mL). The resultant clear yellow solution was stirred over an ice-bath for one hour, after which time it was quenched by pouring into an ice/HCl mixture (2M, 600 mL). This aqueous phase was extracted three times with $CH_2Cl_2$ (200 mL each time). The combined organic extracts were washed aqueous HCl (1M, 200 mL), then $NaHCO_3$ (saturated, 200 mL), and finally NaCl (saturated, 200 mL), before drying over $Na_2SO_4$ and evaporating to afford the title ester **4** as a yellow solid, which was used without further purification. Yield: 86% (8.566 g). $^1$H NMR (400 MHz, $(CD_3)_2SO$): $\delta$ 7.99−7.95 (m, 2H), 7.84−7.81 (m, 2H), 7.76 (d, $J$ = 1.5 Hz, 1H), 7.45 (ddd, $J$ = 8.5 Hz, $J$ = 2.0 Hz, $J$ = 0.5 Hz, 1H), 7.22 (d, $J$ = 8.5 Hz, 1H), 2.46 (s, 3H), 2.38 (s, 3H). $^{13}$C NMR (100 MHz, $(CD_3)_2SO$) $\delta$ 196.87, 163.89, 145.74, 137.41, 135.39, 133.53, 130.92, 130.27, 129.58, 127.97, 123.19, 102.14, 28.83, 19.81.

**Method 3.2.2. Procedure for the esterification of 2′-(4-Nitrobenzoyloxy)-5′-methylacetophenone**

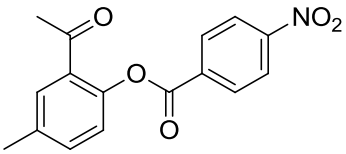

**2′-(4-Nitrobenzoyloxy)-5′-methylacetophenone (7)** Prepared as described above for **6**, but using 2′-hydroxy-5′-methylacetophenone (2.508 g, 16.7 mmol) and 4-nitrobenzoyl chloride (4.324 g, 23.3 mmol). As above for **6**, this compound was used after extractive workup without further purification. Ester **7** obtained in a 98% Yield (4.898 g); mp 274−276 °C; TLC (1:10 EtOAC:Hex) $R_f$ = 0.28; $^1$H NMR (400 MHz, $CDCl_3$): δ 8.38−8.36 (m, 4H), 7.68 (d, *J* = 2 Hz, 1H), 7.42 (ddd, *J* = 12 Hz, *J* = 2 Hz, *J* = 1 Hz, 1H), 7.13 (d, *J* = 8 Hz, 1H), 2.54 (s, 3H), 2.45 (s, 3H). $^{13}$C NMR (100 MHz, $(CD_3)_2CO$) δ 196.79, 163.47, 150.91, 146.75, 136.45, 135.19, 134.02, 131.32, 131.03, 130.22, 123.66, 123.55, 28.65, 19.97.

**Method 3.2.3. Procedure for the synthesis of 4-Methyl-2-(5-(4-iodophenyl)-*1H*-pyrazol-3-yl)phenol**

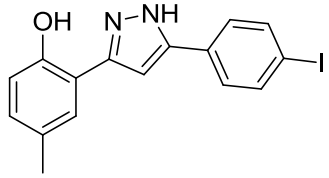

**4-Methyl-2-(5-(4-iodophenyl)-1H-pyrazol-3-yl)phenol (5)** Potassium *tert*-butoxide (613 mg, 5.46 mmol) was dissolved in THF (25 mL). The solution was warmed to 50 °C, and iodo-ester **4** (2.000 g, 5.26 mmol) was added, upon which a yellow precipitate was

observed to form. The mixture was stirred at 50 °C for 30 minutes, then cooled in an ice-bath and quenched by addition of aqueous acetic acid (10% v/v, 20 mL). The aqueous mixture was extracted three times with $CH_2Cl_2$ (50 mL each time). The combined organic extracts were dried over $Na_2SO_4$ and evaporated to afford a yellow solid. This solid was taken up in glacial acetic acid (30 mL) and cooled in an ice-bath. Hydrazine hydrate (“50-60%”, 5.7 mL, ~100 mmol) was added dropwise to the mixture. The ice bath was removed and the mixture was warmed to 65 °C for 16 h. The mixture was then cooled to room temperature and quenched with water (30 mL) and then extracted three times with $CH_2Cl_2$ (50 mL each time). The combined organic extracts were placed over $Na_2SO_4$ and evaporated. The crude product was purified by silica gel column chromatography, eluting with a gradient of 1:10 to 1:1 ethyl acetate/hexanes, to afford the title **5** as a yellow solid. Yield: 68% (1.346 g). Mp: 211-213 °C; TLC (1:4 EtOAC:Hex) $R_f$ = 0.47; $^1$H NMR (400 MHz, $(CD_3)_2CO$) δ 13.03 (bs, 1H), 10.64 (bs, 1H), 7.86 (d, *J* = 8 Hz, 2H), 7.68 (d, *J* = 8 Hz, 2H), 7.58 (s, 1H), 7.28 (s, 1H), 7.01 (d, *J* = 8 Hz, 1H), 6.84 (d, *J* = 8 Hz, 1 H), 2.29 (s, 3H). $^{13}$C NMR (100 MHz, $(CD_3)_2CO$) δ 177.09, 138.16, 135.28, 135.11, 129.74, 127.91, 127.44, 127.03, 124.44, 123.56, 118.14, 116.49, 116.23, 19.77. ESI-TOF MS: m/z = 377.0140 (M + H) calculated for $C_{16}H_{14}N_2OI$: 377.0145. HPLC $t_R$ = 25.2 min.

**Method 3.2.4. Procedure for the Synthesis of 4-Methyl-2-(5-(4-Nitrophenyl)-1H-pyrazol-3-yl)phenol**

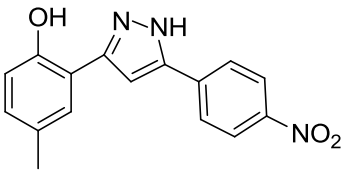


**4-Methyl-2-(5-(4-nitrophenyl)-1*H*-pyrazol-3-yl)phenol (9)** sodium *tert*-butoxide (1.700 g, 17.6 mmol) dissolved in THF (25 mL). The solution was warmed to 50°C, and nitro-ester **7** (3.500 g, 11.7 mmol) was added, upon which an orange precipitate was observed to form. The mixture was stirred at 50 °C for 30 minutes, then cooled in an ice-bath and quenched by addition of aqueous acetic acid (10% v/v, 35 mL). The aqueous mixture was extracted three times with $CH_2Cl_2$ (50 mL each time). The combined organic extracts were dried over $Na_2SO_4$ and evaporated to afford a yellow solid. This solid was taken up in glacial acetic acid (30 mL) and cooled in an ice-bath. Hydrazine hydrate (“50-60%”, 5.7 mL, ~100 mmol) was added dropwise to the mixture. The ice bath was removed and the mixture was warmed to 65 °C for 16 h. The mixture was then cooled to room temperature and quenched with water (30 mL) and then extracted three times with $CH_2Cl_2$ (50 mL each time). The combined organic extracts were over $Na_2SO_4$ and evaporated. The crude product was purified by silica gel column chromatography, eluting with a 3:17 ethyl acetate/hexanes, to afford the title compound **9** as an orange solid. Yield: 67% (2.313 g). Mp: 105-106°C; TLC (1:4 EtOAC:Hex) $R_f$ = 0.24; $^1$H NMR (400 MHz, $(CD_3)_2CO$) δ 12.94 (bs, 1H), 10.81 (bs, 1H), 8.35 (d, *J* = 1.5 Hz, 2H), 8.17 (d, *J* = 9 Hz. 2H), 7.62 (d, *J* = 1.5 Hz, 1H), 7.46 (s, 1H), 7.04 (dd, *J* = 8.5 Hz, *J* = 1.5 Hz, 1H), 6.89 (d, *J* = 6 Hz, 1H), 2.30 (s, 3H). $^{13}$C NMR (100 MHz, $(CD_3)_2CO$)

δ 161.24, 148.25, 136.27, 130.83, 129.35, 128.17, 127.12, 125.08, 124.46, 119.15, 117.37, 116.78, 102.01, 20.55. ESI-TOF MS: *m/z* = 296.1024 (M + H) calculated for $C_{16}H_{14}N_3O_3$: 296.1029. HPLC rt = 31.2 min

**Method 3.2.5.** Procedure for the Synthesis of 4-Methyl-2-(5-phenyl-1H-pyrazol-3-yl)phenol

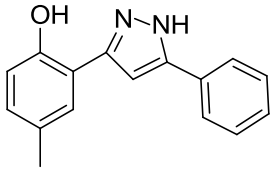


**4-Methyl-2-(5-phenyl-1H-pyrazol-3-yl)phenol (1) (One-Pot Method).** Benzoyl chloride (**10**, 510 µL, 617 mg, 4.4 mmol) was added to a solution of **2** (601 mg, 4 mmol) in pyridine (10 mL), and the mixture was warmed to 50 °C. At 15 min intervals, more 5 (50 µL, 61 mg, 0.4 mmol) was added, until TLC analysis (1:3, ethyl acetate/ hexanes) indicated complete conversion of **2** (Rf = 0.8) into the ester (Rf = 0.7) (three aliquots were added over 45 min, for a total of 660 µL, 800 mg, 5.7 mmol benzoyl chloride in the reaction). While stirring at 50 °C, solid potassium tert-butoxide (987 mg, 8.8 mmol) was gradually added to the reaction mixture. After 15 min, TLC analysis (1:3, ethyl acetate/hexanes) indicated substantial but incomplete conversion of the ester (Rf = 0.7) to the rearranged “dione” (under these conditions, the TLC of this material was a streak extending from the baseline to a major spot with Rf = 0.6). More potassium *ter*-tbutoxide (258 mg, 2.3 mmol) was added, and after an additional 30 min of stirring, TLC analysis indicated complete consumption of the ester. Hydrazine hydrate (“50−60%”, 2.5 mL, ~44 mmol) was added over the course of one minute, followed by glacial acetic acid

(2.0 mL, 2.1 g, 35 mmol). After 1.5 h, TLC analysis indicated completed conversion to the desired product (1:3, ethyl acetate/hexanes, Rf = 0.5). The reaction mixture was poured into an ice/HCl mixture (1 M, 250 mL), which was then extracted three times with ethyl acetate (100 mL each time). The combined organic extracts were washed with $NaHCO_3$ (saturated, 100 mL) and NaCl (saturated, 100 mL) and then dried over $MgSO_4$ and evaporated. The crude product was purified by silica gel column chromatography, eluting with a 1:9 ethyl acetate/ hexanes, to afford the title compound **1** as a yellow solid. Yield 65% (648 mg); mp 160−161 °C (lit.33 156−157 °C). $^1$H NMR (400 MHz, $(CD_3)_2CO$) δ 12.78 (bs, 1H), 10.65 (bs, 1H), 7.908−7.876 (m, 2H), 7.606 (d, *J* = 2 Hz, 1H), 7.542−7.488 (m, 2H), 7.454−7.397 (m, 1H), 7.274 (s, 1H), 7.022 (ddd, *J* = 8.5 Hz, *J* = 2 Hz, *J* = 0.5, 1H), 6.838 (d, *J* = 7.5 Hz, 1H), 2.303 (s, 3H). $^{13}$C NMR (100 MHz, $(CD_3)_2CO$) δ 154.82, 152.95, 145.16, 130.50, 130.28, 129.92, 129.57, 128.79, 127.79, 126.48, 117.33, 117.28, 100.04, 20.59. DART-TOF MS: m/z = 251.1175 (M + H) calculated for $C_{16}H_{15}N_2O$: 251.1184. HPLC rt = 34.3 min.

**Method 3.2.6. Procedure for the synthesis of 4-Methyl-2-(5-(4-aminophenyl)-1H-pyrazol-3-yl)phenol**

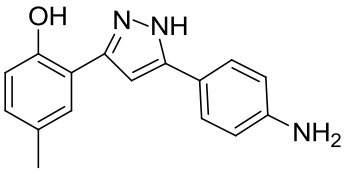


**4-Methyl-2-(5-(4-aminophenyl)-1H-pyrazol-3-yl)phenol (11)** Stannous chloride dihydrate (3.850 g, 17 mmol) was added to a solution of **9** (1 g, 3.4 mmol) in 95% ethanol (30 mL). The mixture was heated to reflux for 16 hr. The mixture was cooled to

room temperature and poured into aqueous NaOH (1 M, 150 mL). The mixture was extracted twice with ethyl acetate (75 mL each time). The combined organic extracts were washed with aqueous NaCl (saturated, 75 mL), then dried over $Na_2SO_4$ and evaporated. The crude product was purified by silica gel column chromatography, eluting with a 1:4 ethyl acetate/hexanes, to afford the title compound **11** as a pale yellow solid. Yield: 71% (638 mg). Mp: 200-202°C; TLC (7:20 EtOAC:Hex) $R_f$ = 0.25; $^1$H NMR (400 MHz, $(CD_3)_2CO$) δ 13.2 (s, 1H), 10.9 (s, 1H), 7.54 (s, 1H), 7.48 (d, *J* = 8.5 Hz, 2H), 7.03 (s, 1H), 6.97 (d, *J* = 8Hz, 1H), 6.79 (d, *J* = 8 Hz, 1H), 6.63 (d, *J* = 8 Hz, 2H), 5.42 (s, 2H), 2.27 (s, 3H). $^{13}$C NMR (100 MHz, $(CD_3)_2CO$) δ 154.17, 149.38, 129.54, 129.34, 127.66, 126.77, 126.69, 126.32, 120.08, 116.72, 116.35, 114.36, 97.06, 19.70. ESI-TOF MS: m/z = 266.1288 (M + H) calculated for $C_{16}H_{16}N_3O$: 266.1287. HPLC rt = 29.0 min.

**Method 3.2.7. Procedure for the synthesis of 4-Methyl-2-(5-(4-Azidophenyl)-1H-pyrazol-3-yl)phenol.**

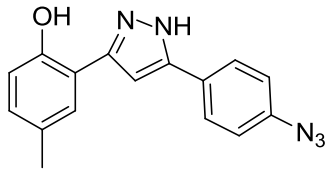


**4-Methyl-2-(5-(4-azidophenyl)-1*H*-pyrazol-3-yl)phenol (12).** Amine **11** (265 mg, 1 mmol) was dissolved in acetonitrile (10 mL) and cooled in an ice-bath. To this was added *tert*-butyl nitrite (178 µL, 154 mg, 1.5 mmol), followed by azidotrimethylsilane (158 µL, 138 mg, 1.2 mmol). The mixture was warmed to room temperature and stirred for one hour, after which the solvent was evaporated, and the crude product was

purified by silica gel column chromatography, eluting with a gradient of 1:10 to 1:1 ethyl acetate/hexanes, to afford the title compound **12** as a yellow solid. Yield: 94% (273 mg). Mp: 153-154 °C; TLC (1:4 EtOAC:Hex) $R_f$ = 0.40; $^1$H NMR (400 MHz, $(CD_3)_2CO$) δ 12.82 (bs, 1H), 10.70 (bs, 1H), 7.93 (d, *J* = 8.5 Hz, 2H), 7.59 (d, *J* = 2 Hz, 1 H), 7.28-7.22 (m, 3H), 7.02 (dd, J = 8.5 Hz, *J* = 2 Hz, 1H), 6.83 (d, *J* = 8 Hz, 1H), 2.30 (s, 3H). $^{13}$C NMR (100 MHz, $(CD_3)_2CO$) δ 153.89, 143.72, 140.18, 129.68, 127.99, 127.14, 126.97, 126.38, 125.50, 119.63, 116.49, 116.37, 99.14, 19.76. ESI-TOF MS: m/z = 291.1196 (M + H) calculated for $C_{16}H_{14}N_5O$: 292.1192. HPLC rt = 33.8 min.

### Method 3.2.8. Procedure for the Photoirradiation of 4-Methyl-2-(5-(4-Azidophenyl)-1H-pyrazol-3-yl)phenol

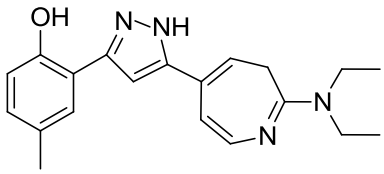


**2-(5-(2-(diethylamino)-3*H*-azepin-5-yl)-1*H*-pyrazol-3-yl)-4-methylphenol (13)** A solution of **11** (40 mg, 0.14 mmol) and diethylamine (0.4 mL) in $C_6D_6$ (1.5 mL) in a quartz NMR tube was irradiated with a 140 W Hanovia Utility Ultraviolet Quartz lamp. The tube was held ~ 10 cm from the light bulb, and a stream of air was blown over the tube to maintain the contents at room temperature. After 5 hours of exposure, the mixture was evaporated under reduced pressure, and the crude product was purified by silica gel column chromatography, eluting with 3:7 ethyl acetate/hexanes, to afford the diethylamine adduct **13**. Yield: 40% (17.3 mg). TLC (1:4 EtOAC:Hex) $R_f$ = 0.36; $^1$H NMR (400 MHz, $(CD_3)_2CO$) δ 10.75 (bs, 1H), 7.54 (s, 1H), 7.21 (d, *J* = 8.0 Hz, 1H), 6.98

(dd, *J* = 8.5 Hz, *J* = 1.5 Hz, 1H ), 6.92 (s, 1H), 6.80 (d, *J* = 8.0 Hz, 1H), 6.04 (d, *J* = 8.0 Hz, 1H), 5.73 (t, *J* = 7.5 Hz, 1H), 3.46 (q, *J* = 7.0 Hz, 4H), 2.28 (s, 3H), 1.29 (bs, 2H), 1.26-1.01(m, 6H). $^{13}$C NMR (100 MHz, $(CD_3)_2CO$) δ 154.05, 152.09, 146.01, 144.21, 142.88, 129.44, 129.40, 127.74, 126.79, 116.56, 116.35, 109.33, 106.77, 99.40, 42.95, 30.97, 19.66, 13.46.

**Method 3.2.9. Synthesis of N-propargyl dansyl amide 42**

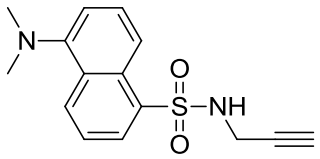


**5-(Dimethylamino)-*N*-(2-propynyl)-1-naphthalenesulfonamide (15)** To a solution of 5 (dimethylamino)naphthalene-1-sulfonyl chloride (2.0 g, 7.41 mmol) in anhydrous $CH_2Cl_2$ (20 mL) were added triethylamine (1.1 mL, 8 mmol) and propargylamine (0.55 mL, 8 mmol); the solution immediately turned from dark yellow to fluorescent. After quenching with 10 ml of phosphate buffer (pH 7) and extraction with 15 ml of $CH_2Cl_2$ **15** was obtained as a yellow solid. TLC (3:10 EtOAC:Hex) $R_f$ = 0.25; $^1$H NMR (400 MHz, $CDCl_3$) δ 8.54 (d, *J* = 8.5 Hz, 1H), 8.30-8.24 (m, 2H), 7.60-7.48 (m, 2H), 7.19 (d, *J* = 7 Hz, 1H), 3.77 (d, *J* = 2.5, 2H), 2.88 (s, 6H), 1.90 (t, *J* = 2.5 Hz, 1H).

**Method 3.2.10. Sonogashira coupling between i-VRT and 15.**

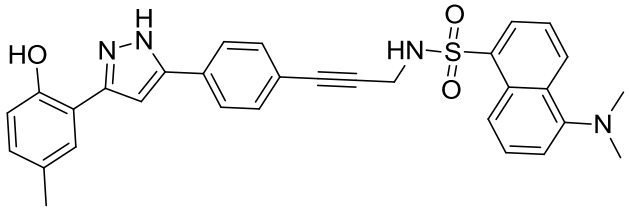


**5-Dimethylamino-*N*-(3-(4-(3-(2-hydroxy-5-methylphenyl)-1*H*-pyrazol-5-yl)phenyl)-2-propynyl)-1-naphthalenesulfonamide (16)** A 10 mL Schlenk tube was fitted with a magnetic stirring bar and a glass stopper and flushed with argon gas. The tube was then charged with 4-Methyl-2-(5-(4-iodophenyl)-1H-pyrazol-3-yl)phenol (203 mg, 0.54 mmol), 5-(dimethylamino)-*N*-(2-propynyl)-1-naphthalenesulfonamide (312 mg, 1.08 mmol) and $PdCl_2$•dppf•$CH_2Cl_2$ (22 mg, 0.027 mmol). The tube was evacuated and backfilled with argon. Under a stream of argon, THF (4 mL), triethylamine (0.12 mL, 0.8 mmol) and finally CuI (4 mg, 0.02 mmol) were added. The tube was sealed, and the mixture was heated to 45 °C for 15 hours and then cooled back to room temperature. The mixture was diluted with ethyl acetate (25 mL) and extracted with 0.1 M HCl (10 mL), then brine (10 mL), then dried over anhydrous sodium sulfate and evaporated under reduced pressure. The crude material was purified by silica gel column chromatography, eluting with 1:4 ethyl acetate/hexanes, to afford the title compound **16** as a yellow solid. Yield: 47% (135 mg). Mp: 216-218°C TLC (3:10 EtOAC:Hex) $R_f$ = 0.19; $^1$H NMR (400 MHz, $(CD_3)_2CO$) δ 12.82 (bs, 1H), 10.62 (bs, 1H), 8.51 (d, *J* = 8.5 Hz, 1H), 8.42 (d, *J* = 8.5, 1H), 8.33 (dd, *J* = 7.5 Hz, *J* = 1.0 Hz, 1H), 7.72 (d, *J* = 8 Hz, 2H), 7.66 – 7.57 (m, 3H), 7.29 – 7.23 (m, 3H), 7.02 (dd, *J* = 8 Hz, *J* = 2 Hz, 1H), 6.94 (d, *J* = 8 Hz, 2H), 6.84 (d, *J* = 8 Hz, 1 H), 4.12 (d, *J* = 5 Hz, 2H), 2.81 (s, 6H), 2.30 (s, 3H).

$^{13}$C NMR (100 MHz, $(CD_3)_2CO$) δ 152.85, 137.24, 137.21, 132.72, 130.98, 130.90, 130.75, 130.59, 130.29, 130.27, 128.93, 128.73, 127.86, 126.08, 124.27, 123.27, 120.40, 117.36, 117.28, 117.12, 115.97, 100.47, 86.47, 83.50, 45.59, 33.77, 20.57 (one 13C signal was not observed after 15000 scans). DART-TOF MS: m/z = 537.1958 (M + H) calculated for $C_{31}H_{29}N_4O_3S$: 537.1960. HPLC rt = 25.2 min.

**Method 3.2.11. Synthesis of Boc-propargyl amine [44]**

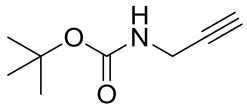


***tert*-Butyl prop-2-ynylcarbamate (17)** To a solution of propargylamine (1.60 g, 29.2 mmol) in $CH_2Cl_2$ (30 mL) at 0 °C was added a solution of di-*tert*-butyl dicarbonate (5.34 g, 30.6 mmol) in $CH_2Cl_2$ (40 mL) via dropping funnel over 25 min, the ice bath was removed, and the resultant solution was stirred at ambient temperature for 60 min. The solvent was removed in vacuo and the crude material was chromatographed on silica gel (EtOAc/hexane, 10/90, $R_f$ = 0.28) to afford the title compound **17** (3.0 g, 66% yield) as a white solid. TLC (3:10 EtOAC:Hex) $R_f$ = 0.3; $^1$H NMR (400 MHz, $CDCl_3$) δ 4.91 (s, 1H), 3.87 (d, *J* = 3 Hz, 2H), 2.18 (t, *J* = 3 Hz, 1H), 1.40 (s, 9H).

**Method 3.2.12. Sonogashira coupling between i-VRT and 17.**

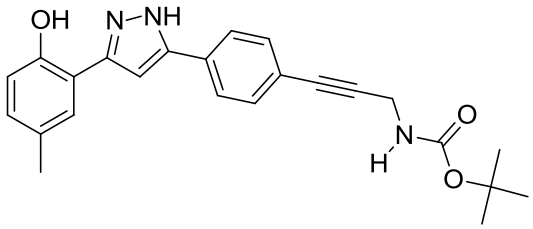

***O-t*-Butyl-*N*-(3-(4-(3-(2-hydroxy-5-methylphenyl)-1*H*-pyrazol-5-yl)phenyl)-2-propynyl)carbamate (18).** Prepared by a method analogous to **16** above, but using **17** (610 mg, 1.62 mmol), **18** (500 mg, 3.24 mmol), $PdCl_2$•dppf•$CH_2Cl_2$ (66 mg, 0.084 mmol), THF (12 mL), triethylamine (0.35 mL, 2.5 mmol) and CuI (11 mg, 0.06 mmol). Title compound **18** was isolated as an orange/brown solid. Yield: 69% (445 mg). Mp 185-187 °C; TLC (3:10 EtOAC:Hex) $R_f$ = 0.37; $^1$H NMR (400 MHz, $(CD_3)_2CO$) δ 12.86 (bs, 1H), 10.66 (bs, 1H), 7.87 (d, *J* = 8 Hz, 2H), 7.60 (d. *J* = 1.5 Hz, 1H), 7.54 (d, *J* = 7 Hz, 2H), 7.31 (s, 1H), 7.03 (dd, *J* = 8.5 Hz, *J* = 2 Hz, 1H), 6.87-6.82 (m, 1H), 6.45 (bs, 1H), 4.13 (d, *J* = 6 Hz, 2H), 2.30 (s, 3H), 1.45 (s, 9H). $^{13}$C NMR (100 MHz, $(CD_3)_2CO$) δ 156.32, 154.70, 136.16, 135.98, 133.02, 130.59, 128.90, 127.87, 126.46, 124.12, 119.04, 117.36, 117.16, 100.53, 89.87, 82.18, 79.38, 31.30, 28.59, 20.58. DART-TOF MS: m/z = 404.1966 (M + H) calculated for $C_{24}H_{26}N_3O_3$: 404.1974. HPLC rt = 19.8 min.

**Method 3.2.13. Procedure for the hydrogen Isotope exchange on 1**

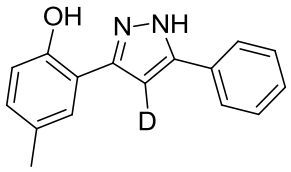

**4-methyl-2-(5-phenyl-1H-pyrazol-3-yl)phenol (21).** To a standard NMR tube containing 1 mL of 1 M NaOH in $D_2O$ was added 1 (25 mg, 0.1 mmol). The tube was

capped and heated in a sand bath at 90 °C. Reaction progress was monitored by periodically collecting a $^{1}$H NMR spectrum and observing the relative integration of the pyrazole C4−H signal at δ 6.7 ppm. After 48 h, the reaction was cooled to room temperature and diluted with 10 mL of $H_2O$. The mixture was cooled in an ice bath and acidified to pH ∼1 by dropwise addition of 1 M HCl. The mixture was extracted with three times with 10 mL $Et_2O$, concentrated under reduced pressure, and purified by preparative TLC eluting with 1:3 EtOAc/hexanes to afford 22 mg (88%) of **1**$_{C4\text{-}D}$ with ∼80% deuteration as determined by $^{1}$H NMR integration. TLC (1:4 EtOAC:Hex) $R_f$ = 0.40; $^{1}$H NMR (400 MHz, $(CD_3)_2CO$) δ 12.78 (bs, 1H), 10.65 (bs, 1H), 7.91−7.88 (m, 2H), 7.61 (d, *J* = 2 Hz, 1H), 7.53−7.49 (m, 2H), 7.45−7.41 (m, 1H), 7.27 (s, 0.2H), 7.02 (dd, *J* = 8.5 Hz, *J* = 1.5 Hz, 1H), 6.84 (d, *J* = 8.5 Hz, 1H), 2.30 (s, 3H). $^{13}$C NMR (100 MHz, $(CD_3)_2CO$) δ 155.94, 154.82, 142.80, 130.49, 129.97, 129.56, 128.80, 127.82, 126.48, 117.33, 117.30, 100.06, 20.58 (one $^{13}$C signal not observed after 13686 scans).

**Method 3.2.14. Procedure for the esterification of 2-acetyl-6-bromo-4-methylphenyl 4-iodobenzoate**

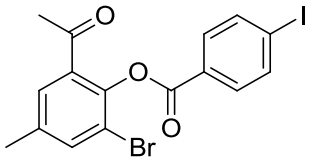


**2-acetyl-6-bromo-4-methylphenyl 4-iodobenzoate (24)** 1-(3-bromo-2-hydroxy-5-methylphenyl)ethanone (1.5 g, 6.55 mmol) was added to an ice-bath cooled suspension of 4-iodobenzoyl chloride (1.9 g, 7 mmol) in pyridine (40 mL). The resultant orange/brownish solution was stirred over an ice-bath for two hours, after which time it

was quenched by pouring into an ice/HCl mixture (2M, 100 mL). This aqueous phase was extracted three times with $CH_2Cl_2$ (50 mL each time). The combined organic extracts were washed aqueous HCl (1M, 50 mL), then $NaHCO_3$ (saturated, 50 mL), and finally NaCl (saturated, 50 mL), before drying over $Na_2SO_4$ and evaporated under reduced pressure. The crude product was purified by silica gel column chromatography, eluting with 1:9 ethyl acetate/hexanes, to afford a white solid **24;** Yield: 75% (2.24 g). Mp 215-217°C; TLC (1:4 EtOAC:Hex) $R_f$ = 0.55; $^1$H NMR (400 MHz, $CDCl_3$): $\delta$ 7.95-7.87 (m, 4H), 7.62 (d, *J* = 1.5 Hz, 1H), 7.57 (d, *J* = 1.5 Hz, 1H), 2.50 (s, 3H), 2.40 (s, 3H). $^{13}$C NMR (100 MHz, $CDCl_3$) $\delta$ 196.67, 163.94, 144.42, 138.21, 137.69, 137.43, 132.72, 131.85, 129.96, 128.41, 118.31, 102.23, 29.53, 20.78.

**Method 3.2.15. Procedure for the synthesis of 2-bromo-6-(5-(4-iodophenyl)-1H-pyrazol-3-yl)-4-methylphenol**

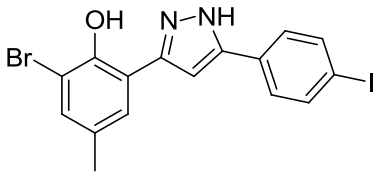


**2-bromo-6-(5-(4-iodophenyl)-1H-pyrazol-3-yl)-4-methylphenol (25)** Potassium *tert*-butoxide (171.60 mg, 17.6 mmol) dissolved in THF (5 mL). The solution was warmed to 50 °C, and 2-acetyl-6-bromo-4-methylphenyl 4-iodobenzoate (350 mg, 0.762 mmol), was added, upon which an orange precipitate was observed to form. The mixture was stirred at 50 °C for two hours, then cooled in an ice-bath and quenched by addition of aqueous acetic acid (10% v/v, 10 mL). The aqueous mixture was extracted three times with $CH_2Cl_2$ (20 mL each time). The combined organic extracts were dried over $Na_2SO_4$

and evaporated to afford a yellow solid. This solid was taken up in glacial acetic acid (20 mL) and cooled in an ice-bath. Hydrazine hydrate (“50-60%”, 3.2 mL, ~100 mmol) was added dropwise to the mixture. The ice bath was removed and the mixture was warmed to 65°C for 16 h. The mixture was then cooled to room temperature and quenched with water (20 mL) and then extracted three times with $CH_2Cl_2$ (30 mL each time). The combined organic extracts were placed over $Na_2SO_4$ and evaporated. The crude product was purified by silica gel column chromatography, eluting with a 1:17 ethyl acetate/hexanes, to afford the title compound **25** as a white solid, yield: 33%. Mp 186-189°C; TLC (1:4 EtOAC:Hex) $R_f$ = 0.48; $^1$H NMR (400 MHz, $(CD_3)_2SO$), 13.07 (bs, 1H), 11.47 (bs, 1H), 7.92 (d, *J* = 8 Hz, 2H), 7.71 (d, *J* = 12 Hz, 2H), 7.62, (s, 1H), 7.38 (s, 1H), 7.34 (s, 1H), 2.31 (s, 3H) ). $^{13}$C NMR (100 MHz, $(CD_3)_2SO$) δ 164.06, 148.38, 138.38, 138.05, 137.64, 132.91, 132.65, 131.53, 130.80, 130.17, 127.89, 127.02, 122.55, 20.18.

### Method 3.2.16. Procedure for the PMB protection of 4-methyl-2-(5-(4-iodophenyl)-1*H*-pyrazol-3-yl)phenol

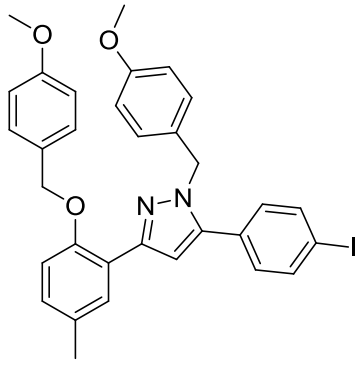


**5-(4-iodophenyl)-1-(4-methoxybenzyl)-3-(2-((4-methoxybenzyl)oxy)-5-methylphenyl)-1*H*-pyrazole (29)** Sodium Hydride (200 mg, 8.3 mmol) was added to a solution of 4-methyl-2-(5-(4-iodophenyl)-1H-pyrazol-3-yl)phenol (250 mg, 0.665 mmol)

in anhydrous DMF (10 mL) at 0°C. The solution was stirred at room temperature for two hours, which was followed by the slow addition of 4-methoxybenzyl chloride (0.3 mL, 2 mmol) via addition funnel. The resulting solution was quenched with $H_2O$ (30 mL) and extracted with ethyl acetate (30 mL) twice. The combined organic extracts were washed with sodium bicarbonate (30 mL), then NaCl (30 mL), before drying over $Na_2SO_4$ and evaporated under reduced pressure. The crude product was purified by silica gel column chromatography, eluting with 1:9 ethyl acetate/hexanes, to afford a brownish/white solid. Yield: 33% (123 mg). TLC (1:4 EtOAC:Hex) $R_f$ = 0.42; $^1$H NMR (400 MHz, $(CD_3)_2CO$) δ 7.74 (d, *J* = 8.5 Hz, 2H), 7.67 (d, *J* = 8.5 Hz, 2H), 7.26 (d, *J* = 8.5 Hz, 2H), 7.22 (dd, *J* = 9 Hz, *J* = 2 Hz, 1H), 7.11 (d, *J* = 8.5 Hz, 1H), 7.05 (d, *J* = 2 Hz, 1H), 6.96 (d, *J* = 8.5 Hz, 2H), 6.86 (d, *J* = 8.5 Hz, 2H), 6.73 (d, *J* = 8.5 Hz, 2H), 6.68 (s, 1H), 5.18 (s, 2H), 5.01 (s, 2H), 3.73 (s, 3H), 3.68 (s, 3H), 2.26 (s, 3H). $^{13}$C NMR (100 MHz, $(CD_3)_2CO$) δ 159.50, 159.04, 154.15, 148.89, 142.03, 137.57, 133.85, 132.20, 130.98, 130.04, 129.77, 129.07, 129.03, 128.75, 127.23, 119.90, 113.76, 113.56, 113.38, 104.19, 91.96, 70.09, 54.66, 54.61, 53.19, 19.60.

**Method 3.2.17. Procedure for the PMB Protection of 1-Bromo-2-naphthol**

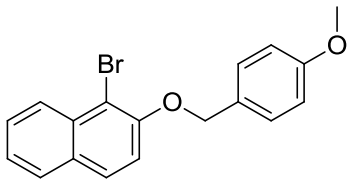


**1-bromo-2-((4-methoxybenzyl)oxy)naphthalene (31)** Sodium Hydride (540 mg, 22.5 mmol) was added to a solution of 1-bromo-2-naphthol (2.0 g, 8.97 mmol) in anhydrous

DMF (10 mL) at 0°C. The solution was stirred at room temperature for two hours, which was followed by the slow addition of 4-methoxybenzyl chloride (1.8 mL, 13.5 mmol) in 5 ml DMF via addition funnel. The resulting solution was quenched with $H_2O$ (50 mL) and extracted three times with DCM (50 mL). The combined organic extracts were washed with sodium Bicarbonate (50 mL), then NaCl (50 mL), before drying over $MgSO_4$ and evaporated under reduced pressure. The crude product was purified by silica gel column chromatography, eluting with 1:9 ethyl acetate/hexanes, to afford a white crystalline solid. Yield: 2.2 g, (75%)**.** TLC (3:10 EtOAC:Hex) $R_f$ = 0.48; $^1$H NMR (400 MHz, $CDCl_3$) δ 8.24 (dd, *J* = 8.5 Hz, *J* = 1.0 Hz, 1H), 7.77 (dd, *J* = 8.0 Hz, *J* = 0.5 Hz, 1H), 7.76 (d, *J* = 9.0 Hz, 1H), 7.57 (ddd, *J* = 8.5 Hz, *J* = 7.0 Hz, *J* = 1.0 Hz, 1H), 7.45 (m, 2H), 7.40 (ddd, *J* = 8.0 Hz, *J* = 7.0 Hz, *J* = 1.0 Hz, 1H), 7.28 (d, *J* = 9.0 Hz, 1H), 6.93 (m, 2H), 5.24 (s, 2H), 3.82 (s, 3H). $^{13}$C NMR (100 MHz, $CDCl_3$) δ 159.46, 153.04, 133.20, 130.08, 128.96, 128.76, 128.72, 128.02, 127.64, 126.31, 124.52, 115.95, 114.00, 110.20, 55.29, 40.74

**Method 3.2.18. Procedure for the Addition of a Terminal Alkyne on Tetraethylene glycol**

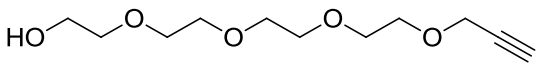


**3,6,9,12-tetraoxapentadec-14-yn-1-ol (34)** Sodium hydride (2.72 g, 113.3 mmol) was added to a solution of tetraethylene glycol (20.0 g, 102.97 mmol) in anhydrous THF (200 mL) at 0°C. The solution was stirred at room temperature for two hours, which was followed by the slow addition of propargyl bromide (12 mL, 113.3 mmol) in 30 mL THF via addition funnel at 0°C. The resulting solution was stirred at room temperature

for 16 h, thereafter the solvent was removed in vacuo and the crude material was chromatographed on silica gel (Acetone/hexane, 60/40, to afford a yellow oil. Yield 5.8g (24.3 %); TLC (6:5 Acetone:Hexane) $R_f$ = 0.33; $^1$H NMR (400 MHz, $CDCl_3$) δ 4.03 (d, *J* = 3.0 Hz, 2H), 3.65-3.45 (m, 14H), 3.42 (t, *J* = 4.5 Hz, 2H), 3.17 (s, 1H), 2.370 (t, *J* = 0.5 Hz, 1H). $^{13}$C NMR (100 MHz, $CDCl_3$) δ 79.38, 77.49, 77.37, 77.17, 76.85, 74.60, 72.39, 70.32, 70.26, 70.22, 70.07, 70.01, 68.80, 61.28, 58.09

*A byproduct of the previous reaction which is a beneficial compound is the di-alkyne was also isolated*

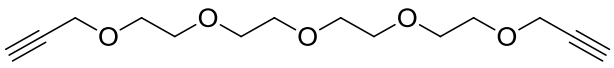

**4,7,10,13,16-pentaoxanonadeca-1,18-diyne (35)**

TLC (6:5 Acetone:Hexane) $R_f$ = 0.47; $^1$H NMR (400 MHz, $CDCl_3$) δ 2.41 (t, *J* = 2.5 Hz, 2H), 3.55-3.75 (m, 16H), 4.18 (d, *J* = 2.5 Hz, 4H). $^{13}$C NMR (100 MHz, $CDCl_3$) δ 79.67, 74.48, 70.61, 70.58, 70.41, 69.12, 58.39

**Method 3.2.19. Procedure for the synthesis of ehtylester of 36**

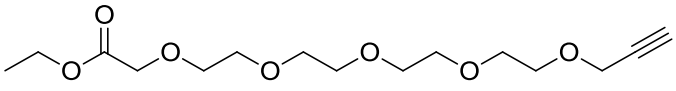

**ethyl 3,6,9,12,15-pentaoxaoctadec-17-yn-1-oate (36)** Sodium hydride (307 mg, 12.8 mmol) was added to a solution of **34** (2.0 g, 8.52 mmol) in anhydrous THF (20 mL) at 0°C. The solution was stirred at room temperature for two hours, which was followed by

the slow addition of ethyl bromoacetate (1.42 mL) in 10 mL THF via addition funnel at 0°C. The resulting solution was stirred at room temperature for 16 h, thereafter the solvent was removed in vacuo and the crude material was chromatographed on silica gel (Acetone/hexane, 60/40, to afford a yellow oil (30%). TLC (6:5 Acetone:Hexane) $R_f$ = 0.21; $^1$H NMR (400 MHz, $CDCl_3$) δ 4.61 (s, 2H), 4.33 (t, *J* = 5 Hz, 2H), 4.24 (q, *J* = 7 Hz, 2H), 4.20 (d, *J* = 2.5 Hz, 2H), 3.74 (t, *J* = 4.5 Hz, 2H), 3.71-3.63 (m, 12H), 2.42 (t, *J* = 2.5 Hz, 1H), 1.28 (t, *J* = 7.5 Hz, 3H). $^{13}$C NMR (100 MHz, $CDCl_3$) δ 86.32, 85.94, 70.69, 70.54, 70.53, 70.46, 70.39, 69.46, 69.20, 67.40, 60.77, 59.13, 30.93, 20.59, 14.34

**Method 3.2.20. Procedure for the Tosylation of Tetraethylene glycol**

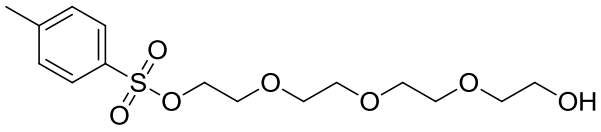


**2-(2-(2-(2-hydroxyethoxy)ethoxy)ethoxy)ethyl 4-methylbenzenesulfonate (42)**

Tetraethylene glycol (10.0 g, 51.49 mmol) was dissolved in chloroform (70 mL) the reaction mixture was cool to -20$^o$C in a NaCl ice bath. 4-Toluenesulfonyl chloride (29.5 g, 154.47 mmol) along with pyridine (54 mL) were added and allowed to stir at -20$^o$C for 5 h. The solvent was evaporated and quenched with ice water (500 mL) and extracted four times with DCM (500 mL). The combined organic extracts were washed with 1M HCl (500 mL), then aq. $NaHCO_3$ (500 mL), followed by $H_2O$ (500 mL). The organic content was dried over $MgSO_4$ and evaporated under reduced pressure. The crude product was purified by silica gel column chromatography, eluting with 3:17 acetone/hexanes, to afford a yellow oil. Yield 3.6 g (20 %).; TLC (7:5 Acetone:Hexane)

$R_f$ = 0.20; $^1$H NMR (400 MHz, $CDCl_3$) δ 7.73 (d, *J* = 8.5 Hz, 2H), 7.29 (d, *J* = 8 Hz, 2H), 4.10 (t, *J* = 5 Hz, 2H), 3.70 (t, *J* = 5.5 Hz, 2H), 3.63 (t, *J* = 5 Hz, 2H), 3.61-3.50 (m, 10H), 2.39 (s, 3H) $^{13}$C NMR (100 MHz, $CDCl_3$) δ 166.28, 162.42, 131.43, 122.97, 114.10, 72.49, 70.76, 70.49, 70.25, 69.47, 67.48, 61.58, 60.56, 14.32.

*A byproduct of the previous reaction which is a beneficial compound is the di-tosylate was also isolated*

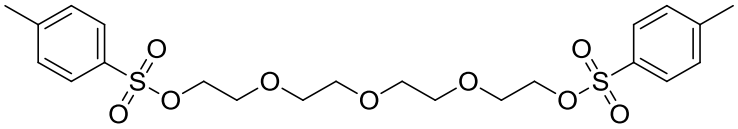

**((oxybis(ethane-2,1-diyl))bis(oxy))bis(ethane-2,1-diyl) bis(4-methylbenzenesulfonate) (43)**

TLC (7:5 Acetone:Hexane) $R_f$ = 0.38; $^1$H NMR (400 MHz, $CDCl_3$) δ 7.75 (d, *J* = 8 Hz, 4H), 7.30 (d, *J* = 10 Hz, 4H), 4.12 (t, *J* = 2 Hz, 4H), 3.64 (t, *J* = 4 Hz, 4H), 3.56-3.48 (m, 8H), 2.40 (s, 6H). $^{13}$C NMR (100 MHz, $CDCl_3$) δ 144.84, 132.94, 129.84, 127.91, 70.66, 70.49, 69.30, 68.62, 21.59.

**Method 3.2.21. Procedure for the synthesis of benzoate ester of Tetraethylene glycol**

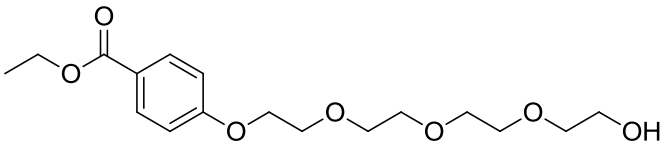

**Ethyl 4-(2-(2-(2-(2-hydroxyethoxy)ethoxy)ethoxy)ethoxy)benzoate (44)**

Mono-tosylated TEG **42** (3.0 g, 8.61 mmol), was dissolved in 15 mL MeCN followed by the addition of $K_2CO_3$ (1.78 g, 12.92 mmol). A solution of ethyl-4-hydroxybenzoate

(2.15 g, 12.92 mmol) in 5 mol MeCN was added to the mixture and allowed to stir at room temperature for 16 hrs. The reaction mixture was then filtered and the acetonitrile was evaporated off. The crude material was purified by column chromatography in 1:4 mixture of acetone:hexanes and the desired compound **44** was achieved in a 74% yield (2.20 g); TLC (7:5 Acetone:Hexane) $R_f$ = 0.45; $^1$H NMR (400 MHz, $CDCl_3$) δ 7.91 (d, *J* = 8 Hz, 2H), 6.67 (d, *J* = 8 Hz, 2H), 4.28 (q, *J* = 14 Hz, *J* = 6 Hz, 2H), 4.13 (t, *J* = 6.5 Hz, 2H), 3.81 (t, *J* = 6 Hz, 2H), 3.70-3.57 (m, 10H), 3.53 (t, *J* = 6 Hz, 2H), 2.96 (s, 1H), 1.31 (t, *J* = 6.5 Hz, 3H). $^{13}$C NMR (100 MHz, $CDCl_3$) δ 166.28, 162.42, 131.43, 122.97, 114.10, 72.7, 72.49, 70.76, 70.57, 70.49, 70.25, 69.47, 67.48, 61.58, 60.56, 14.32.

**Method 3.2.22. Procedure for the Tosylation of propargyl alcohol**

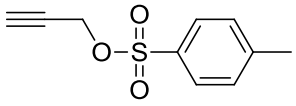

**Prop-2-yn-1-yl 4-methylbenzenesulfonate (46)** Propargyl alcohol (5.3 mL, 89.12 mmol) was dissolved in THF 100 ml followed the addition of NaH (5.3 g, 220 mmol) at 0°C and the stirred at room temperature for 1 hr. This was followed by the slow addition of a solution containing 4-toluenesulfonyl chloride (19 g, 100 mmol) in 100 mL THF via addition and then stirred at room temperature for 16 hrs. The resulting mixture was diluted with 200 mL of ethyl acetate and extracted using water (200 mL). The aqueous phase was washed with a second aliquot of ethyl acetate. The organic phases were combined and dried with $MgSO_4$ and the solvent was evaporated under preduced pressure, then purified on silica gel eluting with a ratio of 5% acetone/95% hexanes.

The desired tosylated propargyl ester **46** was isolated in 66% yield (11.2 g); TLC (7:5 Acetone:Hexane) $R_f$ = 0.47; $^1$H NMR (400 MHz, $CDCl_3$) δ 7.70 (d, *J* = 8.5 Hz, 2H), 7.28 (d, *J* = 8 Hz, 2H), 4.60 (d, *J* = 2.5 Hz, 2H), 2.51 (t, *J* = 2.5 Hz, 1H), 2.35 (s, 3H). $^{13}$C NMR (100 MHz, $CDCl_3$) δ 145.43, 132.59, 129.96, 127.96, 77.69, 75.42, 57.54, 21.53.

**Method 3.2.23. Procedure for the addition of a terminal alkyne on 44.**

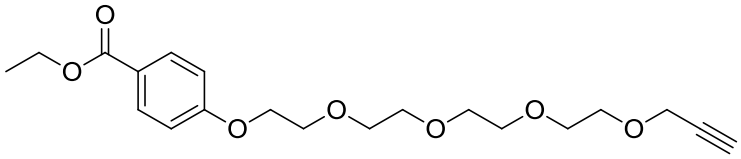

**ethyl 4-(3,6,9,12-tetraoxapentadec-14-yn-1-yloxy)benzoate (47)** Benzoate ester of TEG **44** (1.5 g, 4.38 mmol) was dissolved in THF (35 mL), NaH (263 mg, 10.96 mmol) was added to the solution at 0°C and stirred at room temperature for 1 hr. Propargyl tosylate **46** (1.47 g, 1.5 mmol) in 5 mL THF was then added dropwise and stirring was continued for 16 hrs. The resulting mixture was filtered and the solvent was evaporated under reduced pressure and purified via column chromatography with 10% acetone/90% hexanes as the eluent. The desired compound **47** was isolated in a 63% yield. TLC (7:5 Acetone:Hexane) $R_f$ = 0.48; $^1$H NMR (400 MHz, $CDCl_3$) δ 7.95 (d, *J* = 8 Hz, 2H), 6.90 (d, *J* = 8.5 Hz, 2H), 4.32 (q, *J* = 14 Hz, *J* = 8 Hz, 2H), 4.20-4.13 (m, 4H), 3.85 (t, *J* = 6 Hz, 3H), 3.74-3.60 (m, 12H), 2.41 (t, *J* = 4 Hz, 1H), 1.36 (t, *J* = 4 Hz, 3H). $^{13}$C NMR (100 MHz, $CDCl_3$) δ 166.35, 162.47, 131.49, 123.08, 114.13, 79.65, 77.23, 74.50, 70.88, 70.64, 70.61, 70.41, 69.55, 69.11, 67.56, 60.62, 58.39, 14.37

**Method 3.2.24. Procedure for the synthesis of the VRT-Linker for affinity chromatography**

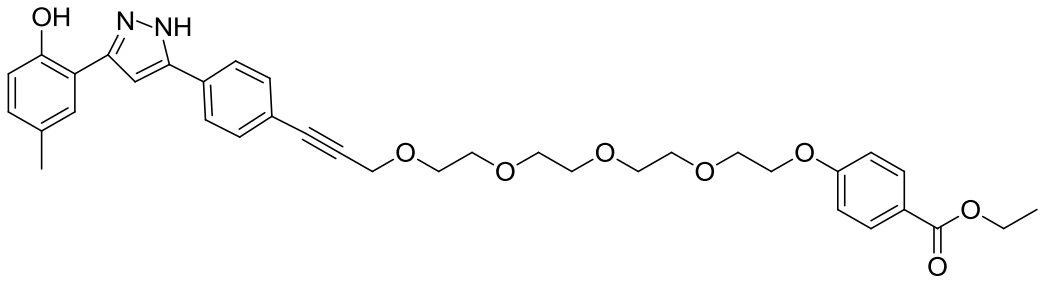


**ethyl 4-((15-(4-(3-(2-hydroxy-5-methylphenyl)-1*H*-pyrazol-5-yl)phenyl)-3,6,9,12-tetraoxapentadec-14-yn-1-yl)oxy)benzoate (48)** Iodo-VRT **5** (106.3 mg, 0.28 mmol), along with 1,1′-bis(diphenylphosphino)ferrocene]dichloropalladium(II), complex with dichloromethane (10.5 mg, 0.015 mmol) were added in a dry Schlenck flask under inert atmosphere, then evacuated and backfilled the flask. Under a stream of argon **47** (215 mg, 0.57 mmol) followed by triethylamine (60 $\mu$L, 0.42 mmol) then evacuated and backfilled with argon again. This was followed by the addition of CuI (3 mg, 0.015 mmol) under inert conditions; the flask was sealed and heated to 45°C for 20 hrs. The resulting reaction mixture was evaporated to remove the solvent and then purified on silica with 10% acetone/90% hexanes as the eluent. The desired compound **48** was isolated in an 84% yield. TLC (7:5 Acetone:Hexane) $R_f$ = 0.39; $^1$H NMR (400 MHz, $CDCl_3$) δ 7.93 (d, *J* = 9 Hz, 2H), 7.60 (d, *J* = 8 Hz, 2H), 7.45 (dd, *J* = 8 Hz, 2H), 7.41 (s, 1H), 7.03 (d, *J* = 8 Hz, 1H), 6.93 (d, *J* = 8 Hz, 1H), 6.89-6.83 (m, 3H), 4.39 (s, 2H), 4.34 (q, *J* = 14 Hz, *J* = 7 Hz, 2H), 4.10 (t, *J* = 5 Hz, 2H), 3.82 (t, *J* = 5 Hz, 2H), 3.76-3.64 (m, 12H), 2.33 (s, 3H), 1.37 (t, *J* = 7 Hz, 3H). $^{13}$C NMR (100 MHz, $CDCl_3$) δ 166.62, 162.44, 153.54, 132.31, 131.47, 129.93, 129.22, 128.42, 126.83, 125.54, 122.85,

122.71, 116.77, 116.17, 114.09, 99.30, 86.32, 85.94, 77.36, 70.69, 70.54, 70.52 70.46, 70.39, 69.46, 69.20, 67.40, 60.77, 59.13, 30.93, 20.59, 14.35

**Biological Activity**

**Method 3.2.25. Fluorescence Emission Spectra Determination of 16.**

A stock solution of **16** (5 mM in DMSO) was diluted to 20 μM in 100% chloroform, 100% methanol, 100% DMSO or buffer containing 20 mM MOPS, 75 mM KI, and 1 mM n-dodecyl-β-D-maltoside (DDM). Emission spectra were obtained with an excitation wavelength of 360 nm, and 4 nm excitation and emission bandpass, at 22°C in a 0.5 cm micro quartz cuvette on a PTI (Photon Technology International, London, ON, Canada) Quantamaster QM/80 steady state spectrofluorimeter. Curves are an average of two measurements at 0.5 nm increments with a 1s integration time and were corrected using a solvent blank measured under identical conditions.

**Method 3.2.26. Continuous Recording Cell-Based Iodide Efflux Assay.**

Using BHK cells stably expressing F508del-CFTR, continuous recording cellbased iodide efflux assays were performed as previously described. In brief, cells were grown to approximately 90−100% confluency. Cells were loaded with NaI loading buffer (3 mM $KNO_3$, 2 mM $Ca(NO_3)_2$, 11 mM glucose, 20 mM HEPES, and 136 mM NaI) at 37 °C for 1 h. NaI loading buffer was aspirated, and cells were washed four times in iodide-free efflux buffer (3 mM $KNO_3$, 2 mM $Ca(NO_3)_2$, 11 mM glucose, 20 mM HEPES, and 136

mM $NaNO_3$). Cells were scraped in 1 mL of iodide-free efflux buffer and collected by centrifugation (350 g for 5 min at 25 °C). Iodide-free efflux buffer was removed, and the cell pellet was resuspended in 400 µL of iodide-free efflux buffer. Iodide efflux was measured at room temperature using an iodide-sensitive electrode (Lazar Research Laboratories, Los Angeles, CA). F508del- CFTR at the cell surface was stimulated with 10 µM forskolin, followed by addition of 10 µM of compound (1, 9, 10, 11, 12, or 15). Five minutes after addition of each compound, Triton X-100 (Sigma) was used to lyse the cells to ensure iodide was properly loaded. The maximal iodide efflux rate was quantified over a 1 min interval associated with the largest positive slope during the 4- to 5-min time period after the addition of the activation cocktail. Traces were recorded using the Digidata 1320A data acquisition system with Clampex 8 software (Molecular Devices, Sunnyvale, CA).

**Method 3.2.27. G551D-CFTR Purification and Reconstitution.**

Mutant G551D-CFTR was purified from Sf9 cells expressing the channel with a C-terminal His10 tag from 0.5 L of culture. Cells were homogenized in the presence of protease inhibitors using an Emulsiflex C3 high-pressure homogenizer (Avenstin, Ottawa, ON. Canada), and plasma membranes were isolated on a 35% sucrose cushion by ultracentrifugation. One-fifth of the membrane pellet was solubilized by the presence of 2% fos-choline 14 (Anatrace, Maumee, OH) for 1 h with resuspension by 30 G needle, and insoluble material was removed by ultracentrifugation. The sample was bound to Ni- NTA (Qiagen Inc. Mississauga, ON, Canada), and the beads were washed with 10−50 mM imidazole buffer containing 1 mM dodecylmaltoside (DDM).

G551D-CFTR was eluted with 600 mM imidazole buffer containing 1 mM DDM, and lower molecular weight contaminants and imidazole were removed by centrifugation with an Amicon Ultra centrifugal filter device (Milipore Corp. Billerica, MA), yielding up to ~0.25 mg of pure G551D-CFTR protein per liter of culture used, in 20 mM MOPS, 75 mM KI, and 1 mM DDM, pH 7.4. G551D-CFTR was reconstituted into 5 mg of egg phosphatidylcholine (Avanti Polar Lipids, Alabaster, AB) at a protein:lipid ratio of approximately 1:300 (w/w) by incubation in the presence of 20 mM MOPS, 75 mM KI, 1 mM DDM, and lipid for 30 min, followed by passage through an Extracti-Gel D detergent-binding column (Pierce Corp. Rockford, IL).

## 4. CONCLUSION

To help reveal the nature of interaction between VRT-532 and the ΔF508-CFTR proteins which still remains a mystery, useful molecular probes for biochemical studies based on the structure of **1** have been synthesized and characterized. The azide derivative **12**, has been shown to display photoreactive capabilities generating a strong electrophile, which is beneficial for photoaffinity labeling experiments. Compounds **5, 9, 11,** and **12** have been shown to maintain the ability to potentiate channel function in live cells expressing the mutant ΔF508-CFTR, concluding that changing the substituent at the 4-position of the parent compounds phenyl ring does not hinder its potentiating capabilities. Utilizing Sonogashira coupling, iodo-VRT **5** and propargyl amine derivatives (**15**, and **17**) provide useful compounds, that include a fluorescent dansyl sulfonamide **16** and Boc protected propargyl amine-VRT **18**. The fluorescent probe **16**, exhibits almost no activity in live cells, but was active as a potentiator in a purified proteoliposome assay, suggesting that **16** maintains the ability to interact with CFTR mutants but that the larger substituent restricts its ability to cross the cell membrane. The environment-dependent fluorescence properties of **16** will make it a useful probe molecule for experiments in purified protein and/or cell lysates. Upon deprotection of Boc protected propargyl amine-VRT **18,** this compound will afford a nucleophilic primary aliphatic amine which can be readily derivatized with electrophiles to prepare new derivatives in the future. Also, it has been demonstrated that the pyrazole C4−H in 1 undergoes gradual exchange in deuterated water, with the intention of exploiting this property to incorporate radioactive tritium. Due to long reaction times and low inclusion of deuterium atoms, a new methodology is currently being studied with hopes of utilizing

the process of protodesilylation for incorporating non radiolabeled deuterium in the “Radiolabeling kit” molecule **26.** Finally, progress towards the synthesis of a stationary phase to be used for affinity chromatography, is in the final stages of completion. The attachment of this compound to a solid support resin remains, but upon completion this can be utilized by our collaborators at the Hospital for Sick Children for affinity chromatography using fragmented mutant CFTR protein, to help elucidate the nature of interaction between VRT-532 and mutant CFTR.

## 5. APPENDIX

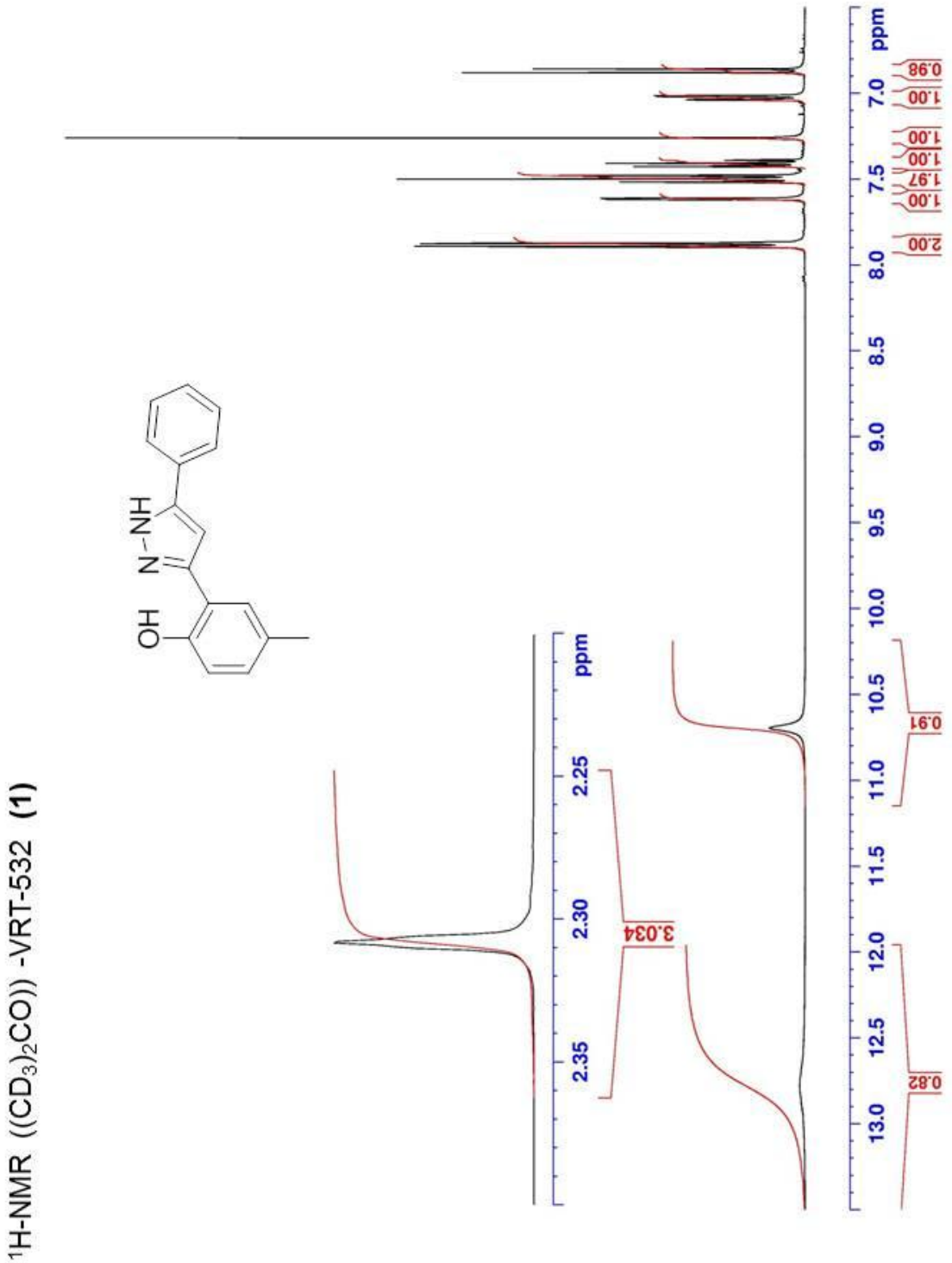
$^1$H-NMR ((CD$_3$)$_2$CO)) -VRT-532 (1)
OH
N
NH
ppm
2.25
2.30
2.35
3.034
ppm
7.0
7.5
8.0
8.5
9.0
9.5
10.0
10.5
11.0
11.5
12.0
12.5
13.0
0.98
1.00
1.00
1.00
1.97
1.00
2.00
0.91
0.82

$^{13}$C-NMR ($(CD_3)_2CO$) ) - VRT-532 **(1)**

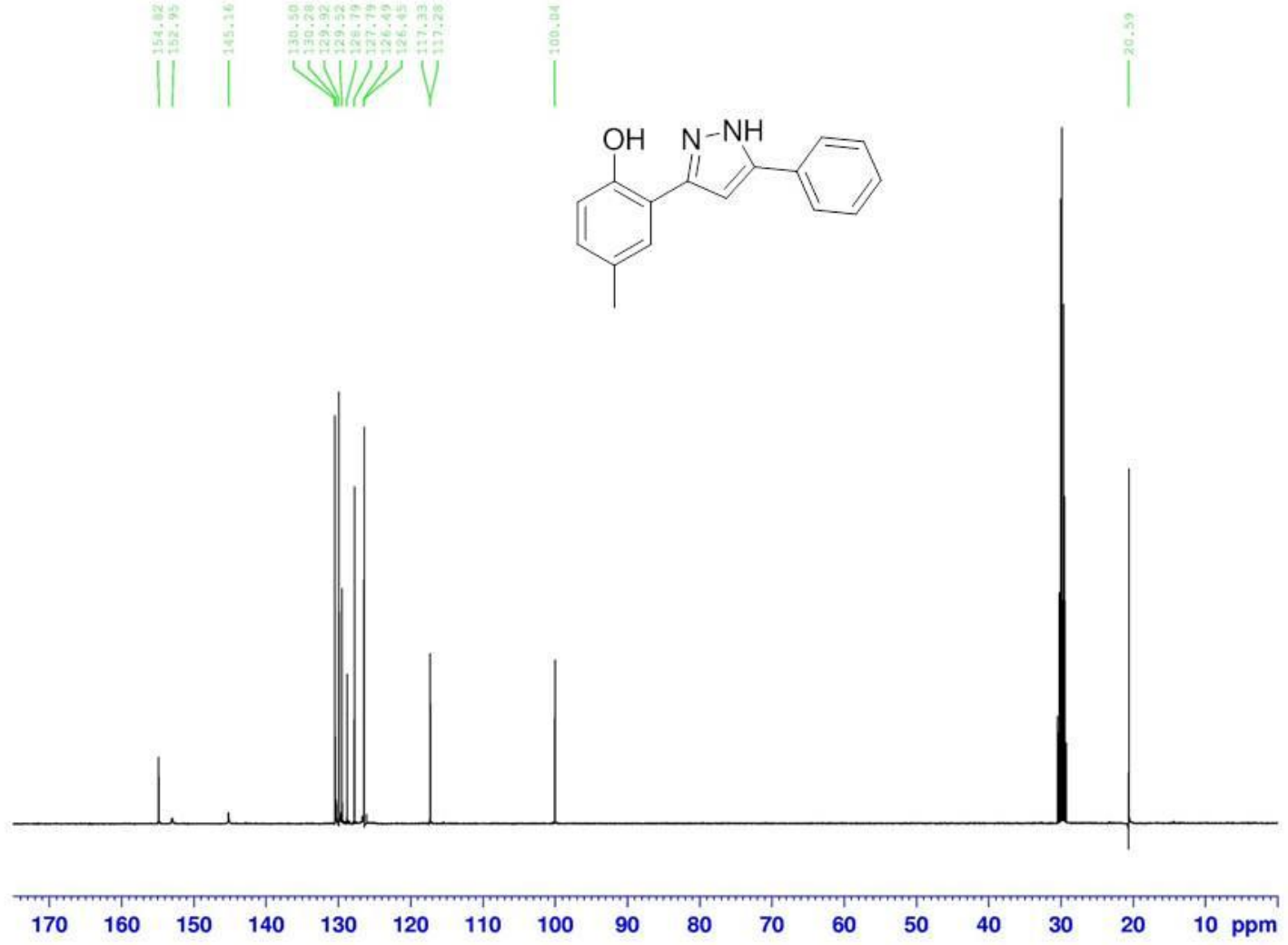

| | | | |
|---|---|---|---|
| Software Version | : 6.3.2.0646 | Date | : 8/22/2012 12:23:53 PM |
| Operator | : manager | Sample Name | : |
| Sample Number | : 003 | Study | : |
| AutoSampler | : SER200 | Rack/Vial | : 1/3 |
| Instrument Name | : HPLC | Channel | : B |
| Instrument Serial # | : None | A/D mV Range | : 1000 |
| Delay Time | : 0.00 min | End Time | : 129.99 min |
| Sampling Rate | : 2.5000 pts/s | | |
| Sample Volume | : 1.000000 ul | | |
| Sample Amount | : 1.0000 | Area Reject | : 0.000000 |
| Data Acquisition Time | : 5/5/2011 4:02:44 PM | Dilution Factor | : 1.00 |
| | | Cycle | : 1 |

Raw Data File : C:\Documents and Settings\All Users\Desktop\Old HPLC stuff\Bashar(C8-VRT)\datb003-20110505-160647.raw
Inst Method : C:\PenExe\TcWS\Ver6.3.1\Examples\Bashar(C8-VRT)\May.5.2011-(C8)-VRTsamplesSEQ from C:\Documents and Settings\All Users\Desktop\Old HPLC stuff\Bashar(C8-VRT)\datb003-20110505-160647.raw
Proc Method : C:\Documents and Settings\All Users\Desktop\Old HPLC stuff\Bashar(C8-VRT)\May.5.2011-(C8)-VRTsamplesSEQ.mth from
Calib Method : C:\Documents and Settings\All Users\Desktop\Old HPLC stuff\Bashar(C8-VRT)\May.5.2011-(C8)-VRTsamplesSEQ.mth from
Report Format File: C:\PenExe\TcWS\Ver6.3.1\Examples\Bashar(C8-VRT)\May.5.2011-(C8)-VRTsamplesSEQ.rpt
Sequence File : C:\PenExe\TcWS\Ver6.3.1\Examples\Bashar(C8-VRT)\May.5.2011-(C8)-VRTsamplesSEQ.seq

# DEFAULT REPORT

| Peak # | Time [min] | Area [µV·s] | Height [µV] | Area [%] | Norm. Area [%] | BL | Area/Height [s] |
|---|---|---|---|---|---|---|---|
| - | 0.001 | 0.00 | 0.00 | 0.00 | 0.00 | | ---------- |
| 1 | 34.373 | 19677480.80 | 661884.96 | 96.96 | 96.96 | BB | 29.7295 |
| 2 | 103.791 | 617680.80 | 120693.03 | 3.04 | 3.04 | BB | 5.1178 |
| | | 20295161.60 | 782577.99 | 100.00 | 100.00 | | |

Warning -- Signal level out-of-range in peak

Missing Component Report

| Component | Expected Retention (Calibration File) |
|---|---|
| May.5.2011-(C8)-VRTsamplesSEQ | 0.001 |

HPLC Chromatogram of VRT-532 **(1)**

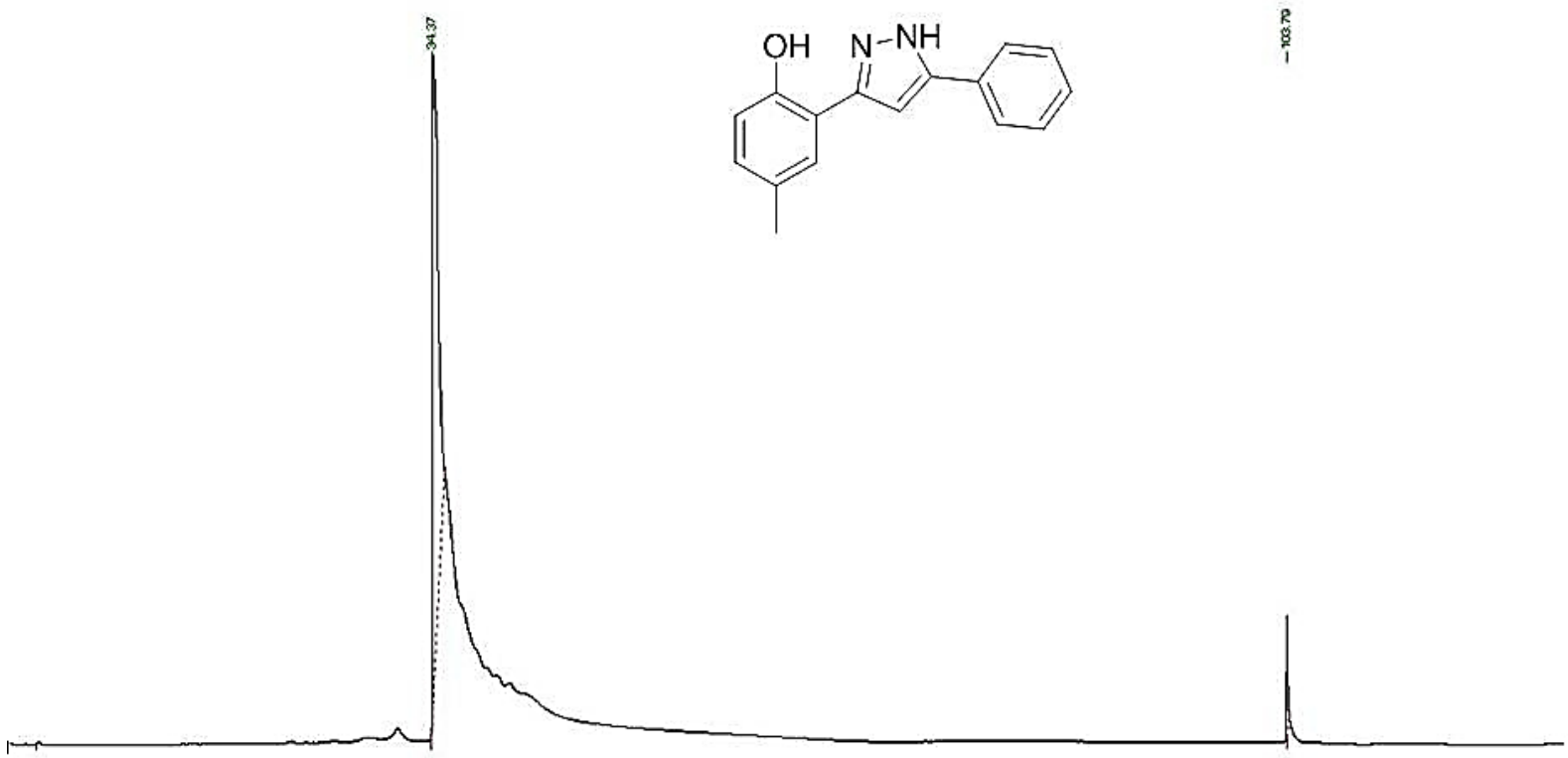

$^1$H-NMR ($(CD_3)_2SO$)) - Iodo-Ester **(4)**

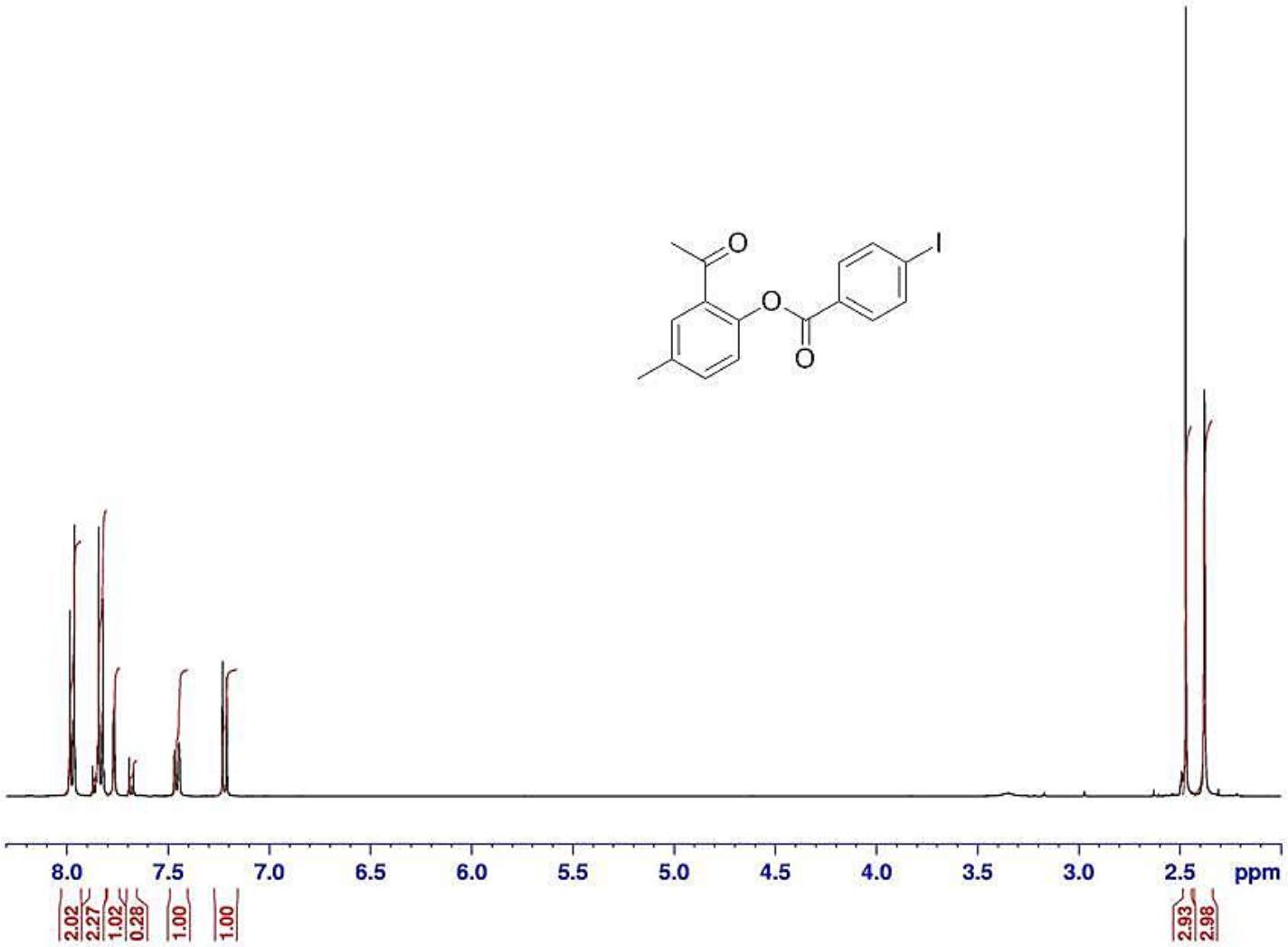

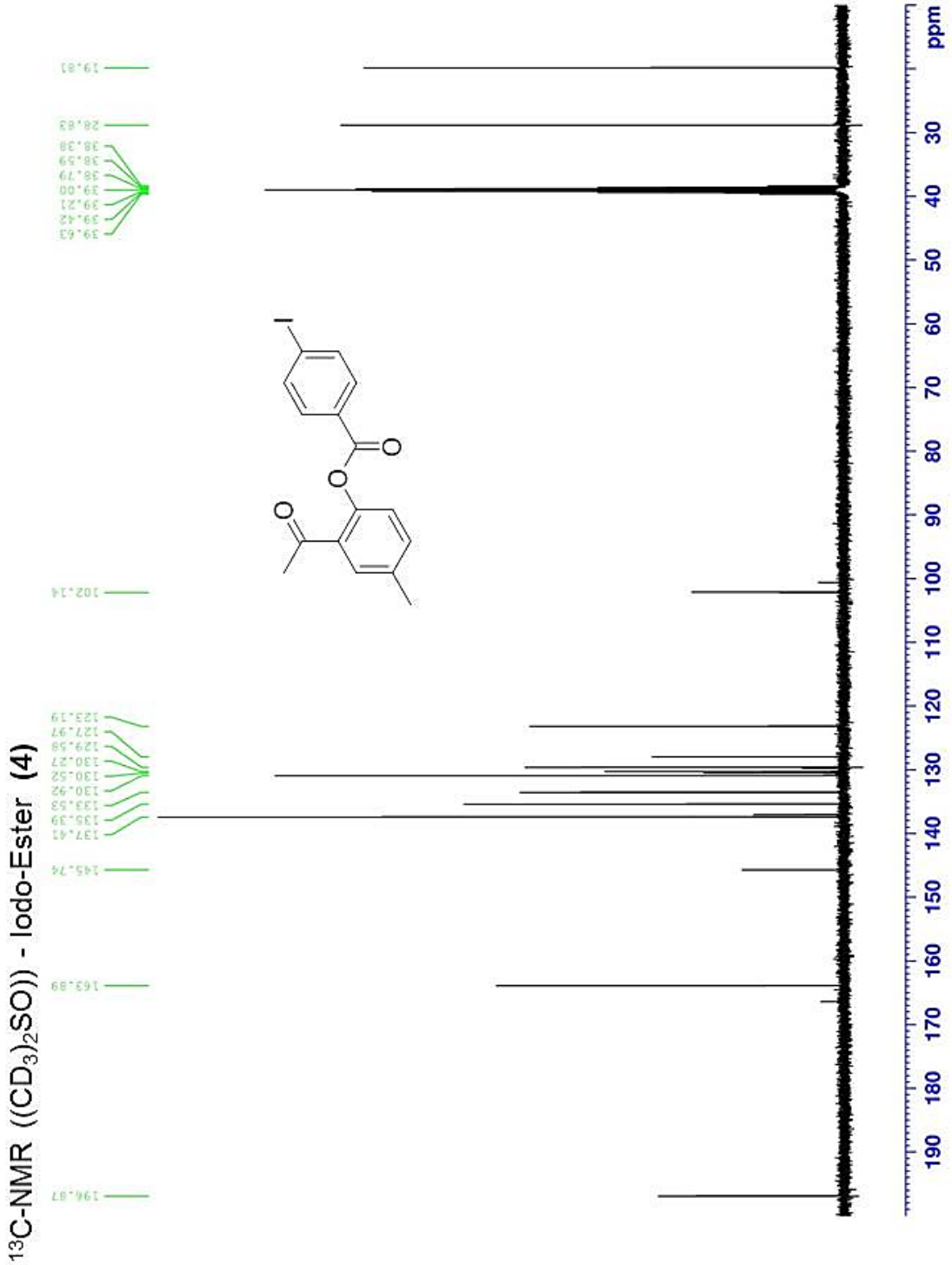
$^{13}$C-NMR ((CD$_3$)$_2$SO)) - Iodo-Ester (4)
196.87
163.89
145.74
137.41
135.39
133.53
130.92
130.52
130.27
129.58
127.97
123.19
102.14
39.63
39.42
39.21
39.00
38.79
38.59
38.38
28.83
19.81
I
O
O
O
ppm
190
180
170
160
150
140
130
120
110
100
90
80
70
60
50
40
30

$^1$H-NMR ($(CD_3)_2CO$)) - Iodo-VRT **(5)**

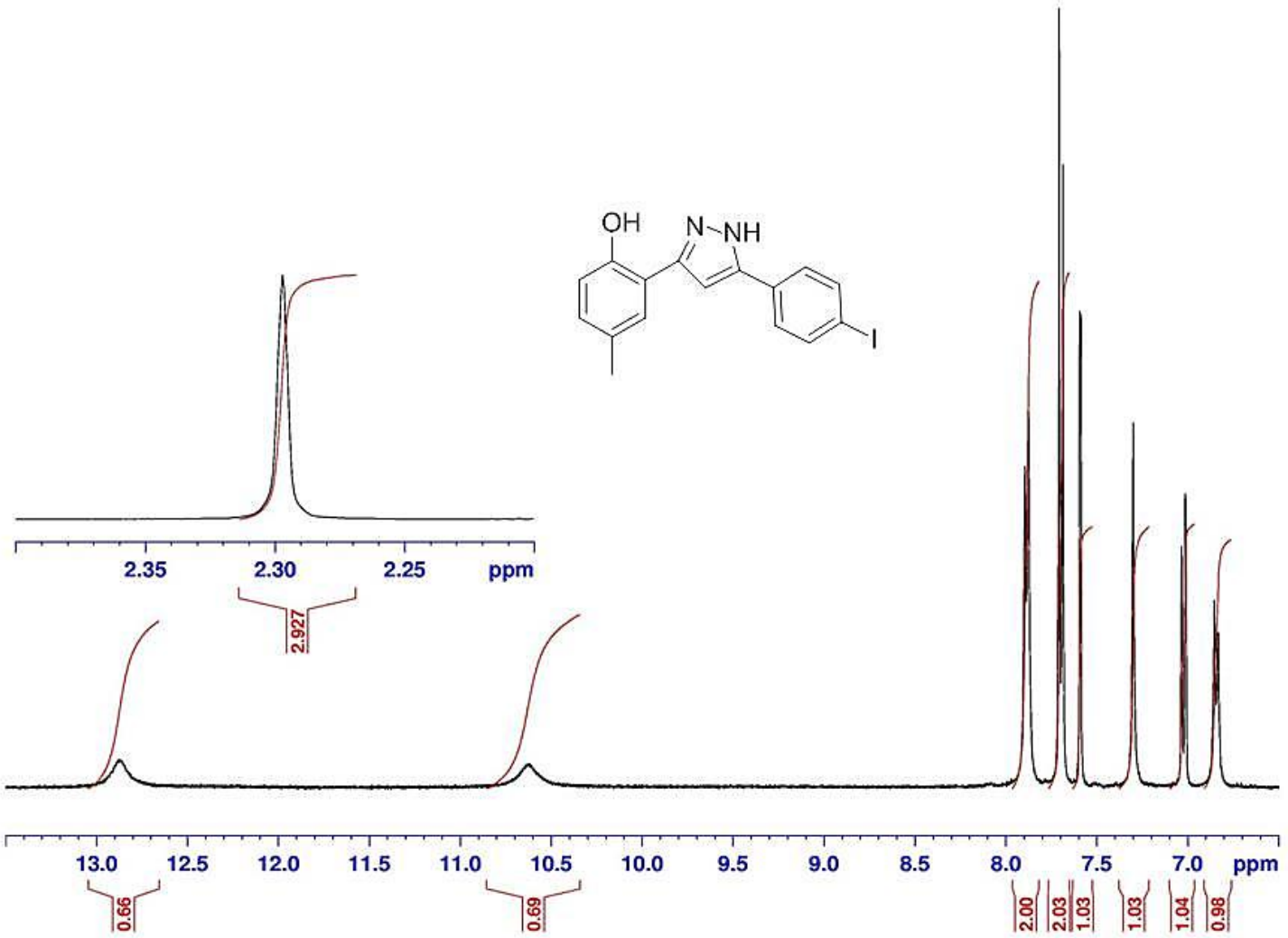

$^{13}$C-NMR ($(CD_3)_2CO$)) - Iodo-VRT **(5)**

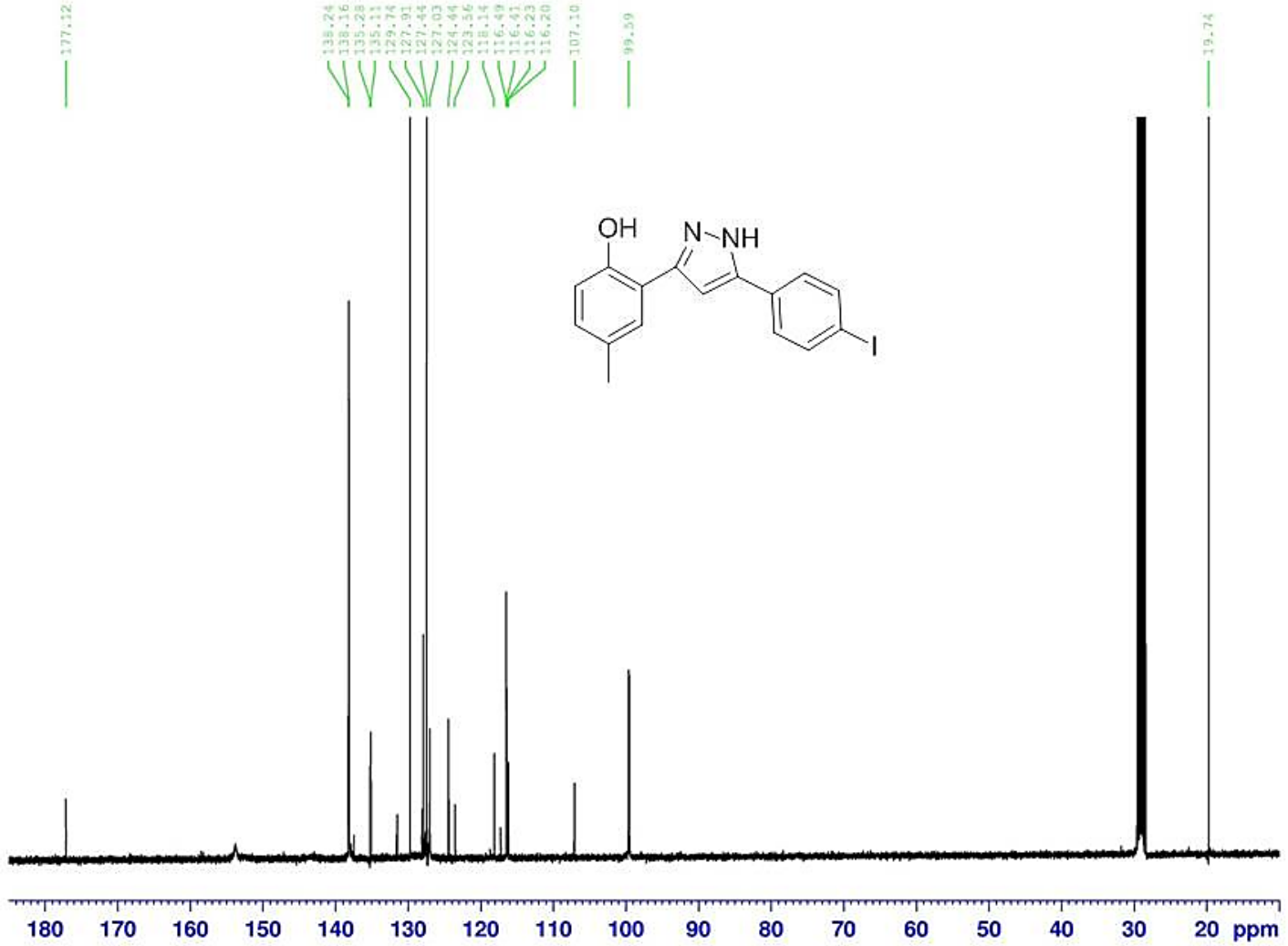

| | | | |
|---|---|---|---|
| Software Version | : 6.3.2.0646 | Date | : 8/21/2012 2:56:27 PM |
| Operator | : manager | Sample Name | : iodo |
| Sample Number | : 001 | Study | : |
| AutoSampler | : SER200 | Rack/Vial | : 1/1 |
| Instrument Name | : HPLC | Channel | : B |
| Instrument Serial # | : None | A/D mV Range | : 1000 |
| Delay Time | : 0.00 min | End Time | : 129.99 min |
| Sampling Rate | : 2.5000 pts/s | | |
| Sample Volume | : 1.000000 ul | Area Reject | : 0.000000 |
| Sample Amount | : 1.0000 | Dilution Factor | : 1.00 |
| Data Acquisition Time | : 7/6/2011 3:27:11 PM | Cycle | : 1 |

Raw Data File : C:\Documents and Settings\All Users\Desktop\Old HPLC stuff\Bashar(C8-VRT)\datb001-20110706-152718.raw
Inst Method : C:\PenExe\TcWS\Ver6.3.1\Examples\Bashar(C8-VRT)\July.6.2011-VRT-samples from C:\Documents and Settings\All Users\Desktop\Old HPLC stuff\Bashar(C8-VRT)\datb001-20110706-152718.raw
Proc Method : C:\Documents and Settings\All Users\Desktop\Old HPLC stuff\Bashar(C8-VRT)\July.6.2011-VRT-samples.mth from
Calib Method : C:\Documents and Settings\All Users\Desktop\Old HPLC stuff\Bashar(C8-VRT)\July.6.2011-VRT-samples.mth from
Report Format File: C:\PenExe\TcWS\Ver6.3.1\Examples\Bashar(C8-VRT)\July.6.2011-VRT-samples.rpt
Sequence File : C:\PenExe\TcWS\Ver6.3.1\Examples\Bashar(C8-VRT)\July.6.2011-VRTseq.seq

# DEFAULT REPORT

| Peak # | Time [min] | Area [µV·s] | Height [µV] | Area [%] | Norm. Area [%] | BL | Area/Height [s] |
|---|---|---|---|---|---|---|---|
| - | 0.001 | 0.00 | 0.00 | 0.00 | 0.00 | | ---------- |
| 1 | 25.823 | 26001140.00 | 258835.95 | 98.54 | 98.54 | BB | 100.4541 |
| 2 | 83.539 | 1443.40 | 542.38 | 0.01 | 0.01 | BB | 2.6612 |
| 3 | 94.905 | 385063.00 | 109069.61 | 1.46 | 1.46 | BB | 3.5304 |
| | | 26387646.40 | 368447.94 | 100.00 | 100.00 | | |

Missing Component Report

| Component | Expected Retention (Calibration File) |
|---|---|
| July.6.2011-VRT-samples | 0.001 |

HPLC Chromatogram of Iodo-VRT **(5)**

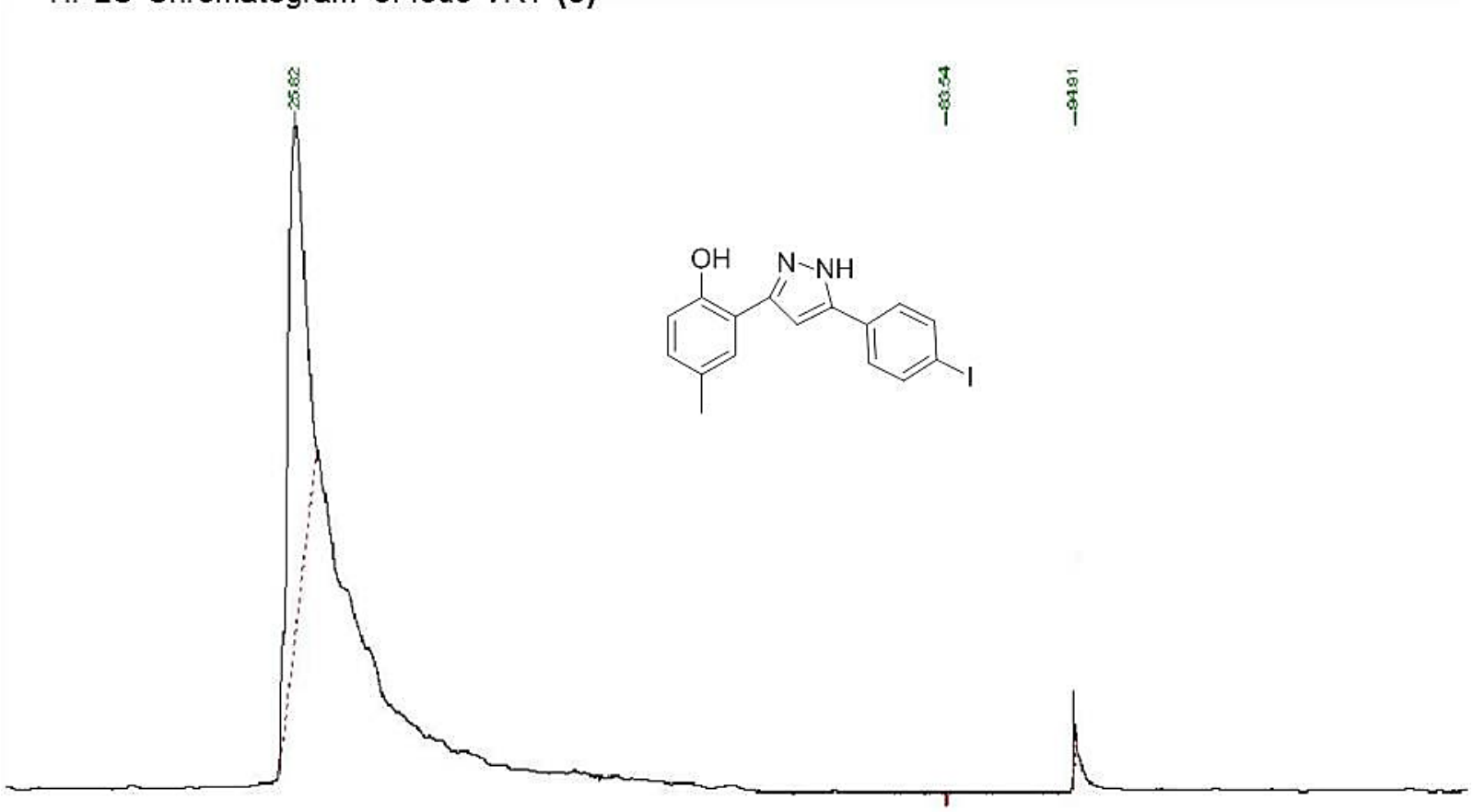

$^1$H-NMR ($(CD_3)_2CO$)) - Nitro-Ester **(7)**

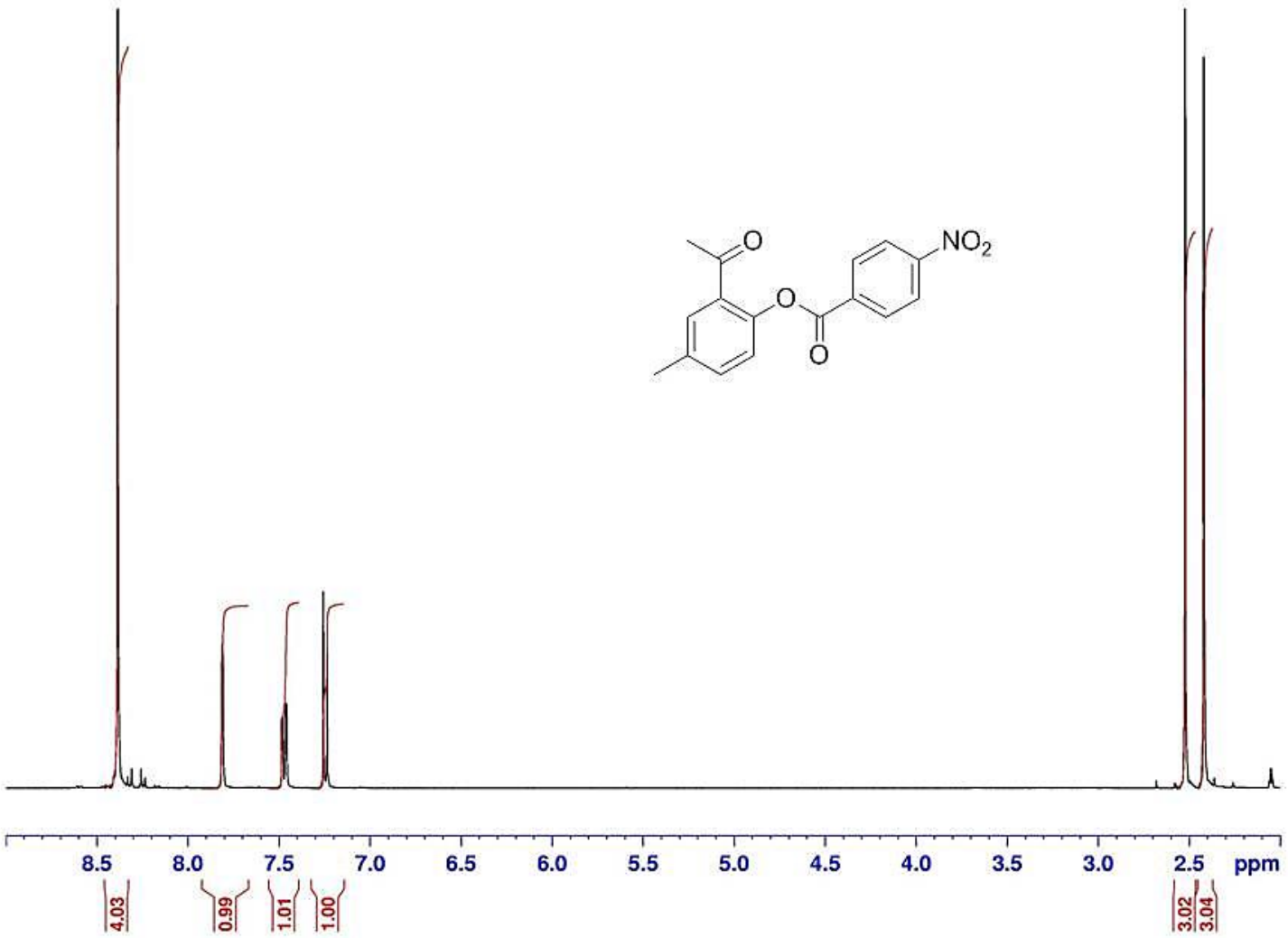

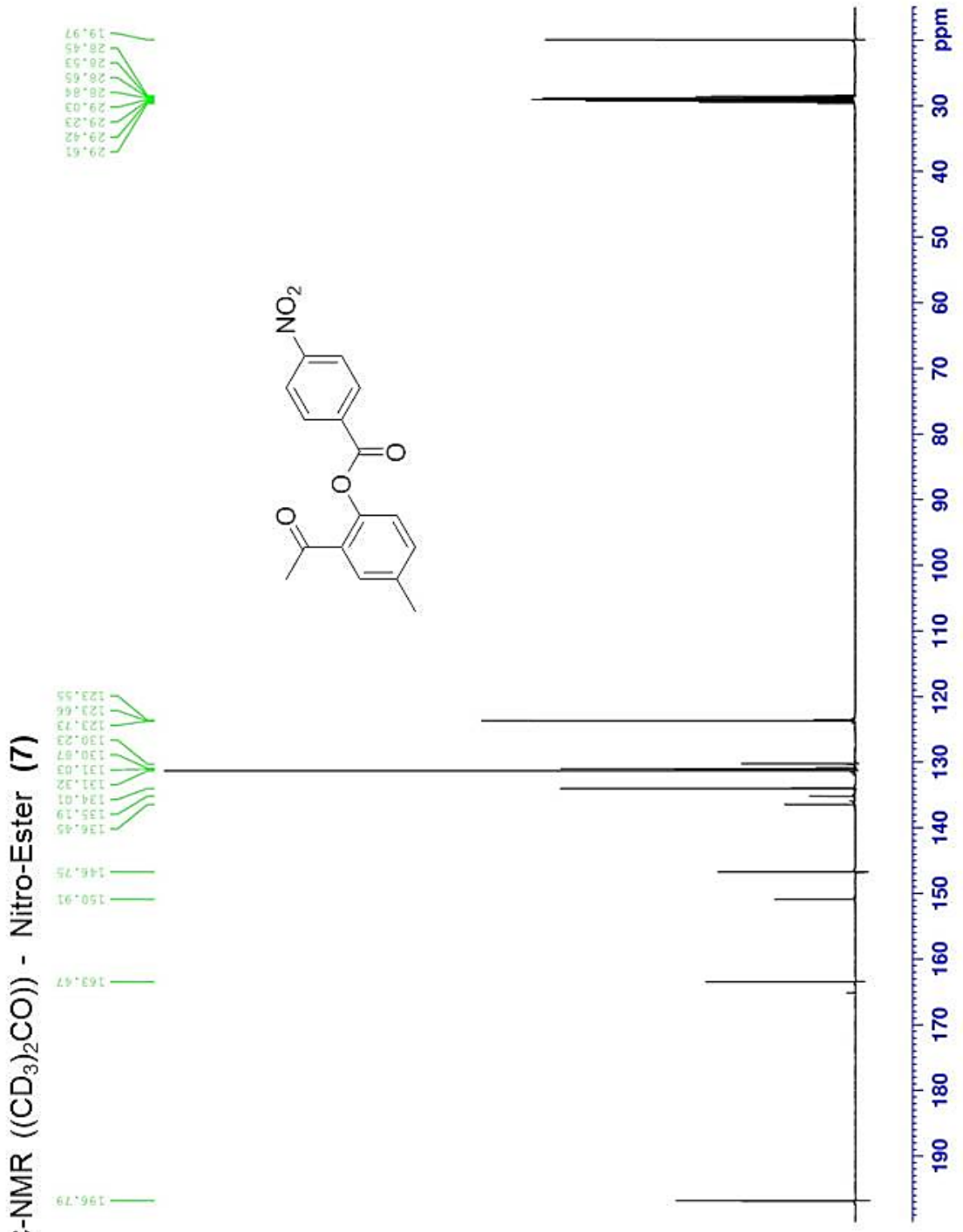
$^{13}$C-NMR ((CD$_3$)$_2$CO)) - Nitro-Ester (7)
NO$_2$
O
O
O
ppm

$^{1}$H-NMR ($(CD_3)_2CO$)) - Nitro-VRT **(9)**

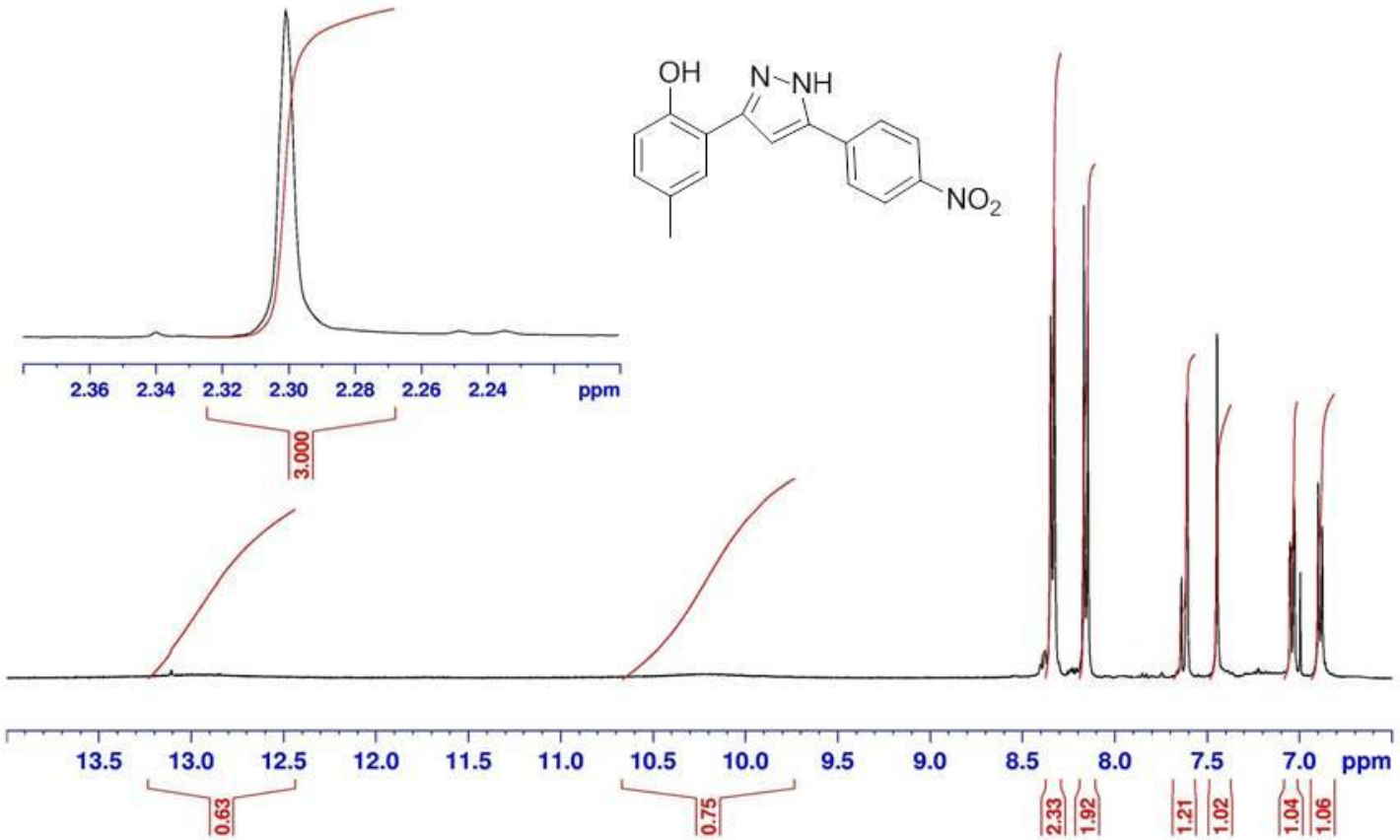

$^{13}$C-NMR $(CD_3)_2CO$ - Nitro-VRT **(9)**

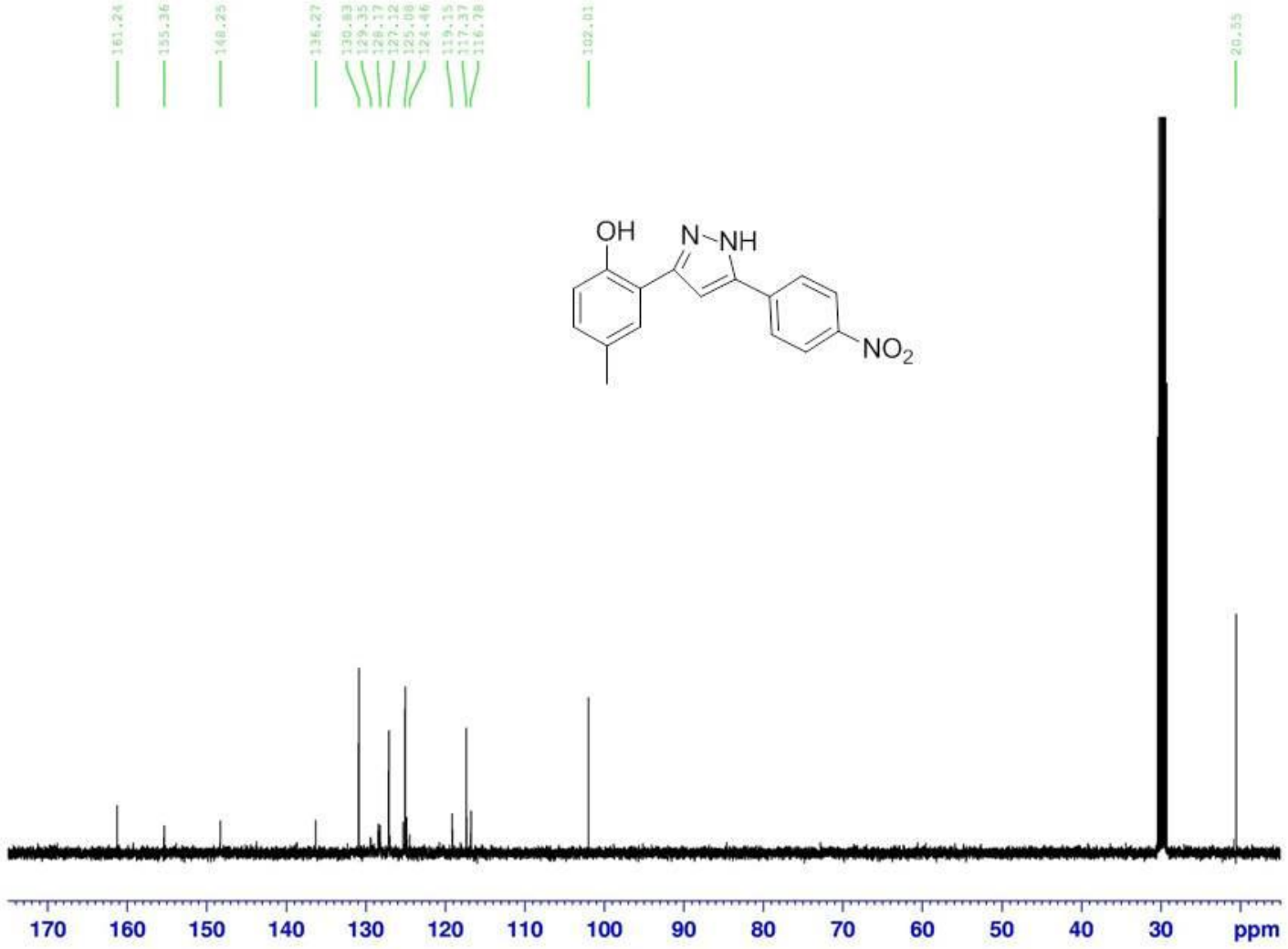

| | | | |
|---|---|---|---|
| Software Version | : 6.3.2.0646 | Date | : 8/21/2012 2:52:33 PM |
| Operator | : manager | Sample Name | : nitro |
| Sample Number | : 002 | Study | : |
| AutoSampler | : SER200 | Rack/Vial | : 1/2 |
| Instrument Name | : HPLC | Channel | : B |
| Instrument Serial # | : None | A/D mV Range | : 1000 |
| Delay Time | : 0.00 min | End Time | : 129.99 min |
| Sampling Rate | : 2.5000 pts/s | | |
| Sample Volume | : 1.000000 µL | | |
| Sample Amount | : 1.0000 | Area Reject | : 0.000000 |
| Data Acquisition Time | : 5/3/2011 9:07:45 PM | Dilution Factor | : 1.00 |
| | | Cycle | : 1 |

Raw Data File : C:\Documents and Settings\All Users\Desktop\Old HPLC stuff\Bashar(C8-VRT)\20110503-211200-nitro.raw
Inst Method : C:\PenExe\TcWS\Ver6.3.1\Examples\Bashar's Files\May.3.2011-(C8)-VRTsamplesMethod from C:\Documents and Settings\All Users\Desktop\Old HPLC stuff\Bashar(C8-VRT)\20110503-211200-nitro.raw
Proc Method : C:\HPLC Data\default.mth from
Calib Method : C:\HPLC Data\default.mth from
Report Format File: C:\PenExe\TcWS\Ver6.3.1\Examples\Bashar's Files\May.3.2011-(C8)-VRTsamplesMethod.rpt
Sequence File : C:\PenExe\TcWS\Ver6.3.1\Examples\Bashar's Files\May.3.2011-(C8)-VRTsamplesSEQ.seq

# DEFAULT REPORT

| Peak # | Time [min] | Area [µV·s] | Height [µV] | Area [%] | Norm. Area [%] | BL | Area/Height [s] |
|---|---|---|---|---|---|---|---|
| 1 | 31.230 | 2583050.80 | 187375.55 | 96.94 | 96.94 | BB | 13.7854 |
| 2 | 103.708 | 81459.80 | 28299.58 | 3.06 | 3.06 | BB | 2.8785 |
| | | 2664510.60 | 215675.13 | 100.00 | 100.00 | | |

Missing Component Report

| Component | Expected Retention (Calibration File) |
|---|---|

All components were found

HPLC Chromatogram of Nitro-VRT **(9)**

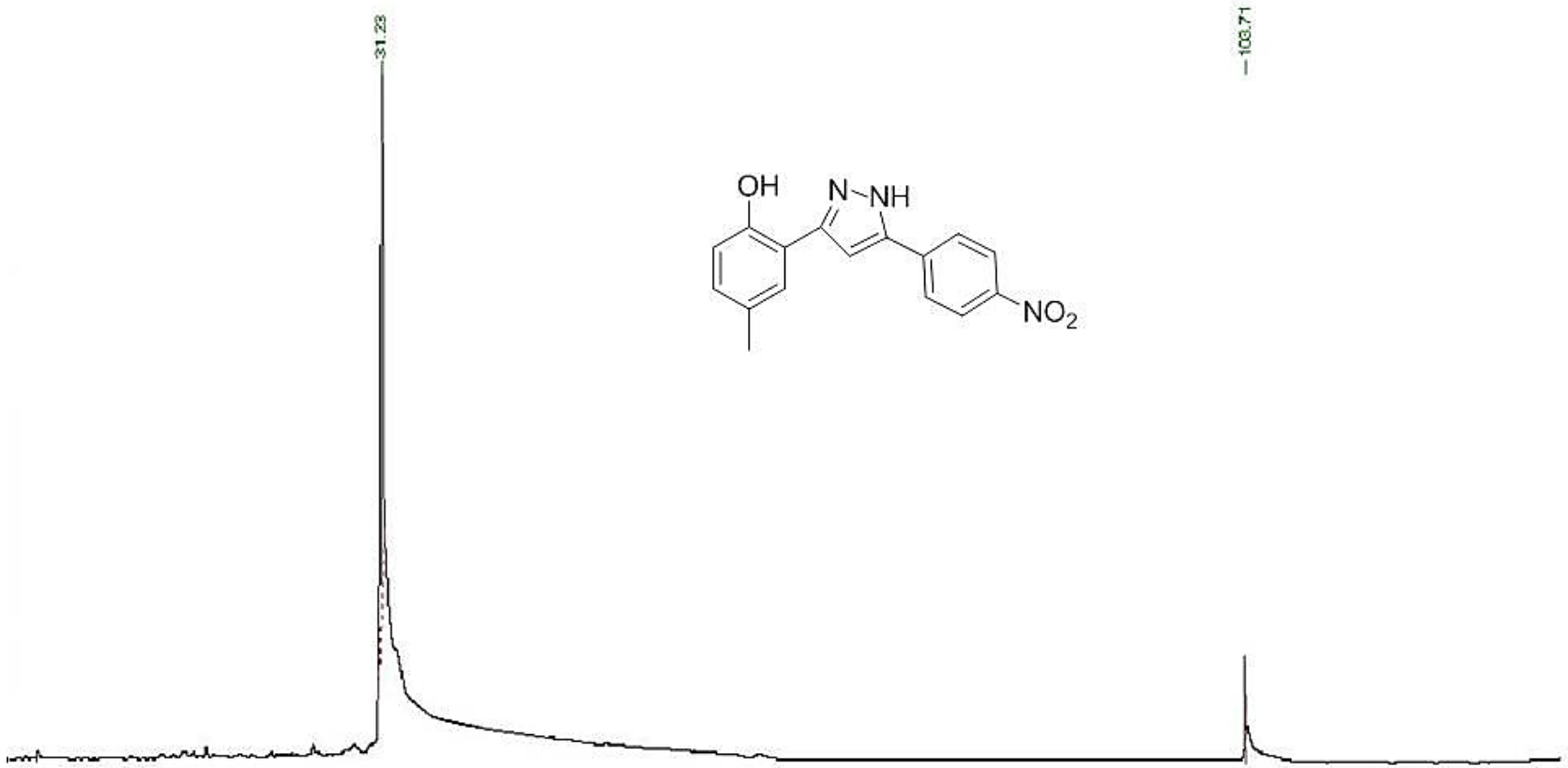

$^{1}$H-NMR $(CD_3)_2CO$) - Amino-VRT- **(11)**

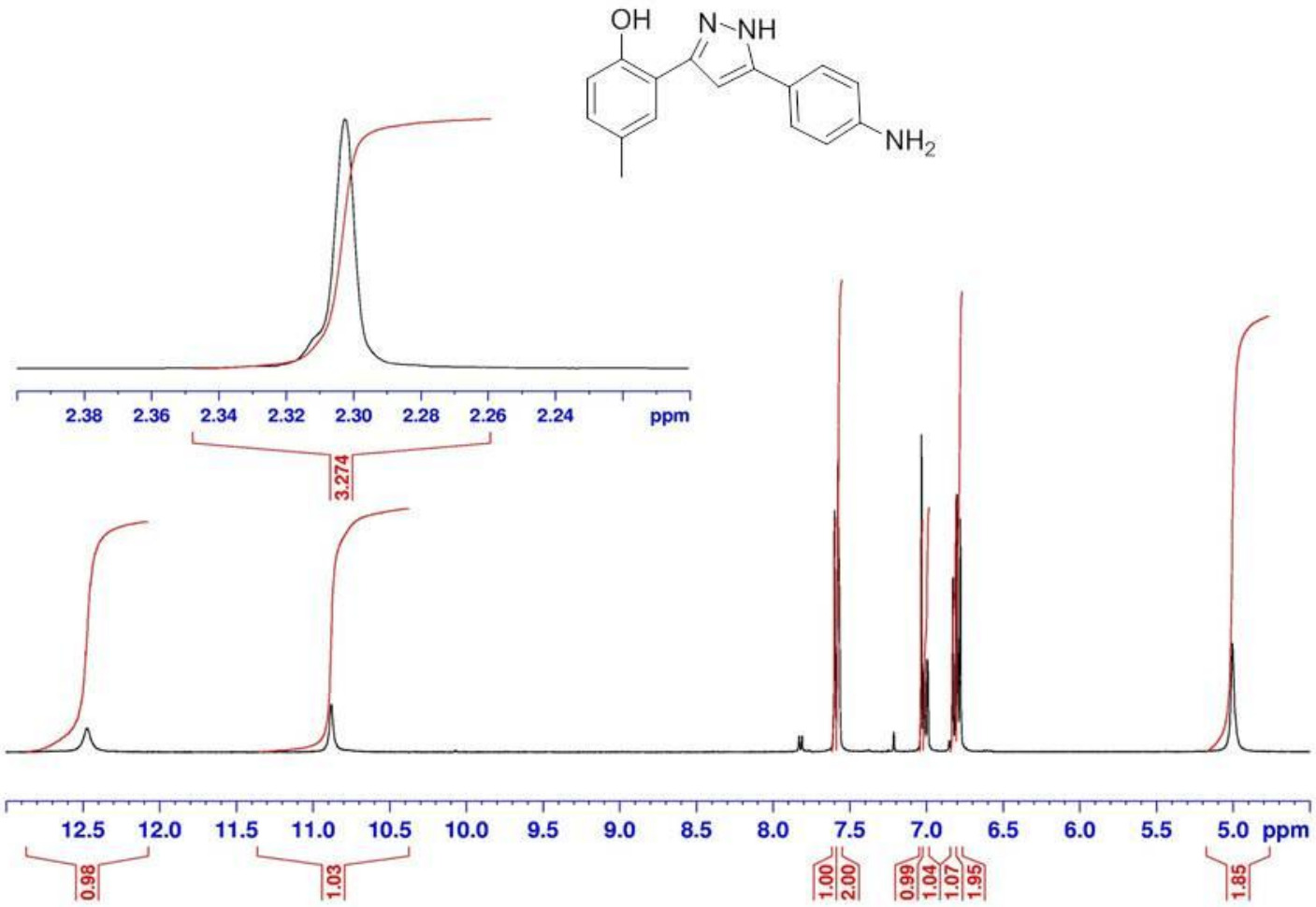

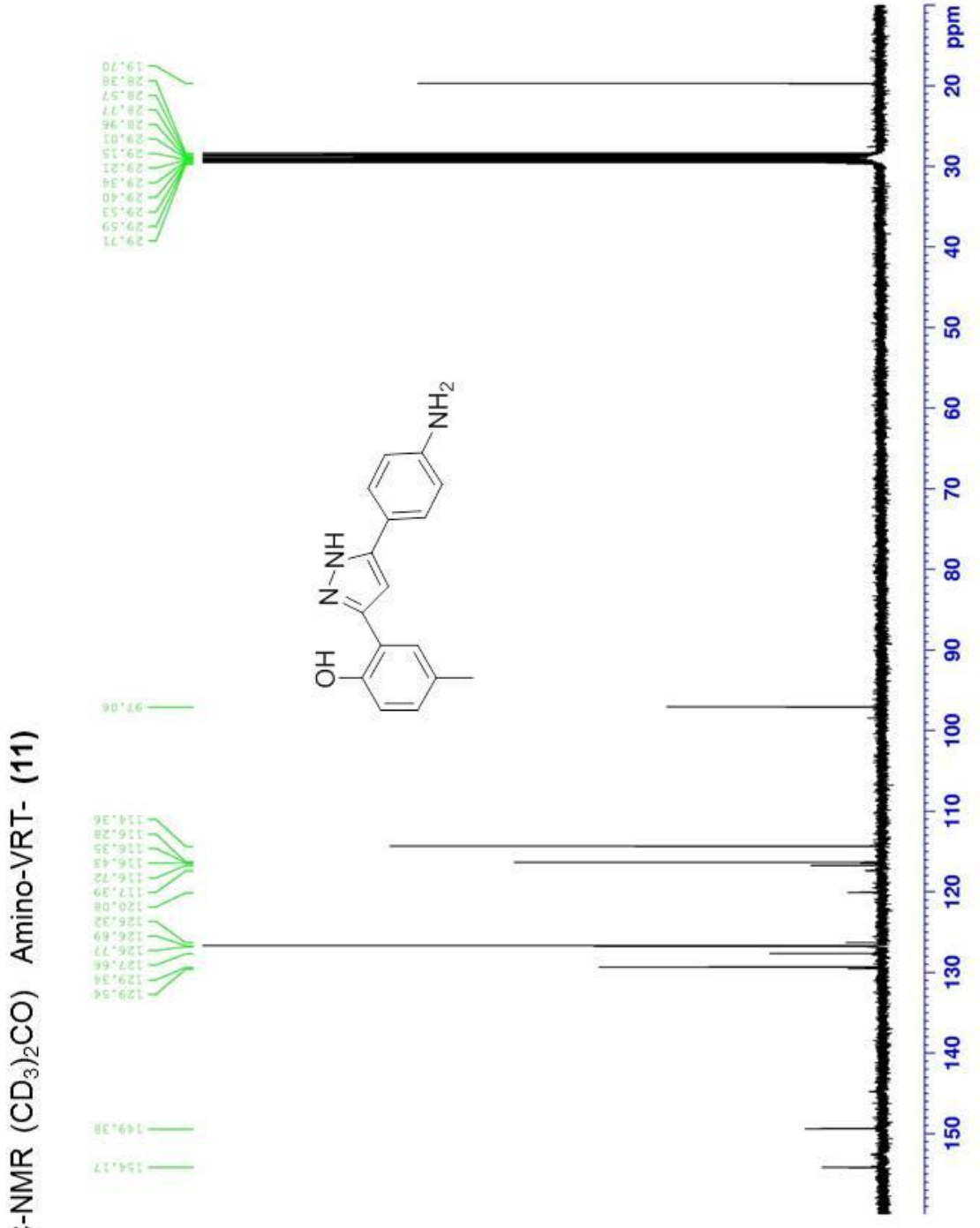
$^{13}$C-NMR $(CD_3)_2CO$) Amino-VRT- **(11)**
$NH_2$
NH
N
OH
ppm

| | | | |
|---|---|---|---|
| Software Version | : 6.3.2.0646 | Date | : 8/21/2012 2:24:50 PM |
| Operator | : manager | Sample Name | : Amino |
| Sample Number | : 001 | Study | : |
| AutoSampler | : SER200 | Rack/Vial | : 1/1 |
| Instrument Name | : HPLC | Channel | : B |
| Instrument Serial # | : None | A/D mV Range | : 1000 |
| Delay Time | : 0.00 min | End Time | : 119.99 min |
| Sampling Rate | : 2.5000 pts/s | | |
| Sample Volume | : 1.000000 µL | Area Reject | : 0.000000 |
| Sample Amount | : 1.0000 | Dilution Factor | : 1.00 |
| Data Acquisition Time | : 5/2/2011 4:34:05 PM | Cycle | : 1 |

Raw Data File : C:\Documents and Settings\All Users\Desktop\Old HPLC stuff\Bashar(C8-VRT)\20110502-163413-amino.raw
Inst Method : C:\PenExe\TcWS\Ver6.3.1\Examples\Bashar's Files\May.2.2011-(C8)-AminoMETHOD from C:\Documents and Settings\All Users\Desktop\Old HPLC stuff\Bashar(C8-VRT)\20110502-163413-amino.raw
Proc Method : C:\HPLC Data\default.mth from
Calib Method : C:\HPLC Data\default.mth from
Report Format File: C:\PenExe\TcWS\Ver6.3.1\Examples\Bashar's Files\May.2.2011-(C8)-AminoMETHOD.rpt
Sequence File : C:\PenExe\TcWS\Ver6.3.1\Examples\Bashar's Files\May.2.2011-(C8)-AminoSEQ.seq

# DEFAULT REPORT

| Peak # | Time [min] | Area [µV·s] | Height [µV] | Area [%] | Norm. Area [%] | BL | Area/Height [s] |
|---|---|---|---|---|---|---|---|
| 1 | 2.494 | 19964.00 | 2864.10 | 0.48 | 0.48 | BB | 6.9704 |
| 2 | 28.996 | 4040103.60 | 150167.40 | 97.93 | 97.93 | BB | 26.9040 |
| 3 | 83.689 | 65403.20 | 23674.68 | 1.59 | 1.59 | BB | 2.7626 |
| | | 4125470.80 | 176706.18 | 100.00 | 100.00 | | |

Missing Component Report

| Component | Expected Retention (Calibration File) |
|---|---|

All components were found

HPLC Chromatogram of Amino-VRT **(5)**

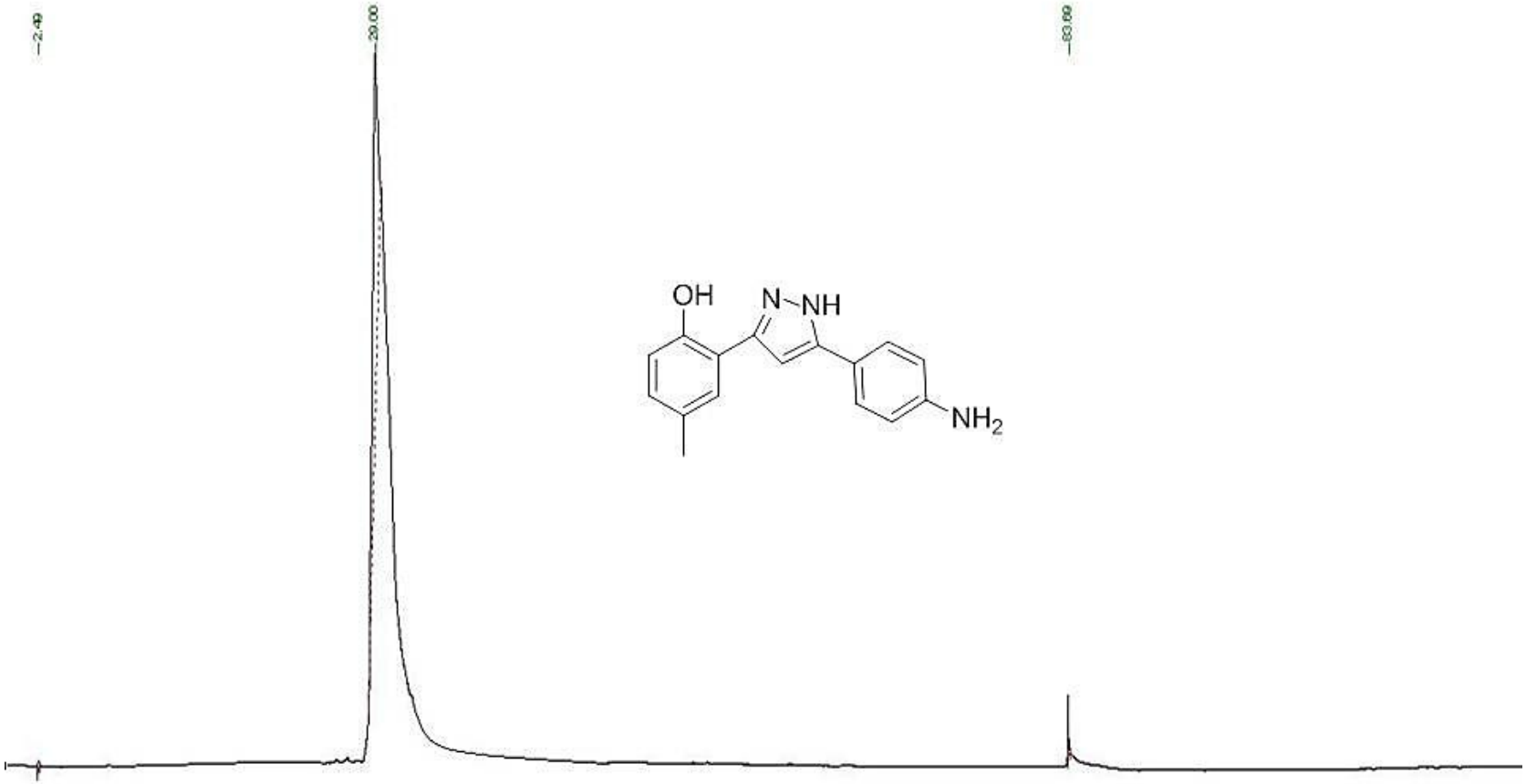

$^{1}$H-NMR $(CD_3)_2CO$) Azido-VRT- **(12)**

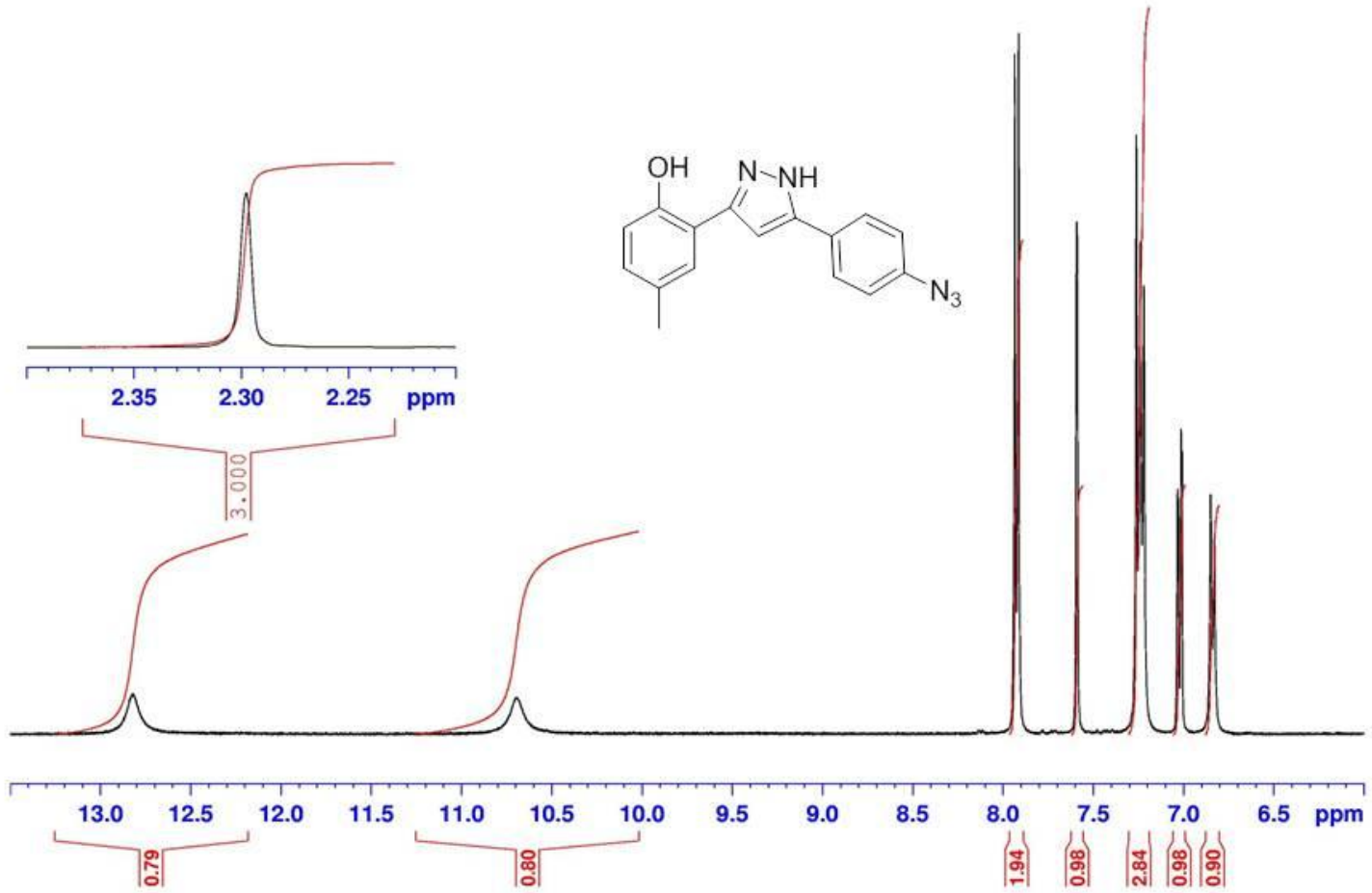

$^{13}$C-NMR $(CD_3)_2CO$) Azido-VRT- **(12)**

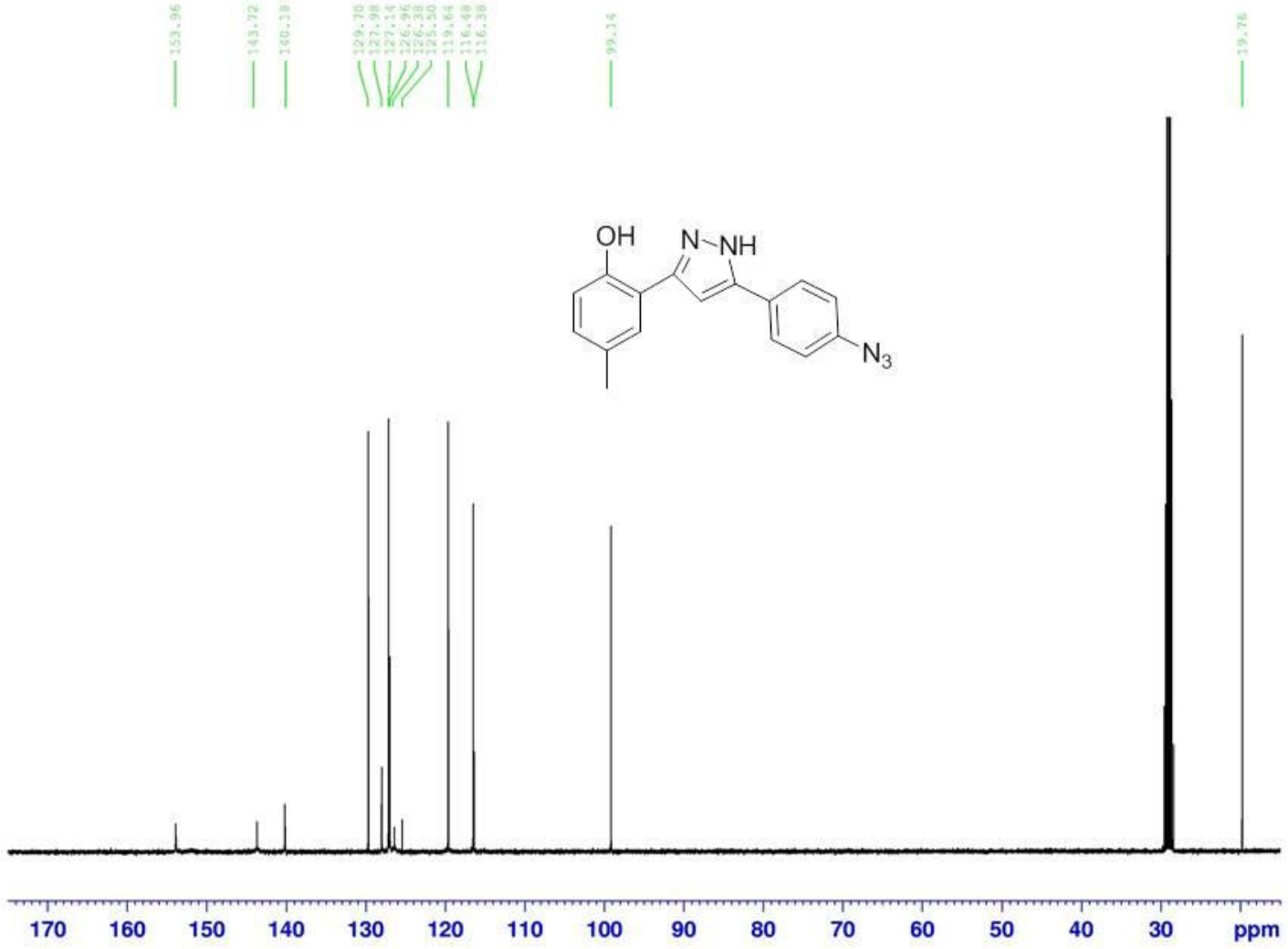

| | | | |
|---|---|---|---|
| Software Version | : 6.3.2.0646 | Date | : 8/21/2012 2:29:04 PM |
| Operator | : manager | Sample Name | : azido |
| Sample Number | : 003 | Study | : |
| AutoSampler | : SER200 | Rack/Vial | : 1/3 |
| Instrument Name | : HPLC | Channel | : B |
| Instrument Serial # | : None | A/D mV Range | : 1000 |
| Delay Time | : 0.00 min | End Time | : 129.99 min |
| Sampling Rate | : 2.5000 pts/s | | |
| Sample Volume | : 1.000000 µL | | |
| Sample Amount | : 1.0000 | Area Reject | : 0.000000 |
| Data Acquisition Time | : 5/3/2011 11:18:45 PM | Dilution Factor | : 1.00 |
| | | Cycle | : 1 |

Raw Data File : C:\Documents and Settings\All Users\Desktop\Old HPLC stuff\Bashar(C8-VRT)\20110503-232253-azido.raw
Inst Method : C:\PenExe\TcWS\Ver6.3.1\Examples\Bashar's Files\May.3.2011-(C8)-VRTsamplesMethod from C:\Documents and Settings\All Users\Desktop\Old HPLC stuff\Bashar(C8-VRT)\20110503-232253-azido.raw
Proc Method : C:\HPLC Data\default.mth from
Calib Method : C:\HPLC Data\default.mth from
Report Format File: C:\PenExe\TcWS\Ver6.3.1\Examples\Bashar's Files\May.3.2011-(C8)-VRTsamplesMethod.rpt
Sequence File : C:\PenExe\TcWS\Ver6.3.1\Examples\Bashar's Files\May.3.2011-(C8)-VRTsamplesSEQ.seq

# DEFAULT REPORT

| Peak # | Time [min] | Area [µV·s] | Height [µV] | Area [%] | Norm. Area [%] | BL | Area/Height [s] |
|---|---|---|---|---|---|---|---|
| 1 | 2.302 | 33079.40 | 4403.79 | 0.12 | 0.12 | BB | 7.5116 |
| 2 | 33.797 | 27931720.80 | 630041.28 | 98.09 | 98.09 | BB | 44.3332 |
| 3 | 103.807 | 511255.60 | 70308.63 | 1.80 | 1.80 | BB | 7.2716 |
| | | 28476055.80 | 704753.69 | 100.00 | 100.00 | | |

Missing Component Report

| Component | Expected Retention (Calibration File) |
|---|---|

All components were found

HPLC Chromatogram of Azido-VRT **(12)**

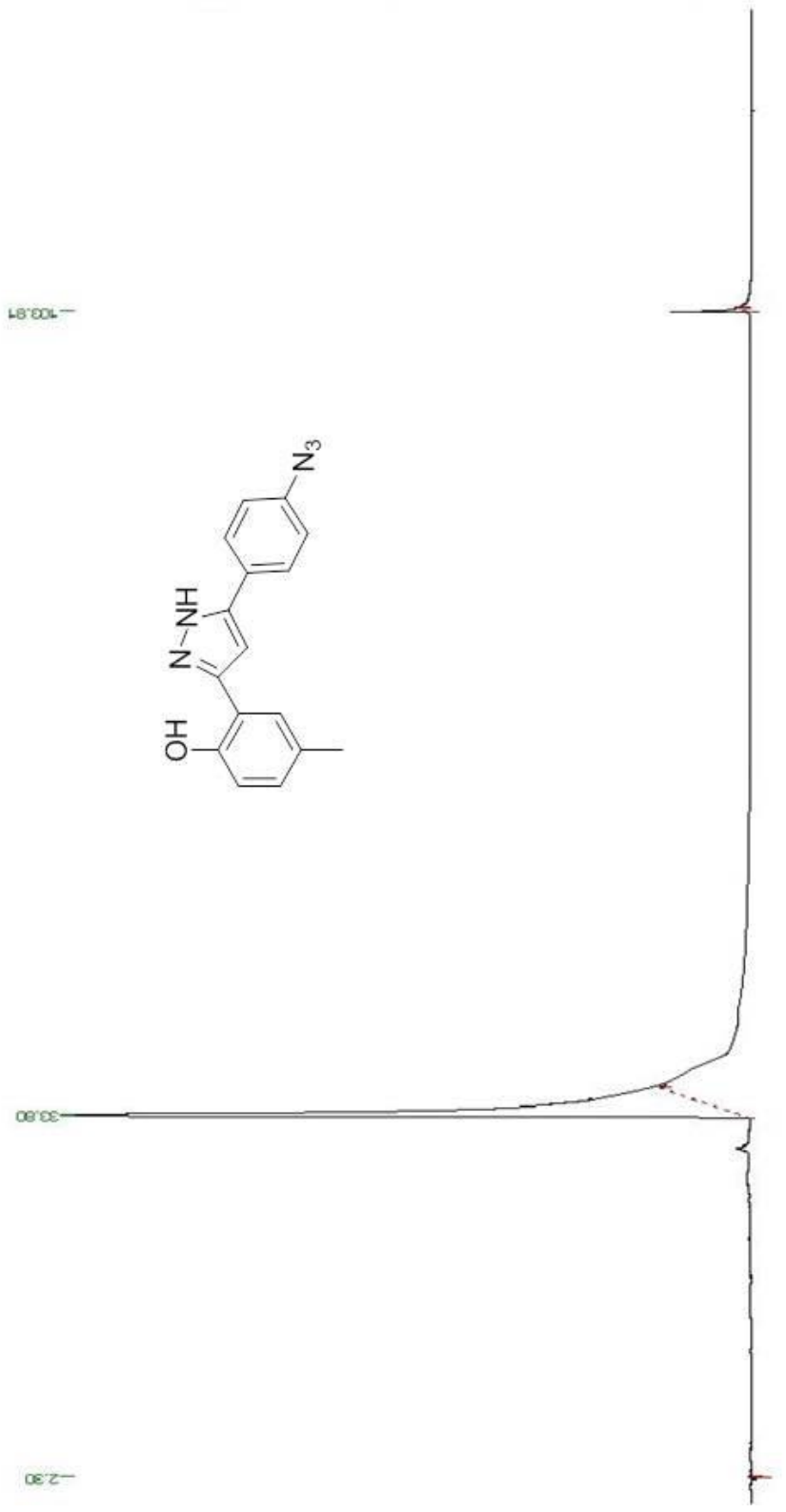

$^{1}$H-NMR ($CDCl_3$) Photolysis product

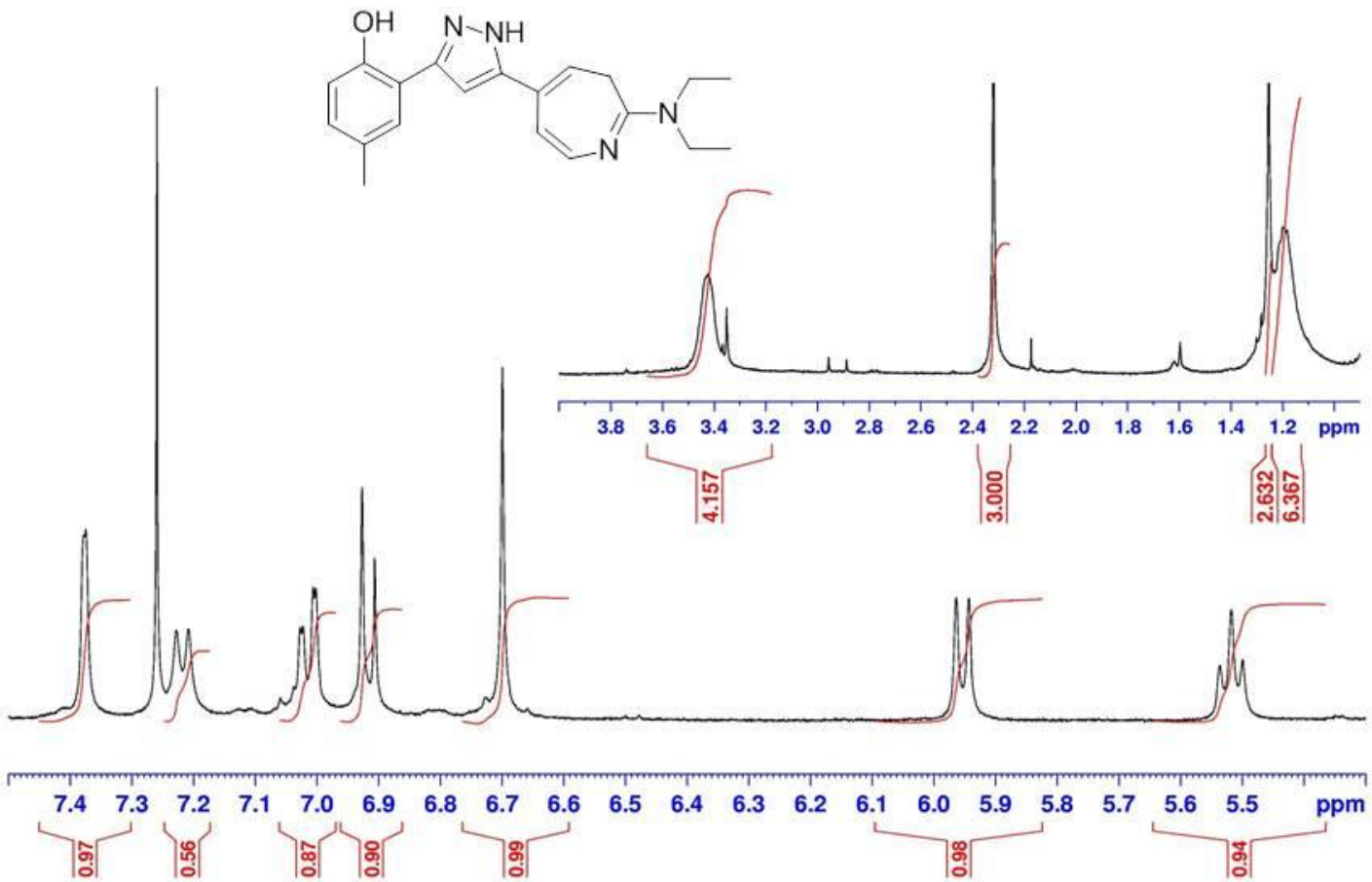

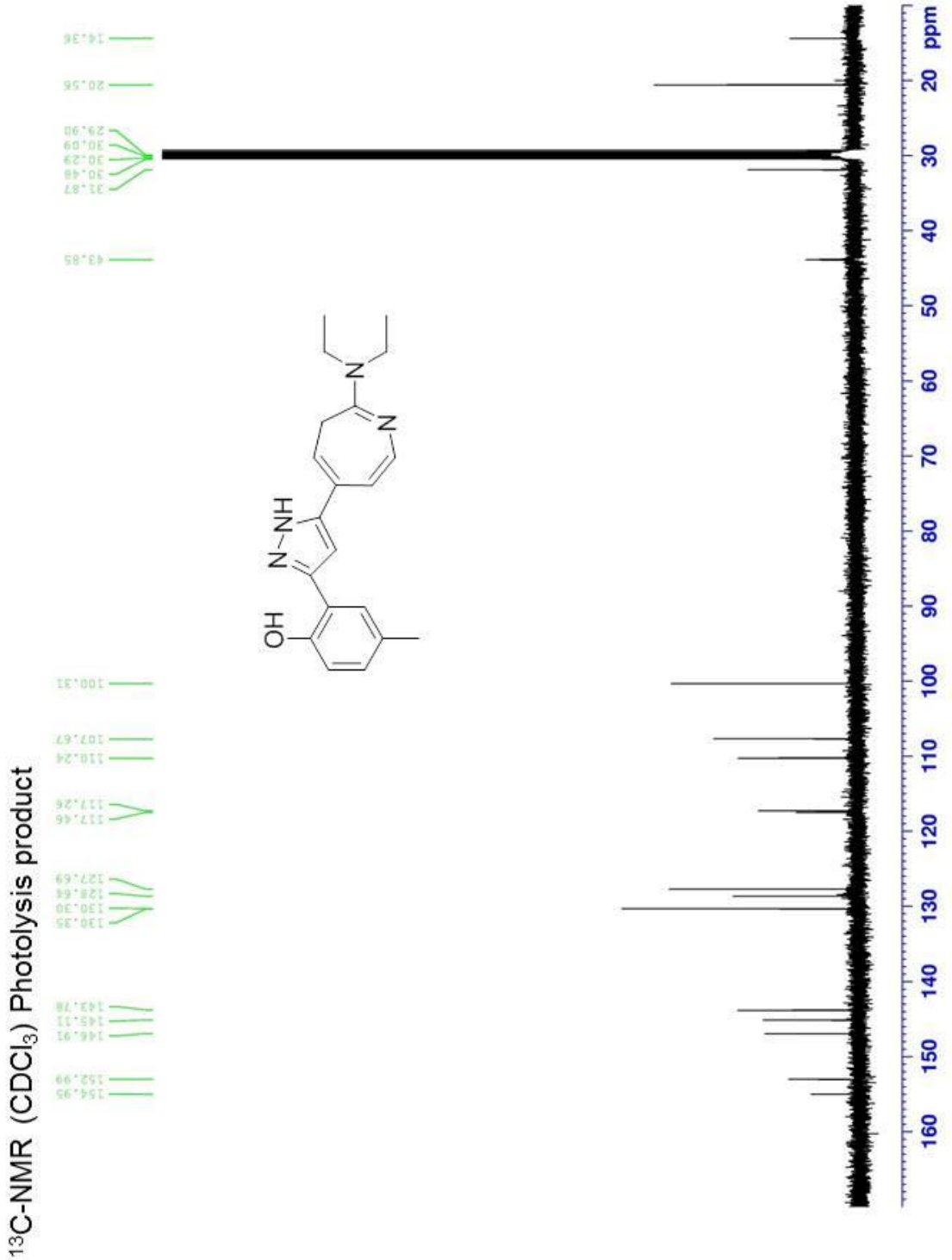
$^{13}$C-NMR ($CDCl_3$) Photolysis product
14.36
20.56
29.90
30.09
30.29
30.48
31.87
43.85
100.31
107.67
110.24
117.46
117.26
127.69
128.64
130.30
130.35
143.78
145.11
146.91
152.99
154.95
N
N
NH
N
OH
20
30
40
50
60
70
80
90
100
110
120
130
140
150
160
ppm

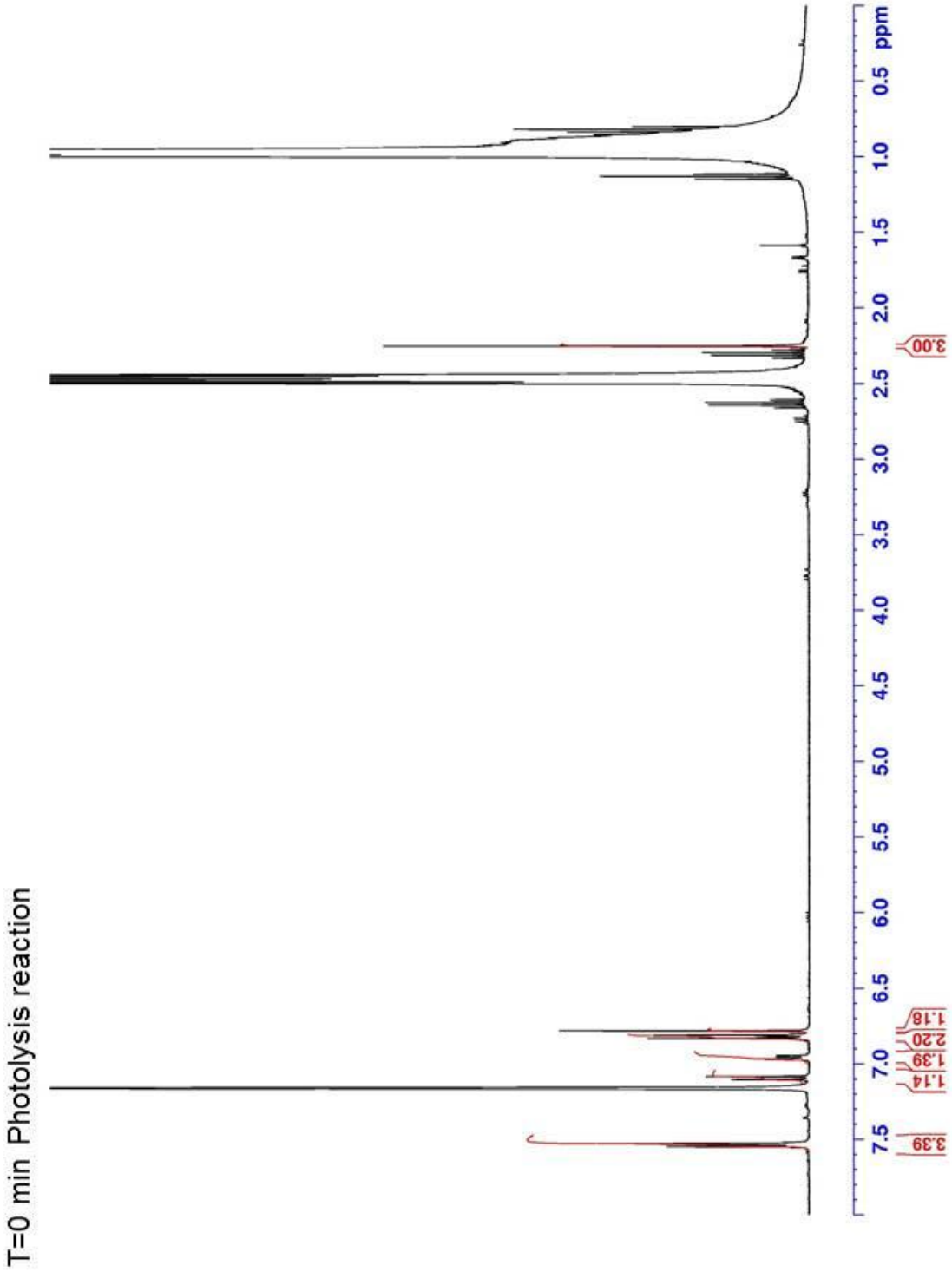
T=0 min Photolysis reaction
7.5
7.0
6.5
6.0
5.5
5.0
4.5
4.0
3.5
3.0
2.5
2.0
1.5
1.0
0.5
ppm
3.39
1.14
1.39
2.20
1.18
3.00

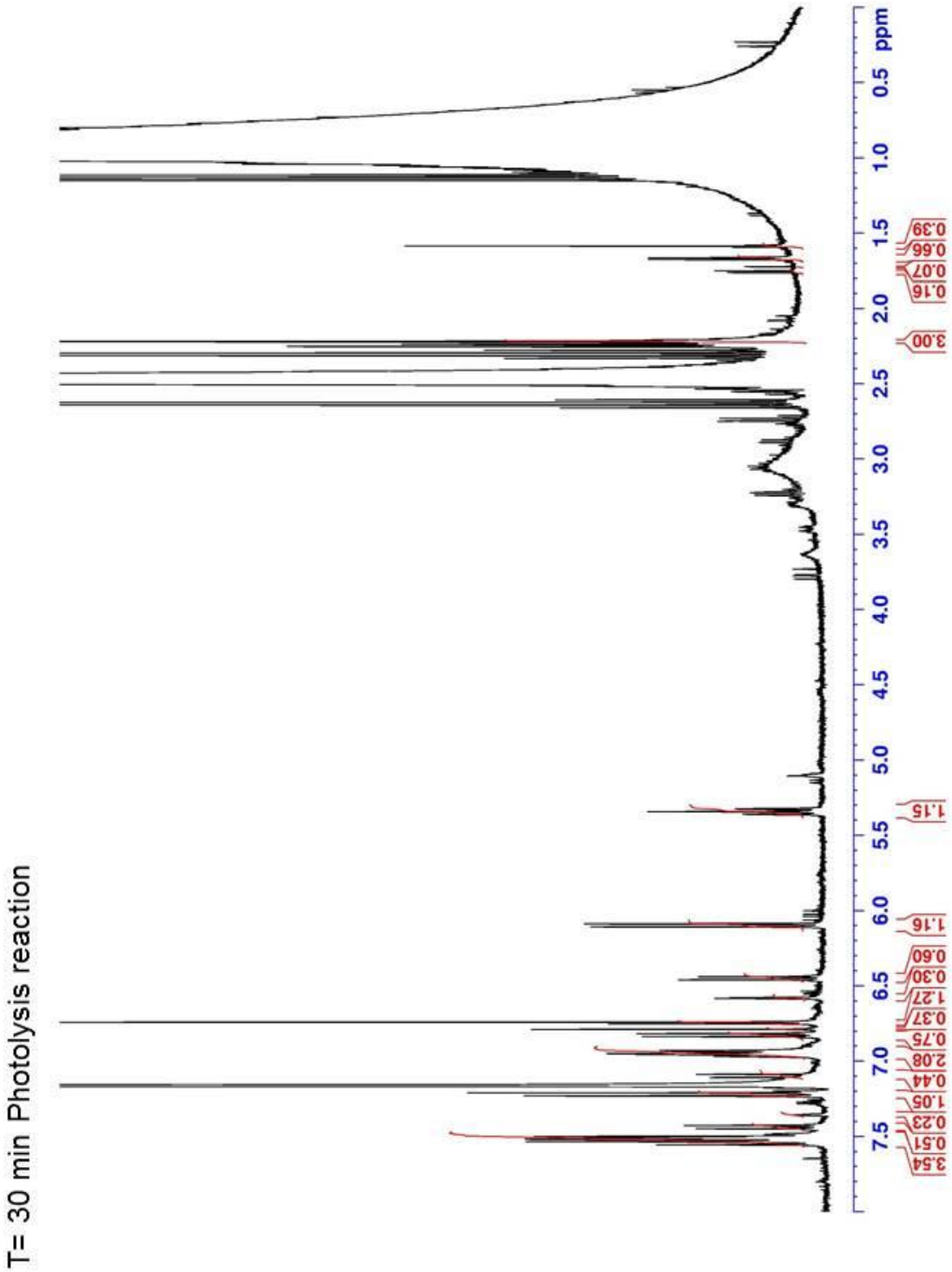
T= 30 min Photolysis reaction
ppm
0.5
1.0
1.5
2.0
2.5
3.0
3.5
4.0
4.5
5.0
5.5
6.0
6.5
7.0
7.5
3.54
0.51
0.23
1.05
0.44
2.08
0.75
0.37
1.27
0.30
0.60
1.16
1.15
3.00
0.16
0.07
0.66
0.39

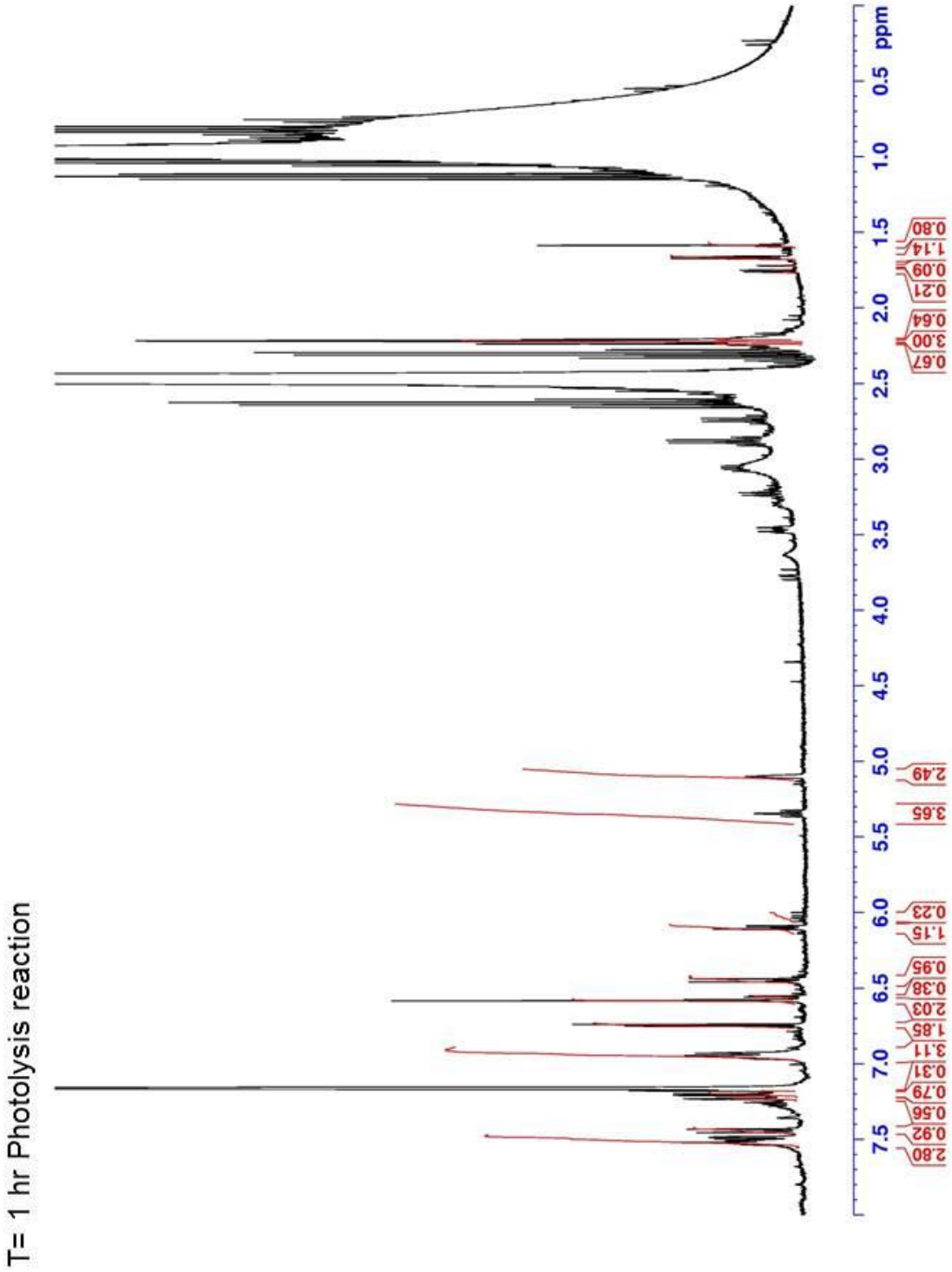
T= 1 hr Photolysis reaction
7.5
7.0
6.5
6.0
5.5
5.0
4.5
4.0
3.5
3.0
2.5
2.0
1.5
1.0
0.5
ppm
2.80
0.92
0.56
0.79
0.31
3.11
1.85
2.03
0.38
0.95
1.15
0.23
3.65
2.49
0.67
3.00
0.64
0.21
0.09
1.14
0.80

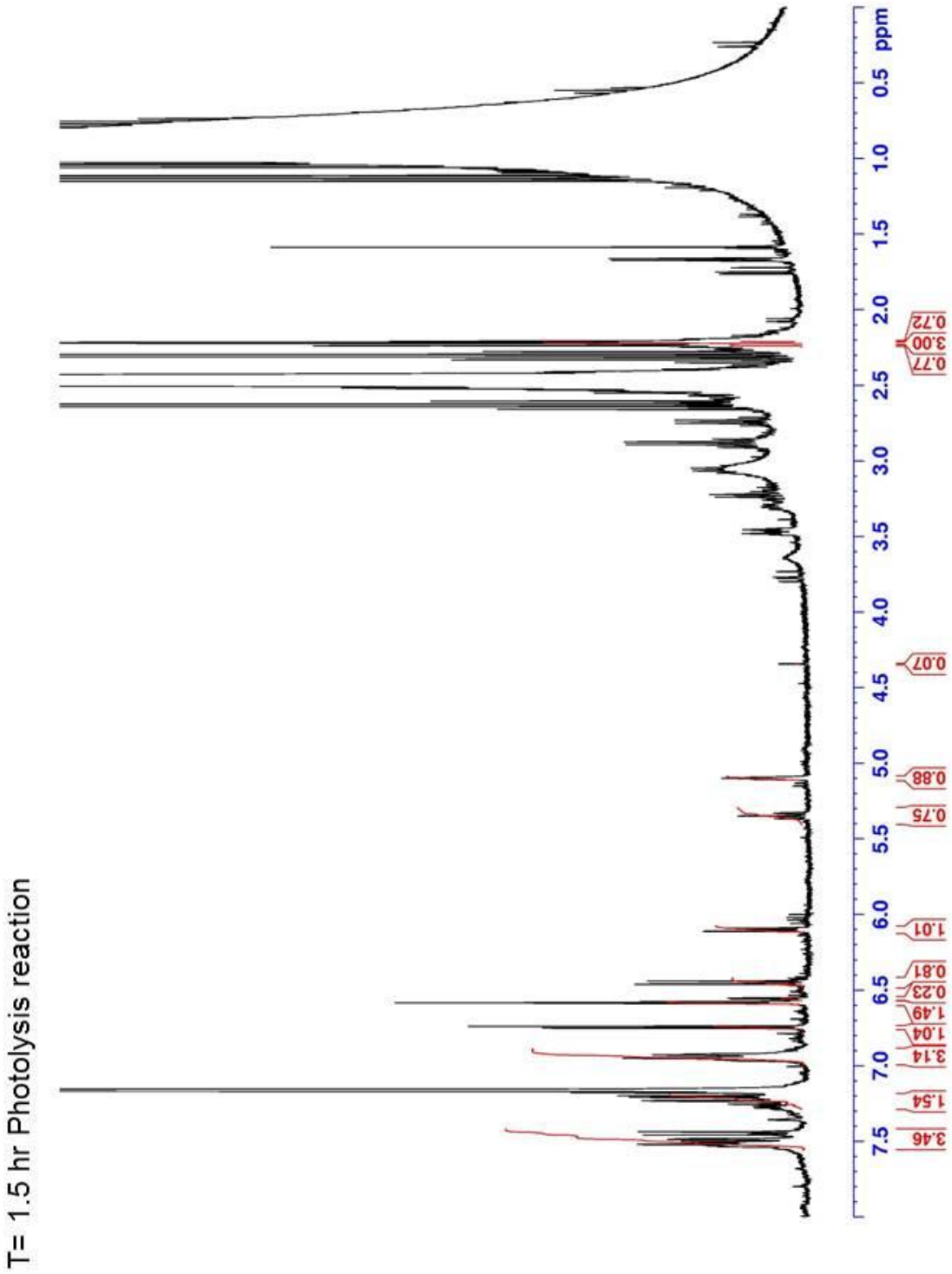
T= 1.5 hr Photolysis reaction
7.5
7.0
6.5
6.0
5.5
5.0
4.5
4.0
3.5
3.0
2.5
2.0
1.5
1.0
0.5
ppm
3.46
1.54
3.14
1.04
1.49
0.23
0.81
1.01
0.75
0.88
0.07
0.77
3.00
0.72

COSY Photolysis product

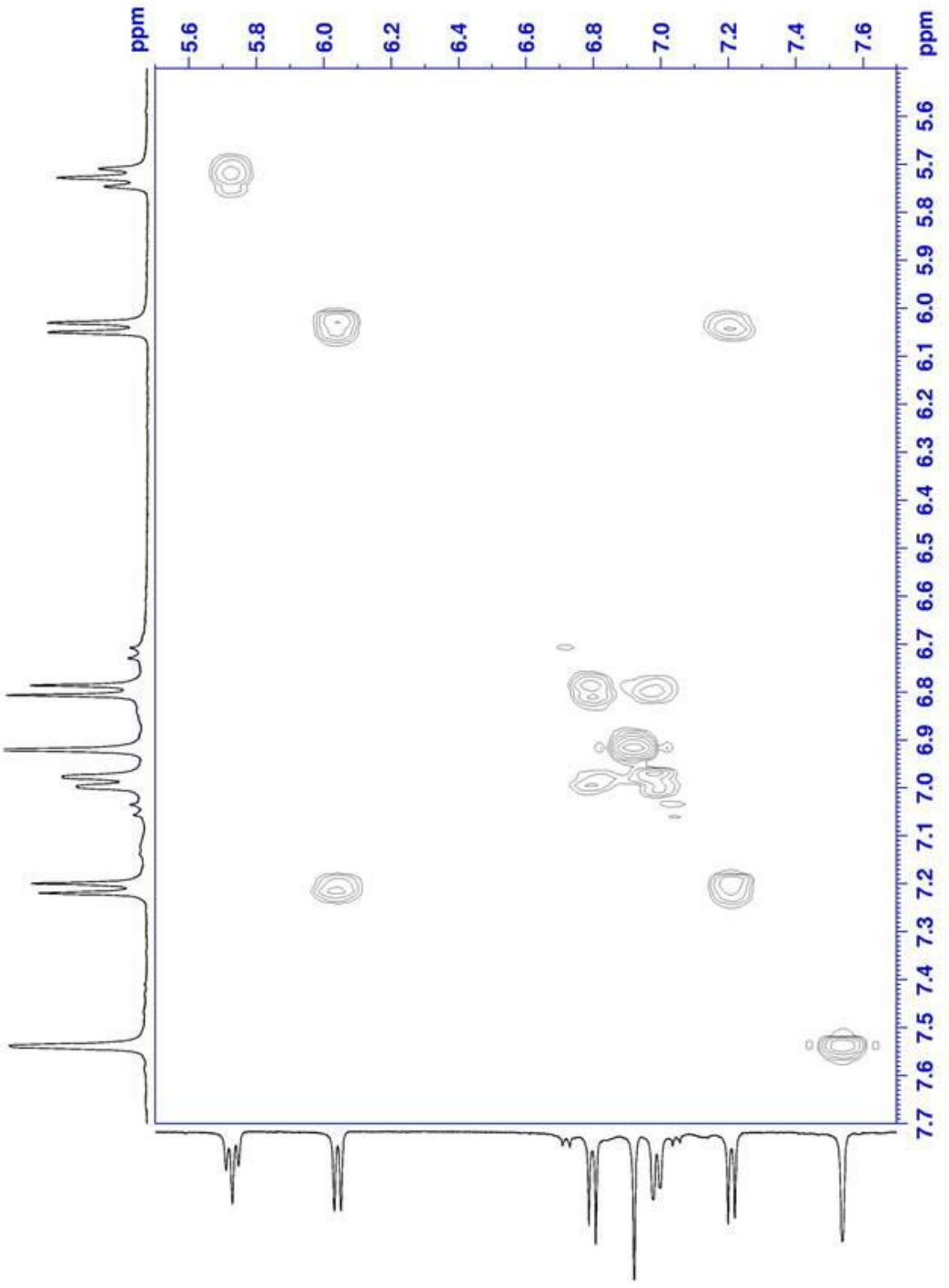

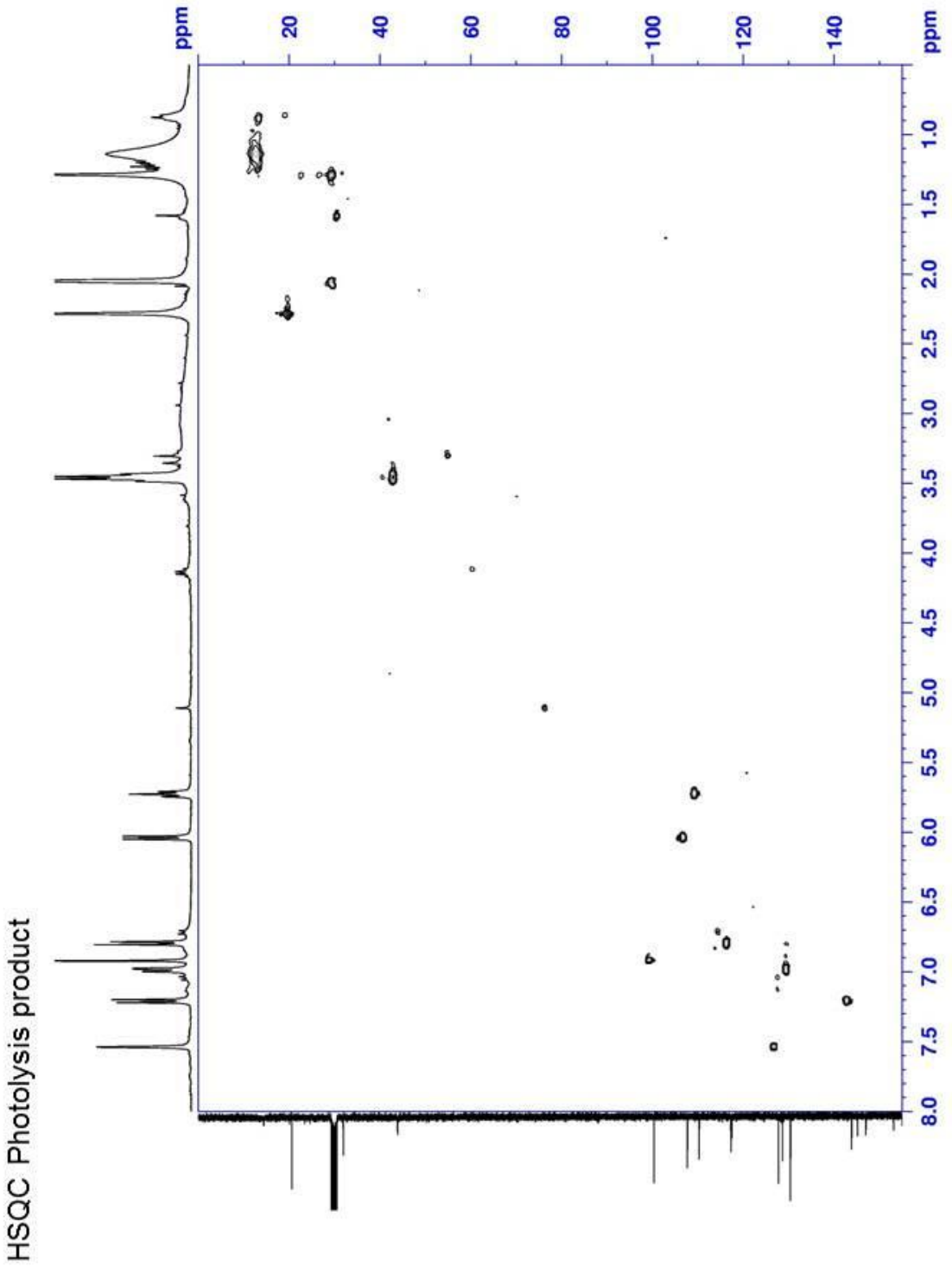
HSQC Photolysis product
ppm
20
40
60
80
100
120
140
ppm
1.0
1.5
2.0
2.5
3.0
3.5
4.0
4.5
5.0
5.5
6.0
6.5
7.0
7.5
8.0

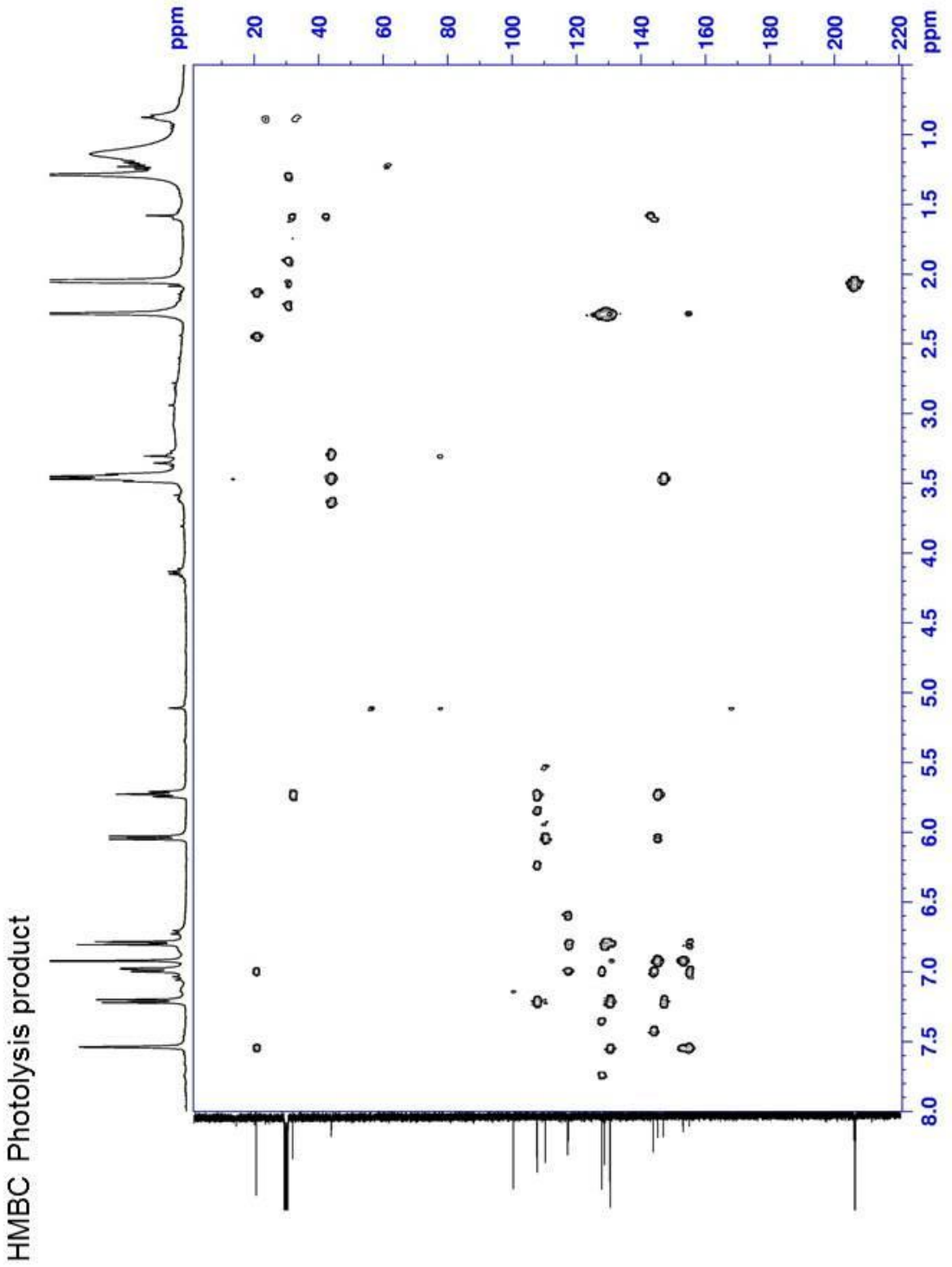
HMBC Photolysis product
ppm
20
40
60
80
100
120
140
160
180
200
220
ppm
1.0
1.5
2.0
2.5
3.0
3.5
4.0
4.5
5.0
5.5
6.0
6.5
7.0
7.5
8.0

$^{1}$H-NMR ($CDCl_3$) Dansyl-amide **(15)**

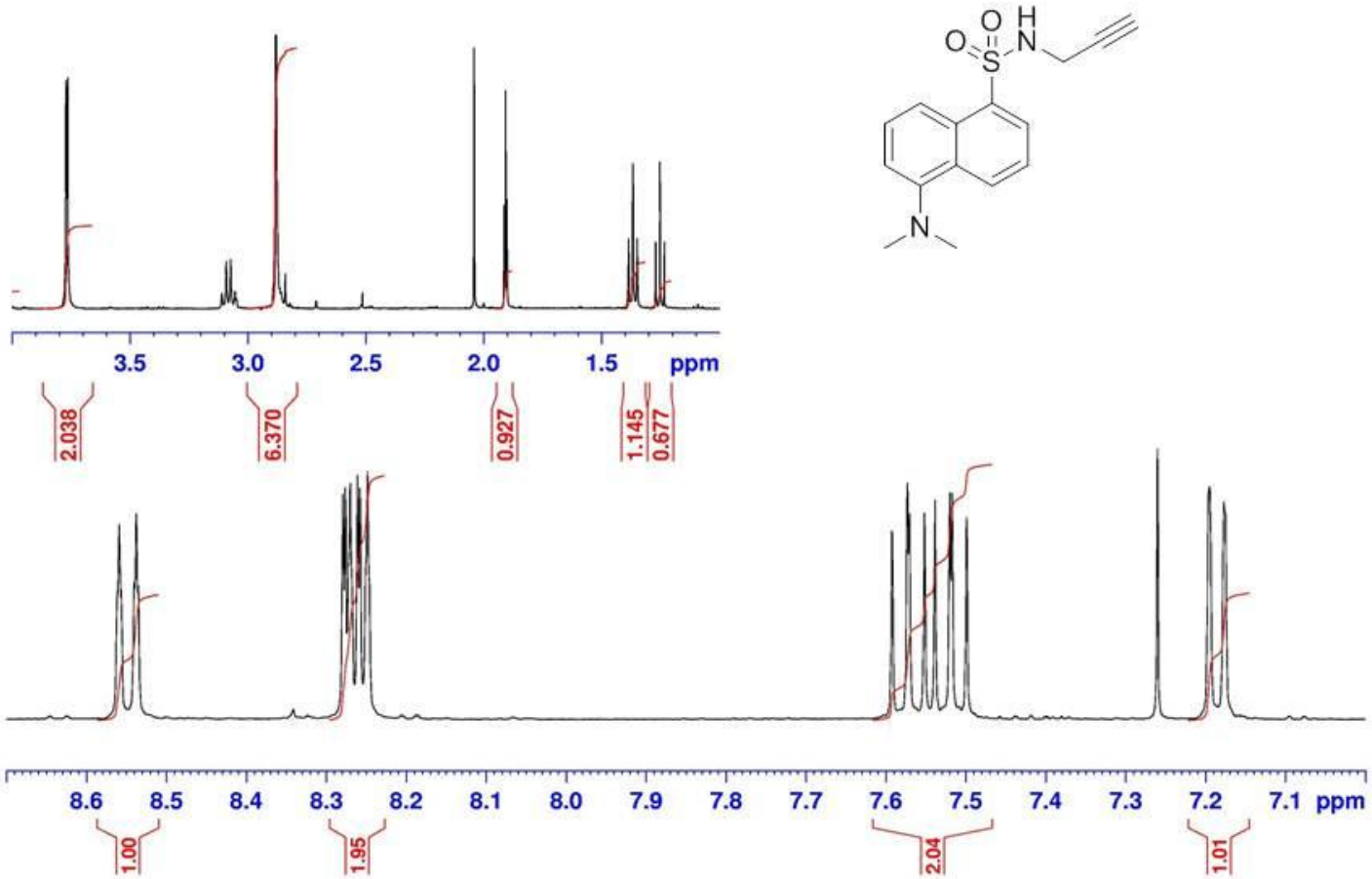

$^{1}$H-NMR ($(CD_3)_2CO$)) DANSYL-VRT **(16)**

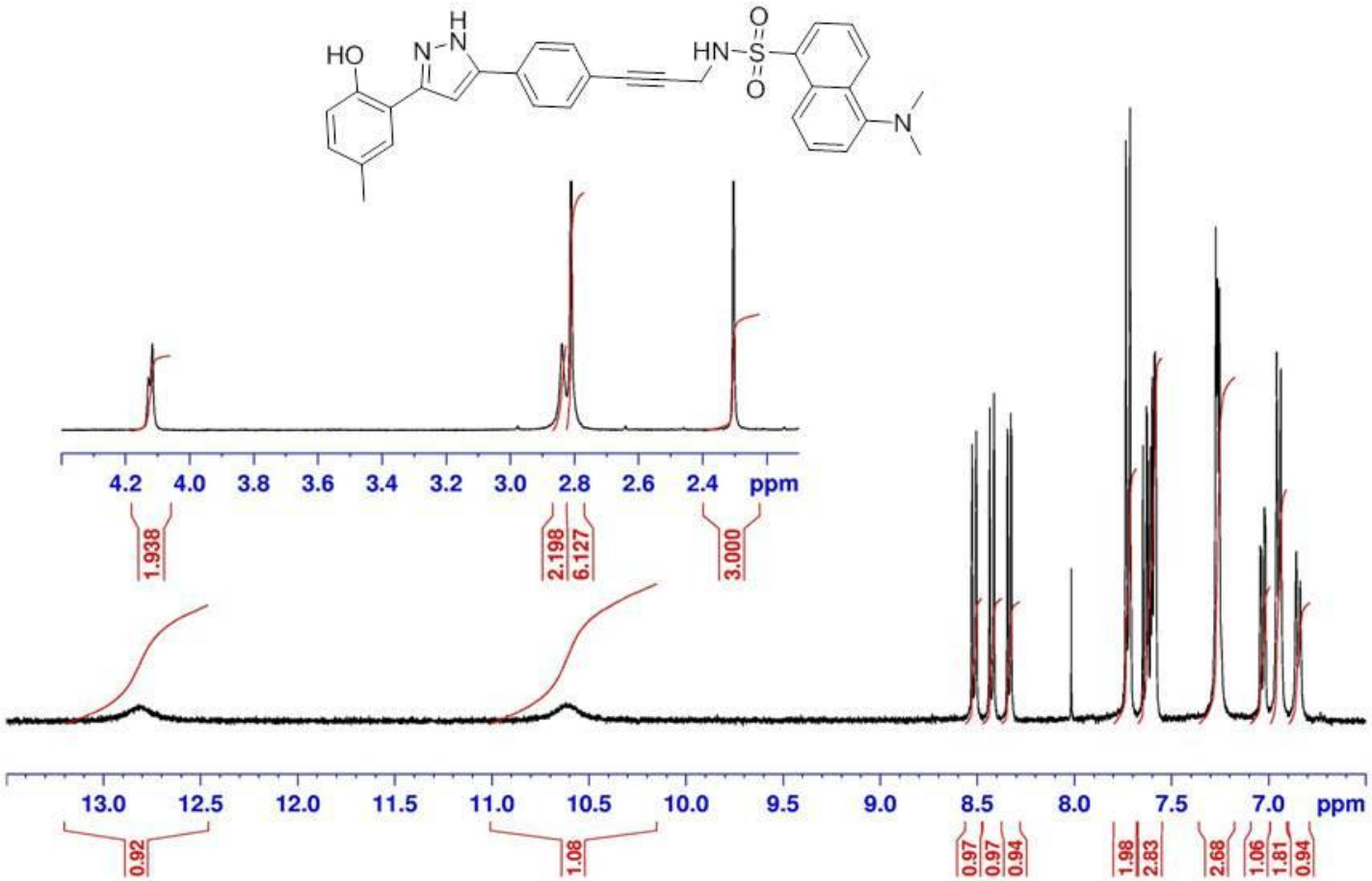

$^{13}$C-NMR ($(CD_3)_2CO$)) Dansyl-VRT **(16)**

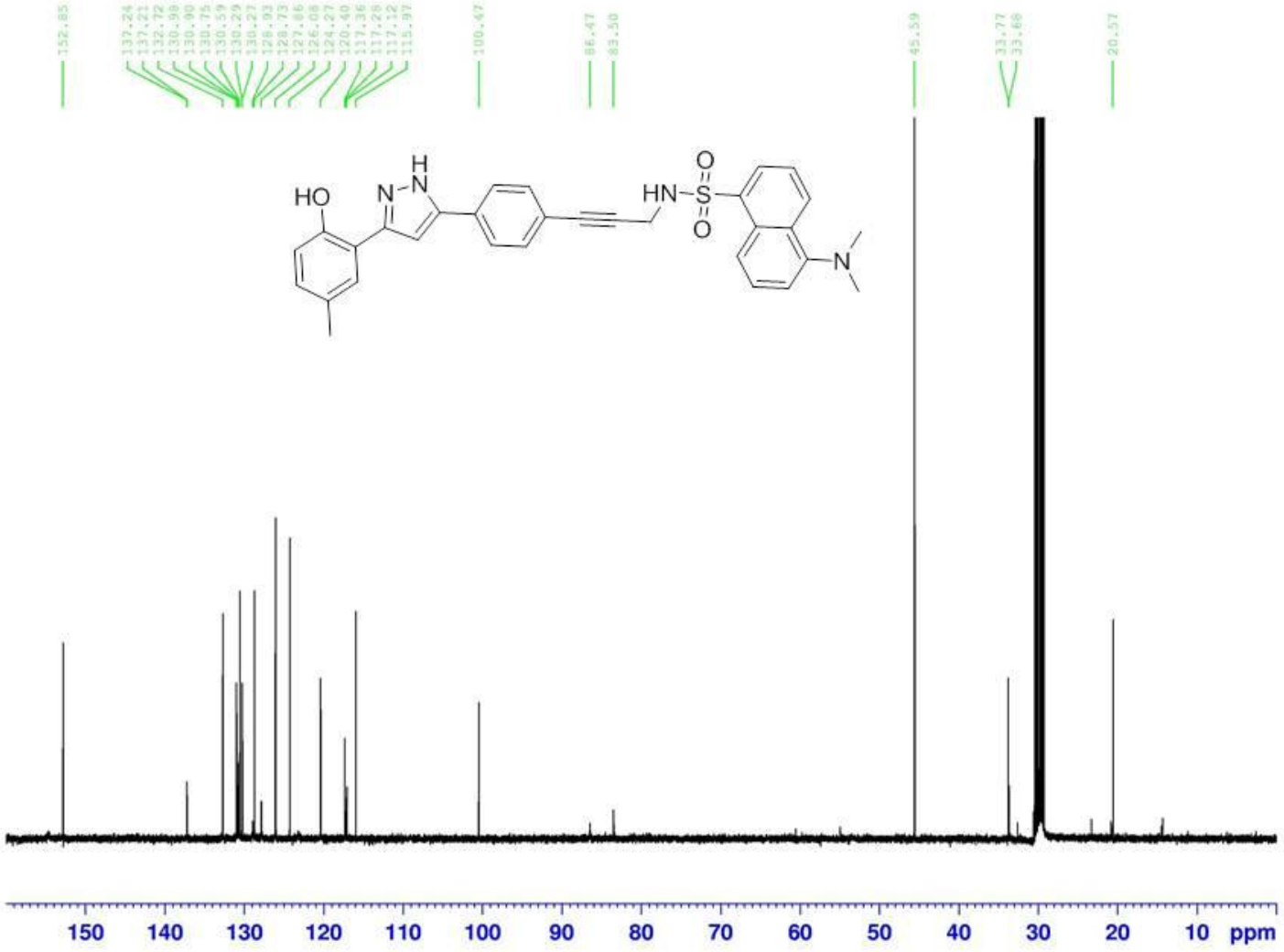

| | | | |
|---|---|---|---|
| Software Version | : 6.3.2.0646 | Date | : 8/22/2012 12:45:28 PM |
| Operator | : manager | Sample Name | : DaNsYl |
| Sample Number | : 001 | Study | : |
| AutoSampler | : SER200 | Rack/Vial | : 1/1 |
| Instrument Name | : HPLC | Channel | : B |
| Instrument Serial # | : None | A/D mV Range | : 1000 |
| Delay Time | : 0.00 min | End Time | : 129.99 min |
| Sampling Rate | : 2.5000 pts/s | | |
| Sample Volume | : 1.000000 µL | | |
| Sample Amount | : 1.0000 | Area Reject | : 0.000000 |
| Data Acquisition Time | : 8/11/2011 4:14:22 PM | Dilution Factor | : 1.00 |
| | | Cycle | : 1 |

Raw Data File : C:\Documents and Settings\All Users\Desktop\Old HPLC stuff\datb001-20110811-161430.raw
Inst Method : C:\PenExe\TcWS\Ver6.3.1\Examples\Bashar(C8-VRT)\August.11.2011-DANSYL-50%method from C:\Documents and Settings\All Users\Desktop\Old HPLC stuff\datb001-20110811-161430.raw
Proc Method : C:\HPLC Data\default.mth from
Calib Method : C:\HPLC Data\default.mth from
Report Format File: C:\PenExe\TcWS\Ver6.3.1\Examples\Bashar(C8-VRT)\August.11.2011-DANSYL-50%method.rpt
Sequence File : C:\PenExe\TcWS\Ver6.3.1\Examples\Bashar(C8-VRT)\August.11.2011-DANSYL-50%seq.seq

# DEFAULT REPORT

| Peak # | Time [min] | Area [µV·s] | Height [µV] | Area [%] | Norm. Area [%] | BL | Area/Height [s] |
|---|---|---|---|---|---|---|---|
| 1 | 6.663 | 1156683.60 | 21820.63 | 11.77 | 11.77 | BB | 53.0087 |
| 2 | 25.241 | 8672948.80 | 94476.16 | 88.23 | 88.23 | BB | 91.8004 |
| | | 9829632.40 | 116296.78 | 100.00 | 100.00 | | |

Missing Component Report

| Component | Expected Retention (Calibration File) |
|---|---|

All components were found

HPLC Chromatogram of Dansyl-VRT **(16)**

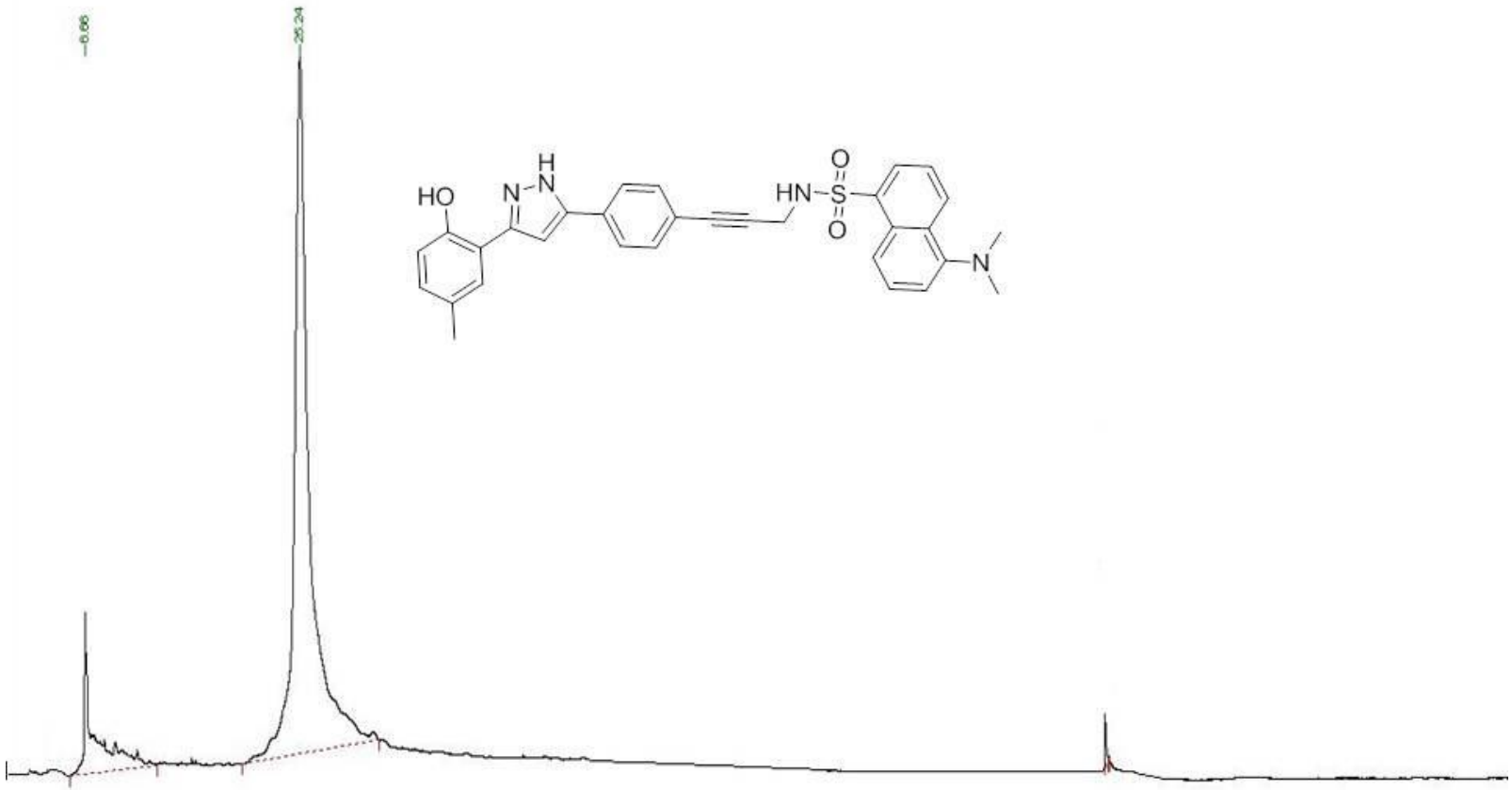

$^{1}$H-NMR ($CDCl_3$) BOC-propargylamine **(17)**

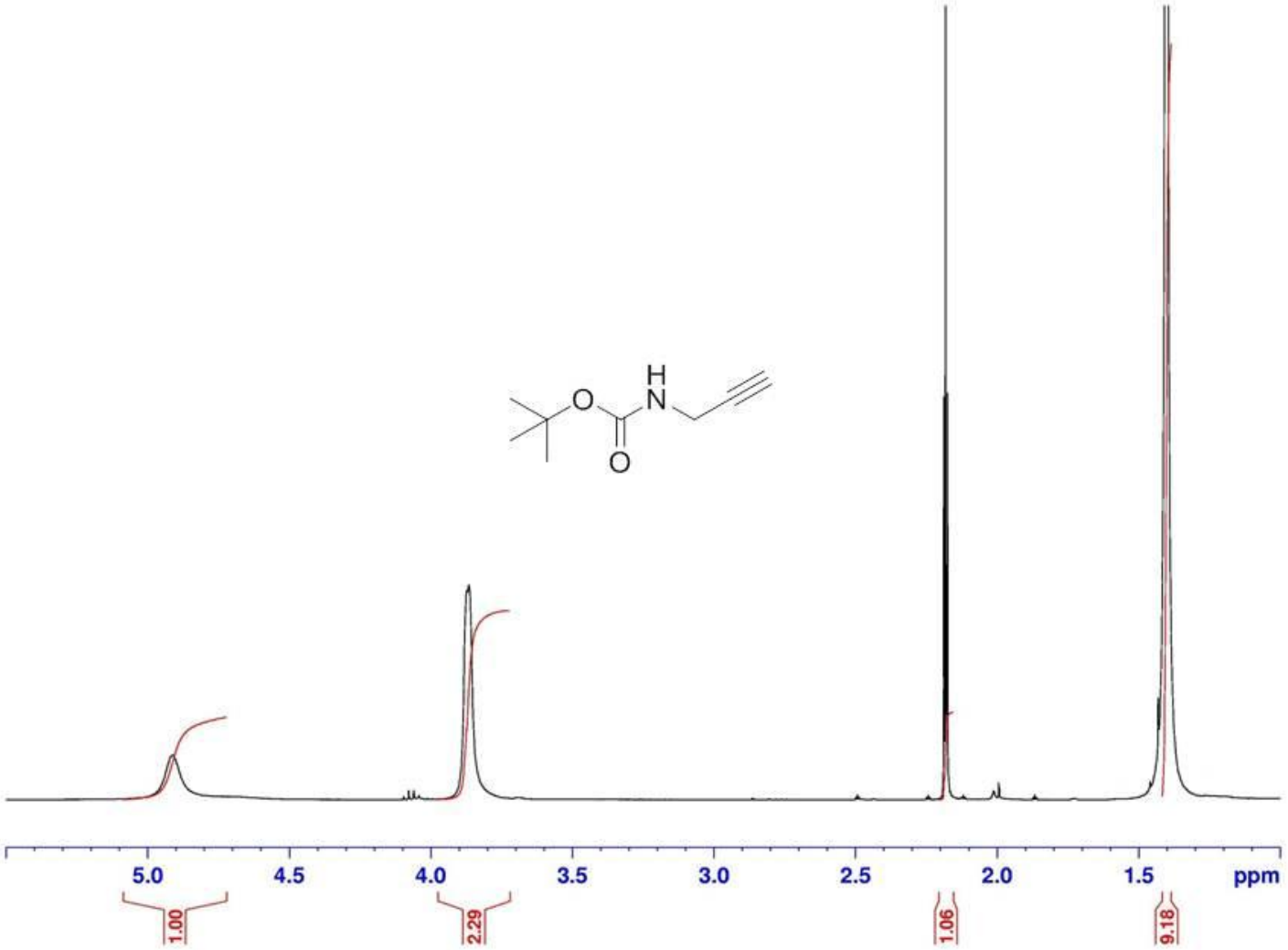

$^{1}$H-NMR ($(CD_3)_2CO$)) BOC-VRT **(18)**

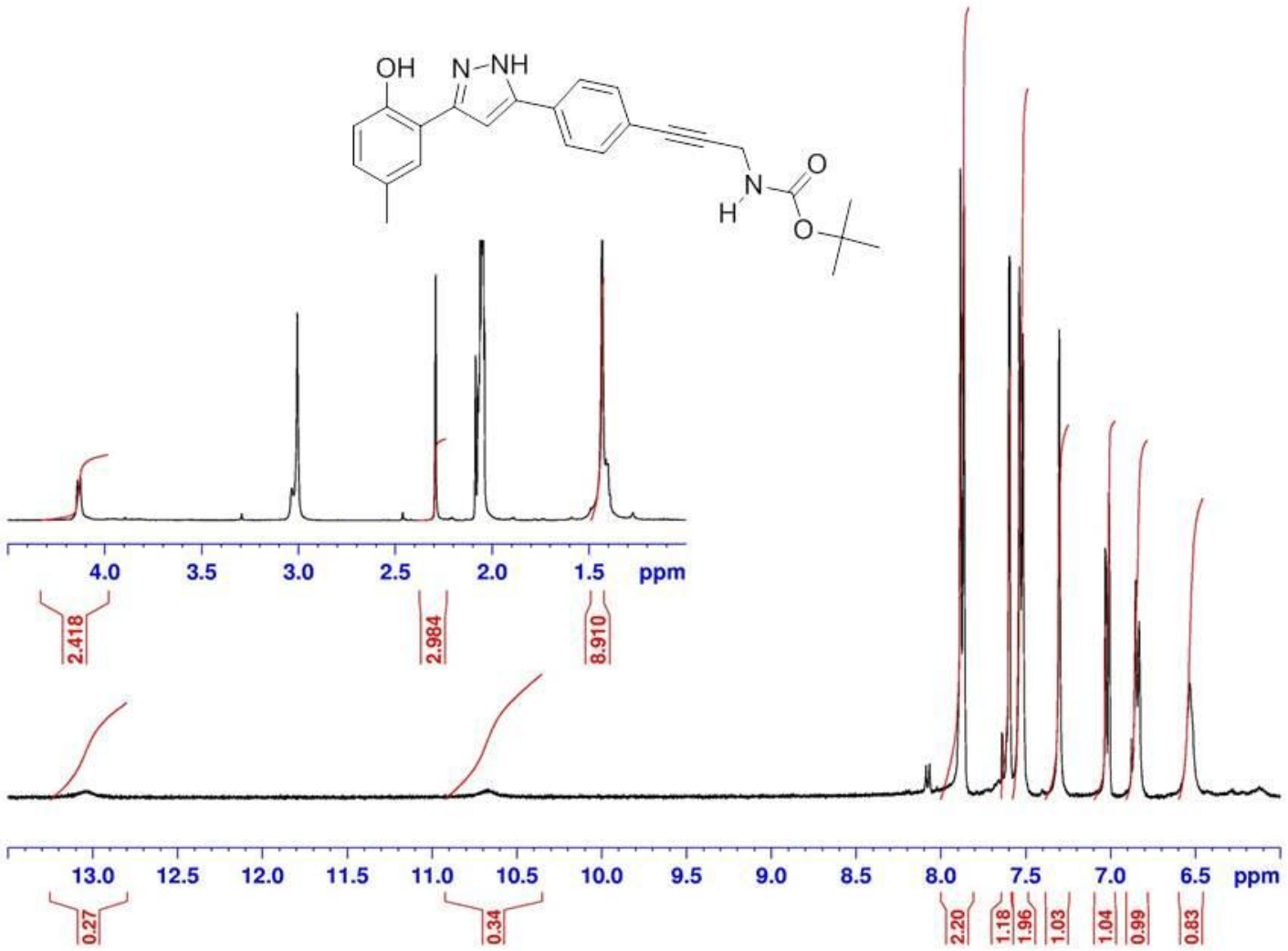

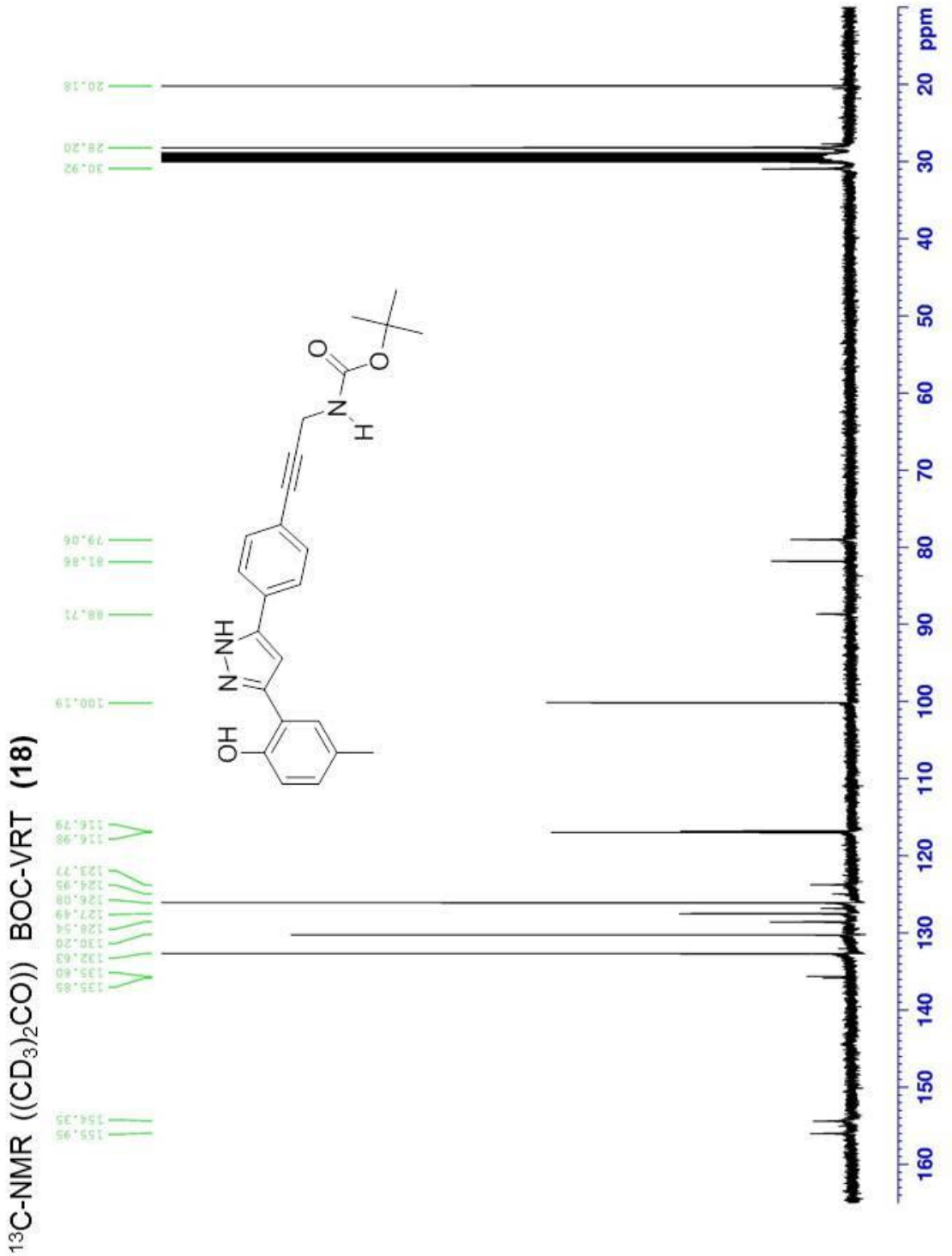
$^{13}$C-NMR ((CD$_3$)$_2$CO)) BOC-VRT (18)
20.18
28.20
30.92
79.06
81.86
88.71
100.19
116.79
116.98
123.77
124.95
126.08
127.49
128.54
130.20
132.63
135.60
135.85
155.95
156.35
HO
N
NH
O
O
N
H
20
30
40
50
60
70
80
90
100
110
120
130
140
150
160
ppm

| | | | |
|---|---|---|---|
| Software Version | : 6.3.2.0646 | Date | : 8/22/2012 12:37:19 PM |
| Operator | : manager | Sample Name | : BOC |
| Sample Number | : 001 | Study | : |
| AutoSampler | : SER200 | Rack/Vial | : 1/1 |
| Instrument Name | : HPLC | Channel | : B |
| Instrument Serial # | : None | A/D mV Range | : 1000 |
| Delay Time | : 0.00 min | End Time | : 129.99 min |
| Sampling Rate | : 2.5000 pts/s | | |
| Sample Volume | : 1.000000 ul | | |
| Sample Amount | : 1.0000 | Area Reject | : 0.000000 |
| Data Acquisition Time | : 7/8/2011 10:21:50 AM | Dilution Factor | : 1.00 |
| | | Cycle | : 1 |

Raw Data File : C:\Documents and Settings\All Users\Desktop\Old HPLC stuff\Bashar(C8-VRT)\datb001.raw
Inst Method : C:\PenExe\TcWS\Ver6.3.1\Examples\Bashar(C8-VRT)\July.8.2011-BOCmethod from C:\Documents and Settings\All Users\Desktop\Old HPLC stuff\Bashar(C8-VRT)\datb001.raw
Proc Method : C:\Documents and Settings\All Users\Desktop\Old HPLC stuff\Bashar(C8-VRT)\July.8.2011-BOCmethod.mth from
Calib Method : C:\Documents and Settings\All Users\Desktop\Old HPLC stuff\Bashar(C8-VRT)\July.8.2011-BOCmethod.mth from
Report Format File: C:\PenExe\TcWS\Ver6.3.1\Examples\Bashar(C8-VRT)\July.8.2011-BOCmethod.rpt
Sequence File : C:\PenExe\TcWS\Ver6.3.1\Examples\Bashar(C8-VRT)\July.8.2011-BOCseq.seq

# DEFAULT REPORT

| Peak # | Time [min] | Area [µV·s] | Height [µV] | Area [%] | Norm. Area [%] | BL | Area/Height [s] |
|---|---|---|---|---|---|---|---|
| - | 0.001 | 0.00 | 0.00 | 0.00 | 0.00 | | ---------- |
| 1 | 19.733 | 28865683.60 | 190211.01 | 97.37 | 97.37 | BB | 151.7561 |
| 2 | 94.341 | 778217.20 | 76569.35 | 2.63 | 2.63 | BB | 10.1636 |
| | | 29643900.80 | 266780.36 | 100.00 | 100.00 | | |

Missing Component Report

| Component | Expected Retention (Calibration File) |
|---|---|
| July.8.2011-BOC | 0.001 |

HPLC Chromatogram of BOC-VRT **(18)**

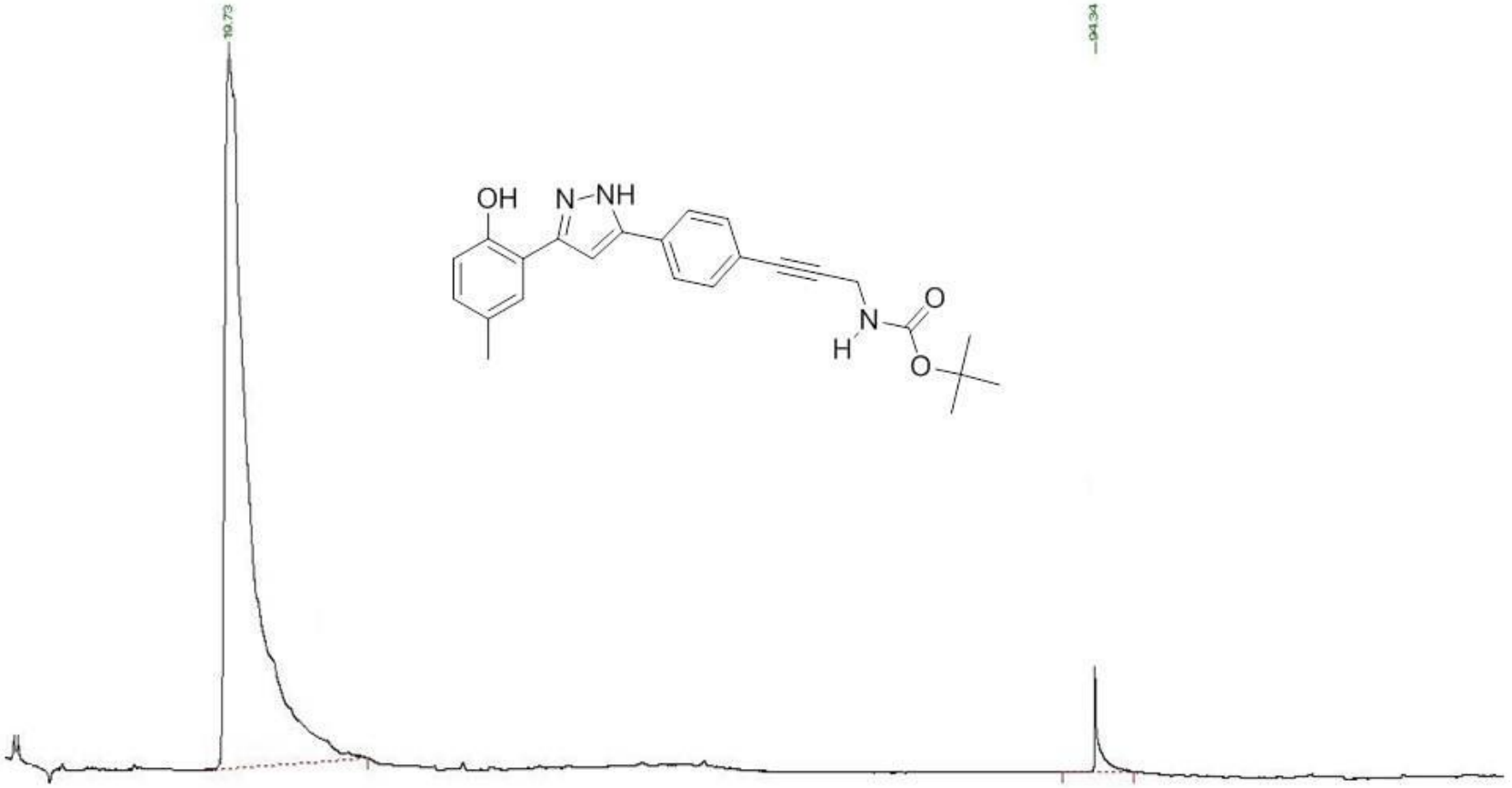

$^{1}$H-NMR ($(CD_3)_2CO$)) D-VRT **(21)**

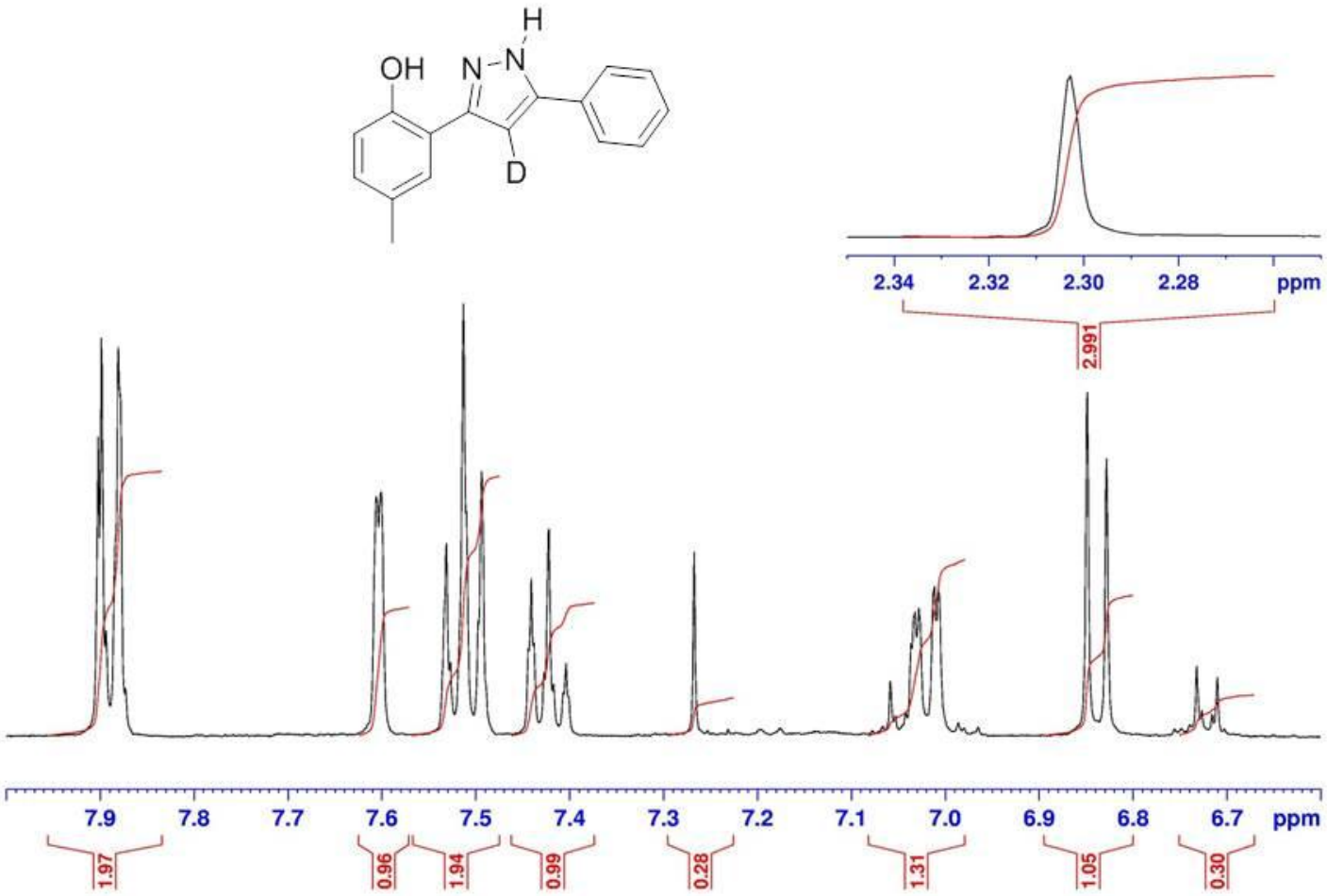

$^{13}$C-NMR ($(CD_3)_2CO$)) D-VRT **(21)**

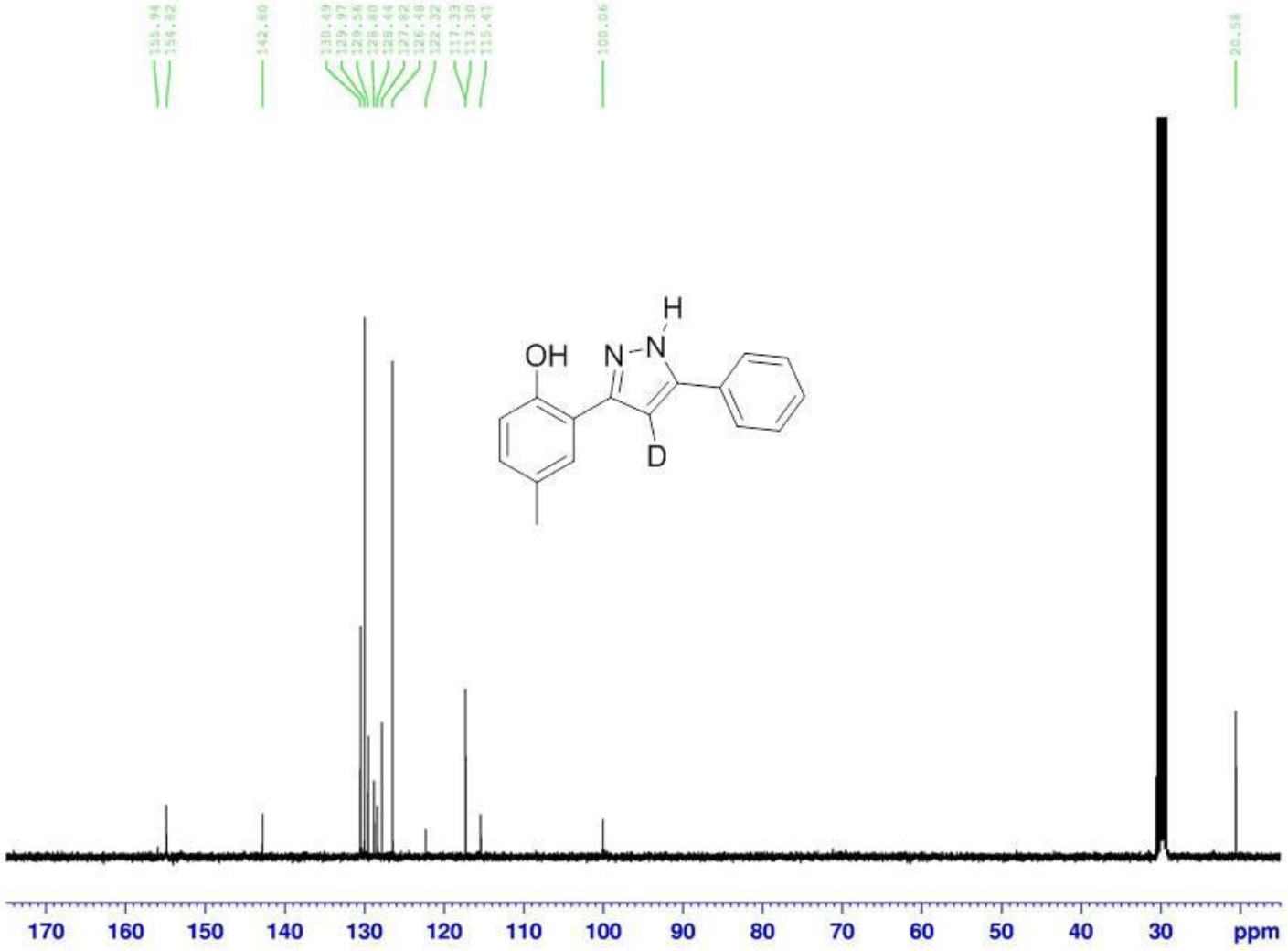

$^{1}$H-NMR ($CDCl_3$) I,Br-Ester **(21)**

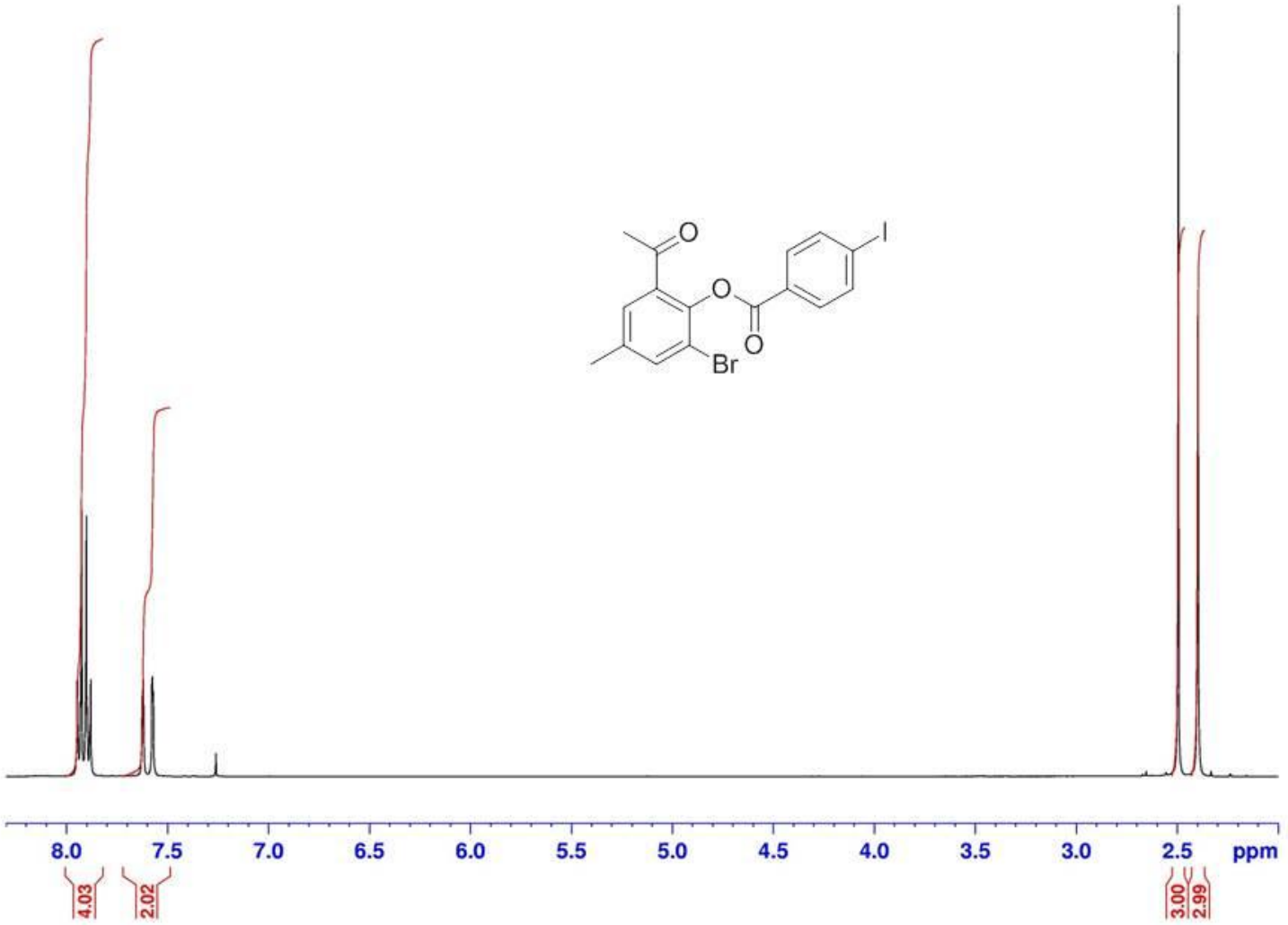

$^{13}$C-NMR ($CDCl_3$) I,Br-Ester **(21)**

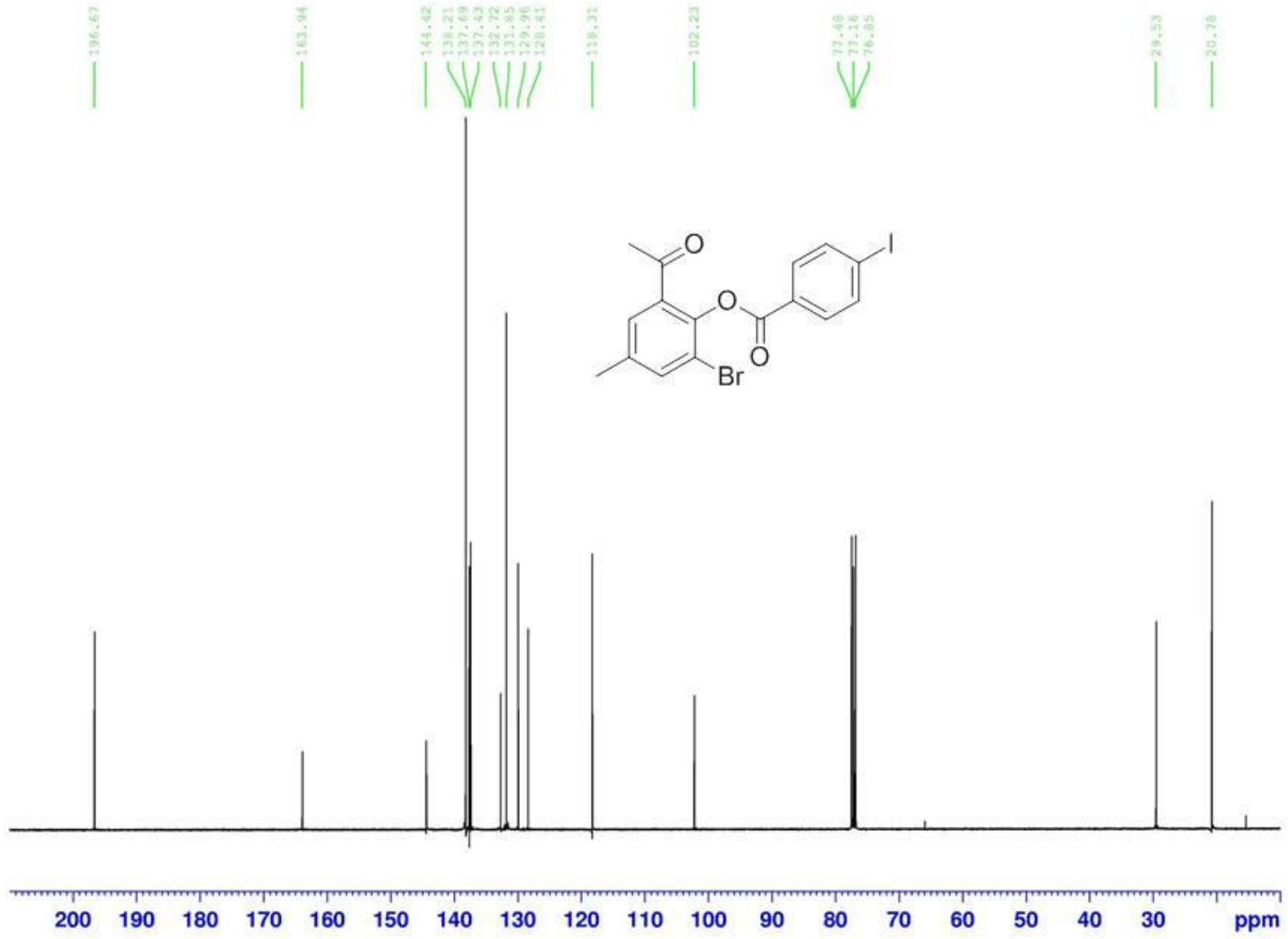

$^1$H-NMR $(CD_3)_2SO$) I,Br-VRT **(25)**

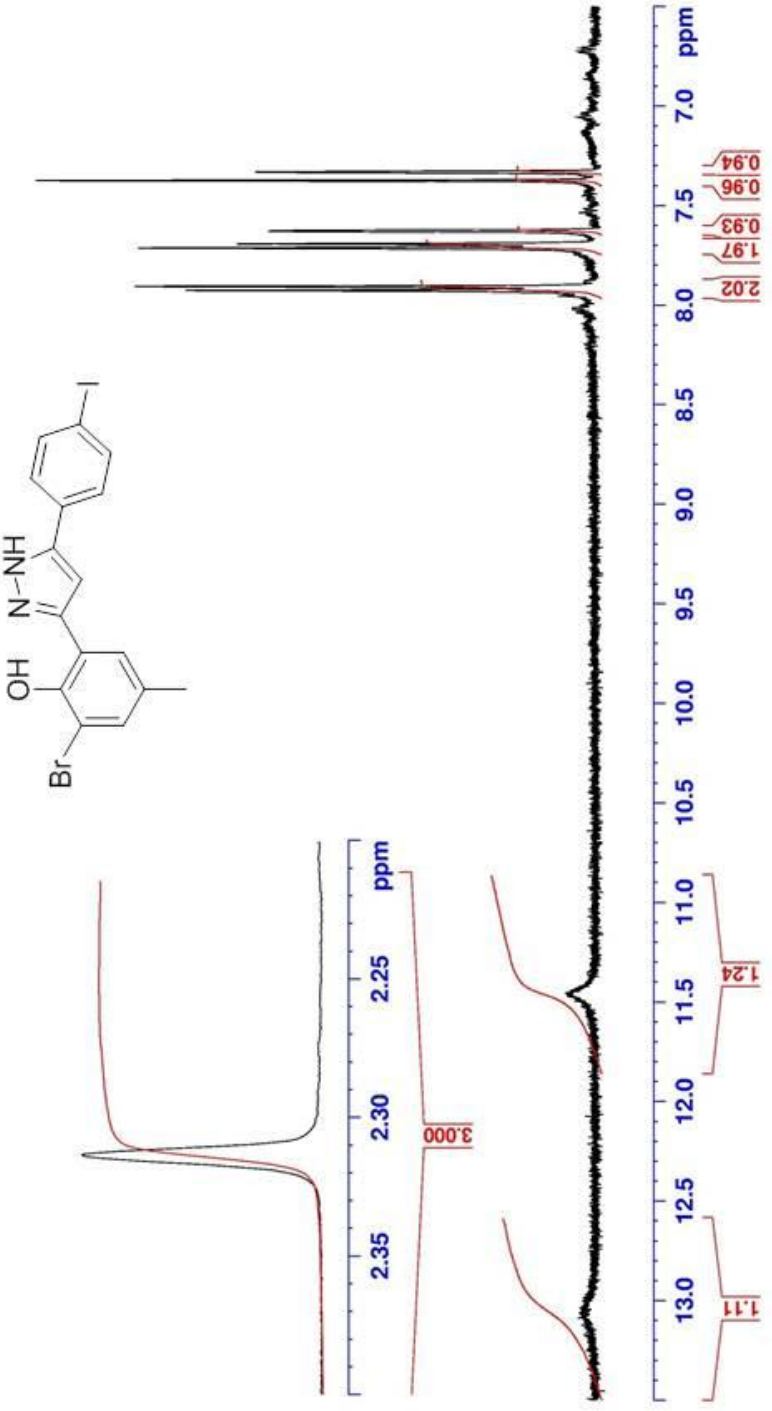

$^{13}$C-NMR $(CD_3)_2SO$) I,Br-VRT **(25)**

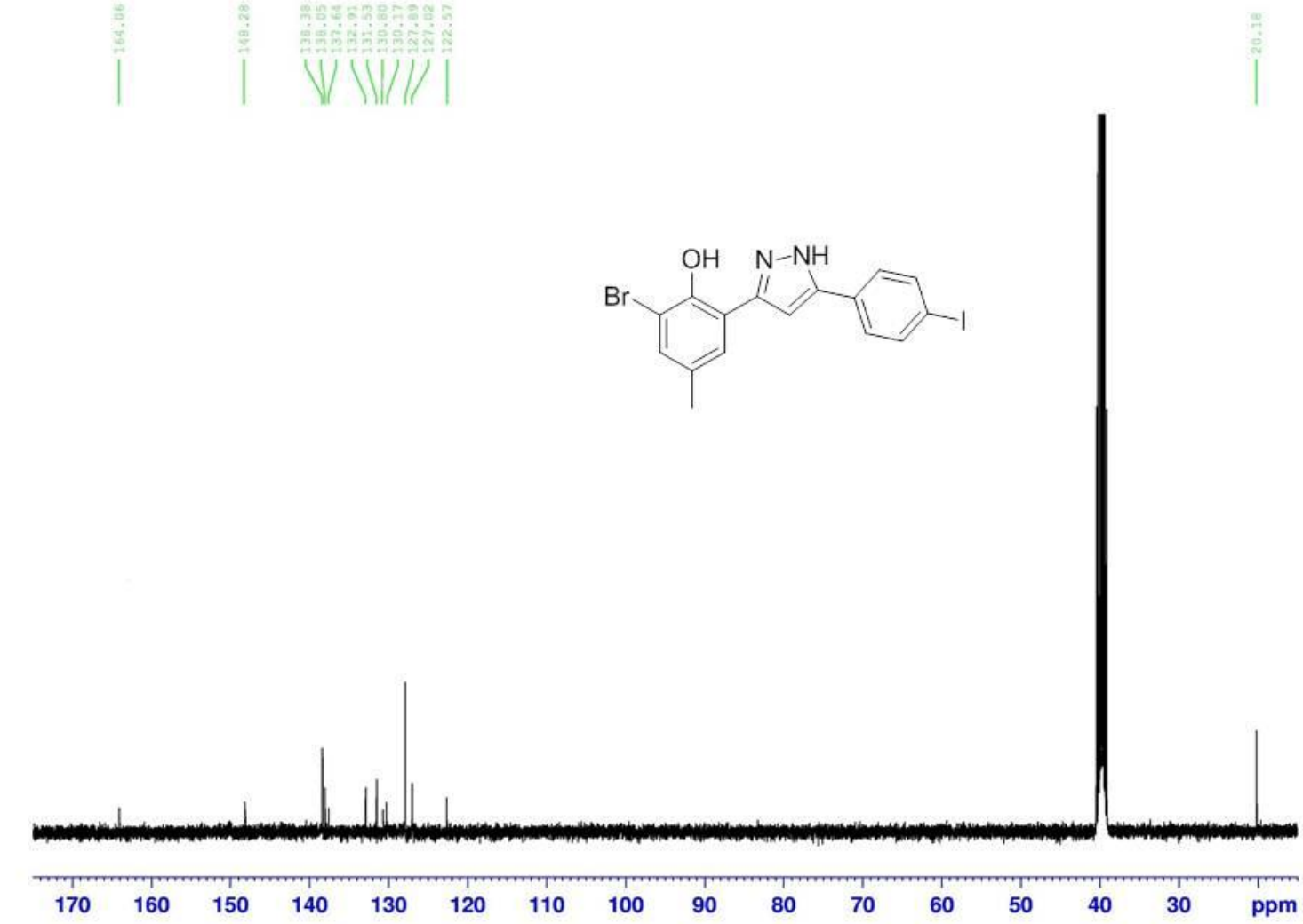

$^1$H-NMR $(CD_3)_2CO$) PMB-VRT **(29)**

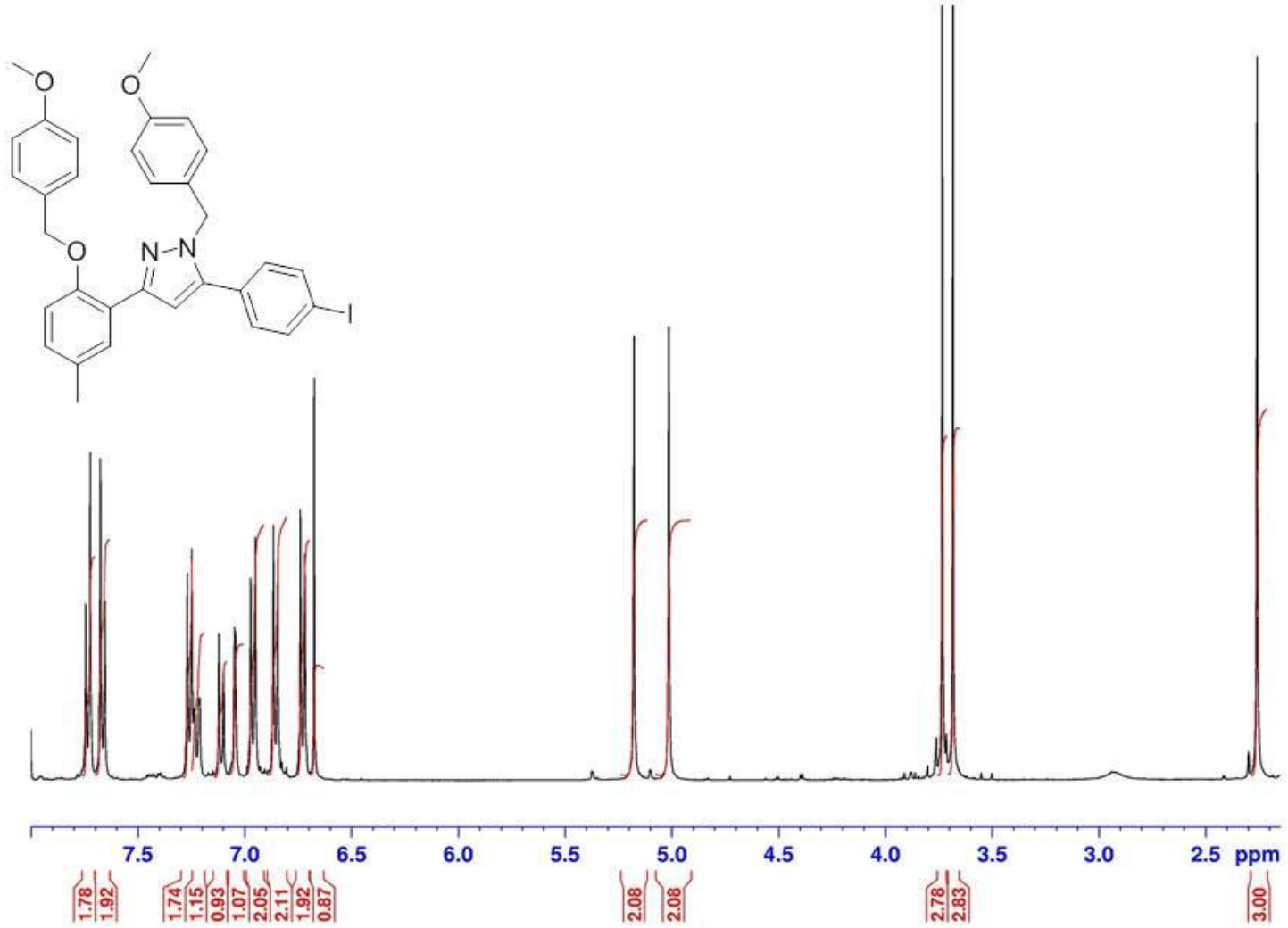

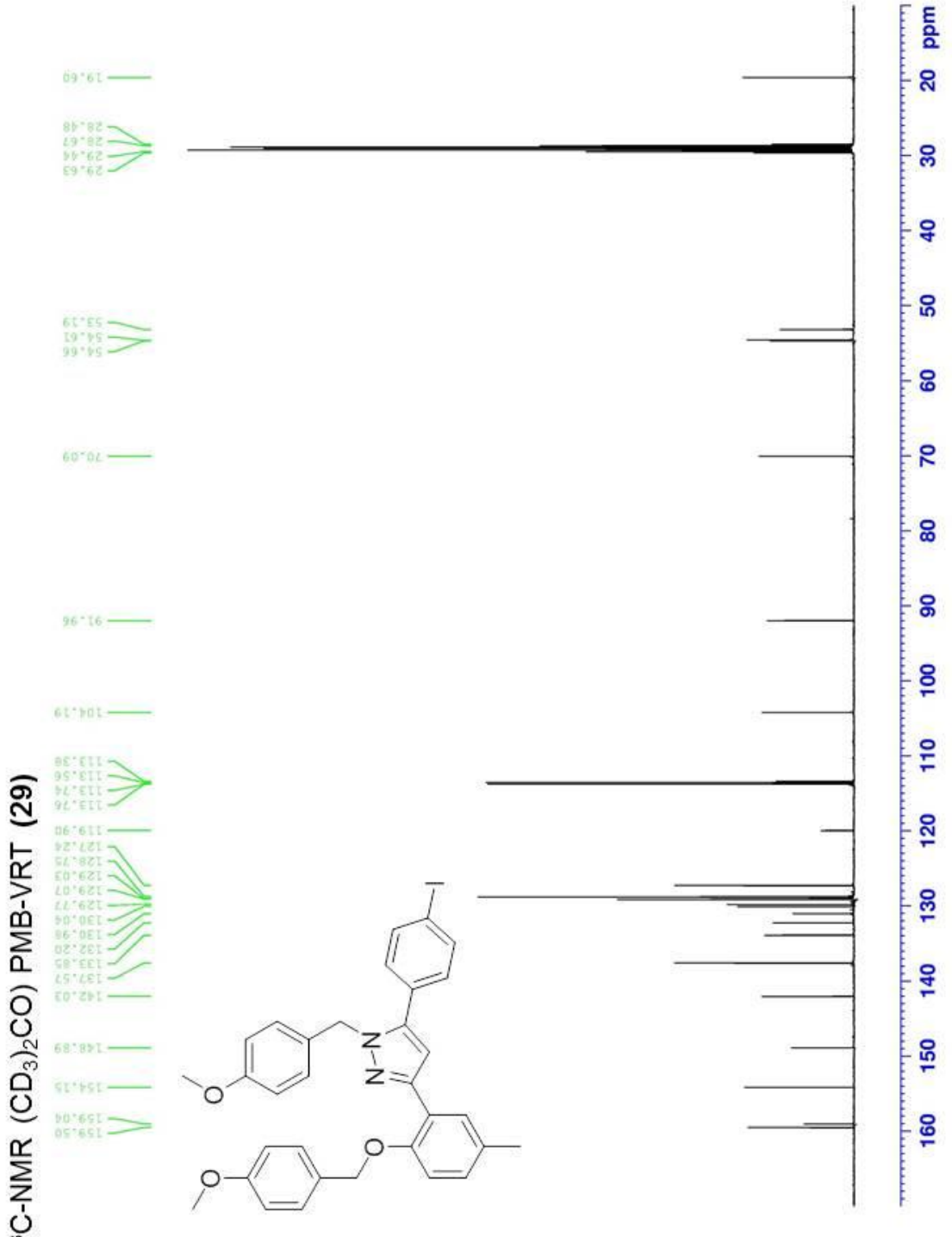
$^{13}$C-NMR ($CD_3)_2CO$) PMB-VRT **(29)**
159.50
159.04
154.15
148.89
142.03
137.57
133.85
132.20
130.98
130.04
129.77
129.07
129.03
128.75
127.24
119.90
113.76
113.74
113.56
113.38
104.19
91.96
70.09
54.66
54.61
53.19
29.63
29.44
28.67
28.48
19.60
ppm
20
30
40
50
60
70
80
90
100
110
120
130
140
150
160

$^{1}$H-NMR ($CDCl_3$) PMB-Naphthalene (**31**)

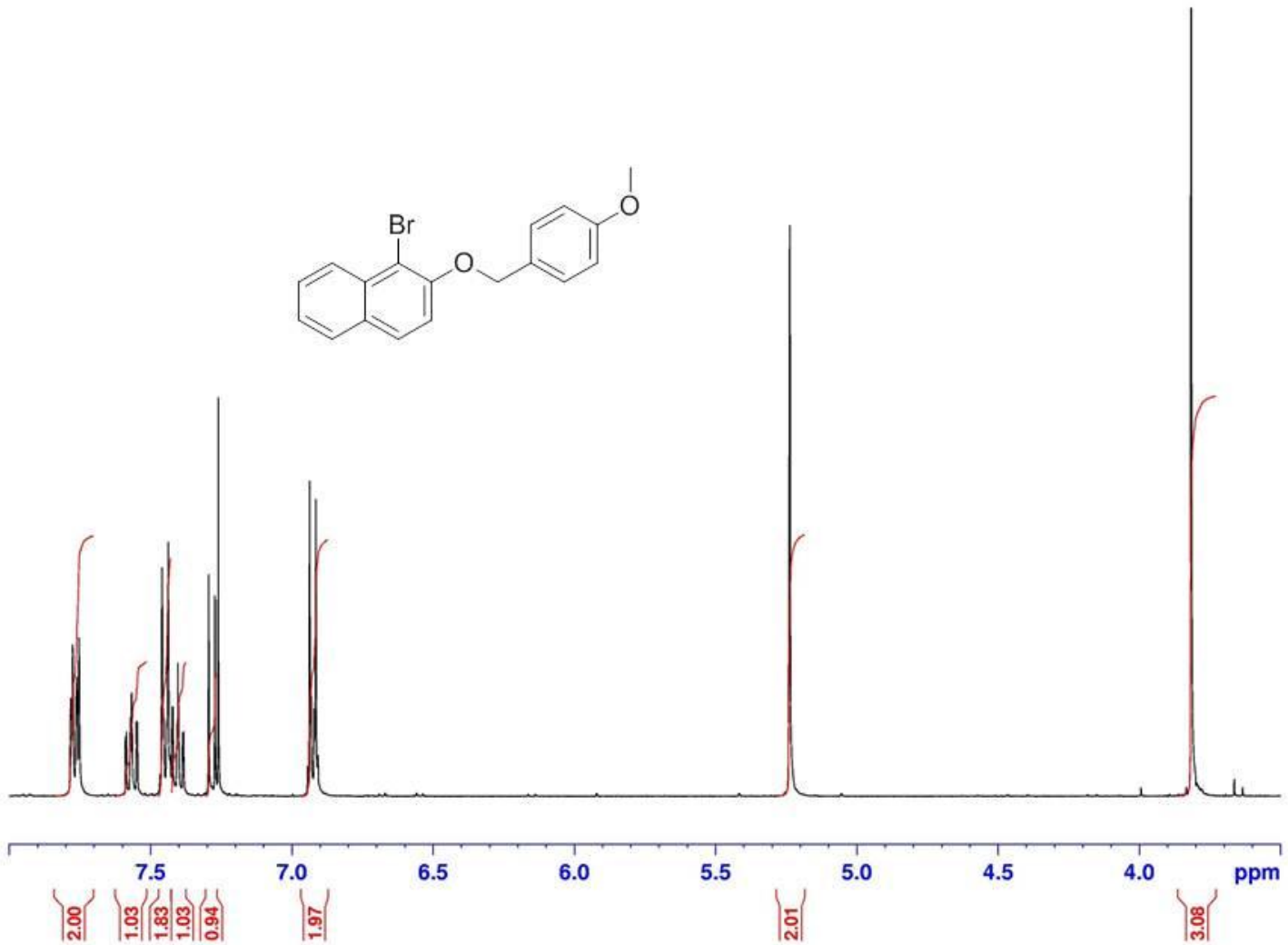

$^{13}$C-NMR ($CDCl_3$) PMB-Naphthalene (**31**)

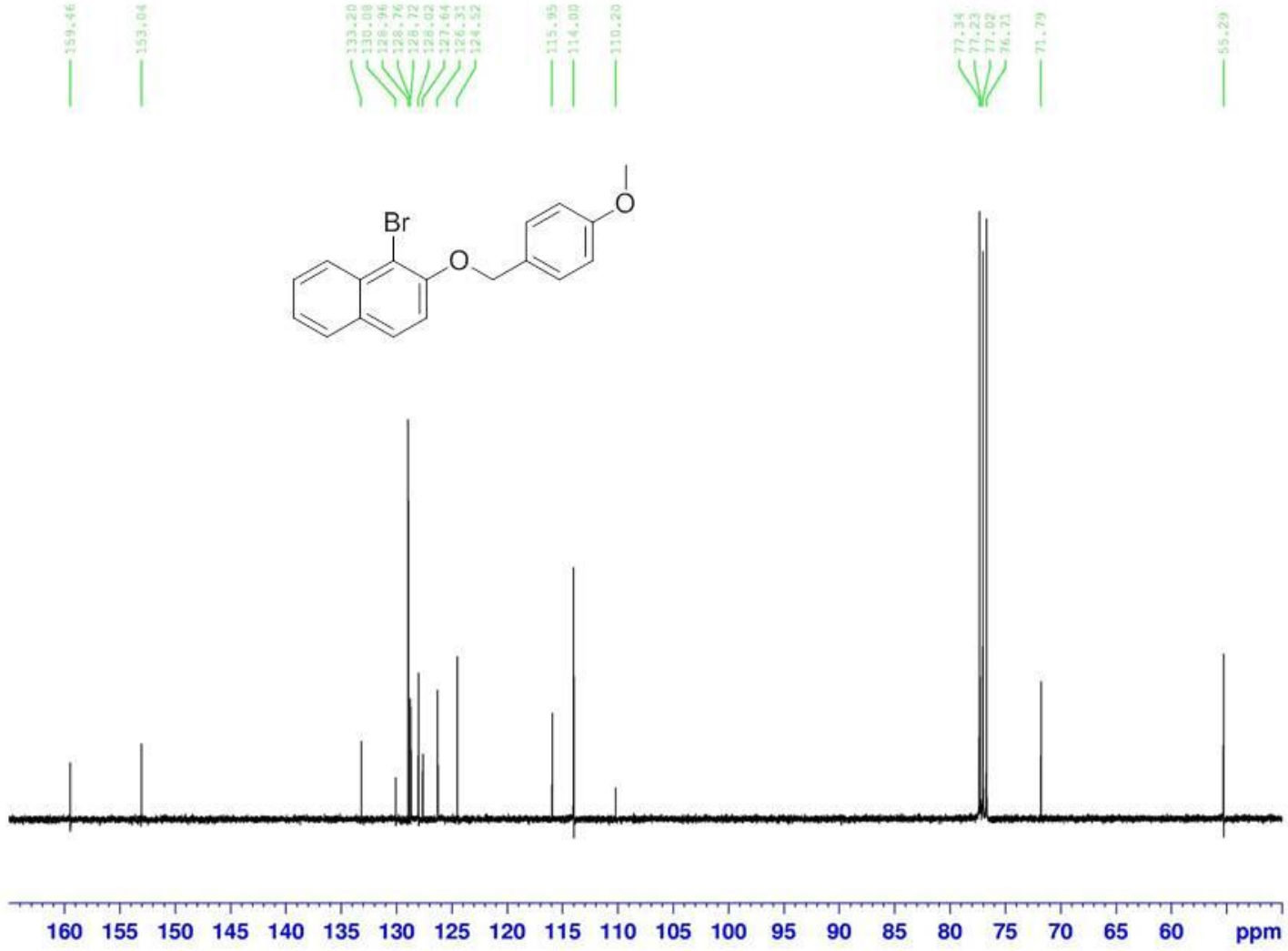

$^{1}$H-NMR ($CDCl_3$) Propargyl-TEG **(34)**

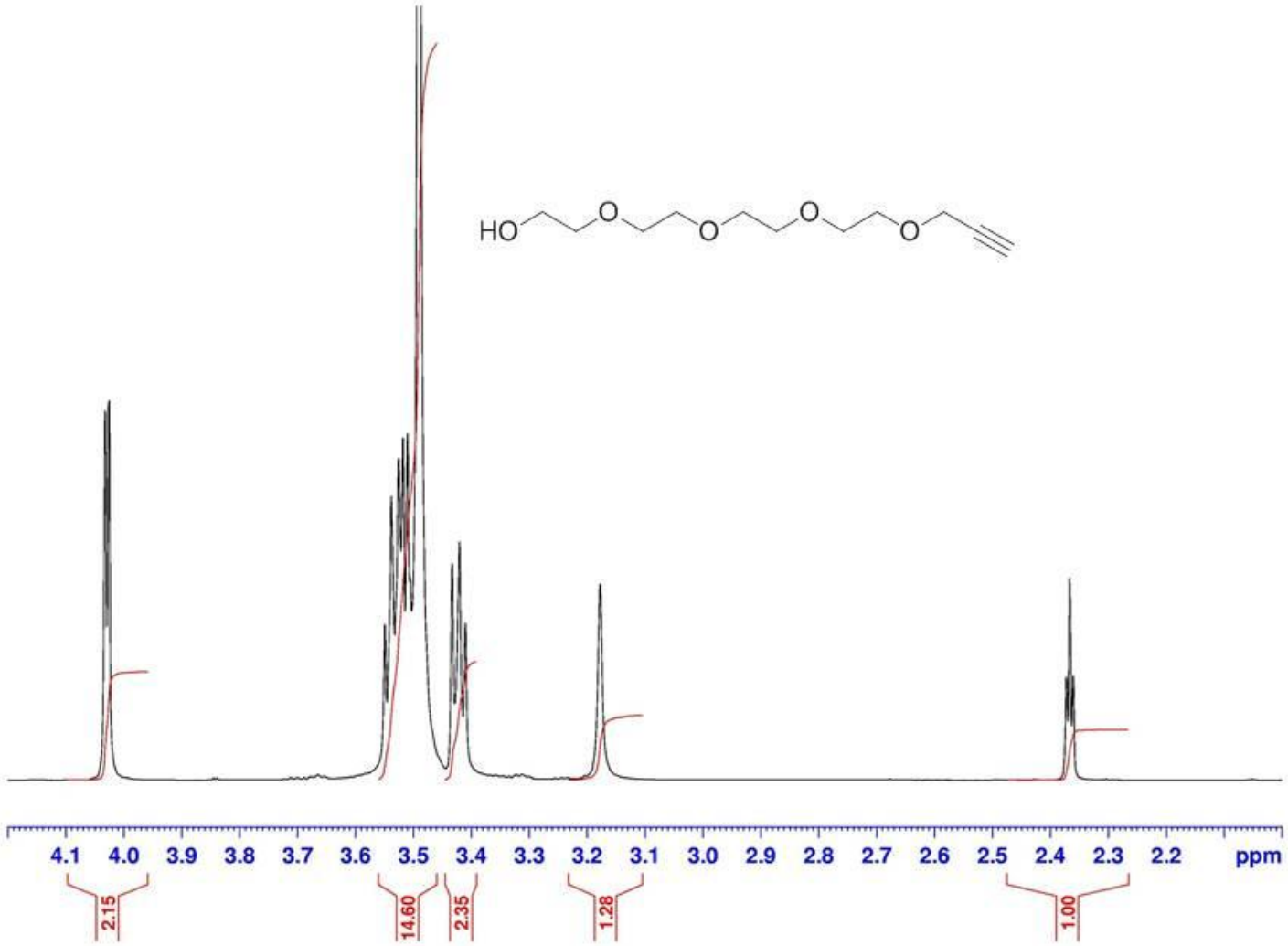

$^{13}$C-NMR ($CDCl_3$) Propargyl-TEG **(34)**

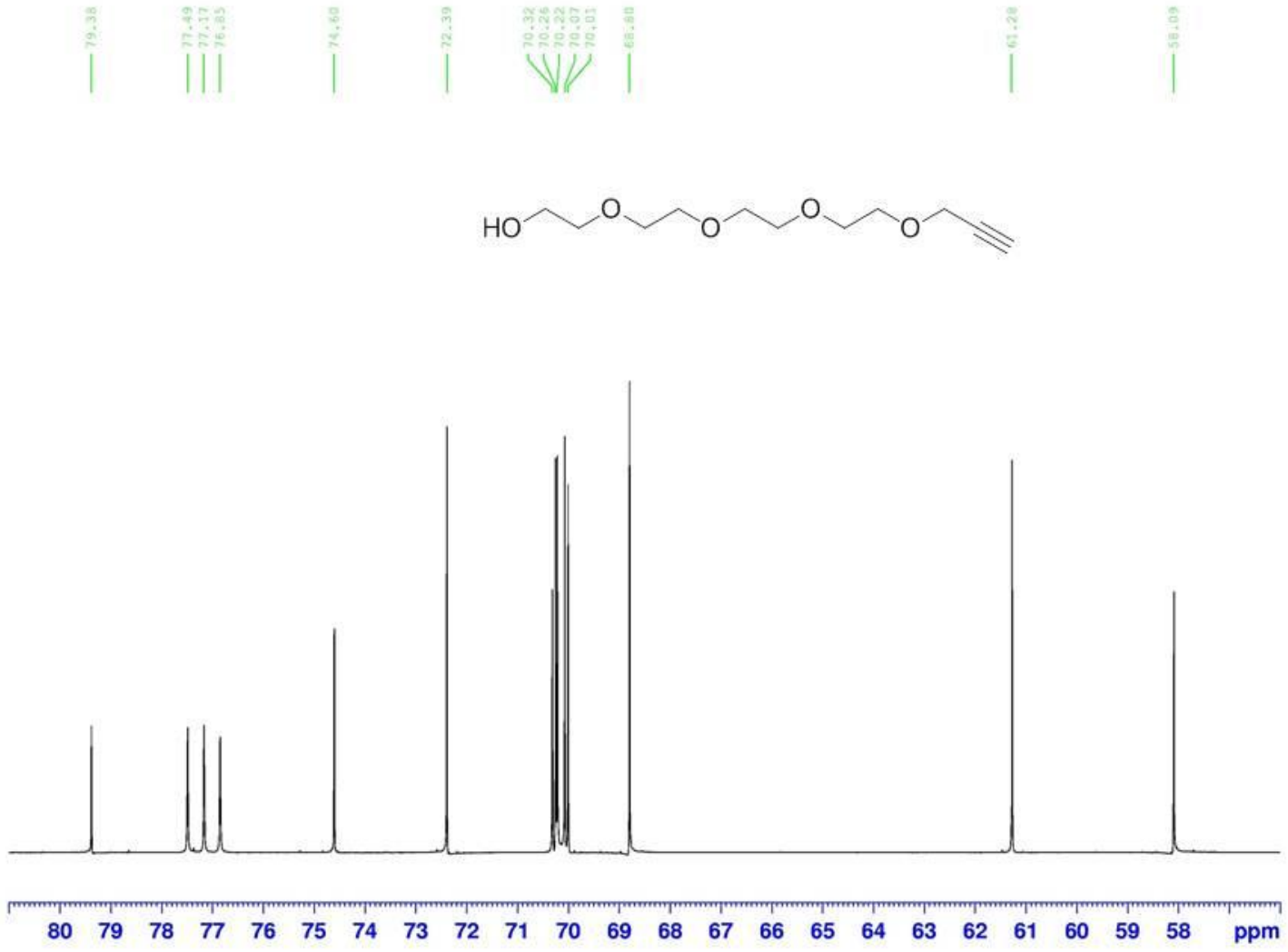

$^{1}$H-NMR ($CDCl_3$) Di-propargyl-TEG **(35)**

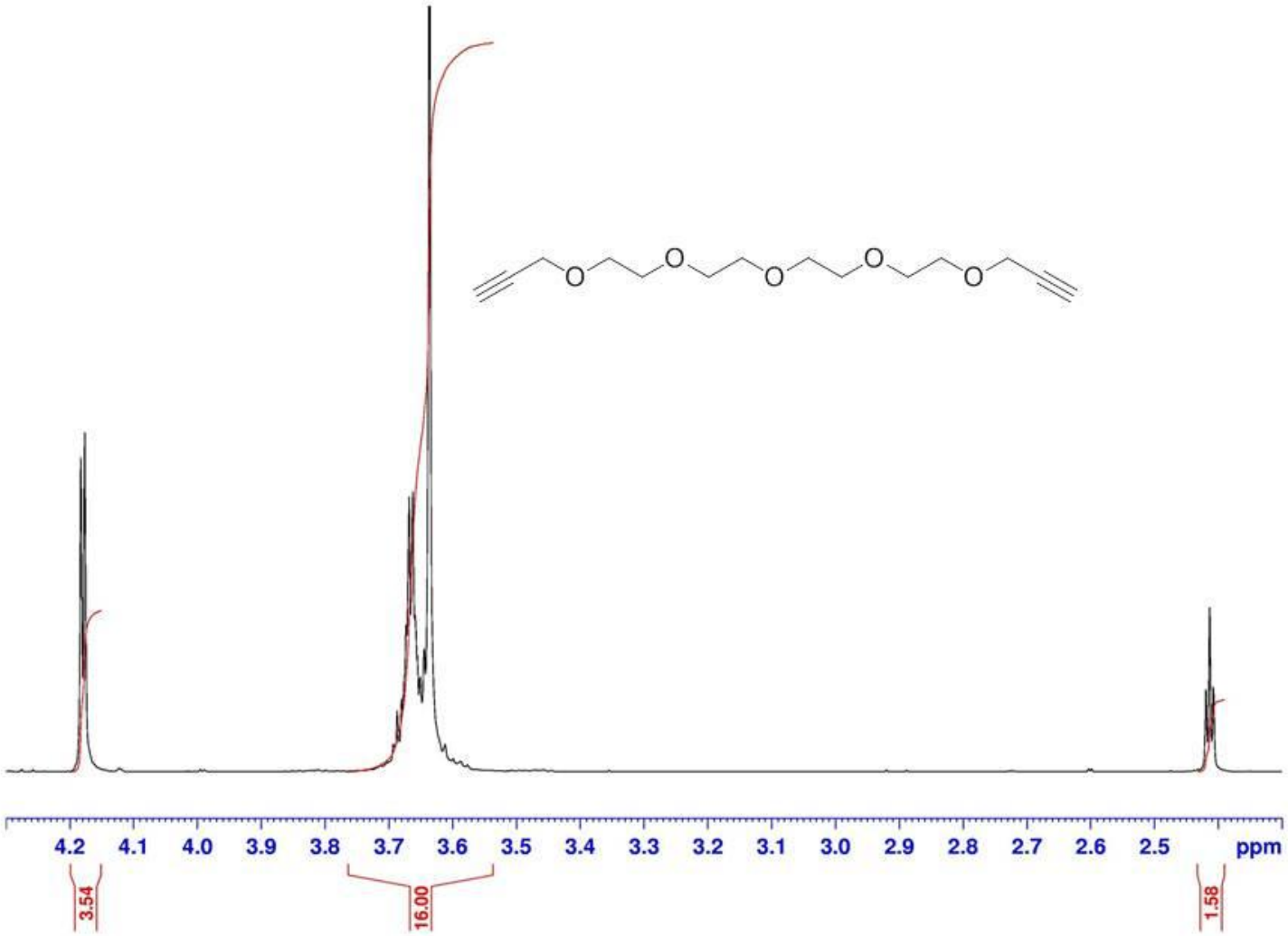

$^{13}$C-NMR ($CDCl_3$) Di-propargyl-TEG **(35)**

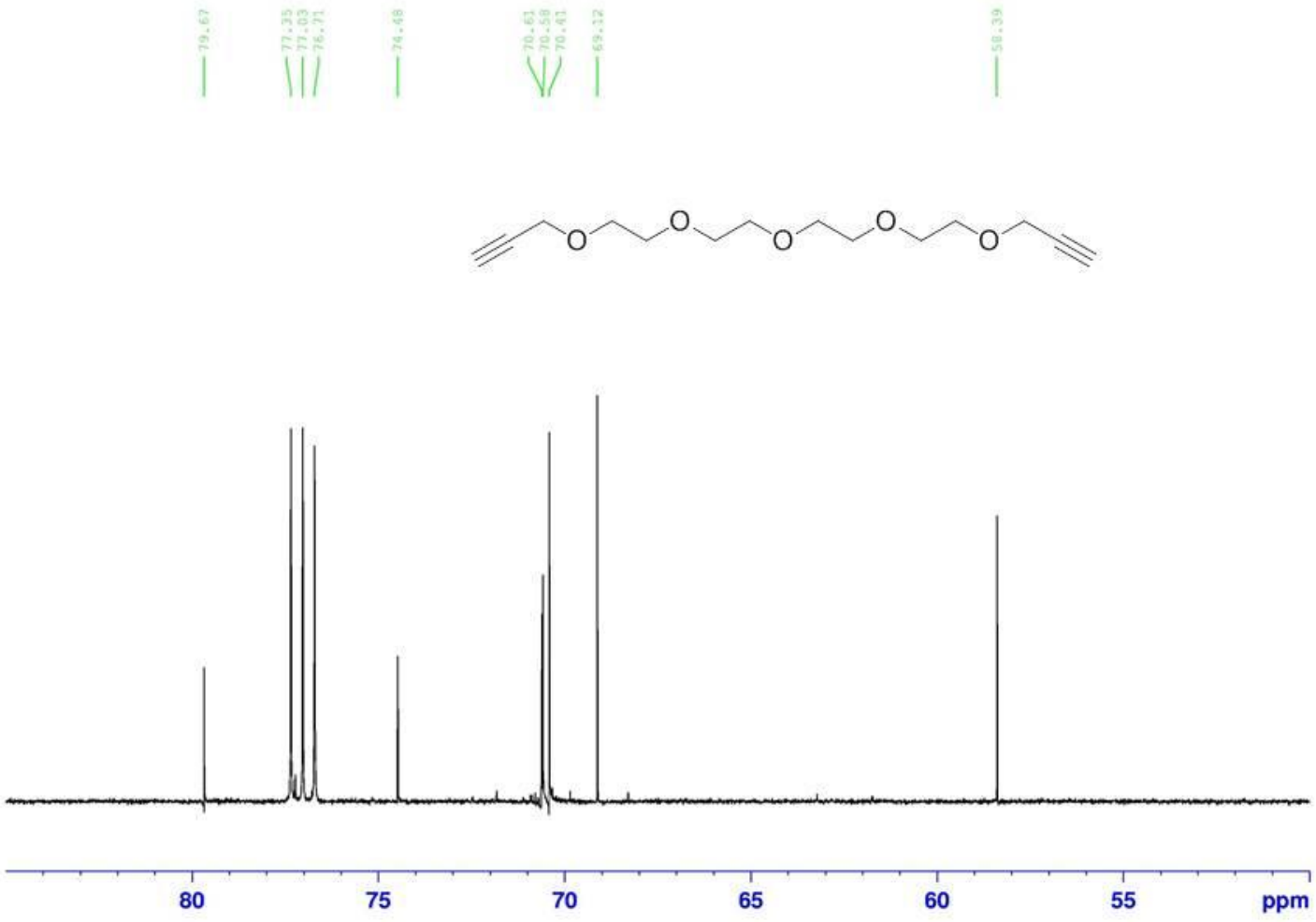

$^{1}$H-NMR ($CDCl_3$) Ethyl ester of propargyl-TEG **(36)**

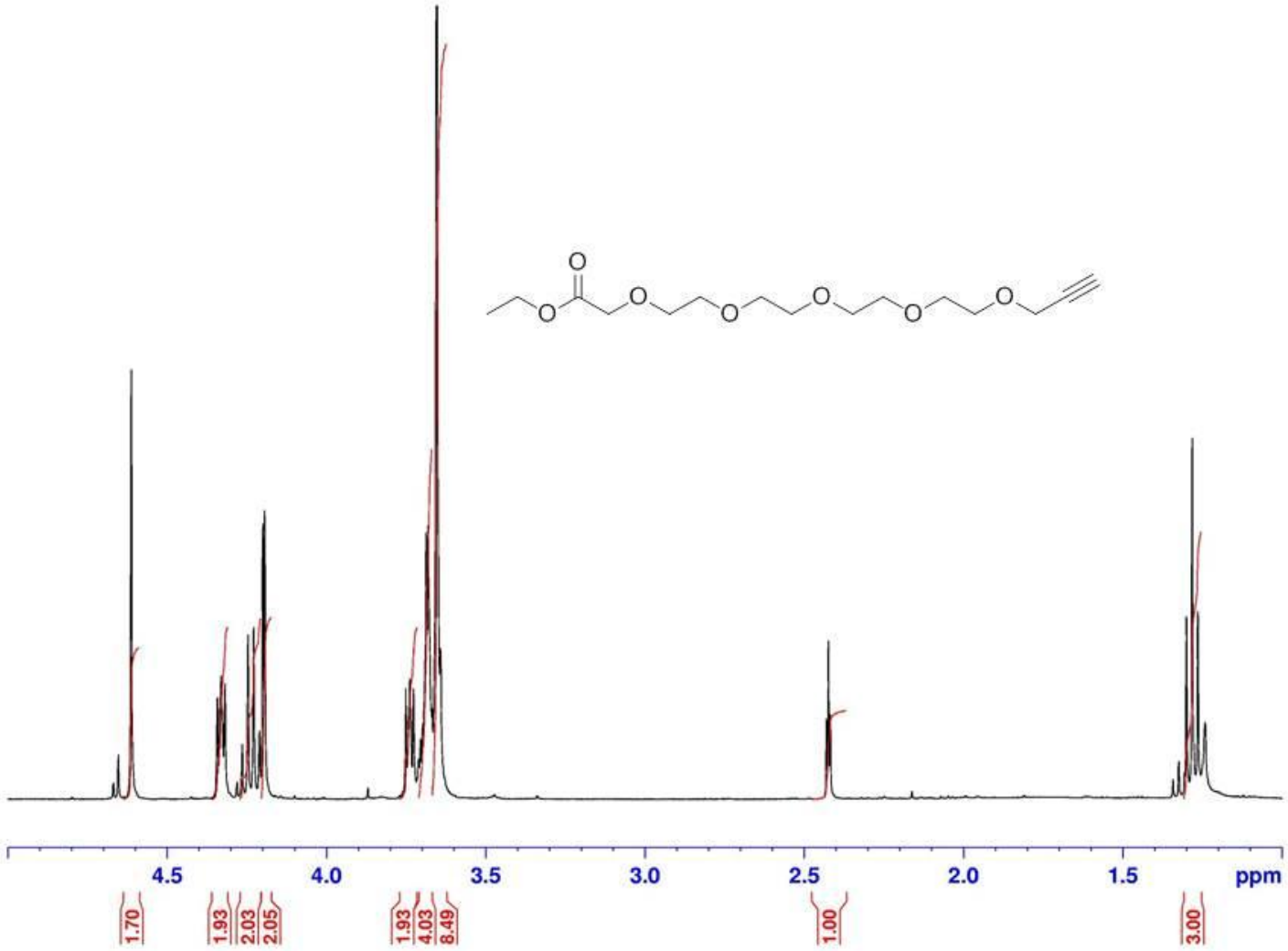

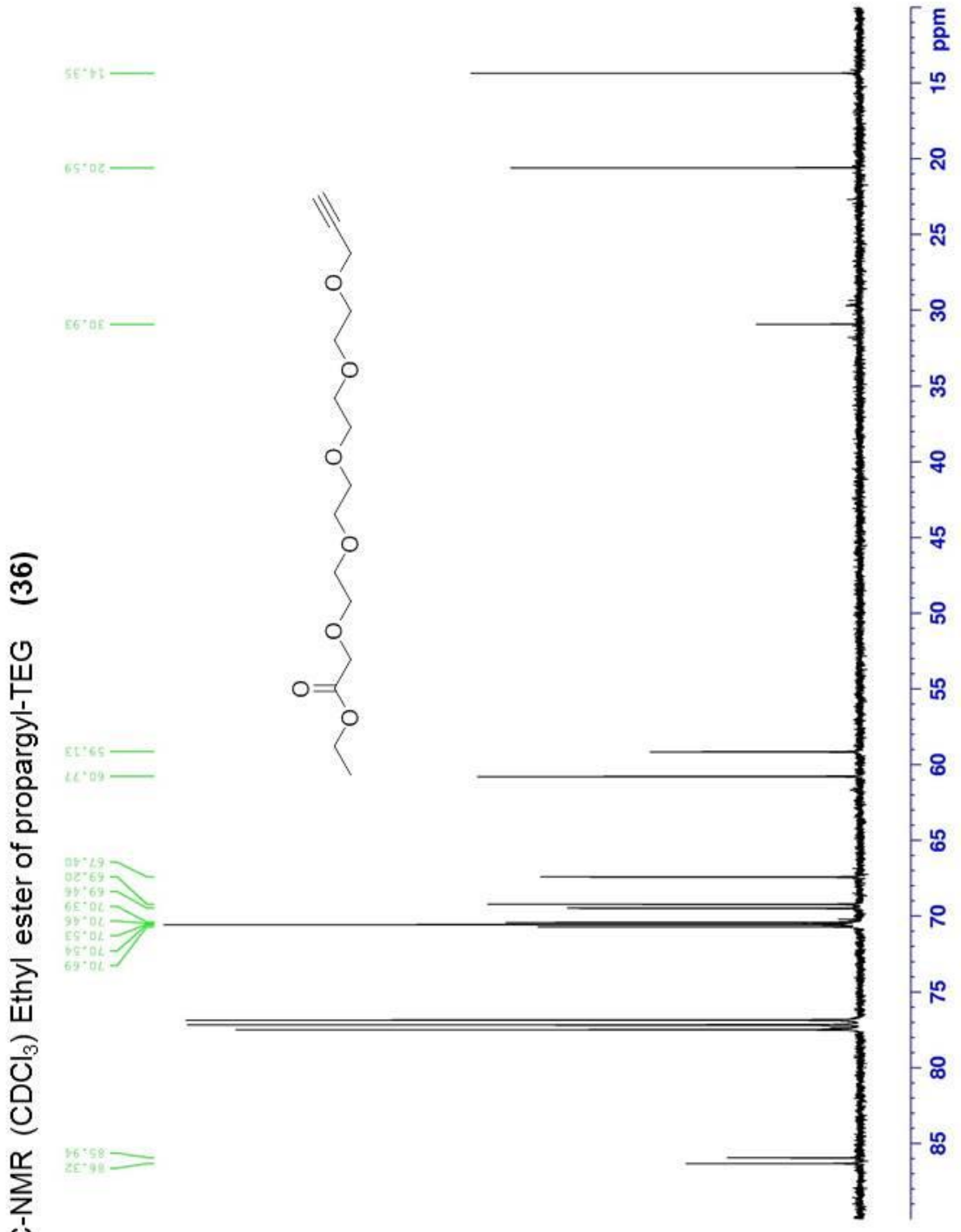
$^{13}$C-NMR ($CDCl_3$) Ethyl ester of propargyl-TEG (36)
14.35
20.59
30.93
59.13
60.77
67.40
69.20
69.44
70.39
70.46
70.53
70.54
70.69
85.94
86.32
ppm
15
20
25
30
35
40
45
50
55
60
65
70
75
80
85

$^{1}$H-NMR ($CDCl_3$) Mono-TSO-TEG **(42)**

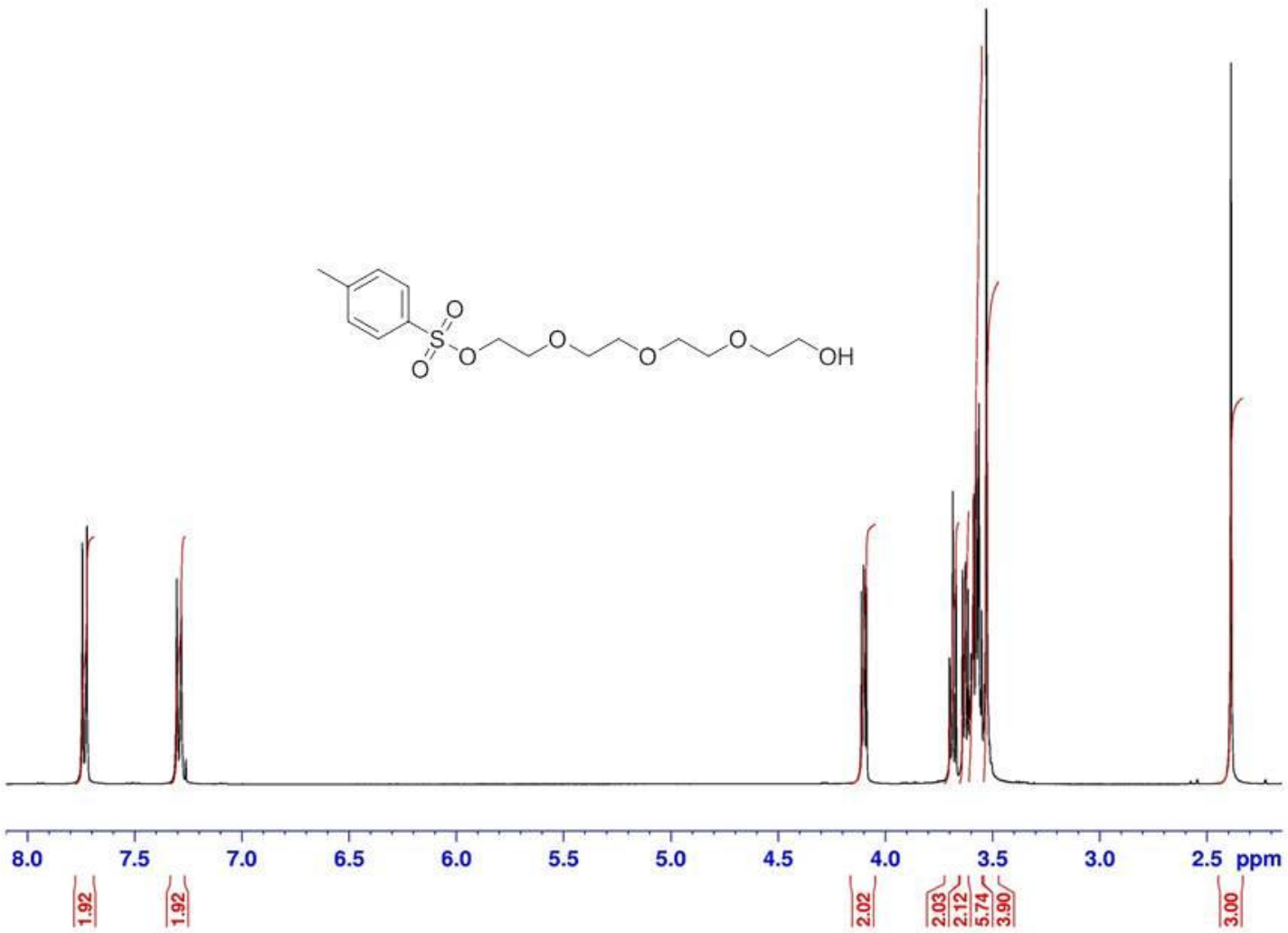

$^{13}$C-NMR ($CDCl_3$) Mono-TSO-TEG **(42)**

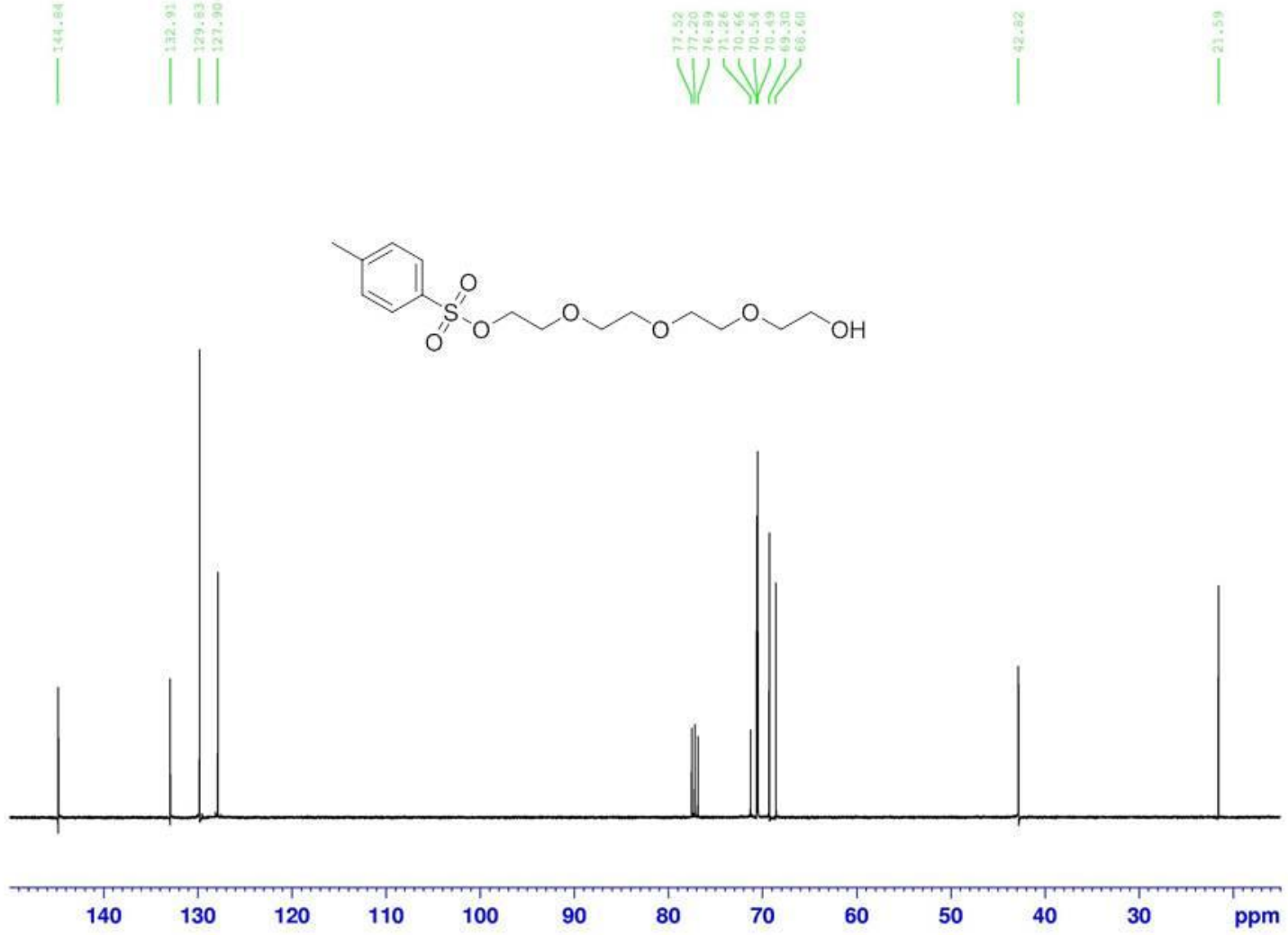

$^{1}$H-NMR ($CDCl_3$) Di-TSO-TEG **(43)**

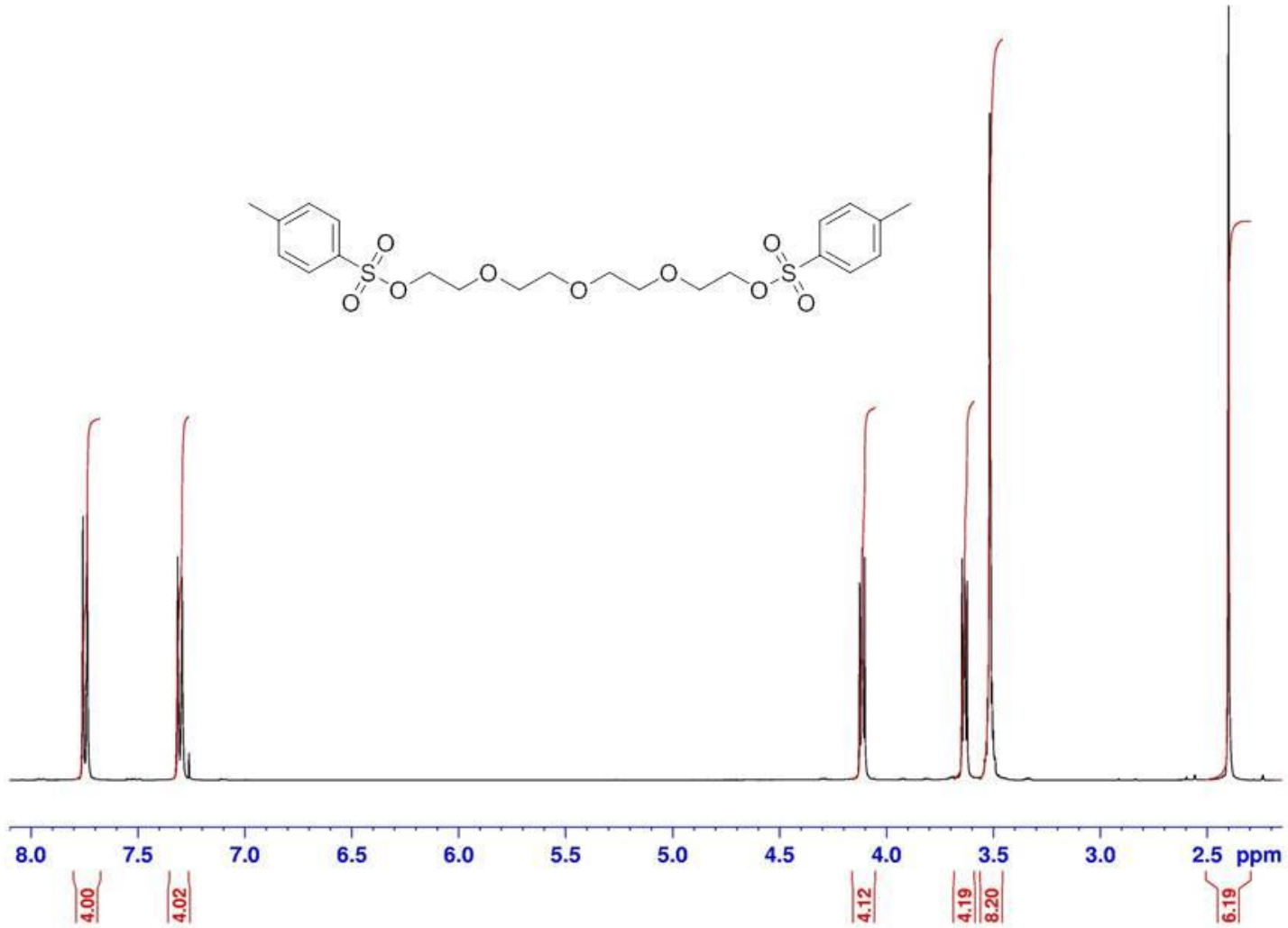

$^{13}$C-NMR ($CDCl_3$) Di-TSO-TEG **(43)**

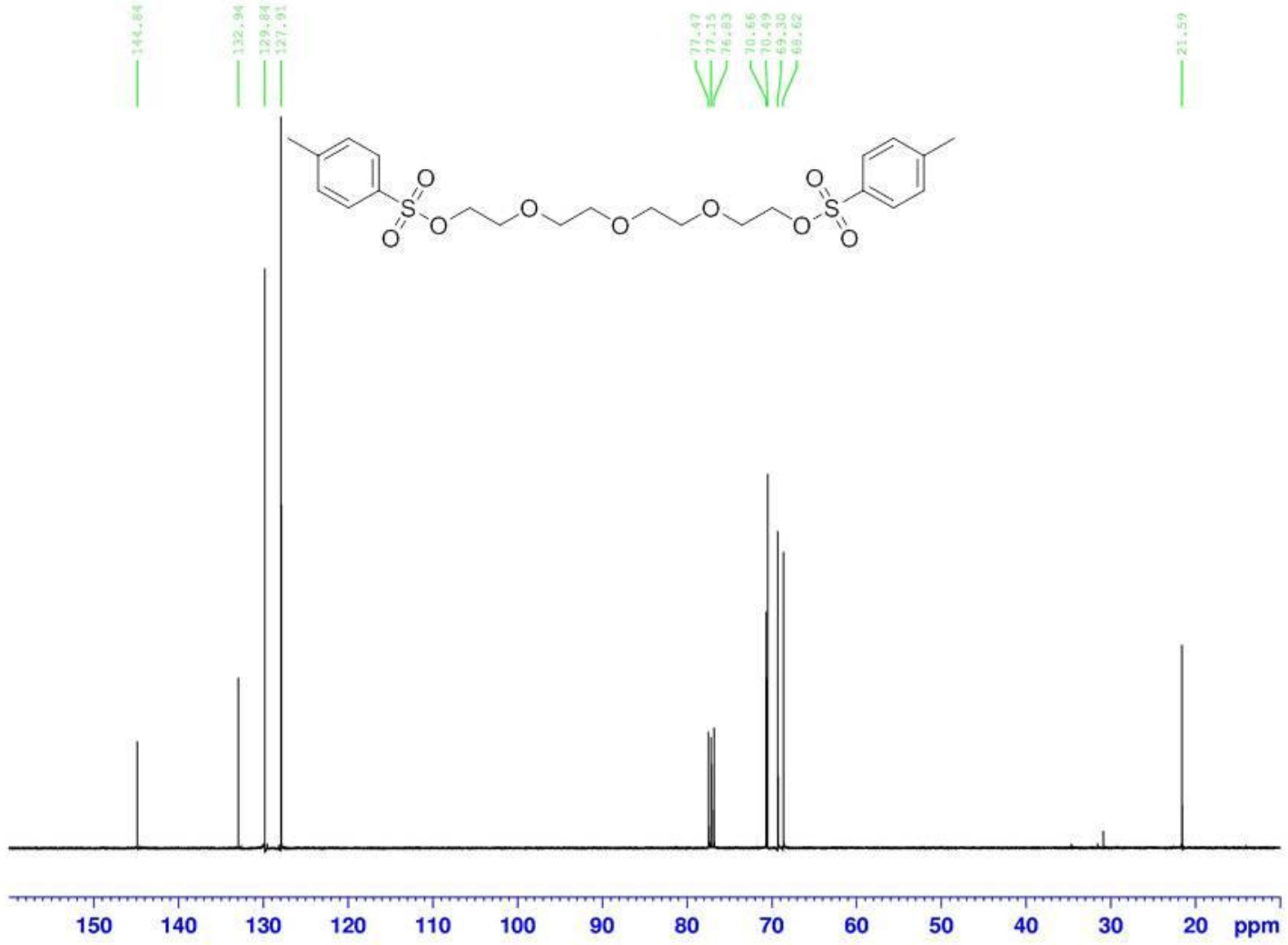

$^{1}$H-NMR ($CDCl_3$) Benzoate ester of TEG **(44)**

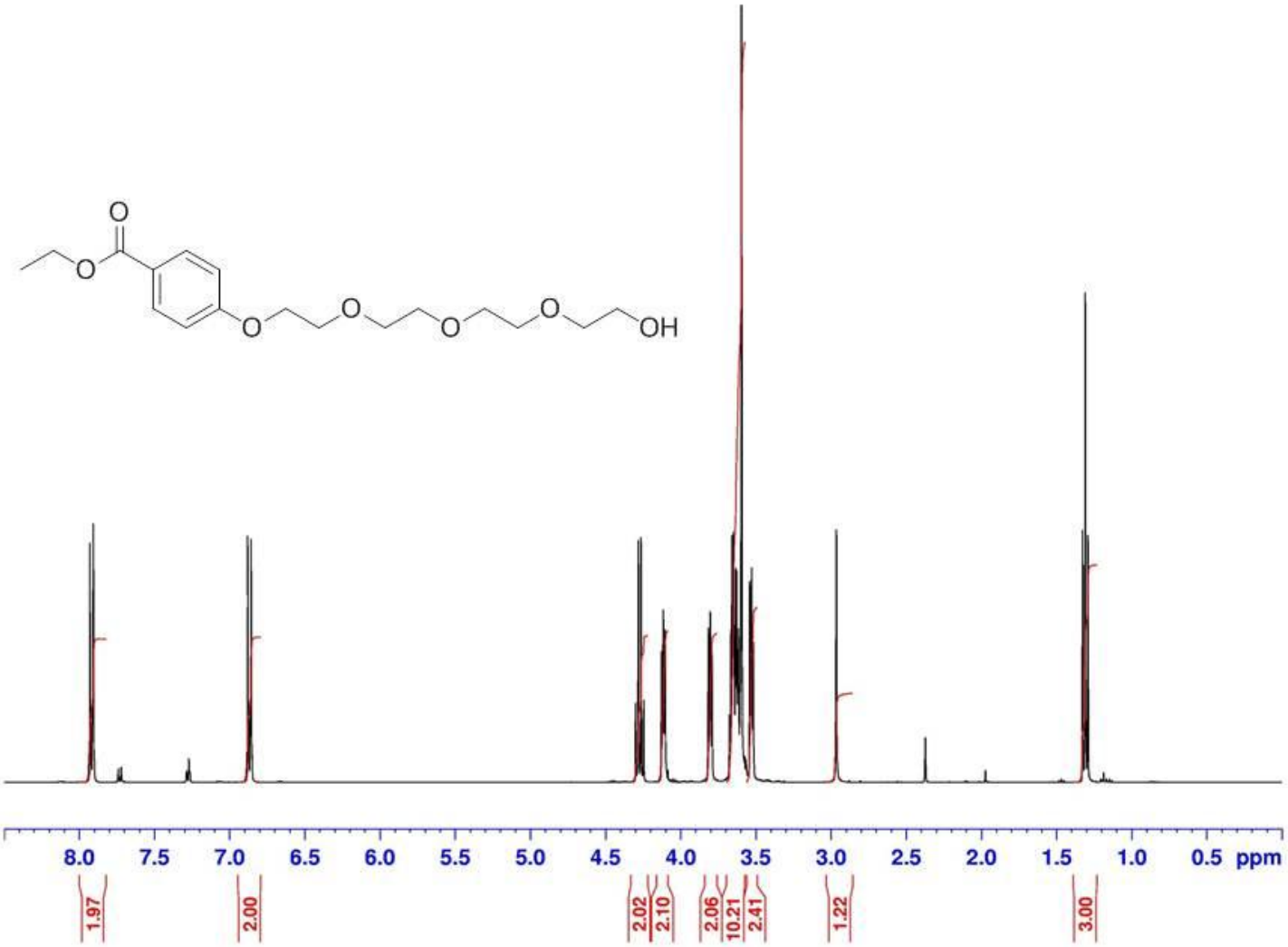

$^{13}$C-NMR ($CDCl_3$) Benzoate ester of TEG **(44)**

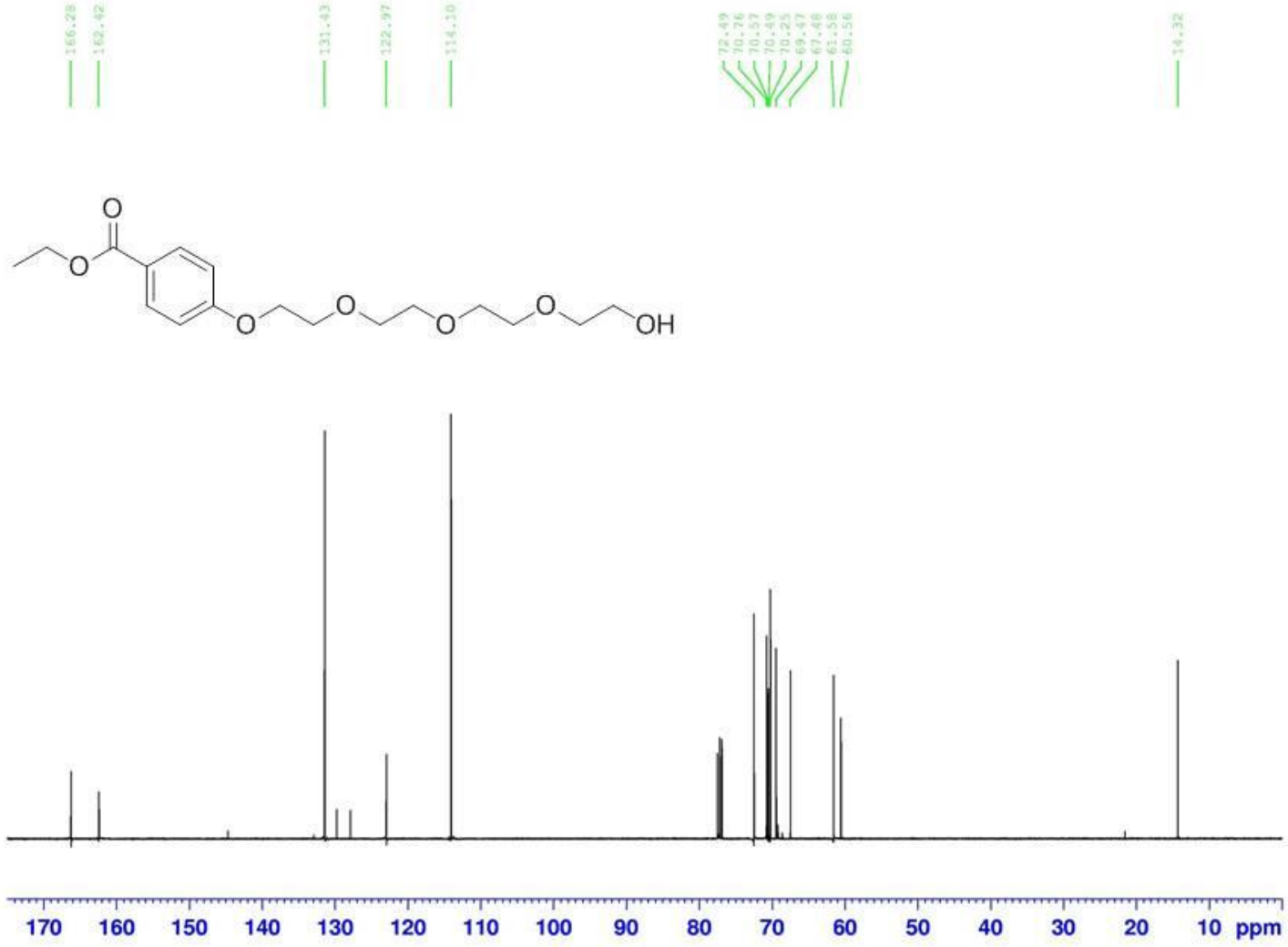

$^{1}$H-NMR ($CDCl_3$) Propargyl-TSO **(46)**

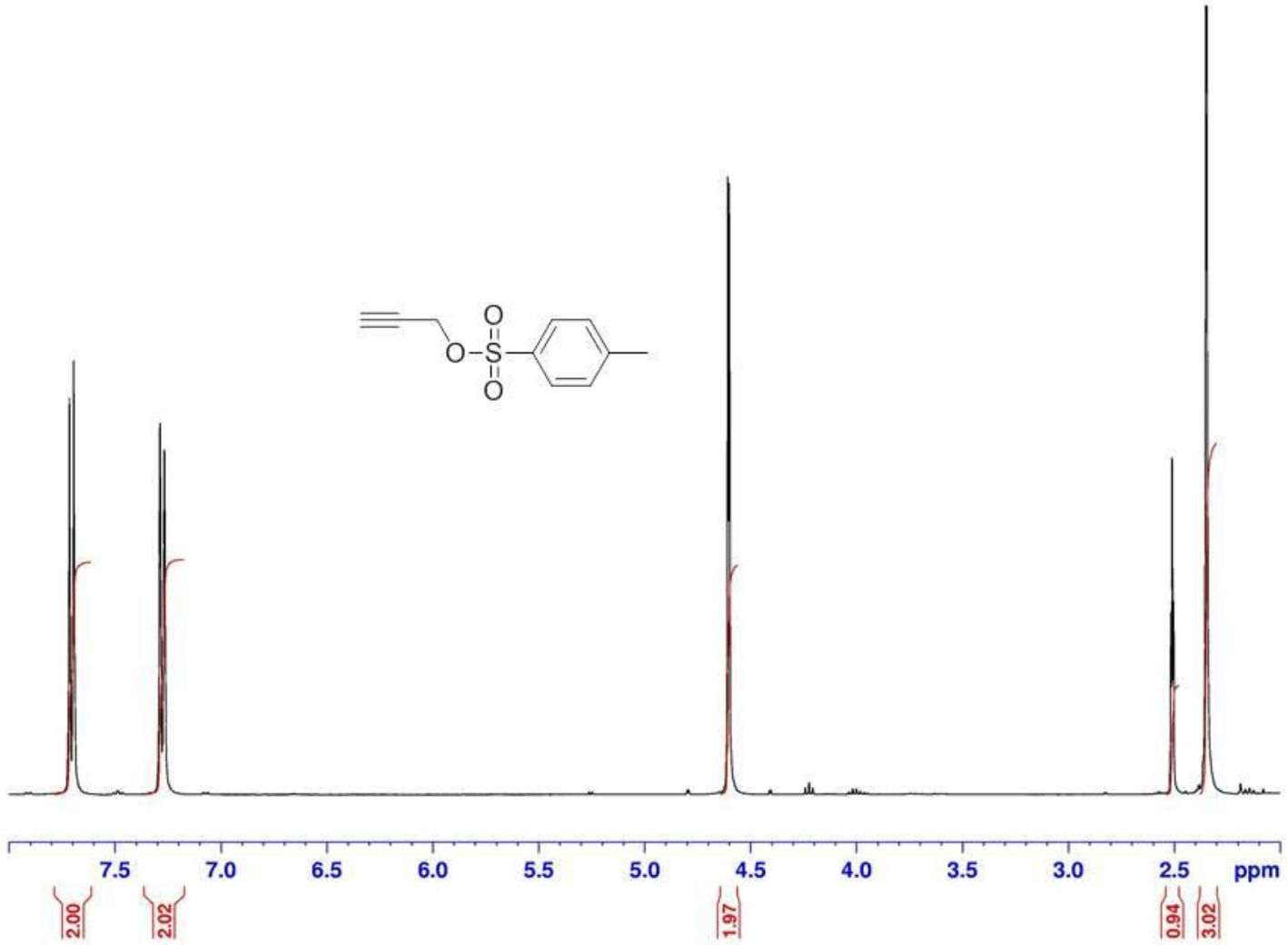

$^{13}$C-NMR ($CDCl_3$) Propargyl-TSO **(46)**

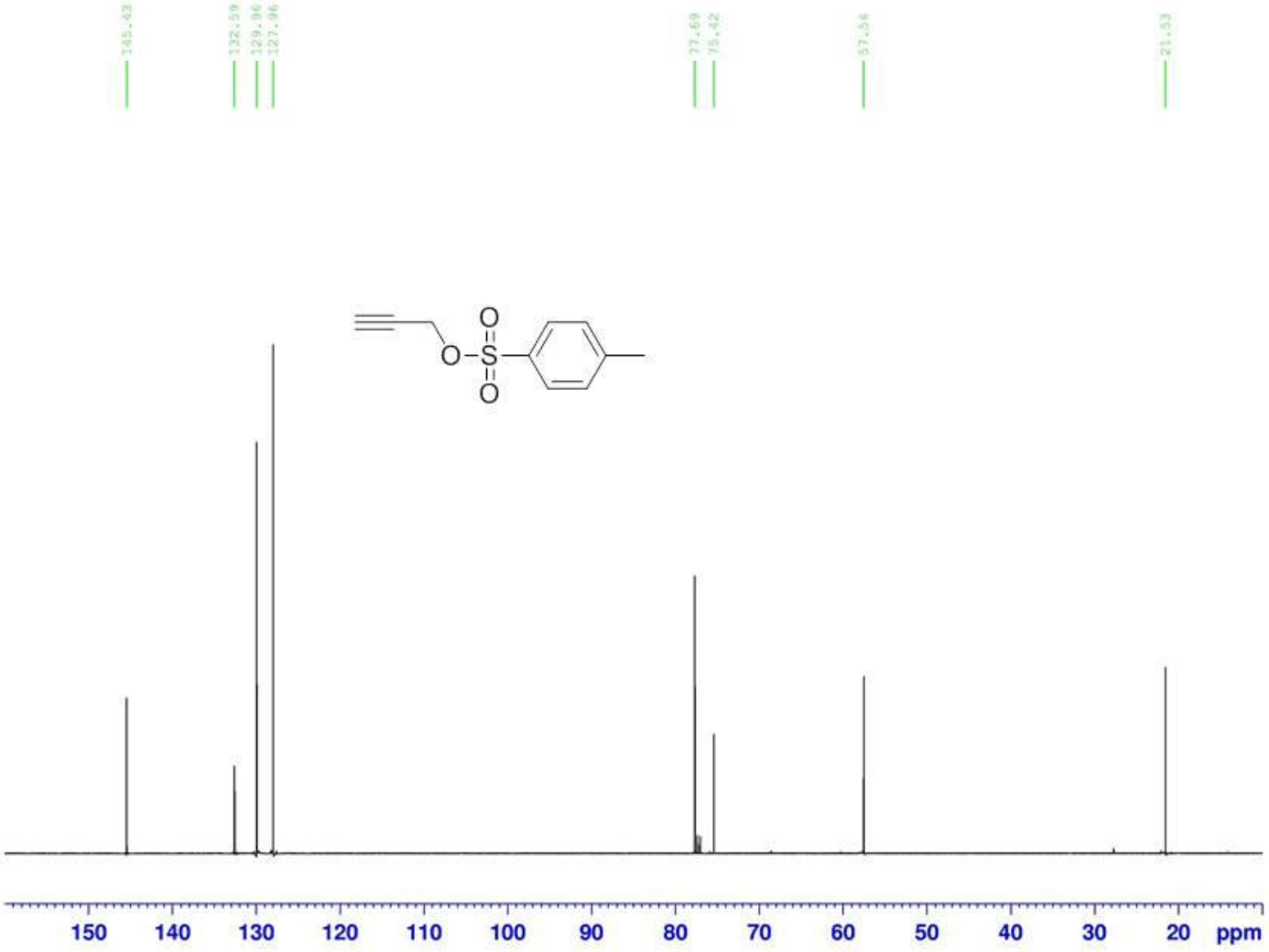

$^{1}$H-NMR ($CDCl_3$) Benzoate ester of Prop-TEG **(47)**

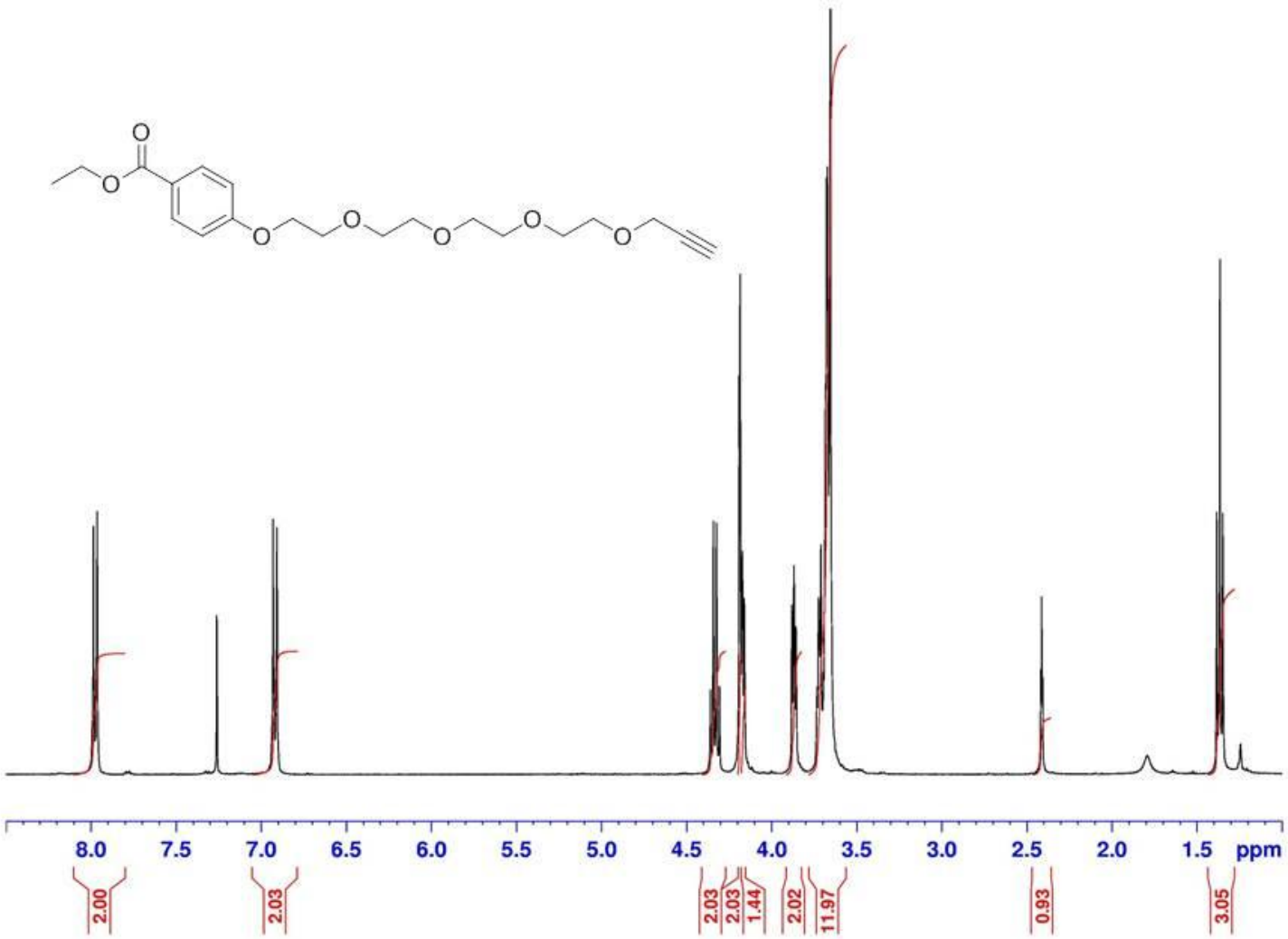

$^{13}$C-NMR ($CDCl_3$) Benzoate ester of Prop-TEG **(47)**

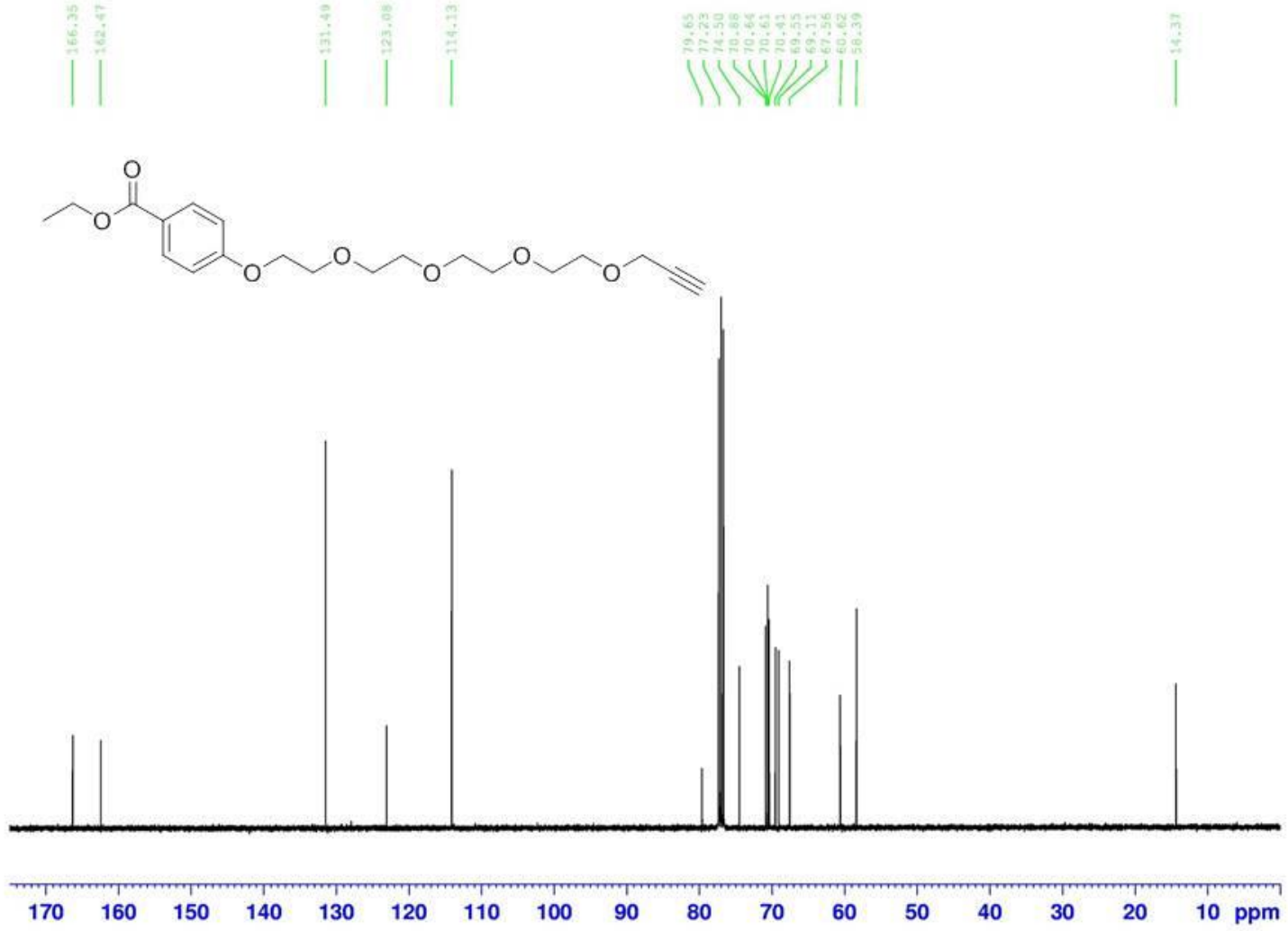

$^{1}$H-NMR ($CDCl_3$) VRT-Linker **(48)**

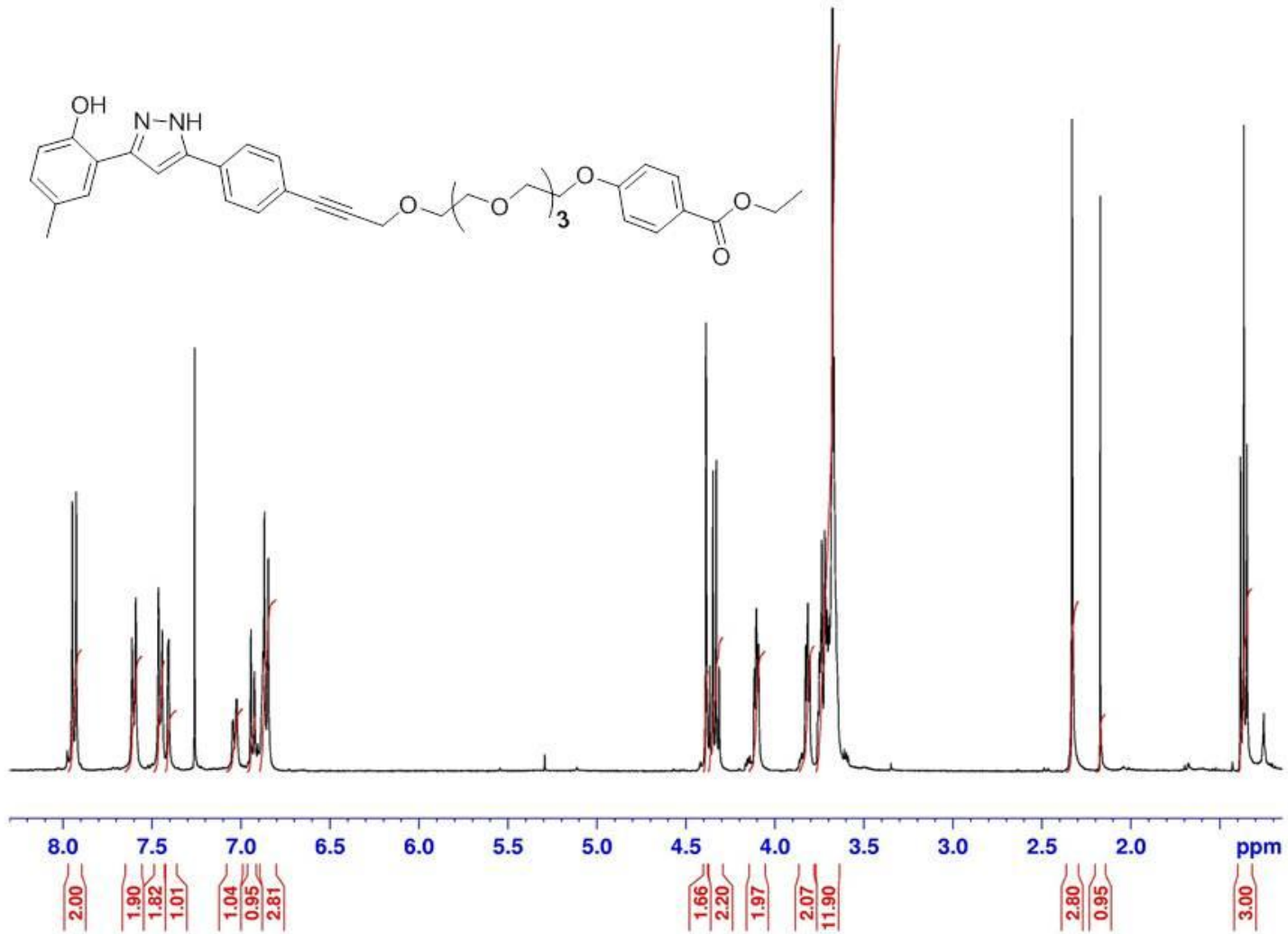

$^{13}$C-NMR ($CDCl_3$) VRT-Linker **(48)**

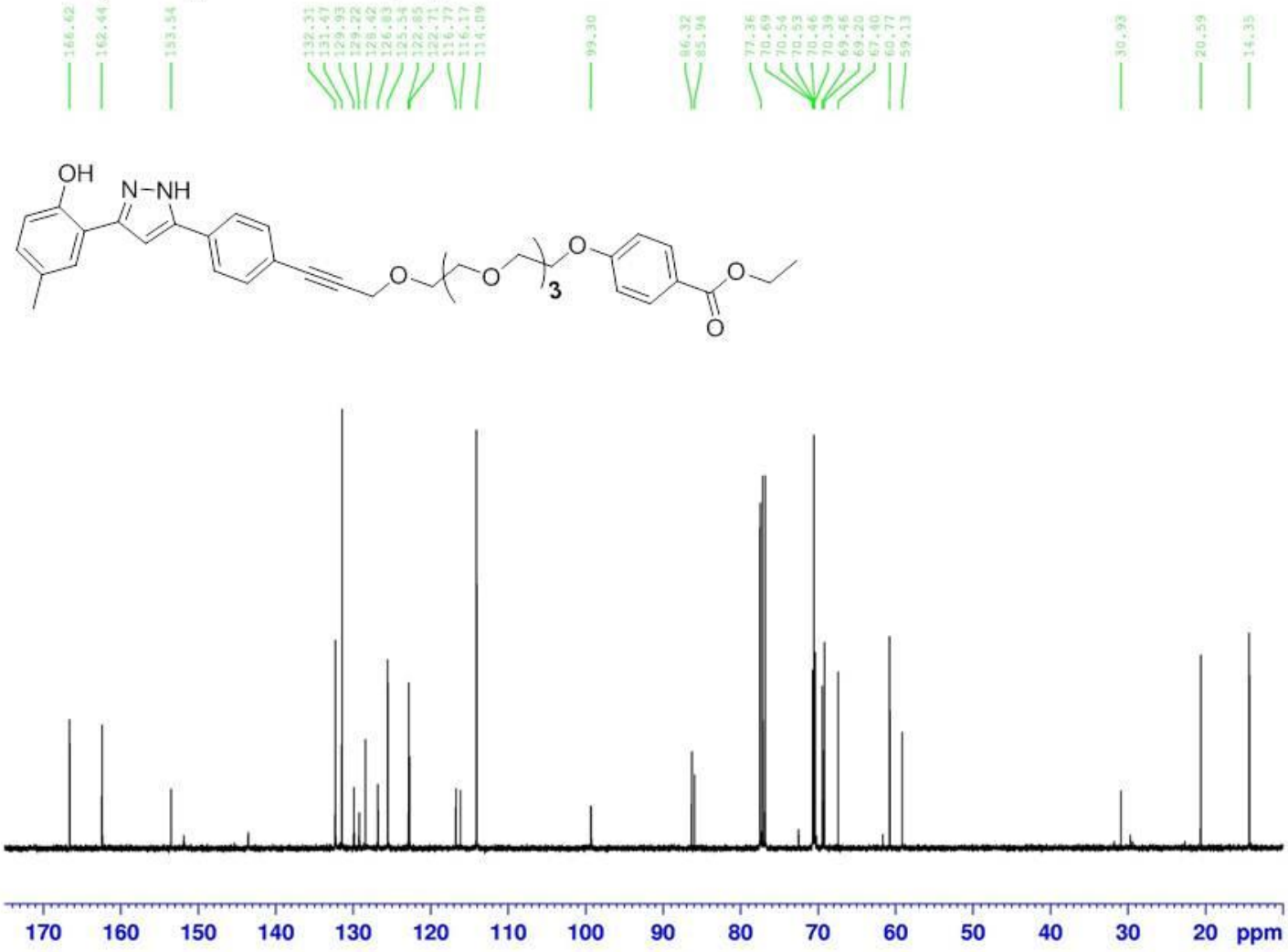

## 6. REFERENCES


1. *Canadian Cystic Fibrosis Patient Data Registry Report*; 2008, 9. Available online at http://www.cysticfibrosis.ca/assets/files/pdf/ CPDR_ReportE.pdf.

2. Riordan, J. R.; Rommens, J. M.; Kerem, B.-S.; Alon, N.; Rozhamel, R.; Grzelczak, Z.; Zielenski, J.; Lok, S.; Plavsic, N.; Chou, J.L.; Drumm, M. L.; Iannuzi, M. C.; Collins, F.; Tsui, L.-C. Identification of the cystic fibrosis gene: cloning and characterization of complementary DNA. *Science.,* **1989**, *245,* 1066-1073.

3. Anderson, D.H. Cystic fibrosis of the pancreas and its relation to celiac disease: A clinical and pathological study. *Am. J. Dis. Child*. **1938,** *56*, 344-399.

4. Di Sant' Agnese, P.A.; Darling, R.C.; Perera, G.A.; Shea, E. Abnormal electrolyte composition of sweat in cystic fibrosis of the pancreas: clinical significance and relationship to the disease. *Pediatrics*, **1953**, *12*, 549-563.

5. Bolliger, C.T. In Cystic fibrosis *in the 21st century;* Bush, A., Ed.; Karger: New York, 2006; Vol. 34, pp 2-8.

6. Harris. A.; Leir, S.H.; Blackledge, N. R.; Ott, C.J. Novel regulatory mechanism for the CFTR gene. *Biochem. Soc. Trans*. **2009**, *37*, 843-848.

7. Kunzelmann. K.; Mall. M. Pharmacotherapy of the ion transport defect in cystic fibrosis. *Clin Exp Pharmacol Physiol.* **2001***, 28,* 857–867.

8. Cheng, S.H.; Gregory, R.J.; Marshall, J.; Paul, S.; Souza, D.W.; White, G.A.; O'Riordan C.R.; Smith, A.E. Defective intracellular transport and processing of

CFTR is the molecular basis of most cystic fibrosis, *Cell,* **1990***, 63***,** 827–834.

9. Sharma, M.; Pampinella, F.; Nemes, C.; Benharouga, M.; So, J.; Du, K.; Bache, K.G.; Papsin, B.; Zerangue, N.; Stenmark, H.; Lukacs, G.L. Misfolding diverts CFTR from recycling to degradation: quality control at early endosomes. *J Cell Biol,* **2004***, 164***,** 923–933.

10. Serohijos, A.W. Hegedus, T.; Aleksandrov, A.A.; He, L.; Cui, L.; Dokholyan, N.V.; Riordan, J.R. Phenylalanine-508 mediates a cytoplasmic-membrane domain contact in the CFTR 3D structure crucial to assembly and channel function. *Proc. Natl. Acad. Sci. USA*, **2008,** *105,* 3256–3261.

11. Chan, H.C.; Ruan, Y.C.; He, Q.; Chen, M.H.; Wen, H.C.; Wen, M.X.; Chen, Y.; Xie, C.; Zhang, X.H.; Zhou, Z. The cystic fibrosis transmembrane conductance regulator in reproductive health and disease*. J. Physiol,* **2009,** *587***,** 2187–2195.

12. Bertrand, C.A.; Frizzell, R.A. The role of regulated CFTR trafficking in epithelial secretion. *Am J Physiol Cell Physiol,* **2003**, *285*, 1-18.

13. Rosser, M.F.N.; Grove, D.E.; Cyr, D.M The Use of Small Molecules to Correct Defects in CFTR Folding, Maturation, and Channel Activity. *Current Chemical Biology*, **2009**, *3*, 420-431.

14. Meacham, G.C.; Lu, Z.; King, S.; Sorscher, E.; Tousson, A.; Cyr. D.M. The Hdj-2/Hsc70 chaperone pair facilitates early steps in CFTR biogenesis. *EMBO J.* **1999**, *8*, 1492-505.

15. Bobadilla, J.L.; Milan Macek, M.Jr.; Fine, J.P.; Philip M. Farrell, P.M. Cystic Fibrosis: A Worldwide Analysis of CFTR Mutations.Correlation With Incidence Data and Application to Screening. *Hum Mutat,* **2002**, *19*, 575-606.

16. Rowntree, R.K.; Harris, A. The Phenotypic Consequences of CFTR Mutations Annals of *Human Genetics,* **2003** *67*,471–485.

17. Edward, F.; McKone, E.F.; Goss, C.H.; Moira, L.; Aitken, M.L. CFTR genotype as a predictor of prognosis in cystic fibrosis. *CHEST*, **2006**, *130,* 1441-1447.

18. Döring, G.; Elborn, J.S.; Johannesson, M.; de Jonge, H.; Griese, M.; Smyth, A.; Heijerman H. Clinical trials in cystic fibrosis. *J Cyst Fibros*. **2007**, 6(2), 85-99.

19. Ratjen. F.; Grasemann. H. Emerging therapies for cystic fibrosis lung disease. *Expert Opin. Emerging Drugs.* **2010**, *15*, 653-659.

20. Lukacs, G.L.; Verkman, A.S. CFTR: folding, misfolding and correcting the DF508 conformational defect. *Trends. Mol Med***,** **2012**, *18*, 81-91

21. Clarke, D. M.; Bartlett, C.; Loo, T. W.; Wang, Y. Correctors promote maturation of cystic fibrosis transmembrane conductance regulator (CFTR)-processing mutats by binding to the protein. *J. Biol. Chem.* **2007**, 282, 33247-33252

22. Robert, R.; Carlile, G.W.; Pavel, C.; Liu, N.; Anjos, S.M.; Liao, J.; Luo, Y.; Zhang, D.; Thomas, D.Y.; Hanrahan, J.W. Structural analog of sildenafil identified as a novel corrector of the F508del-CFTR trafficking defect. *Mol. Pharmacol*. **2008**, *73 (2),* 478-489

23. Carlile, G.W.; Robert, R.; Zhang, D.; Teske, K.A.; Luo, Y.; Hanrahan, J.W.; Thomas, D.Y. Correctors of protein trafficking defects identified by a novel high-throughput screening assay *ChemBioChem*, **2007***, 8(9),* 1012-1020.

24. Van Goor, F.; Straley, K. S.; Cao, D.; Gonzalez, J.; Hadida, S.; Hazlewood, A.; Joubran, J.; Knapp, T.; Makings, L. R.; Miller, M.; Neuberger, T.; Olson, E.; Panchenko, V.; Rader, J.; Singh, A.; Stack, J. H.; Tung, R.; Grootenuis, P. D. J.;

Negulescu, P. Rescue of ΔF508- CFTR trafficking and gating in human cystic fibrosis airway primary cultures by small molecules. *Am. J. Physiol., Lung Cell Mol. Physiol.* **2006**, *290*, 1117−1130.

25. Wang, Y.; Bartlett, M. C.; Loo, T. W.; Clarke, D. M. Specific Rescue of Cystic Fibrosis Transmembrane Conductance Regulator Processing Mutants Using Pharmacological Chaperones. *Mol. Pharmacol.* **2006**, *70*, 297−302

26. Wellhauser, L.; Kim Chiaw, P.; Pasyk, S.; Li, C.; Ramjeesingh, M.; Bear, C. E. A Small-Molecule Modulator Interacts Directly with ΔPhe508-CFTR to Modify Its ATPase Activity and Conformational Stability. *Mol. Pharmacol.* **2009**, *75*, 1430−1438.

27. McKone, E. F.; Aitken. M. L. Cystic fibrosis: disease mechanisms and therapeutic targets. *Drug Discovery Today: Disease Mechanism.,* **2004**, *1*, 137-143

28. Cyr, D. M.; Grove, D.E.; Rosser, M.F.N.; The use of small molecules to correct defects in CFTR folding, maturation and channel activity. *Curr. Chem. Biol*., **2009,** *3,* 420-431.

29. Zeitlin, P. L. Emerging drug treatments for cystic fibrosis*. Expert Opin. Emerging Drugs,* **2007**, *12,* 329-336

30. Rickman, B.H.; Nuckolls, C.; Shu, S.; Rheingold, A.L.; Fox, J.M.; Willmore, N.D.; Liu, L.; Katz, T.J. An effective synthesis of functionalizes Helicenes. *J. Am. Chem. Soc.* **1997**, *119*, 10054-10063

31. Alkhouri, B.; Denning, R A.; Chiaw, P.K.; Eckford, P.D.W.; Yu, W.; Li, C.; Bogojeski, J.J.; Bear, C. E.; Viirre. R.D. Synthesis and Properties of Molecular Probes for the Rescue Site on Mutant Cystic Fibrosis Transmembrane Conductance Regulator*. J. Med. Chem.* **2011**, *54*, 8693−8701.

32. Senderowitz, H.; Noy, E. Combating Cystic Fibrosis: In Search for CF Transmembrane Conductance Regulator (CFTR) Modulators. *Chem. Med. Chem*, **2011**, *6,* 243 – 251.

33. Kreindler, J. L. Cystic fibrosis: Exploiting its genetic basis in the hunt for new therapies. *Pharmacol Ther.* **2010** *125*, 219–229.

34. Zeitlin, P. L. Pharmacologic restoration of DF508 CFTR-mediated chloride current. *Kidney International*, **2000**, *57*, 832–837.

35. Thool, A. W.; Ghiya, B. J. Synthesis of 2-hydroxy-4,6- diphenylpyrimidines and their antimicrobial activity. *J. Ind. Chem. Soc.* **1988**, *65*, 522−524.

36. Zhu, W.; Ma, D. Synthesis of aryl and vinyl azides via prolinepromoted CuI-catalyzed coupling reactions. *Chem. Commun.* **2004**, 888−889.

37. Barral, K.; Moorhouse, A. D.; Moses, J. E. Efficient Conversion of Aromatic Amines into Azides: A One-Pot Synthesis of Triazole Linkages. *Org. Lett.* **2007**, *9,* 1809−1811.

38. Ghosh, P. B.; Whitehouse, M. W. 7-Chloro-4-nitrobenzo-2-oxa- 1,3-diazole: A New Fluorigenic Reagent for Amino Acids and other Amines. *Biochem. J.* **1968**, *108*, 155−156.

39. Sydnes, O.; Issei Doi, I.; Ayako Ohishi, A.; Masaki Kuse, M.; Isobe, M. Determination of Solvent-Trapped Products Obtained by Photolysis of Aryl Azides in 2,2,2 Trifluoroethanol. *Chem Asian J,* **2008**, *3(1),* 102-112.

40. Weber, G. Polarization of the Fluorescence of Macromolecules 2. Fluorescent Conjugates of Ovalbumin and Bovine Serum Albumin. *Biochem. J.* **1952**, *51*, 155−167.

41. Dorman, G. Photoaffinity Labelling in Biological Signal Transduction. *Top. Curr. Chem.* **2001**, *211*, 169−225.

42. Bolletta, F.; Fabbri, D.; Lombardo, M.; Prodi, L.; Trombini, C.; Zaccheroni, N. Synthesis and Photophysical Properties of Fluorescent Derivatives of Methylmercury. *Organometallics,* **1996,** *15*, 2415−2417.

43. Chinchilla, R.; Najera, C. The Sonogashira Reaction: A Booming Methodology in Synthetic Organic Chemistry. *Chem. Rev.* **2007**, *107*, 874−922.

44. Casara, P.; Danzin, C.; Metcalf, B; Jung, M. Stereospecific Synthesis of (2*R*,5*R*)-Hept-6-yne-2,5-diamine: A Potent and Selective Enzyme-Activated Irreversible Inhibitor of Ornithine Decarboxylase (ODC). *J. Chem. Soc., Perkin Trans,* **1985**, *1* 2201−2207.

45. Savage, M. D. An introduction to avidin-biotin technology and options for biotinylation. *BioMethods*, **1996,** *7*, 1-29.

46. Qiu, H.; Yinsheng Wang, Y. Probing adenosine nucleotide-binding proteins with an affinity labeled-nucleotide probe and mass spectrometry. *Anal. Chem.* **2007**, *79*, 5547-5556.

47. Taki, M.; Sisido, M. Leucyl/phenylalanyl(L/F)-tRNA-protein transferase-mediated aminoacyl transfer of a nonnatural amino acid to the N-terminus of peptides and proteins and subsequent functionalization by bioorthogonal reactions. *J. Pept. Sci.*, **2007**, *88(2)*, 263-271.

48. Isin, E.M.; Elmore, C.S.; Nilsson, G.N.; Thompson, R.A.; Weidolf, L. Use of Radiolabeled Compounds in Drug Metabolism and Pharmacokinetic Studies. *Chem. Res. Toxicol.*, **2012**, 25 *(3)*, 532–542.

49. Crist N. Filer, C.N. GABAergic radioligands labelled with tritium. *J. Label Compd. Radiopharm.* **2010**, *53*, 120–129.

50. Fathabad, N.C.; Choghamarani, A.G. Chemoselective and Catalytic Trimethylsilylation of Alcohols and Phenols by 1,1,1,3,3,3-Hexamethyldisilazane and Catalytic Amounts of $PhMe_3N^+Br_3^-$ . *Chin*. *J*. *Catal*., **2010**, *31*, 1103–1106

51. Amantini, D.; Fringuelli, F.; Pizzo, F.; Vaccaro, L. Efficient O-trimethylsilylation of alcohols and phenols with trimethylsilyl azide catalyzed by tetrabutylammonium bromide under neat conditions. *J. Org. Chem.,* **2001,** *66(20)***,** 6734-6737.

52. Yadollahi, B.; Mirkhani, V.; Tangestaninejad, S.; Karimian, D. Rapid and efficient protection of alcohols and phenols, and deprotection of trimethylsilyl ethers catalyzed by a cerium-containing polyoxometalate. *Appl***.** *Organomet***.** *Chem***.** **2011,** *25(2),* 83-86**.**

53. Luc, L.; Olivier, C.; Salah, G.; Fathi, M.; Suzanne, B.; Claude, B.; Rene, M. Selective and Potent Monoamine Oxidase Type B Inhibitors: 2-Substituted 5-Aryltetrazoles Derivatives. *J. Med. Chem.* **1995***, 38(24), 4786-4792*

54. Katz, T.J.; Liu, L; Willmore, N.D.; Fox, J.M.; Rheingold, A.L.; Shi, S.; Nuckolls, C.; Rickman, B.H. An Efficient Synthesis of Functionalized Helicenes. *J. Am. Chem. Soc*., **1997,** *119(42)*, 10054-10063.

55. Wataru, S.; Soichiro, O.; Chizuko, K.; Mitsuo, K. A molecular gyroscope having phenylene rotator encased in three-spoke silicon-based stator. *Chem. Lett.*, **2007**, *36(8)*, 1076-1107

56. Liu, Y.; Guo, Z.; Jin, Y.; Xue, X.; Xu, Q.; Zhang, F.; Liang, X. Click oligo(ethylene glycol)**: An excellent orthogonal stationary phase to C18 for two-dimensional reversed-phase/reversed-phase liquid chromatography. *J. Chromatogr.* **2008,** *1206(2),* 153-159.

57. Sun, X.L.; Stabler, C.L.; Cazalis, C.S.; Chaikof, E.L. Carbohydrate and protein immobilization onto solid surfaces by sequential Diels-Alder and azide-alkyne cycloadditions. *Bioconjug Chem.* **2006**,*17(1)*, 52-57.

58. Bhosale, S.; Bhosale, S.; Wang, T.; Kopaczynska, M.; Jurgen-Hinrich Fuhrhop, J.H. Hydrophobic and Hydrophilic Yoctowells as Receptors in Water *J. Am. Chem. Soc.*, **2006**, *128 (7)*, 2156–2157.

59. Losey, E.A.; Smith, M.D.; Meng, M; Best, M.D. Microplate-Based Analysis of Protein-Membrane Binding Interactions via Immobilization of Whole Liposomes Containing a Biotinylated Anchor. *Bioconjug Chem*., **2009***, 20(2),* 376-383.

60. Chan, L.J.; Seok, O.N.; Cho, S.; Hye, S.; Lee, Jung, L. Efficient in situ esterification of carboxylic acids using cesium carbonate. Org. *Prep. Proced. Int.,* **1996**, *28(4),* 480-483.

61. Baccaro, A.; Marx, A. Enzymatic Synthesis of Organic-Polymer-Grafted DNA. *Chem. Eur. J.*, **2010**, *16,* 218-226.

62. Liu, Y.; Kuzuya, A.; Sha, R.; Guillaume, J.; Wang, R.; Canary, J.W.; Nadrian, C.S. Coupling Across a DNA Helical Turn Yields a Hybrid DNA/Organic Catenane Doubly Tailed with Functional Termini., *J. Am. Chem. Soc.*, **2008,** *130 (33),* 10882–10883.

63. Singh, I.A; Rebecca, B. Palladium-catalyzed coupling of stannyl allenes with aryl iodides. *Synth. Commun.*, **1994**, *24(6),* 789-99.